Prevalence of resistance-nodulation-cell division-type efflux pumps and their contribution to antimicrobial resistance in *Acinetobacter baumannii*

Dissertation

zur

Erlangung des Doktorgrades (Dr. rer. nat.)

der

Mathematisch-Naturwissenschaftlichen Fakultät

der

Rheinischen Friedrich-Wilhelms-Universität Bonn

Vorgelegt von

Jennifer Nowak

aus Menden

Bonn 2016

Angefertigt mit Genehmigung der Mathematisch-Naturwissenschaftlichen Fakultät
der Rheinischen Friedrich-Wilhelms-Universität Bonn

1. Gutachter: Prof. Dr. Harald Seifert

2. Gutachter: Prof. Dr. Hans-Georg Sahl

Promotionsdatum: 12.01.2017

Erscheinungsjahr: 2017

Die vorliegende Arbeit wurde im Zeitraum von Februar 2012 bis März 2016 am Institut für Medizinische Mikrobiologie, Immunologie und Hygiene an der Uniklinik Köln unter der Leitung von Univ.-Prof. Dr. med. Harald Seifert angefertigt.

Hiermit versichere ich an Eides statt,

- dass ich die Dissertation persönlich, selbständig und ohne fremde Hilfe angefertigt und andere Quellen und Hilfsmittel als die in der Arbeit angegebenen nicht benutzt habe; insbesondere, dass wörtlich oder sinngemäß entnommene Stellen und Abbildungen aus Veröffentlichungen anderer Autoren als solche kenntlich gemacht worden sind,

- dass ich in der Dissertation einzelne Formulierungen und Sätze wörtlich oder mit geringen Veränderungen aus eigenen Veröffentlichungen übernommen habe, die im Einzelnen (aus Gründen der Lesbarkeit) nicht als solche kenntlich gemacht worden sind. Im Original habe ich diese Veröffentlichungen persönlich, selbständig und ohne fremde Hilfe angefertigt. Die aus anderen Quellen direkt oder indirekt übernommenen Daten und Konzepte wurden unter Angabe der Quelle kenntlich gemacht. Die Rechte zur Wiederverwendung der Veröffentlichungen habe ich mit Bestätigung des jeweiligen Verlages erhalten. Es handelt sich dabei um folgende Publikationen:
    - Nowak, J., Seifert, H., and Higgins, P.G. 2015. *Prevalence of eight resistance-nodulation-division efflux pump genes in epidemiologically characterized Acinetobacter baumannii of worldwide origin.* J Med Microbiol, 64: 630-5
    - Nowak, J., Schneiders, T., Seifert, H., and Higgins, P.G. 2016. *The Asp20-to-Asn Substitution in the Response Regulator AdeR Leads to Enhanced Efflux Activity of AdeB in Acinetobacter baumannii.* Antimicrob Agents Chemother, 60: 1085-90,

- dass ich mich bis zu diesem Tage noch keiner Doktorprüfung unterzogen habe. Ebenso hat die von mir vorgelegte Dissertation noch keiner anderen Fakultät oder einem ihrer Mitglieder vorgelegen,

- dass ein Dienststraf- oder Ehrengerichtsverfahren gegen mich weder geschwebt hat noch gegenwärtig schwebt.

Köln, im Juli 2016

(Jennifer Nowak)

Danksagung

Mein größter Dank gilt meinem Doktorvater **Prof. Dr. Harald Seifert** für die Möglichkeit, während der letzten vier Jahre in seinem Labor an einem spannenden Thema arbeiten und meine Ergebnisse auf nationalen sowie internationalen Konferenzen präsentieren zu können. Herzlichen Dank für die uneingeschränkte Unterstützung.

Des Weiteren möchte ich mich recht herzlich bei **Prof. Dr. Hans-Georg Sahl** für die bereitwillige Übernahme des Zweitgutachtens bedanken.

Special thanks go to **Dr. Paul G. Higgins**. As a mentor he was always providing a helping hand, inspiration, fruitful discussions as well as constructive criticism and challenging questions and tasks. He taught me to be critical and question everything. Thank you!

Ein riesen Dankeschön gilt meinen Labor-Mädels **Danuta Stefanik, Dr. Esther Wohlfarth, Kiki Xanthopoulou, Steffi Gerson** und **Anne Schulte**, die mir zu jeder Zeit hilfsbereit zur Seite standen und mich moralisch unterstützten.

Vielen Dank auch an **Marco Schwabe** und **Andrea Stammegna** für die regelmäßige Herstellung von Nährmedien, sowie an **Edel van Gumpel, Sandra Winter, Martina Wolke, Dr. Oleg Krut** und **Dr**. **Michael Schramm** für ihre Hilfsbereitschaft bei methodischen Fragen.

I would like to thank **Dr. Thamarai Schneiders, Dr. Alexandr Nemec, Prof. Dr. Martinus Pos and Dr. Ravi Marreddy for** their willingness to discuss my work and giving advice.

Für ihre Unterstützung und aufheiternde Gespräche möchte ich mich bei **Dr. Sarah Wilmschen, Lars** und **Stephan Neumann, Sascha Neuhaus, Betty Machova, Dr. Birgit Blissenbach, Dr. Tina Tosetti, Dr. Raja Ganesan, Dr. Tew Kamlovit, Dr. Alex Wailan, Marc Herb, Alex Gluschko, Sandra Schramm** und **Pia Wiegel** bedanken.

Von Herzen ein Dankeschön an **Inga Gerlings, Melli Arens** und **Andrea Filla** für ihre Unterstützung und ihren Glauben an mich. Bei **meinen Eltern und meinem Bruder** möchte ich mich von ganzem Herzen für ihre Liebe, Unterstützung und ihr Vertrauen bedanken und, dass sie mich immer dann erden, wenn mir alles über den Kopf wächst.

Table of contents

List of figures

List of figures contd.

List of tables

Index of abbreviations

ABC	- ATB-binding cassette
Acb	- *A. calcoaceticus* - *A. baumannii*
ARDRA	- Amplified ribosomal DNA restriction analysis
AFLP	- Amplified fragment length polymorphism
AbaR	- *A. baumannii* resistance island
BLAST	- Basic Local Alignment Search Tool
Bp	- Base pair
CCCP	- Carbonyl cyanide m-chlorophenyl hydrazone
Cfu	- Colony forming unit
ESKAPE	- Group of bacteria that escape the effects of antibacterial drugs
GtU	- Genotypically unique
HAMP	- Histidine kinase, adenylyl cyclase, methyl-accepting chemotaxis protein and phosphatase
IC	- International clone
ICU	- Intensive care unit
IPTG	- Isopropyl β-D-1-thiogalactopyranoside
IS*Aba*	- Insertion sequence *A. baumannii*
Kbp	- Kilobase pair
LB	- Luria Bertani
M	- Molar
MALDI-TOF MS	- Matrix-assisted laser desorption-ionization-time-of-flight mass spectrometry
MATE	- Multidrug and toxic compound extrusion
MDR	- Multidrug resistance/resistant
MFP	- Membrane fusion protein
MFS	- Major facilitator superfamily
MH	- Mueller Hinton
MIC	- Minimal inhibitory concentration
MurNAc	- N-acetylmuramic acid
NaCl	- Sodium chloride
NBD	- Nucleotide binding domain
NCBI	- National Center for Biotechnology Information
NMP	- 1-(1-naphtylmethyl)-piperazine
OD	- Optical density
Oe	- Overexpression
Oof	- Out-of-frame
OXA	- Oxacillinase
PAβN	- Phenylalanine arginyl β-naphtylamide
PACE	- Proteobacterial antimicrobial compound efflux
PDR	- Pandrug resistant
qRT-PCR	- Semi-quantitative real-time polymerase chain reaction
RND	- Resistance-nodulation-cell division
Rpm	- Rounds per minute
SDS	- Sodium dodecyl sulfate
SMR	- Small multidrug resistance
Spp.	- Species
TAE	- Tris-acetate EDTA
TMD	- Transmembrane domain
TMS	- Transmembrane segment
U	- Unit
VAP	- Ventilator-associated pneumonia
XDR	- Extensively drug resistant
X-gal	- 5-bromo-4-chloro-3-indolyl-β-D-galactopyranoside

1. Introduction

In 2011, the World Health Organisation announced antimicrobial resistance as the third greatest threat to human health [1]. Acquired antimicrobial resistance is defined as resistance of a microorganism (including bacteria, fungi, parasites and viruses) to an antimicrobial agent that was originally effective in treating the infection caused by the microorganism. As a consequence, standard treatments become ineffective and patients remain infected for a prolonged period, increasing the risk of spreading the microorganisms to others, and elevating health care expenses. Furthermore, there is a greater risk of death, particularly in immunocompromised patients or patients suffering from severe underlying diseases, when infected with multidrug resistant (MDR) organisms, as only limited treatment options are available [2].

Bacteria that are increasingly prevalent in our hospitals and are increasingly resistant to many of the applied antimicrobial agents have been termed "ESKAPE" organisms and include *Enterococcus faecium*, *Staphylococcus aureus*, *Klebsiella pneumoniae*, *Acinetobacter baumannii*, *Pseudomonas aeruginosa* and *Enterobacter* species [3]. Of these pathogens, *A. baumannii* was considered susceptible to most of the antimicrobials in the 1970s, however resistance to all first-line antibiotics has now been described [4, 5]. Within this thesis, the role of *A. baumannii* as a successful pathogen in the health care environment will be illustrated. As a main emphasis, bacterial efflux pumps, which promote the resistance to multiple drugs in *A. baumannii,* will be explained and discussed.

1.1 The genus Acinetobacter

The genus *Acinetobacter* is a member of the family *Moraxellaceae* within the class of γ-*Proteobacteria* and is defined as Gram-negative, strictly aerobic, oxidase-negative, glucose non-fermenting, catalase-positive, indole- and nitrate negative, non-fastidious bacteria with a G + C content of 40-48% [6, 7]. On blood agar plates these organisms form smooth, sometimes mucoid, pale yellow to greyish white colonies (Fig. 1.1A). Depending on the growth phase, the cells' shape can vary from coccoid to coccobacillary (Fig. 1.1B, C).

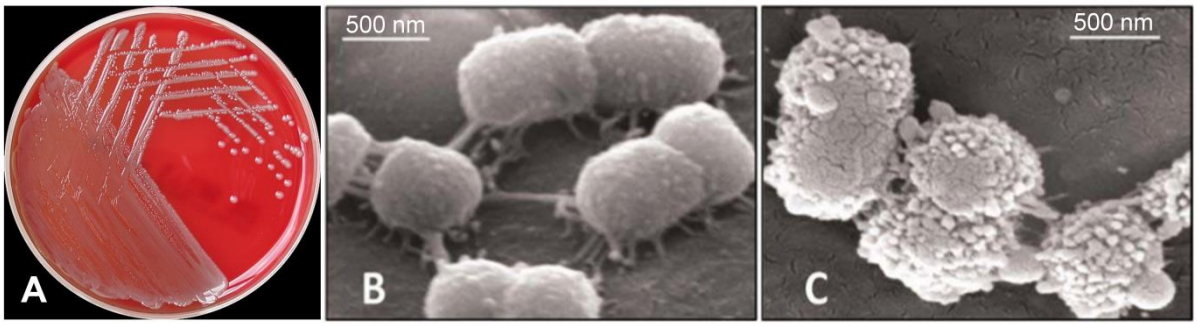

Figure 1.1 Morphology of *A. baumannii*. (A) Appearance of *A. baumannnii* on blood agar plate. Taken from Jakubů [8]. Scanning electron micrograph of *A. baumannnii* strains (B) AYE and (C) ACICU. Adapted from Visca *et al*. [9].

It took 60 years from its first isolation until the genus designation *Acinetobacter* was officially acknowledged. Although the Dutch microbiologist Bijernick was the first one who detected an *Acinetobacter* strain from a soil sample in 1911, originally named *Micrococcus calcoaceticus*, it was not until 1954 when Brisou and Prevot proposed the current genus name [10]. Detailed phenotypical analysis of Baumann *et al.* finally lead to the official acknowledgement of the genus *Acinetobacter* in 1971 [11, 12].

The name *Acinetbacter* derives from the Greek ακινετοσ (akinetos), meaning non-motile rod. However, recent studies have shown that *Acinetobacter*, in particular the species *A. baumannii,* indeed shows motile activity (Fig. 1.2), moving along wet surfaces in a 'twitching' manner by retraction of type IV pili. Furthermore, *A. baumannii* responds to light; driven by blue-light-sensing photoreceptors, it is motile in the absence of light [13-15].

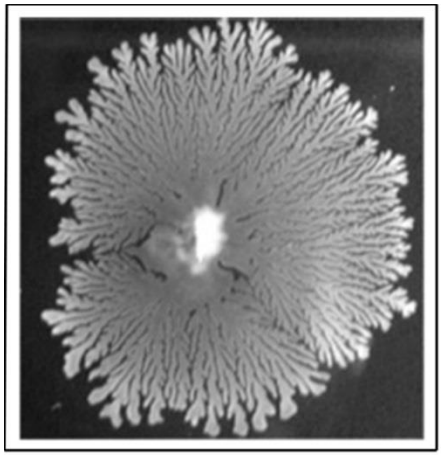

Figure 1.2 A colony of *A. baumannii* spreading over the surface of an agar plate. Taken from Wilharm [16].

1.1.1 Acinetobacter species and identification techniques

In 1986, studies based on DNA-DNA hybridisation by Bouvet and Grimont enabled the identification of species within the *Acinetobacter* genus [17]. To date, the genus comprises 62 species, with 57 published names (e.g. *A. baumannii*, *A. baylyi*, *A*. *calcoaceticus*, *A. lwoffii*, *A. nosocomialis*, *A. seifertii* and *A. pittii)* and 5 provisional designations such as *Acinetobacter* DNA group 6 (http://apps.szu.cz/anemec/Classification.pdf). Due to their close genetic relatedness and similar phenotypic properties, it is often challenging to discriminate between these species using phenotypic or taxonomic methods. As the best-known example, *A. baumannii*, *A. calcoaceticus*, *A. nosocomialis*, *A. pittii and A. seifertii* are often grouped together in the so-called "*A. calcoaceticus* - *A. baumannii* (Acb) complex" [18, 19]. However, from the clinical perspective this grouping is unsatisfactory as antibiotic susceptibilities and clinical significance of these five species differ from each other [20-22]. To facilitate a better identification of the species, molecular techniques such as amplified ribosomal DNA restriction analysis (ARDRA) [23] and high-resolution amplified fragment length polymorphism (AFLP) [24] have been used. Allowing the identification of genetic fingerprints typical of each species, these methods are able to properly discriminate between them. However, these techniques are almost exclusively applied in reference laboratories. In diagnostic microbiological laboratories, most often the semi-automated matrix-assisted laser desorption-ionization-time-of-flight mass spectrometry (MALDI-TOF MS) or automated Vitek2 system is used for species identification. Whereas MALDI-TOF MS generates mass spectra specific for each species, which can subsequently be matched to spectra in an online database [25], Vitek2 measures metabolic activities (e.g. acidification, alkalinisation, enzyme hydrolysis) to distinguish species [26]. Furthermore, PCR-based approaches based on species-specific DNA regions, such as the $bla_{OXA\text{-}51}$ carbapenemase gene intrinsic to *A. baumannnii* or sequencing of the DNA gyrase subunit B encoding gene *gyrB*, are used [27, 28]. However, so far a gold standard to discriminate between *Acinetobacter* species (*Acinetobacter* spp.) has not been established. Therefore, due to varying specificity and sensitivity of the applicable methods, data sets from different laboratories should be compared with caution if different methods where used for species identification.

1.1.2 Natural habitat of Acinetobacter spp.

In 1968, Baumann reported that he isolated *Acinetobacter* spp. from 28 of 30 soil samples and 29 of 30 water samples taken in California (USA) [29]. Since then, this genus has been considered as ubiquitous in nature. More recent studies confirmed these findings by isolating *A. nosocomialis* and *A. baylyi* from soil [30, 31]. Similarly, *A.baylyi*, *A. bouvettii* and *A. towneri*, among others, were cultivated from activated sludge [32]. Even in the extreme environment of Andean lakes, five different *Acinetobacter* spp. could be isolated [33]. However, human carriage has also been reported. In 1997, Seifert *et al.* reported colonization of skin and mucous membranes in 43% of healthy individuals, where *A. lwoffii* and *A. johnsonii* were found to be the most prevalent [34]. In a similar study conducted in the UK, *Acinetobacter* skin carriage was found in 44% of 192 healthy humans, with *A. lwoffii* again accounting for most of the isolates (61%) [35]. Investigating the faecal carriage, isolates could be cultivated among 25% of healthy people with *A. johnsonii* being the predominant species [36]. Among hospitalised patients, 75% were found positive for *Acinetobacter* spp. [34].

Based on the early dogma of *Acinetobacter* being an environmental organism, *A. baumannii* has also been described as such, although no appropriate reference supports this assumption [37]. Instead, *A. baumannii* is almost exclusively found in the hospital environment, emerging as an opportunistic nosocomial pathogen. Occasional reports of *A. baumannii* occurring in the environment (vegetables, soil, aquacultures) are available [38-40], but it is not clear whether these infrequent findings are due to contamination or contact with humans, or if the environment indeed serves as natural reservoir. *A. baumannii* isolates recovered from human lice [41], vegetables collected in supermarkets, greengrocers and private gardens [38] as well as from surfaces like tables in parks and game consoles, which themselves are inanimate but in contact with humans, [42] rather speak for a human-associated natural reservoir. Furthermore, pets like dogs, cats and horses, were found to be colonized by *A. baumannii* [43, 44]. Causing clinical outbreaks worldwide (meaning that multiple patients within a hospital are infected with the same strain), this organism has developed to the clinically most relevant species among the genus *Acinetobacter*.

1.1.3 Clinical relevance of Acinetobacter spp.

The first case of a community-acquired *Acinetobacter* infection was reported in two patients with excessive alcohol consumption in the US in 1977 [45]. However, incidences of **community-acquired *Acinetobacter* infections** have increasingly been reported during the last 15 years. Due to the prolonged lack of reference methods for species identification, care should be taken when reviewing reports interpreting which *Acinetobacter* spp. are involved in infections. Nevertheless, *A. baumannii*, *A. nosocomialis* and *A. pittii* have been implicated in community-acquired infections, with *A. baumannii* being the most predominant [46]. Infections include primarily pneumonia, skin infections, secondary meningitis, and endocarditis, which mostly occur in elderly people and are often associated with (chronic) underlying diseases, such as diabetes mellitus [47-49]. Interestingly, *A. baumannnii* infections have mainly been reported during summer in tropical and subtropical areas like Southeast Asia and tropical Australia [50, 51]. Possible reasons for this phenomenon have yet to be elucidated. More recently, *A. baumannii* was isolated from wounds of survivors of natural disasters, such as earthquakes [52, 53] and a tsunami [54]. Overall, community-acquired infections caused by *A. baumannii* are rare and rather based on single events. Nevertheless, a mortality rate between 40-60% has been correlated especially with community-acquired pneumonia caused by this species, underlining its clinical impact [55].

Within hospitals, the situation is different. An increasing number of health-care associated outbreaks of multidrug resistant *A. baumannii*, ranging from a hospital-specific to inter-hospital as well as inter-continental dissemination, have been described around the world. Similar to community-acquired infections, **hospital-acquired infections** are mainly due to *A. baumannii*, *A. nosocomialis* and *A. pittii*, with *A. baumannii* being the most frequent. Whereas, *A. nosocomialis* and *A. pittii* isolates are relatively susceptible to antimicrobials and cause sporadic infections with mortality rates between 7-18% [56, 57], *A. baumannii* outbreaks are often clonal and spread nationally as well as internationally [6, 9]. Furthermore, infections are associated with prolonged hospital stay and considerable morbidity and mortality in up to 58% of cases [58-60]. The situation in intensive care units (ICUs) and surgical units is of particular severity. As these wards host critically ill patients with impaired host defences, the units including its patients create an optimal niche for opportunistic bacteria such as *A. baumannii*. Due to the high incidence of antimicrobial usage in these environments, opportunistic pathogens develop antibiotic resistance and

spread among patients. Indeed, during the past three decades *A. baumannii* has been increasingly reported to cause a large variety of nosocomial infections among immunocompromised patients, such as ventilator-associated-pneumonia (VAP), bloodstream infection following invasive procedures, as well as wound and urinary tract infections, meningitis and soft-tissue infections [61]. Due to its appearance in infections subsequent to injuries sustained in conflict areas such as Afghanistan and Iraq, *A. baumannii* was colloquially referred to as "Iraqibacter" by American military personal [62].

Analysing clinical *A. baumannii* outbreaks worldwide, three clones have been characterized to predominantly emerge and spread epidemically across hospitals, which therefore have been called international clones (IC) 1-3 (formerly called EUI-III) [63, 64]. Within a large survey using imipenem-resistant *A. baumannii* isolates, five further epidemic lineages (IC4-8) were identified [65]. The spread of clonal lineages is proposed to be triggered by transfer of colonized patients between wards and hospitals [66-68], and ultimately airline travel facilitates intercontinental dissemination [69, 70]. It is of particular concern that isolates within these clones display increasing resistance against multiple antimicrobial agents. Whereas in the 1970s *A. baumannii* was associated with susceptibility to most antimicrobials, today this organism is displaying resistance against all first-line antibiotics [37]. Outbreaks of multidrug [71-73], extensively drug [74-76] and even pandrug resistant [4, 5] strains have been described (see Table 1.1 for definitions).

Table 1.1 Standardized international terminology to describe acquired resistance profiles.
Adapted from Magiorakos *et al*. [77] with permission from Elsevier.

Type of resistance	Definition
Multidrug resistance (MDR)	Non-susceptibility to ≥1 agent in ≥ 3 antimicrobial classes*
Extensively drug resistance (XDR)	Non-susceptibility to ≥1 agent in all but ≤ 2 antimicrobial classes*
Pandrug resistance (PDR)	non-susceptibility to all antimicrobial agents*

*for a list of approved antimicrobials against *Acinetobacter* spp. see *Suppl. Table I*

1.1.4 A. baumannii – a persisting hospital pathogen

Special traits of *A. baumannii* that contribute to its predominant appearance in hospital settings include its resistance to desiccation, biofilm formation and its genomic plasticity, which allows the easy acquisition of resistance determinants.

Investigating the **desiccation tolerance** of *A. baumannii* isolates on dry surfaces, Jawad *at el*. reported a mean survival time of 27 days on glass coverslips [78]. This survival time was considerably longer in comparison to other *Acinetobacter* spp. [79, 80] as well as to *E. coli* and other *Enterobacteriaceae* [6]. Even a long-term survival of more than 4 months has been reported [81]. With this unique trait, *A. baumannii* dissemination is facilitated in the hospital environment. If a patient with a silent *A. baumannii* colonization is hospitalized, in particular if transferred from another hospital, the organism may spread to the surrounding environment by air droplets and scales of skin [82]. Isolates have indeed been recovered from pillows, bed curtains, and furniture during outbreaks [67, 83]. The *A. baumannii* colonies on these surfaces can in turn be picked up on the hands of medical personal, further spreading the isolate within the ward or the hospital.

Additionally, the ability to **form biofilm** facilitates the adherence of *A. baumannii* isolates to biotic as well as abiotic surfaces [84]. Comparing the biofilm formation of species of the Acb-complex to species which are not part of the complex, members of the Acb-complex were threefold more likely to form a biofilm on a liquid-solid interface [85, 86]. This creates a particular problem with medical devices including mechanical ventilators and catheters, serving as additional reservoirs (humans being the primary reservoir) [87]. After invasive procedures, patients that are already in a critical health state may easily have contact with persisting *A. baumannii* clones, which in the worst case exhibit MDR. Indeed, invasive procedures have been described as a risk factor of getting *A. baumannii* infections in the hospital setting [6, 68, 88].

The upregulation of innate resistance mechanisms [89] and its ability to **easily acquire antimicrobial resistance determinants** are key features which help *A. baumannii* to withstand the antibiotic pressure it is facing in hospital settings. Its genomic plasticity can be exemplified by the acquisition of variable genomic regions called resistance islands. These islands are inserted into the chromosome and encode multiple genes conferring resistance to distinct antimicrobials. In the MDR *A. baumannii* isolate AYE, Fournier *et al.* identified a

resistance island of 86 kb in size named AbaR1 [37]. Of the 88 encoded genes, 45 were predicted to be resistance genes, conferring resistance against aminoglycosides, β-lactams, chloramphenicol, and tetracycline, amongst others. Furthermore, this resistance island was composed of mobile genetic elements and also contained genes derived from other pathogenic Gram-negative organisms such as *Pseudomonas*, *Salmonella* and *E. coli*, illustrating inter-species genomic exchange. To date, 26 further resistance islands have been described (AbaR2-AbaR27) in various *A. baumannii* isolates originating from all over the world [90-96]. They are all slightly different in their composition [which, and how many (resistance) genes are encoded] but were always inserted into the same chromosomal region, disrupting a putative ATPase open reading frame. In addition to resistance islands, further often broad-host-range mobile genetic elements have been characterized in *A. baumannii (*transposons, insertion sequences, integrons) which either introduce new resistance genes or upregulate the expression of innate resistance mechanisms thereby contributing to antimicrobial resistance in this organism [97-99]. Altogether, the outlined genome plasticity of *A. baumannii* facilitates its ability to acquire resistance determinants, ultimately leaving limited treatment options against infections and impairing the control of hospital outbreaks.

1.1.5 Antimicrobial resistance mechanisms in A. baumannii

Different antibiotic classes have been discovered or developed to inhibit bacterial cell growth (bacteriostatic mode of action) or kill bacteria by causing cell death (bactericidal mode of action). Cellular processes targeted by antimicrobials approved against *Acinetobacter* spp. *(Suppl. Table I)* include cell wall, DNA, RNA and protein synthesis as well as folate synthesis. To date, resistance mechanisms against all of the currently available antimicrobial agents have been described in *A. baumannii*, which include decreased permeability, enzymatic inactivation and modification of antimicrobials, target-site modification, and active efflux. Below, the activity of relevant antimicrobial classes is described followed by the description of specific resistance mechanisms displayed by *A. baumannii*. Resistance mechanisms and the antimicrobial site of action are illustrated in Fig. 1.3.

Ribosomes, which drive protein synthesis from mRNA templates, are divided into two subunits – the 30S and the 50S subunit. **Aminoglycosides** (e.g. amikacin and gentamicin)

inhibit protein synthesis by binding to the 16S ribosomal RNA of the 30S subunit of the ribosome. As a consequence, the incoming mRNA is misread and non-functional proteins are generated. In bacteria, drug-modifying enzymes have been described, which prevent aminoglycosides from binding to the ribosome. In *A. baumannii* three types of aminoglycoside-modifying enzymes, including aminoglycoside acetlytransferases (e.g. AacC1-4), nucleotidyltransferases (e.g. AntA1-4), and phosphotransferases (e.g. AphA1-6), have been discovered [100-102]. In addition, methylation of residues in the aminoglycoside-binding site of the 16S ribosomal RNA (e.g. by ArmA), which impairs aminoglycoside binding, is another resistance mechanisms leading to high-level aminoglycoside resistance [103, 104].

Similar to aminoglycosides, **tetracyclines** (e.g. tetracycline and minocycline) and **glycylcyclines** (tigecycline) interfere with RNA synthesis by targeting the 30S ribosomal subunit. However, in contrast, the transfer RNA binding site is blocked so that the aminoacyl-transfer RNA cannot attach to the mRNA, and thus peptide chain elongation is inhibited. Active efflux mediated through the tetracycline-specific efflux pumps TetA and TetB are the primary cause of resistance to tetracyclines in *A. baumannii* [105, 106]. Furthermore, the ribosomal protection protein Tet(M) protects the ribosome from tetracyclines via a shielding mechanism [107]. Initially designed to not be a substrate of tetracycline-specific efflux pumps [108], the synthetic antimicrobial tigecycline showed promising *in vitro* activity against most *A. baumannii* isolates and was hoped to be affective against MDR isolates [109, 110]. However, it was later revealed that tigecycline is a substrate of polyspecific efflux pumps [111, 112]. Furthermore, mutations in the gene encoding an S-adenosyl-L-methionine-dependent methyltransferase (*trm*) [113] as well as a 1-acyl-sn-glycerol-3-phosphate acyltransferase (*plsC*) [114] have been shown to decrease tigecycline susceptibility in *A. baumannii* strains that were serially passaged in tigecycline.

Targeting the 50S ribosomal subunit and thereby preventing the translocation of the aminoacyl-transfer RNA within the ribosome, **chloramphenicol** and **macrolides** (e.g. azithromycin and erythromycin) induce translational termination. For both antimicrobial classes, specific drug modifying enzymes (the acetyltransferase Cat for chloramphenicol and Mph for macrolides [115, 116]) as well as specific efflux pumps (CmlA in the case of chloramphenicol [37] and Mel2 in macrolides [117]) have been associated with resistance in *A. baumannii*.

Quinolones (e.g. nalidixic acid) inhibit DNA synthesis by targeting the bacterial DNA gyrase (topoisomerase II) and topoisomerase IV which are needed to relieve topological stress and decatenate DNA during DNA replication. By modifying quinolones with the addition of a fluorine at the C6 carbon (generating **fluoroquinolones**, e.g. ciprofloxacin, levofloxacin), the affinity to topoisomerases was increased. However, amino acid substitutions in the chromosomal DNA gyrase (due to mutations in the DNA gyrase encoding genes *gyrA* and *gyrB*) or topoisomerase IV (mutations in encoding genes *parC* and *parE)*, respectively, interfere with target site binding and subsequently lead to resistance in *A. baumannii* [118-120]. In particular ciprofloxacin resistance has most often been associated with two specific mutations, resulting in the Ser83→Leu substitution in GyrA and Ser80→Leu change in ParC.

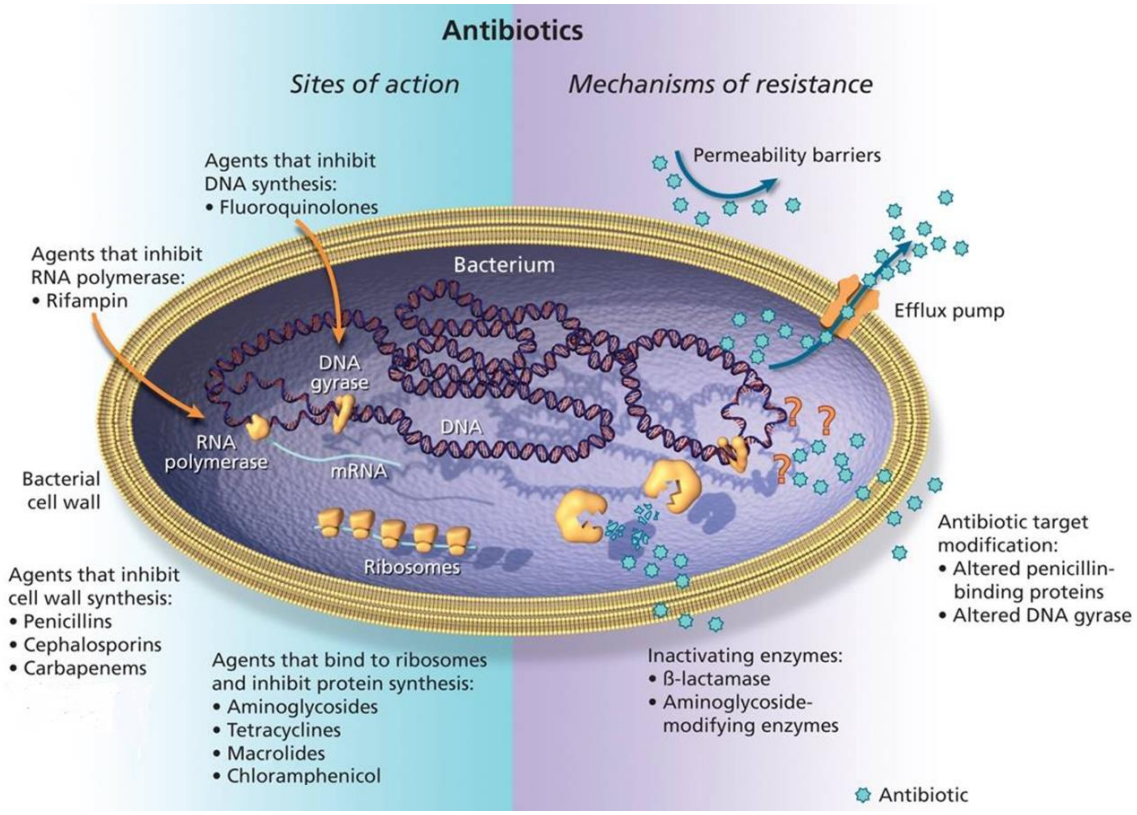

Figure 1.3 Antibiotic modes of action and bacterial strategies to resist. Antibiotics target different cellular processes (e.g. DNA, RNA, protein or cell wall synthesis) leading to bacterial cell death or reduced cell growth. Bacteria however, developed different strategies to combat the antibiotic action, including modification of the antibiotic target, inactivation of the drug, decreased influx and increased efflux of the agents. Adapted from Mulvey *et al.* [121] with permission.

RNA synthesis is inhibited by **rifampicin**. Binding to the active centre of the bacterial RNA polymerase, transcription initiation is inhibited. Resistance to rifampicin is conferred by mutations in *rpoB* encoding the β-subunit of the RNA polymerase. Furthermore, rifampicin

can be inactivated by enzymatic ribosylation mediated by ADP-ribosyltransferases, such as Arr-2 [122].

In Gram-negative bacteria, the cell wall consists of cross-linked peptidoglycan layers which are linked to the outer membrane (containing lipopolysaccharides, phospholipids and channel forming porins) by lipoproteins. Each peptidoglycan layer consists of an alternating order of the sugar derivates N-acetylglucosamine and N-acetylmuramic acid (MurNAc). MurNAc is further linked to peptide side chains (e.g. D-alanine). The crosslinking of peptidoglycan layers during cell wall synthesis is catalysed by transpeptidases, which link the D-alanine peptide side chains strengthening the peptidoglycan layers. Structurally mimicking the naturally occurring D-alanine-D-alanine structure, **β-lactam** antibiotics inhibit the crosslinking of peptidoglycan. The transpeptidases tightly bind to the antibiotic forming long-lived complexes. As a consequence, poorly crosslinked peptidoglycan is produced and the cell wall is unable to resist turgor pressure which subsequently leads to cell lysis. With regards to *A. baumannii* infections, it is **carbapenems** (e.g. meropenem and imipenem), a subclass of β-lactams, that are the drugs of choice. The most clinically significant mechanism to inactivate carbapenems is through the production of carbapenem-hydrolysing β-lactmases. Carbapenemases (e.g. OXA-23, OXA-58, NDM-1, NMD-2, IMP-1, VIM-1), have been reported worldwide in *A. baumannii*, leading to a vast limitation of treatment options for combatting *A. baumannii* infections [123, 124].

Cell death as described for β-lactams is also induced by **polymyxins,** such as colistin, which bind to lipid A of lipopolysaccharides at the bacterial membrane. By binding to the cell membrane, polymyxins alter the membrane structure, leaving it more permeable. Target modification by adding a phosphoethanolamine moiety to lipid A, driven by increased expression of the two-component regulatory genes *pmrAB*, has been identified in colistin-resistant isolates [125].

In bacteria, folate is essential for cell growth and replication as it is used for purine biosynthesis (thus DNA synthesis) and the synthesis of amino acids (glycine, methionine, serine). **Sulphonamides** (e.g. sulfamethoxazole) and **trimethoprim** inhibit the bacterial folate metabolism targeting the enzymes necessary for the generation of the folate intermediate dihydropteroic acid (sulphonamides) or inhibiting the last step in folate synthesis which generates tetrahydrofolic acid (trimethoprim). A bactericidal effect is achieved when both antimicrobials are administered in combination (as co-trimoxazole). In *A. baumannii* the

generation of usually plasmid-encoded isoenzymes (*sul* or *dfr* genes) has been reported, which show reduced affinity to both antimicrobials [124]. Furthermore, efflux has been associated with decreased susceptibility to trimethoprim or co-trimoxazole, respectively [89, 126, 127].

All the above mentioned resistance mechanisms are specific to one antimicrobial class or even single drugs. However, decreased membrane permeability as well as increased drug efflux contributes to multidrug resistance by affecting multiple antimicrobial classes.

Porins, or porin channels are water-filled outer membrane pores that allow the passive diffusion of substances, including antimicrobials, across the outer membrane. Due to the small number and size of these porins in *Acinetobacter*, its outer membrane permeability is less than 5% compared to other Gram-negative bacteria, preventing drug influx and thus promoting resistance [128, 129]. In particular, loss of the outer membrane porins CarO, OprD or the 33-36kDa protein have been associated with carbapenem resistance [130-132].

Increased expression of efflux pumps that actively expel multiple, structurally different classes of antimicrobials out of the cell, has been shown to confer multidrug resistance in *A. baumannii*. Exported antimicrobials include aminoglycosides, β-lactams, carbapenems cephalosporins, chloramphenicol, fluoroquinolones, erythromycin, tetracyclines and tigecycline [112, 126, 133].

1.2 Bacterial efflux pumps

Bacterial efflux pumps are chromosomally or plasmid encoded components of the bacterial membrane that capture and excrete metabolic end products and deleterious substances from within the cell to the extracellular environment [134, 135]. Lowering the intracellular concentration of toxic compounds, the ancient function of efflux pumps is thought to aid bacterial survival in a harmful environment [136]. Bacterial tolerance to structurally diverse compounds like bile salts, detergents, solvents, dyes and antibiotics was reported to be conferred by efflux pumps [134, 137, 138]. In particular, the efflux of antibiotics is allowing bacteria to survive despite high concentrations of antimicrobial agents, leading to a resistance phenotype. Since the first discovery of chromosomally encoded efflux pumps in Gram-negative bacteria in 1993 [139, 140], the ever-increasing identification and characterization of overexpressed transporters that confer multidrug resistance, particularly in the ESKAPE pathogens, underlines the grave threat they cause to health care environments.

Based on their primary structure and energy source, bacterial efflux pumps are classified into five distinct families, including the ATP (adenosine triphosphate)-binding cassette (ABC) superfamily, the multidrug and toxic compound extrusion (MATE) family, the major facilitator superfamily (MFS), the small multidrug resistance (SMR) family and the resistance-nodulation-cell division (RND) family (Fig. 1.4). These individual efflux families are described in the following section, mostly referring to studies performed in *E.coli*, with the main focus on RND-type transporters.

1.2.1 Transporter of the ABC superfamily

Efflux pumps belonging to the ABC superfamily are uniporters which use the binding and hydrolysis of ATP as an energy source to pump out their substrates [141]. Organised as dimers, ABC transporters consist of four domains, two cytoplasmic nucleotide-binding domains (NBD) and two trans-membrane domains (TMDs) embedded in the intracellular membrane (Fig. 1.5) [142]. Each of the two NBDs harbour an ATP binding site and the TMDs, consisting of 12-20 transmembrane segments (TMS), form a transmembrane pore which serves as a path across the intracellular membrane [143].

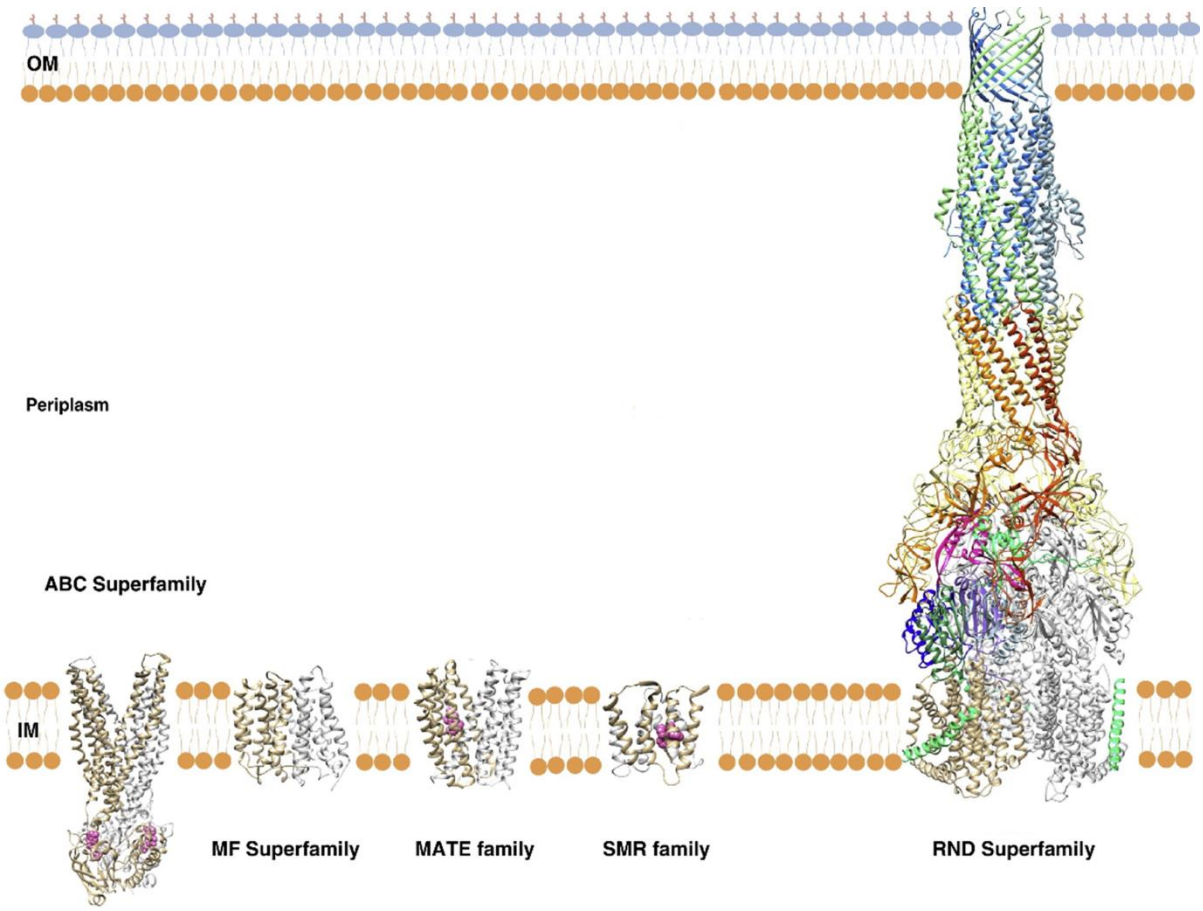

Figure 1.4 Composition of efflux pump families in Gram-negative bacteria. Transporters of the ABC-, MFS-, MATE- and SMR-type transporters are antiporters which span the inner membrane. They extrude ligands from the cytoplasm to the periplasm. The RND-type pumps are tripartite spanning the inner and the outer membrane. As a consequence, substrates are exported from the periplasm to the extracellular environment. OM: outer membrane; IM: inner membrane; modified from Du *et al*. [136].

Substrate extrusion is accomplished by ATP-dependent conformational changes of the transporter [144-146]. Although the chronological order of events has not yet been elucidated, it is proposed that in the absence of bound substrates and ATP, ABC efflux pumps are in an inward-facing 'open' confirmation (Fig. 1.5) [147]. Thereby, the assumed substrate-binding chamber formed by the two TMDs within the membrane is facing the cell interior. Upon direct substrate binding to the TMDs and binding of two ATP molecules within the NBD dimer interface (looking like a 'cassette'), the NBDs dimerize. This conformational change involves the closure of the inward-facing and the opening of the outward-facing confirmation of the TMDs. In this stage the two TMDs diverge into two discrete 'wings' that point away from each other towards the periplasm (in the case of Gram-negative bacteria). ATP hydrolysis, the release of ADP and transport of the substrate, leads to the dissociation of

the NBD dimers and sets the ABC pump back to its initial inward facing configuration ready for the next cycle.

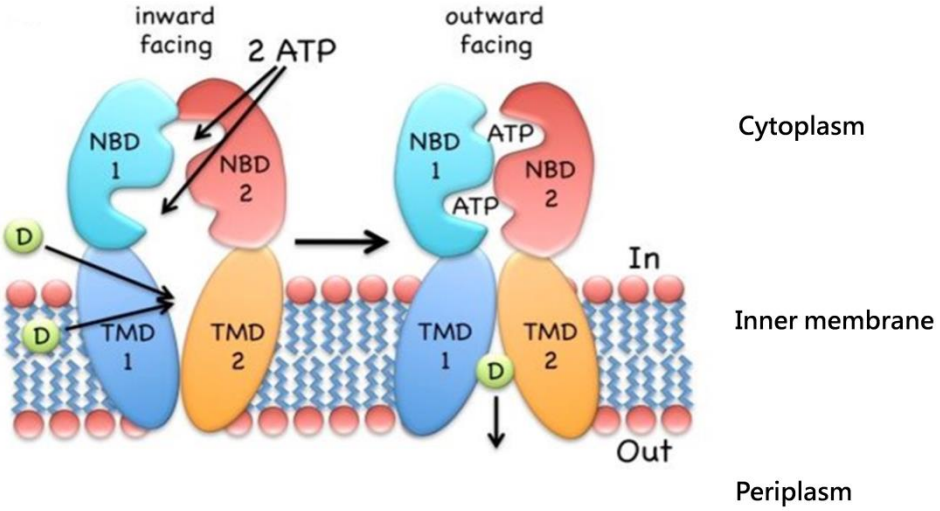

Figure 1.5 Export mechanism of ABC transporters. Being in the inward-facing conformation, ABC pumps bind their substrates "D" (drug) in the cytoplasm or the inner leaflet of the membrane. Following, two molecules of ATP are bound, resulting in a dimerization of the nucleotide binding domains (NBDs) and a conformational change of the transmembrane domains (TMDs) to the outward-facing configuration, results in the export of the substrate to the periplasm. Adapted from Wilkens [147].

In Gram-negative bacteria there are only a small number of examples of this exporter family. The best studied bacterial ABC pump is MacB in *E.coli*, which particularly raises macrolide MIC values when overexpressed [148]. In contrast to typical primary ABC pumps, the MacB dimer interacts with the periplasmic adaptor protein MacA, which is assumed to connect MacB to the outer membrane pore TolC, without a direct connection between the pump and the pore [149, 150]. As the outer membrane pore spans the extracellular membrane, this trimeric complex facilitates the efflux of MacB substrates from the cytoplasm directly to the extracellular space.

1.2.2 Pumps of the MF superfamily

With more than 1000 identified members to date, the MFS superfamily comprises the largest protein transporter group [151]. Usually composed of 400-600 amino acid residues, MFS pumps are antiporters using the electrochemical gradient across the inner membrane as an energy source for the export of substrates from the cytosol to the periplasm [151, 152]. MFS transporters generally function as monomers and comprise two domains, each of which is composed of six to seven distorted α-helices making a total of 12-14 TMS spanning

the inner membrane (Fig. 1.4). Thereby, both helical bundles are connected by a long, flexible central loop and the N- as well as the C-terminus are located in the cytoplasm. Four membrane helices face away from the interior, whereas the remaining helices form an internal cavity. The composition of this central pore, lying between both the N- and the C-domains, has been reported to determine the substrate specificity of the MFS pump. Whereas a cavity comprised of many hydrophilic residues is associated with the transport of specific substrates (e.g. tetracyclines in the case of TetA pump [153]), MFS pumps with a hydrophobic core, like EmrD in *E. coli*, have been reported to have a broad substrate specificity transporting a multitude of lipophilic compounds, including proton uncouplers, quaternary ammonium compounds and SDS [154, 155]. Cationic dyes, chloramphenicol and fluoroquinolones have also been reported as substrates of MdfA, another MFS efflux pump in *E.coli* [155].

MFS pumps are proposed to transport their substrate via an alternating-access mechanism, involving two major conformations, the inward-facing and the outward facing configuration [152]. Crystal structures have revealed the protonated inward-facing composition of the *E. coli* MFS pumps EmrD and MdfA [154, 156]. Thereby, an inverse V- or heart-shape of the monomer was reported with the internal cavity open to the cytoplasm (Fig. 1.6 A). The substrate binding site within the hydrophobic cavity was found right in the middle of the membrane. Substrates are suggested to reach the binding site via the inner membrane leaflet or the cytoplasm. Upon binding, rotation between the N-and the C-terminal domains around the axis parallel to the membrane lead to an outward-facing form of the monomer (Fig. 1.6 C). In this conformation the internal cavity is open to the periplasm and substrate translocation can occur via an H^+-antiport.

Similar to the MacAB ABC-type exporter, the presence of tripartite MFS pumps was proposed. As an example, the *E. coli* MFS efflux pump EmrB has been reported to form dimers and a complex with the accessor protein EmrA, encoded upstream of EmrB [157]. It was hypothesised that binding to an outer membrane pore would facilitate the substrate transport from the cytoplasmic site directly to the extracellular space.

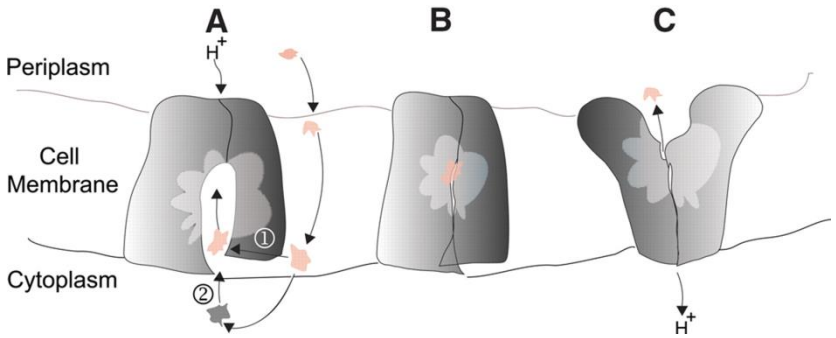

Figure 1.6 Transport mechanism of MFS efflux pumps. A. In its protonated state, MFS transporter show an inward-facing conformation and can bind ligands from the inner leaflet of the bilayer (1) or the cytoplasm (2). B. Binding of the substrates leads to an occluded and further to C. an outward facing conformation. The pump is deprotonated and the ligand is released to the periplasm. Taken from Yin *et al*. [154]. Reprinted with permission from AAAS.

1.2.3 Transporters of the MATE family

In Gram-negative bacteria, efflux transporters of the MATE family have been associated with fluoroquinolone resistance and reduced susceptibility to aminoglycosides [158, 159]. These pumps are antiporters ranging from 400 to 700 amino acid residues, which use the proton or cation gradient (Na^+) across the inner membrane to extrude their substrates from the cytoplasm to the periplasm. Regarding the structure of MATE exporters, two lobes, a C-terminal and an N-terminal lobe, each of which consists of six transmembrane helices, form a cleft within the inner membrane (Fig. 1.4) [160]. In its outward-facing conformation, the Na^+-driven MATE pump NorM of *Vibrio cholerae* was reported to form a V-shape structure, similar to pumps of the MFS family (Fig. 1.6). Thereby, the two lobes which are connected by a cytoplasmic loop, form an internal cavity between them displaying an opening to the extracellular space. Within the internal cavity, which is divided into the larger N-lobe and a C-lobe cavity, a drug binding pocket (N-lobe cavity) as well as the cation-binding site (C-lobe cavity) have been identified. Analysis of the archeal H^+-gradient driven pump PfMATE suggests that the bound substrate is released into the extracellular environment (periplasm in the case of Gram-negative bacteria) upon a protonation-dependent bending of the first transmembrane helix which results in the collapse of the N-lobe [161]. Until today MATE transporters could only be captured in their outward-open configuration. However, proton/cation binding or release has been shown to induce essential rearrangements of the seventh and eighth transmembrane helix which might play a role in the conformational change between the outward-open and the inward-open state [161-163].

1.2.4 Exporters of the SMR family

Proton-motive-force driven SMR efflux transporters comprise the smallest group of exporter proteins. These hydrophobic proteins functioning as homodimers are only 100 -120 amino acid residues in length and composed of four TMS (Fig. 1.4) [136]. Considering the orientation of the dimer, contradictory results were published. Whereas X-ray crystallography of the *E. coli* SMR transporter EmrE showed an antiparallel arrangement of the two protomers, being embedded in opposite directions within the membrane [164], a parallel composition was achieved by chemical crosslinking [165]. However, the first three TMS of each monomer together form the substrate binding cavity whereas TMS4, which is almost perpendicular to the membrane, is responsible for dimer formation [164]. Similar to the other primary efflux pumps, it is suggested that substrates are moved across the membrane via the alternating access model [166]. Nuclear magnetic resonance studies of EmrE enabled the observation of the conformational change of the two protomers upon substrate binding [167]. Thereby, the configuration of the protomers is identical in the inward- and the outward-facing state, merely their orientation in the membrane is opposite. However, in contrast to the MATE and MFS superfamilies, two protons are exchanged for one substrate molecule. Furthermore, the substrate and the protons are competing for the same binding site (conserved Glu14 residue within TMS1) [168]. Upon substrate encounter, the protonated glutamate residue becomes deprotonated and binds the substrate instead.

Antibiotic classes translocated by SMR pumps in Gram-negative bacteria include aminoglycosides in *P. aeruginosa* [169] and colistin, erythromycin, rifampicin and tetracycline in *Klebsiella pneumoniae* [170].

1.2.5 Efflux pumps of the RND family

Among the efflux pump classes, members of the RND family exhibit the widest range of substrates including commonly used antibiotics, as well as antiseptics, detergents, bile salts, disinfectants and dyes, and thus show the highest clinical significance in Gram-negative bacteria [134, 137, 138]. No homologues of efflux pumps belonging to this family exist in mammals [171]. With the typical **tripartite composition** of these pumps, spanning the inner as well as the outer membrane, compounds are exported directly to the extracellular environment and the intracellular concentrations of compounds toxic for the bacterial cell is lowered efficiently. The best-characterized member of this family is the AcrAB-TolC system

in *E. coli* which in the following section will serve as the paradigm RND-type efflux pump. AcrAB-TolC is composed of three components – the transporter AcrB, an outer membrane pore TolC and a periplasmic adaptor protein, also called membrane fusion protein (MFP), AcrA [172]. It is suggested that the AcrAB-TolC system form a 3AcrA: 3AcrB: 3TolC complex (Fig. 1.7) [173].

The **transporter** AcrB is composed of a transmembrane and a periplasmic domain [174, 175]. The TMD spans the entire width of the inner membrane whereby each monomer of the AcrB trimer is arranged in a 12-stranded β-barrel. The transporter protrudes from the inner membrane into the periplasm by α-helical bundles forming an internal cavity.

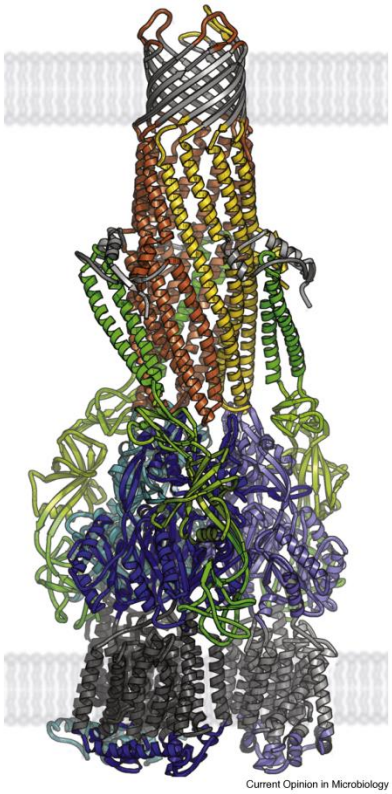

Figure 1.7 Tripartite assembly of the *E. coli* RND-type efflux pump AcrAB-TolC. AcrA is shown in green, AcrB subunits are depicted in blue and TolC barrels are coloured in yellow/orange. Membrane bound domains are grey. Reprinted from Blair *et al.* [176] with permission from Elsevier.

The wide substrate range exhibited by RND-type pumps can be attributed to multiple binding sites within the transporter protein. Computer simulations and co-crystallization experiments have revealed **three binding pockets** within the periplasmic domain of AcrB, suggesting that RND-type efflux pumps bind their substrates from the periplasm and extrude them through the outer membrane pore [175, 177, 178]. It should be noted that AcrD, another RND-type efflux pump in *E. coli*, is able to transport aminoglycosides even from the

cytoplasm [179]. The **proximal binding pocket** lies at the surface of the periplasmic domain at the entrance of the internal cavity, whereas the **distal binding pocket** is situated deeper within the cavity (Fig. 1.9 A, B). Both binding pockets are connected by a flexible loop (Fig. 1.9 C) [178]. Interactions with transported ligands are favoured by aromatic, charged and polar amino acid residues that are enriched within the binding pockets. Low-molecular-weight drugs, such as minocycline, are predicted to directly bind to the deep distal binding pocket, without interacting with the proximal binding pocket [180]. In contrast, high-molecular-weight substrates (e.g. chloramphenicol and ethidium) are believed to first bind to the proximal binding pocket and in the transport process they are forced to the distal pocket [181, 182]. The distal binding pocket is further divided into two different binding portions, a **wider 'cave' portion** and a **narrower 'groove' portion** (Fig. 1.8) [183]. Antimicrobial agents like minocycline, levofloxacin, erythromycin, rifampicin and tetracycline are predicted to bind to the upper 'groove' portion. Chloramphenicol, however, seems to bind to the lower 'cave' portion and ciprofloxacin seems to bind to both portions. Co-crystallization of ampicillin with AcrB revealed another binding site within the central cavity [184-186]. As for high-molecular-weight ligands, it is predicted that after initial binding at this potential third binding site, drugs eventually translocate to the distal binding pocket. However, the functional significance of this third binding site has not been determined yet.

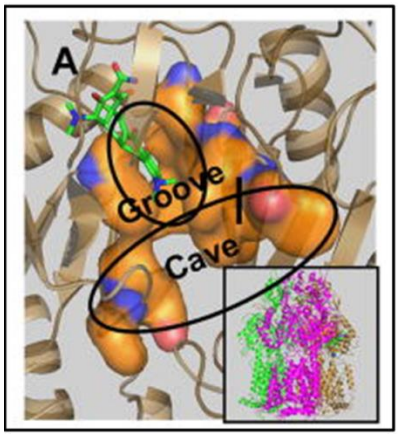

Figure 1.8 Distal binding pocket within AcrB. The distal binding pocket (orange) is divided into two portions the wider cave binding portion and the narrow groove binding portion. Minocycline (green) is bound to the groove portion. AcrB protomer assembly is shown in the right corner. Taken from Nikaido *et al*. [187] by permission of Oxford University Press.

The discoveries and investigations on efflux pump inhibitors gave further insights into the architecture of the distal binding pocket. The first two compounds discovered with inhibitory effects on broad substrate efflux pumps in Gram-negative bacteria are phenylalanine arginyl

β-naphtylamide (PAβN) and 1-(1-naphtylmethyl)-piperazine (NMP) [188, 189]. Investigations in *E. coli* have shown that PaβN and NMP act as RND substrates binding to the 'groove' portion of the distal binding pocket in AcrB [135, 190]. As it was impossible for minocycline to bind to any subsite of the pocket, it is suggested that binding of efflux pump inhibitors distorts the binding pocket, thereby inhibiting substrate binding.

Regarding the transport mechanism, a '**three step functional rotation'** model has been proposed (Fig. 1.9) [175, 191]. Thereby, AcrB is believed to show an asymmetrical configuration with each protomer sequentially rotating between three conformations. In the **loose conformation**, substrates are allowed to access the pump as the cavity within the protomer is opened to the periplasm. This cavity is connected to the binding pockets by a channel. In the **tight configuration,** the binding pocket expands to accommodate the substrates. In this way, drugs enter the cavity from the periplasm and move along the channel to bind to the different sites in the distal binding pocket. At this stage the exit tunnel from the binding site is blocked. Upon protonation, the **extrusion configuration** is triggered [192, 193]. The proton is thought to enter from the periplasm, binding to specific Asp residues in the TMD of AcrB, promoting the conformational change [193]. As a consequence, the periplasmic opening to the tunnel is closed, whereas the exit tunnel is opened. Furthermore, shrinking of the binding pocket leads to the extrusion of the substrate.

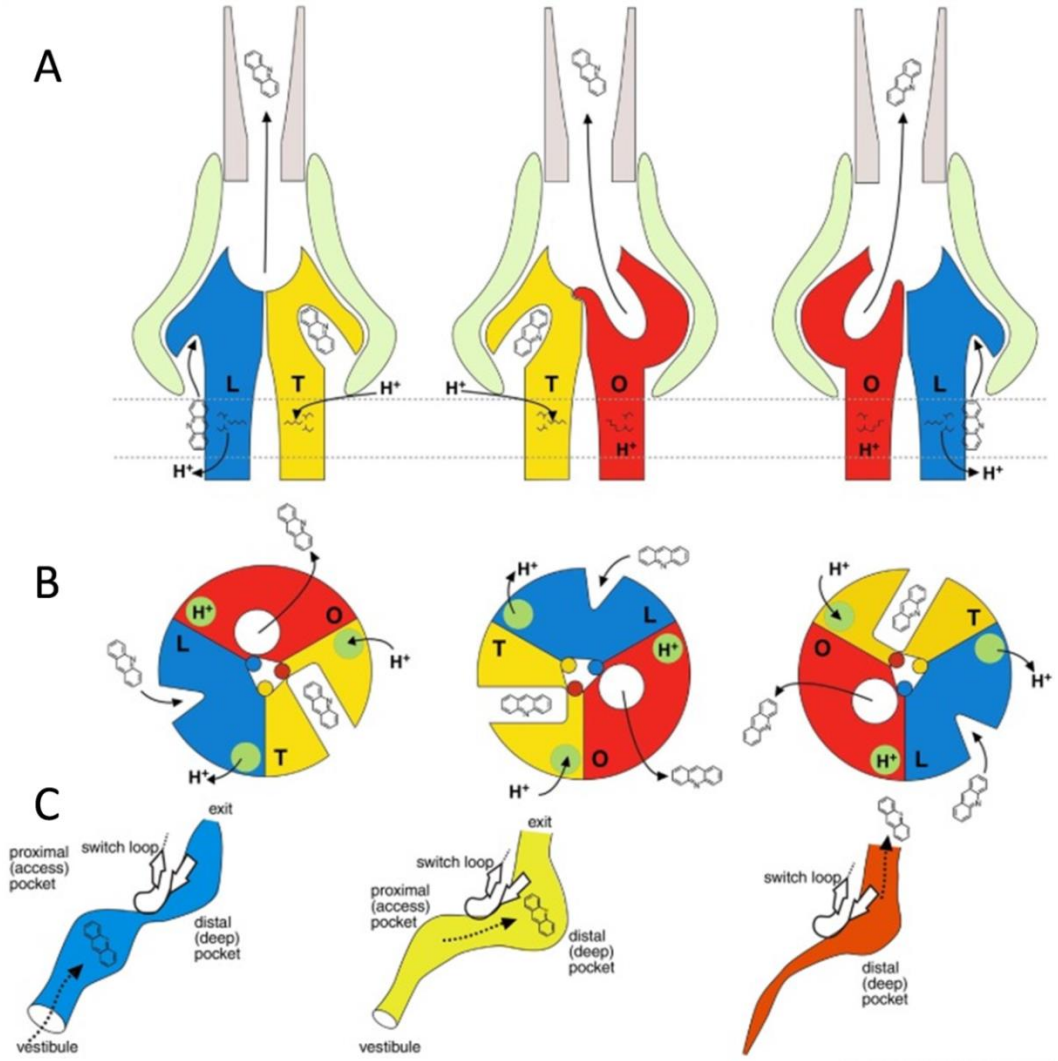

Figure 1.9 Three step functional rotation mechanism of AcrB shown (A) in a cross section (two protomers each of AcrB (blue, yellow, or red), AcrA (green), TolC (grey) , (B) from the aerial perspective and (C) illustrating the paths of the drug along the vestibule/cavity (C). Upon drug binding and proton coupling, AcrB undergoes different conformational changes, access/loose (L; blue), binding/tight (T; yellow), extrusion/open (O; red), in order to export the encountered substrate. Adapted from Du *et al*. [136].

The **MFP AcrA** consists of a long α-hairpin domain and the N-and C-terminal ends together form a compact β-roll domain (Fig. 1.7) [194]. In between, a central lipoyl domain ensures flexibility of the two domains facilitating the assembly of the MFP to the other efflux pump components. AcrA is predicted to preassemble with AcrB via its N- and C- terminal ends close to the inner membrane [173]. Complete assembly of the tripartite RND complex is achieved by AcrA recruiting the outer membrane pore TolC via its α-hairpin domain.

Each **TolC** monomer is characterized by three structurally distinct domains: the 12-stranded β-barrel lies within the outer membrane to form an open pore; the α-helical barrel is protruding from the outer membrane to the periplasm and a mixed α/β- folding is situated

in the periplasm (Fig. 1.7) [195]. Altogether these three domains form an exit tube for substrates. Before its assembly, the TolC tunnel is closed. Once recruited to the complex, conformational changes in AcrA are thought to trigger a shift in TolC so that the tip of the periplasmic end of the channel shifts from the closed to the open state [173]. Due to this transition it is likely that substrates pass through the TolC channel and ultimately are expelled to the extracellular environment. Until today, it has not yet been fully established whether only AcrA is assembled with the outer membrane pore, or if interactions between the top of the periplasmic domain of AcrB and the α-barrel domain of TolC are favoured [172, 196].

Regarding the gene composition of RND-type efflux systems, in *E. coli* the genes encoding AcrAB form an operon, whereas TolC is encoded elsewhere [197]. In other species like *P. aeruginosa*, a three gene operon with a specific outer membrane pore has been described for AcrAB-TolC homologs (e.g. MexAB-OprK) [140].

1.2.6 Physiological function of efflux pumps

Efficiently expelling a large number of noxious agents including antimicrobials, detergents, disinfectants, dyes, and antiseptics [198-200], the ancient function of efflux pumps has been attributed to aid the **survival** in competitive and hazardous environments [136]. In addition to the mentioned agents, host derived substrates like bile salts, fatty acids and steroid hormones have also been shown to be exported by efflux pumps, generally allowing adaption and survival within the host. In fact, among all substrates, *E. coli* AcrAB has been shown to exhibit the highest affinity for bile salts [201], which are abundant in the intestine of vertebrates – the natural habitat of *E. coli*.

Investigations in *E.coli* suggest that efflux transporters, in particular AcrAB, are the **first line of defence** when bacteria are exposed to antibiotics. Serially challenging *E. coli* cells with increasing concentrations of tetracycline led to an increased expression of genes relevant for either regulating, or directly coding for components of AcrAB [202, 203]. Resistance to β-lactams and quinolones increased concomitantly with tetracycline resistance. However, when the highest concentration of tetracycline was maintained, this increased expression of *acrB* declined in later cultures and instead cells developed mutations in genes usually targeted by antibiotics such as DNA gyrase or the 30S subunit of the ribosome [202]. These results suggest that polyspecific efflux systems are used as an initial strategy to combat

antibiotic exposure, but if bacteria are facing consistent concentrations of antibiotics, accumulated mutations in key antibiotic targets constitute the better survival strategy.

In order to efficiently confer **antimicrobial resistance**, a synergistic interplay between drug influx and efflux is crucial [204, 205]. The influx of toxic compounds is controlled by the outer membrane permeability. In *E. coli* an effective permeability barrier is achieved by the regulation of porin expression – their expression is decreased when the influx of toxic compounds threatens cell survival and increased when a high concentration of nutrients is required [206]. As described in Chapter 1.1.5, *P. aeruginosa* and *A. baumannii* have a smaller number and size of porins, as compared to *E. coli*, leading to a very slow drug influx. This reduced uptake allows efflux pumps to successfully reduce the intracellular concentration of drugs to sub-inhibitory concentrations by extruding them out of the cell. In *E. coli* for example, a simultaneous reduction in porin synthesis and upregulation of efflux pumps was detected in the process of adapting to tetracycline exposure [207].
Furthermore, the interplay between different efflux pump classes further enhances antimicrobial resistance [208, 209]. Thereby, toxic compounds are transported to the periplasm by primary pumps of the MATE, SMR, ABC or MFS family, residing in the inner membrane and pumping substrates from the cytoplasm. From there, ligands are expelled to the extracellular environment by RND systems. Once the intracellular concentration of toxic molecules exceeds the capacity of the transporters, overexpression of pumps is induced, leading to a resistant phenotype [204]. Crossing the inner and the outer membrane, mainly RND-type efflux systems contribute significantly to antibiotic resistance. In the last decades, an increasing number of enterobacterial species, isolated from patients undergoing antibiotic treatment, have been found to have their MDR phenotype associated with increased expression of either AcrAB or AcrAB-like transporters [138, 210]. Thus, under antibiotic pressure, extrusion of antimicrobials by RND transporters seems to be a very efficient bacterial survival strategy.

The exporters' capacity to extrude substrate also comes into play during **cellular stress** responses. Levels of AcrAB in *E. coli* have been found to be elevated during stress responses induced by exposure to high salt, ethanol or bile salt concentrations [211]. Regarding oxidative stress, promoted by high levels of H_2O_2, the ABC efflux pump MacAB of *Salmonella* was reported to be essential for cell survival [212]. Similarly in *Stenotrophomonas maltophilia*, SmeIJK contributes to oxidative stress resistance [213]. On the other hand,

reduced *acrB* expression in *K. pneumonia* correlated with reduced tolerance to bile salt, oxidative, and hyperosmotic stress [214].

Various investigations suggest a correlation between efflux pump expression and **biofilm formation**. Inhibiting or deleting any of 9 efflux pumps that confer multidrug resistance in *Salmonella typhimurium* led to impaired biofilm formation [215]. However, this effect has not been observed in all species. In *P. aeruginosa*, deletion of RND pumps had no effect on the cells ability to form biofilms [216]. Moreover, considering an interplay between biofilms and efflux pumps, the investigation of gene expression during biofilm growth in *E. coli* revealed the upregulation of 20 transporter genes [217].

A direct effect of efflux pumps on bacterial **pathogenicity and virulence** has been shown upon transporter inactivation. AcrB or *tolC* deficient *S. typhimurium*, for example, poorly colonized the avian gut and did not persist [218]. A reduced infection rate of mice was determined for *K. pneumoniae* strains lacking the *acrAB* genes [219]. Furthermore, by individually deleting 3 of the 4 best-studied efflux transporters in *P. aeruginosa* (MexAB-OprM, MexEF-OprM, MexXY-OprM), its ability to invade epithelial cells declined significantly [220]. At the same time, an epidemic *P. aeruginosa* strain overexpressing MexAB-OprD displayed enhanced killing of fruit flies compared to a laboratory reference strain [221].

The advantages that accompany the overexpression of efflux pumps allow bacteria to survive in hazardous environments. However, there are also disadvantages for the cell. Given the polyspecificity of these transporters, metabolites required for cell growth and division have also been reported to be substrates [222-224]. In addition, pump synthesis and functioning is an energy-driven process [183]. Investigations have shown that the unregulated overexpression of efflux pumps not only led to increased overall resistance but also to decreased cell growth [127, 225]. Therefore, transporters are usually tightly regulated. Nevertheless, upon exposure to toxic substrates, their expression has to be rapidly induced.

1.2.7 Efflux pump regulation

The transcription of efflux systems is strictly regulated by a combination of local regulators, global response regulators or two-component regulatory systems, through either repression or activation. Mutations in the genes encoding regulators are often accompanied by overexpression of efflux pumps, and are thus often associated with an MDR phenotype.

Local regulators are usually encoded adjacent to the structural components of the efflux pump (Fig. 1.10) and most of them are members of the MarR, MerR or TetR family, acting as transcriptional repressors [226-228]. MDR clinical isolates often harbour mutations in these local regulators supporting the fact that these regulators usually undermine the overexpression of efflux transporters. Under normal conditions, the local repressor binds to the promoter of an efflux pump operon and inhibits transcription (Fig. 1.10). However, specific effector molecules (e.g. antibiotics [229], bile salts [230], ethidium bromide [231], rhodamine 6G [232]) can bind to the repressor. The resulting conformational change in the regulator protein blocks its DNA binding, or releases the repressor from the bound promoter, so that the exporter gene is transcribed. This negative regulation of efflux pump expression is an advantage to the cell as no additional time and energy has to be spent in order to generate a transcriptional activator needed for a positive regulation. Thus, bacterial cells can respond more rapidly to environmental changes.

In addition to, or instead of local regulators, efflux pump expression can be positively controlled by **global regulators**. The three global regulators MarA, Rob and SoxS, for example, regulate AcrAB and TolC of *E. coli* in addition to at least another 40 genes [233]. Although all three belong to the XylS/AraC regulator family and bind to the same DNA sequence in the promoter of *acrAB*, the so called marbox (Fig. 1.10), the activation of AcrAB by each regulator proceeds in response to different environmental conditions or stimuli. In the case of **MarA**, salicylate was reported to be a driving effector for *acrAB* gene transcription [234]. The *marA* gene is encoded within the *marRAB* operon, with *marR* and *marB* encoding local repressors of the operon [235]. Salicylate can bind to the MarR repressor, inducing a conformational change and thereby inhibiting its binding to the *marRAB* promoter. Mutations in the *marR* gene can have a similar effect. As a consequence, MarA is expressed and activates *acrAB* transcription.

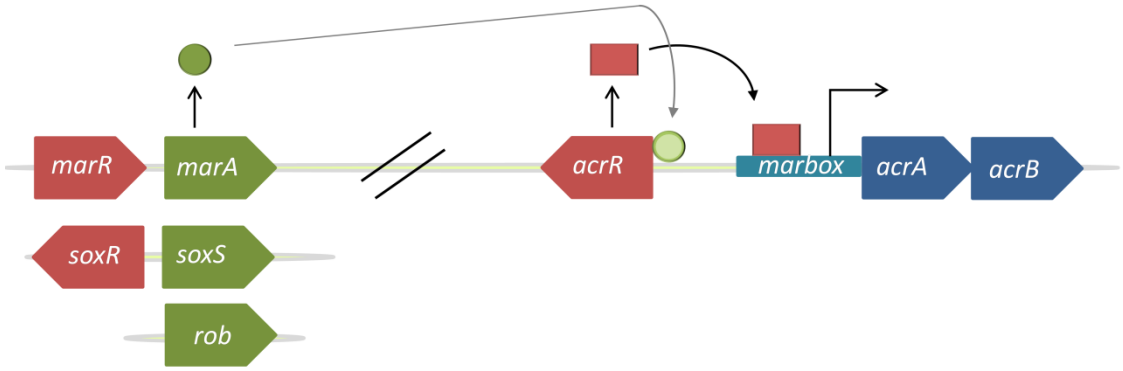

Figure 1.10 Regulation of *acrAB* gene expression. In *E. coli* the expression of the RND pump encoding genes *acrAB* are regulated by the global regulators MarA, SoxS and Rob, and the local repressor AcrR. Adapted from Blair *et al.* [236] with permission.

The **Rob regulator** is assumed to induce efflux pump expression once it undergoes a conformational change. Bile salts for example can bind Rob at its non-binding DNA domain [237]. The resulting conformational change allows the Rob regulator to bind to the marbox. Upon oxidative stress however, *acrAB* gene transcription dependents on the global regulators **SoxRS** [238]. In this case, reactive oxygen species oxidise SoxR, which in turn oxidises SoxS. Being in its oxidised active form, SoxS binds to the promoter of *acrAB* and promotes its expression. Under oxidative stress, the AcrAB pump of *Salmonella* has been shown to be regulated in the same manner [239].

The **two-component regulatory system** is widely distributed among prokaryotes, and senses and responds to various environmental signals and stimuli [240]. It is composed of two components, a sensor histidine kinase, and a cognate cytoplasmic response regulator, which each are composed of two domains. Environmental stimuli (e.g. changes in osmolarity, nutrients, presence of antibiotics) are sensed at the periplasmic sensor domain of the senor kinase leading to the autophosphorylation of the cytoplasmic kinase domain at a conserved histidine residue (H149; Fig. 1.11). This autophosphorylation is catalysed by the ATPase which is part of the cytoplasmic domain of the sensor kinase. Following, the kinase catalyses the transfer of its phosphoryl-group to the receiver domain of the response regulator via a conserved aspartate residue, rendering the regulator in its activated form. Upon activation, the regulator is now able to bind to the promoter region of the efflux pump genes with its effector domain to induce expression. Phosphorylation of the sensor kinase and the transfer of the phosphoryl-group can be reversed by its phosphatase activity; by switching between phosphorylation and dephosphorylation activities, the expression of downstream genes can further be controlled.

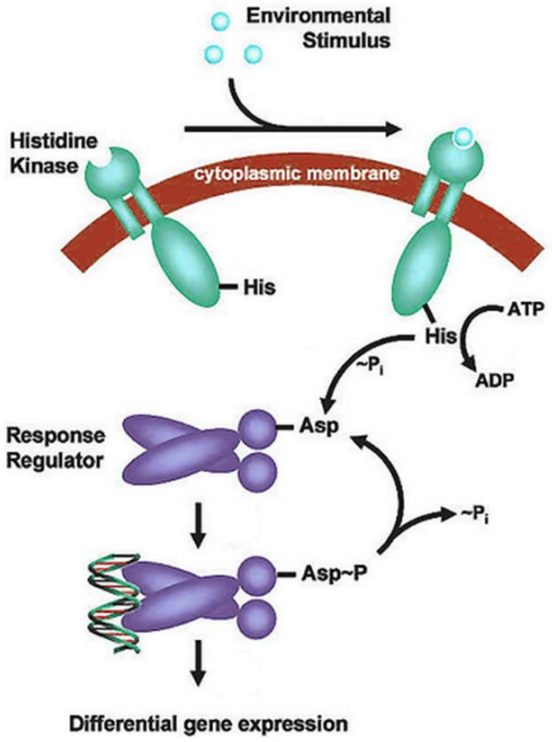

Figure 1.11 Signal transduction pathway of the two-component regulatory system. Upon environmental changes the sensor kinase gets autophosphorylated. The phosphoryl-transfer to the response regulator is bringing it to its active form, inducing differential gene expression. Taken from Cann [241].

As an example, sensing an acidic environment, the PhoPQ two-component system of *Salmonella* activates the expression of the ABC-type efflux pump MacAB [242], whereas the BaeSR system responds to transition metals (copper or zinc) by inducing MdtABC and AcrD expression [243].

1.3. Efflux pumps in Acinetobacter spp.

To date, efflux pumps have been reported in isolates of *A. baumannii*, *A. baylyi*, *A. nosocomialis*, *A. pittii*, *A. radioresistens, A. oleivorans* and the *A.* genomic species 17. But it is in *A. baumannii* that their overexpression has been associated with an MDR phenotype.

1.3.1 The RND-type efflux pump AdeABC in A. baumannii

The RND-type system AdeABC (*Acinetobacter* drug efflux) was the first efflux pump that was characterized in *A. baumannii* [126]. The genes encoding the pump are contiguous and directly orientated with overlapping stop and start codons for AdeAB, which is indicative of an operon (Fig. 1.12). The *adeABC* operon encodes the MFP AdeA, the transporter AdeB, and the outer membrane pore AdeC.

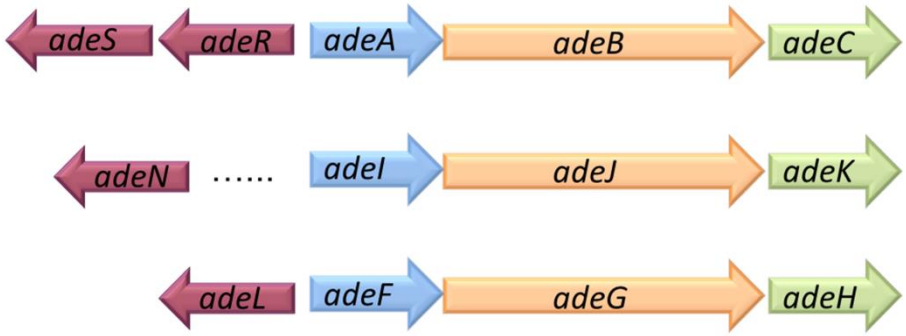

Figure 1.12 Gene composition of the three characterized RND-type efflux pumps in *A. baumannii*. Genes encoding the RND efflux systems display an operon formation. Whereas the two-component system AdeRS and the LysR regulator AdeL are encoded directly upstream of the pump they control, AdeN is encoded >800 kbp upstream of *adeIJK*.

Insertional inactivation of AdeB in an *adeB*-overexpressing MDR clinical *A. baumannii* isolate revealed that this RND system conferred antimicrobial resistance to aminoglycosides and low-level resistance to chloramphenicol, fluoroquinolones, erythromycin, tetracycline, and trimethoprim (Table 1.2) [126]. Later studies correlated *adeB* overexpression with decreased susceptibility to netilmicin, certain β-lactams (cefepime, cefpirome, cefotaxime) and tigecycline [244-246]. The impact on carbapenem susceptibility is still under debate; studies showing no efflux involvement in carbapenem susceptibility [247, 248] as well as observations attributing a 2-8-fold increase in the resistance to carbapenems to efflux have been published [89, 249, 250]. Expressing AdeABC in a heterologous *E. coli* strain, the efflux properties of the *A. baumannii* efflux system was compared to that of the *E. coli* pump AcrAB-TolC [251]. On the one hand, β-lactams could be identified as substrates of AdeABC,

which was impossible to detect in *A. baumannii* due to the expression of endogenous β-lactamases. On the other hand, Sugawara *et al.* found out that the transport of cefepime, ciprofloxacin and tetracyclines is more efficient by AdeABC but weaker to benzylpenicillin, oxacillin, nitrocefin, ethidium bromide and novobiocin, compared to AcrAB-TolC.

Analysing an internal 850-bp fragment of *adeB* amongst 50 *A. baumannii* isolates belonging to IC1–3, 11 *adeB* sequence types were detected, varying in 2 to 45 bases [252]. This sequence variability in *adeB* correlated well with genotypic clustering of these isolates performed beforehand. Thus, it was speculated whether *adeB* typing might be used as a method for rapid identification of distinct lineages in *A. baumannii*.

Regarding the prevalence of the *adeB* gene in *A. baumannii*, controversial data have been published, ranging from 70% to 96% [105, 244, 253, 254]. These differences are mainly due to different study designs. Whereas in some studies species identification was not always performed using reference methods and/or the isolates investigated came from one particular hospital [253, 254], advanced studies included isolates from different European countries, that were divided into IC1, IC2, and genotypically unique isolates [105, 244]. Apart from the distinct study designs, in each study only one primer pair was used to detect the *adeB* gene. Owing to the high variability of the *adeB* sequence [252], false-negative results are likely to occur by this approach. Additionally, in the study of Nemec *et al.*, *adeC* was detected in only 41% of the clinical isolates, in which *adeAB* was present [244]. These data suggest that AdeAB could recruit another outer membrane pore to form a functional tripartite system, as it has been reported before for other bacterial genera [255, 256].

The AdeABC efflux system is regulated by the two-component regulatory system AdeRS, with AdeS being the sensor kinase and AdeR being the response regulator [257]. Both genes are located directly upstream of the *adeABC* operon and transcribed in the opposite direction (Fig. 1.12). AdeRS are suggested to be transcriptional activators of AdeABC, as their inactivation led to increased susceptibility [257]. However, to date no signal directly inducing *adeABC* expression via AdeRS has been described. Using the *A. baumannii* reference strain ATCC 19606, Bazyleu *at al.* reported downregulation of *adeB*, when *A. baumannii* cells were exposed to lower-than-normal incubation temperatures (30°C instead of 37°C), high osmolarity obtained by adding 0.3 M sucrose, or when 4 mM salicylate was supplemented to the growth medium [258]. There was no correlation between the decreased levels of *adeB* and *adeR* expression suggesting that the number of *adeR* transcripts is not crucial for *adeB*

regulation. Using the same reference strain, Fernando *et al*. reported a growth-phase dependent expression of *adeB*, with *adeB* being less expressed at high cell density [259]. Furthermore, *adeA* has been shown to be overexpressed upon NaCl exposure [260].

Different substitutions in the positive regulators AdeRS have been associated with antimicrobial resistant phenotypes in *A. baumannii* clinical isolates mediated by increased expression of the AdeB transporter (Fig. 1.13). For example in AdeS, alterations within functional conserved domains like the periplasmic sensor domain (Gly30→Asp) [261], the HAMP region (histidine kinase, adenylyl cyclase, methyl-accepting chemotaxis protein and phosphatase; Ala94→Val, Gly103→Asp, Asn125→Lys) [91, 246] and the HAMP linker region (Met62→Ile) [246] as well as amino acid changes near to its autophosphorylation site (Thr153→Met) [257] have been described and allied with increased levels of *adeB* transcripts and antimicrobial resistance (Fig. 1.13). Further substitutions in the catalytic core of AdeS (Arg152→Lys, His189→Tyr) and the ATPase domain (Ile252→Ser, Gly336→Ser) catalysing the autophosphorylation were described by Yoon *et al*. [262]. Substitutions in AdeR associated with AdeABC overexpression have been described in the signal receiver domain (Asp20→Asn, Pro56→Ser, Ala91→Val) [89, 246, 262], the α5 helix of the receiver domain (Pro116→Leu) [257] as well as in the effector domain (Leu192→Arg, Glu219→Ala) [262] (Fig. 1.13). Furthermore, a truncated AdeS generated by the insertion of the IS element IS*Aba*1 led to increased expression of *adeB* [99, 111]. In the latter study, Sun *et al.* were the first to describe a molecular mechanism behind the antimicrobial resistance phenotype by introducing several recombinant *adeRS* constructs into an *adeRS*-deficient *A. baumannii* strain. In contrast, with the insertion of IS*Aba*1 in *adeR*, no expression of *adeAB* could be detected [263].

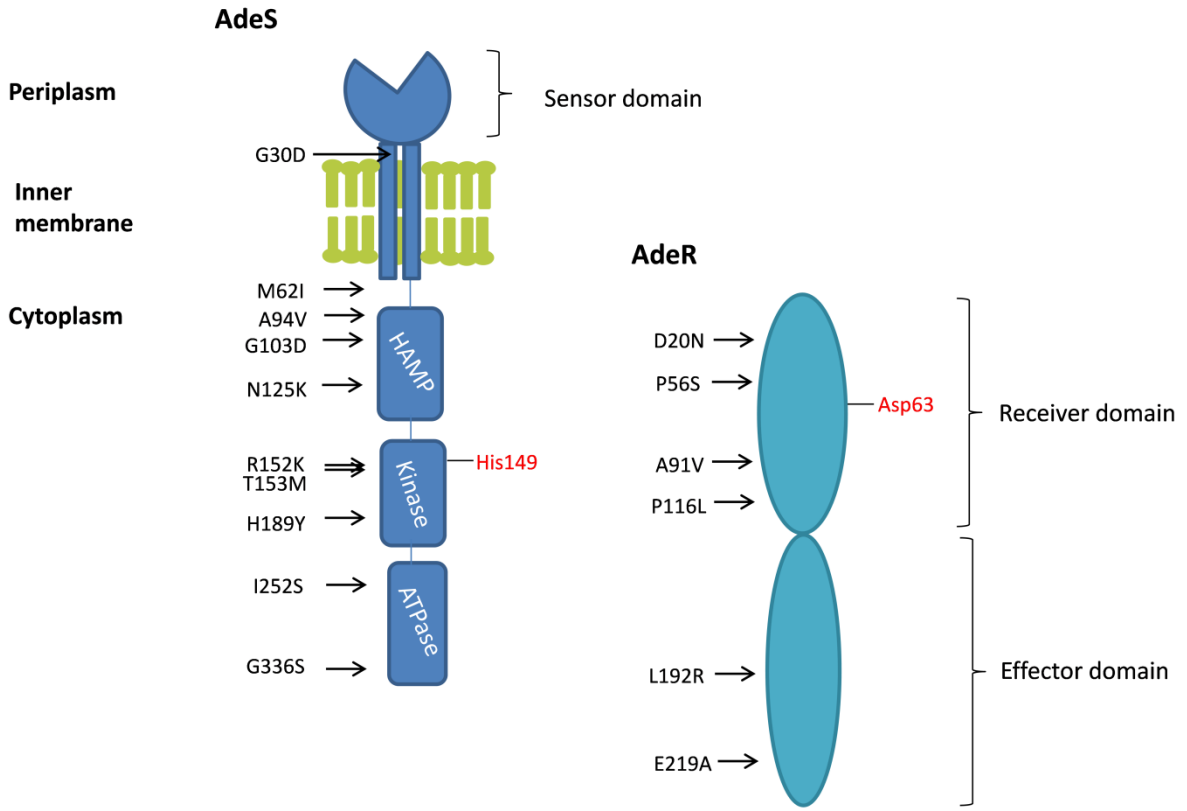

Figure 1.13 Substitutions within the different AdeS and AdeR domains associated with increased *adeB* expression. The HAMP domain of AdeS transduces the signal sensed by the periplasmic sensor domain. ATP is bound in the ATPase domain which catalyses the autophosphorylation of the kinase domain. The signal is further transduced to the receiver domain of the response regulator AdeR by the kinase domain, transferring the phosphate-group from His149 of AdeS to Asp63 of AdeR. Subsequently, the effector domain of AdeR is activated and binds to its regulon. HAMP; histidine kinase, adenylyl cyclase, methyl-accepting chemotaxis protein and phosphatase domain.

Nevertheless, *adeB* overexpressing *A. baumannii* have also been described without any mutations in the *adeRS* regulatory genes compared to the isogenic parents [246, 264]. Lin *et al.* proposed BaeSR to be another two-component system regulating *adeABC* expression [265], but direct binding of BaeR to the *adeA* promoter could not be demonstrated [266]. Recently, Yoon *at al.* reported several short nucleotide polymorphisms within *adeRS* characteristic for *A. baumannii* strains belonging to IC1 and IC2 [262]. Interestingly, in this context the mutation leading to the Ala94→Val substitution in the HAMP linker domain of AdeS was reported to be a polymorphism of isolates belonging to IC1, and thus was erroneously reported as responsible for increased *adeABC* expression. Therefore, it is necessary not to rely on associations, but to further investigate substitutions within the regulatory genes and their possible effect on *adeB* expression and antimicrobial susceptibility.

1.3.2 Other RND-type efflux pumps in A. baumannii

The *adeIJK* operon encodes the second RND-type efflux pump in *A. baumannii* (Fig. 1.12) [127]. Pumping out β-lactams, carbapenems, cephalosporins, chloramphenicol, co-trimoxazole, erythromycin fluoroquinolones, fusidic acid, novobiocin, rifampicin, tetracyclines, tigecycline as well as acridine, pyronine, safranin and SDS this system in part showed an overlapping substrate profile compared to AdeABC (Table 1.2) [127, 251]. Thus, it is not surprising that a synergistic effect of both pumps has been investigated on the extrusion of fluoroquinolones, tetracyclines and tigecycline [267]. In the initial report characterizing AdeIJK, it was indicated that this efflux system does not have a major effect on antimicrobial resistance, as its overexpression was toxic for the host cell [127]. Furthermore, *adeIJK* transcription levels in isolates overexpressing the pump have been reported to be lower than the level of overexpressed *adeABC* [261]. Nevertheless, using tetracycline gradients, spontaneous low-level resistance mutants overexpressing *adeIJK* were obtained, suggesting that AdeIJK can be overexpressed up to a certain threshold [261]. Expression above this threshold seems toxic to the cell.
AdeIJK is negatively regulated by AdeN (Fig. 1.12) [133]. This TetR transcriptional repressor found 813 kbp upstream of the *adeIJK* operon, is constitutively expressed and does not regulate its own expression. In addition to *A. baumannii*, AdeN homologues could also be detected *in A. calcoaceticus, A. nosocomialis* and *A. pittii* [133].

In 2010, a third RND-efflux pump encoding operon, *AdeFGH*, was described (Fig. 1.12) [112]. Selecting an AdeABC- and AdeIJK-defective *A. baumannii* mutant in the presence of chloramphenicol and norfloxacin, Coyne *et al.* generated an *adeFGH* overexpressing mutant. This strain exhibited high-level resistance to chloramphenicol, fluoroquinolones and trimethoprim as well as decreased susceptibility to tetracyclines, tigecycline and co-trimoxazole. The susceptibility to SDS and dyes like acridine orange, ethidium bromide and safranin O was also affected (Table 1.2). Structural components of the efflux system were detected in 40 of 44 clinical *A. baumannii* isolates. Unlike AdeIJK, AdeFGH is not thought to contribute to intrinsic resistance, as it is not constitutively expressed. As mutations in the LysR transcriptional regulator AdeL were detected in *adeFGH* overexpressing strains, it is thought to control the transcription of this pump [112]. AdeL is encoded directly upstream of the *adeFGH* operon, and is transcribed in the opposite direction (Fig. 1.12). Mutations in *adeL* have been described either in the C-terminal domain, possibly affecting the interaction

of the regulator with the RNA polymerase, or at a domain that is thought to be involved in signal recognition (Val139→Gly) and thus might lead to a signal-independent activation of AdeL. However, effector molecules or conditions which lead to an AdeL-dependent overexpression of *adeFGH* have not been described so far.

Table 1.2 Chromosomally encoded efflux pumps in *A. baumannii* and their associated substrates.

Efflux pump family	Name of efflux pump	Associated substrates	References
RND	AdeABC	amikacin, benzalkonium, benzylpenicillin, cefepime, cefotaxime, cefpirome, chloramphenicol , chlorhexidine, ciprofloxacin, cloxacillin, erythromycin, ethidium bromide, gentamycin, imipenem, kanamycin, levofloxacin, meropenem, methyl viologen, minocycline, netilmicin, nitrocefin, novobiocin, norfloxacin, ofloxacin, oxacillin, pefloxacin, SDS, sparfloxacin, tetracycline, tigecycline, tobramycin, trimethoprim	[89, 244-246, 249-251, 268]
	AdeIJK	acridine orange, benzalkonium, cefepime, chloramphenicol, ciprofloxacin, cloxacillin, co-trimoxazole, crystal violet, doripenem, doxycycline, ertapenem, ethidium bromide, fusidic acid, levofloxacin, meropenem, methyl viologen, minocycline, moxifloxacin, nitrocefin, novobiocin, oxacillin, pyronine, SDS, safranin, tetracycline, ticarcillin, tigecycline, trimethoprim	[127, 133, 251, 268, 269]
	AdeFGH	acridine orange, chloramphenicol, fluoroquinolones, ethidium bromide, safranin, SDS, tetracycline, tigecycline ,trimethoprim,	[112]
MFS	CraA	chloramphenicol	[270]
	AmvA	acridine orange, acriflavine, benzalkonium chloride, deoxycholate, erythromycin, ethidium bromide, methyl viologen	[271]

Table 1.2 contd. Chromosomally encoded efflux pumps in *A. baumannii* and their associated substrates.

Efflux pump family	Name of efflux pump	Associated substrates	References
MATE	AbeM	acriflavine, ciprofloxacin, chloramphenicol, doxorubicin, erythromycin, ethidium bromide, gentamicin, norfloxacin, ofloxacin, rhodamine 6G, triclosan, trimethoprim	[272]
SMR	AbeS	acridine orange, acriflavine, benzalkonium chloride, ciprofloxacin, deoxycholate, erythromycin, ethidium bromide, methyl viologen, novobiocin, rhodamine 123, SDS	[273]
PACE	AceI	chlorhexidine	[274]

1.3.3 Non RND-type efflux pumps in A. baumannii

In addition to the three RND-type efflux pumps that are predominantly associated with an MDR phenotype, two MFS pumps, as well as one member each of the MATE or the MFS superfamily have been characterized in *A. baumannii*.

CraA, standing for chloramphenicol resistance *Acinetobacter*, is one of the MFS-type efflux exporters with chloramphenicol being the only substrate of the pump (Table 1.2) [270]. It is believed to contribute to intrinsic resistance to this fenicol, however it has not yet been established if *craA* is constitutively expressed. However, it is overexpressed in response to NaCl, thus osmotic stress might constitute a stimulus for its expression [260]. Regarding its prevalence, it was present in all of 82 tested *A. baumannii* strains [270].

The second MFS pump, AmvA, is associated with decreased susceptibility to mainly, detergents, disinfectants and dyes, with erythromycin being the only antibiotic affected (Table 1.2) [271]. AmvA was described with 4-TMS and reported to be overexpressed in isolates that display elevated antimicrobial resistance.

The role of AbeM, a member of the MATE-type efflux family, on antimicrobial resistance in *A. baumannii* still remains to be elucidated as its functionality has only been investigating in *E. coli* strains defective in their main RND-type efflux pump AcrAB [272]. Thereby,

aminoglycosides, chloramphenicol, erythromycin, fluoroquinolones, trimethoprim as well as dyes and triclosan were exported (Table 1.2). *A. baumannii* isolates overexpressing *abeM* did not display a specific resistance phenotype, suggesting for a very weak effect of this pump [245, 275].

Inactivation of the SMR efflux pump AbeS followed by subsequent complementation affected the MIC values of chloramphenicol, erythromycin, fluoroquinolones, nalidixic acid, novobiocin, dyes and detergents (Table 1.2) [273]. Recently, Lytvynenko *et al.* determined residues involved in the substrate recognition of AbeS [276]. Amino acid substitution at position 3, 16 and 42 revealed increased resistance to acriflavine and ethidium, but not benzalkonium.

In 2013 a new type of efflux pump, called AceI (Acinetobacter chlorhexidine efflux) was identified in *A. baumannii* [274]. Expression of *aceI* was induced by chlorhexidine, which is also a substrate of the pump (Table 1.2). Thus, AceI was described as a representative of a new transporter family, called proteobacterial antimicrobial compound efflux (PACE) family [277].

1.3.4 Chromosomally encoded efflux systems in other Acinetobacter spp.

There are only a few studies focusing on efflux systems in *Acinetobacter* species other than *A. baumannii*. In *A. pittii* the efflux pump AdeXYZ was detected [253]. Chu *et al.* did not succeed in their attempts to disrupt *adeY*, thus, based on hydrophobicity analysis, protein sequence similarity and gene organisation, AdeXYZ is assumed to be a RND-type efflux system. Using a PCR-based approach, *adeY* was detected in 90% of *A. pittii* isolates collected in a hospital in Hong Kong between 1997-2000 [253]. Furthermore, the gene was found in one isolate each of *A. nosocomialis* and the *Acinetobacter* genomic species 17. BLAST analysis revealed a similar efflux system in the *A. baylyi* strain ADP1.

AdeDE, encoding the MFP AdeD and the transporter AdeE, is another system identified in *A. pittii*, with AdeE sharing 50% amino acid identity to AdeB. Inactivating AdeE, Chau *et al.* demonstrated decreased susceptibility to aminoglycosides, carbapenems, ceftazidime, chloramphenicol, fluoroquinolones, erythromycin, rifampicin and tetracycline [278]. Within the aforementioned isolate collection from the hospital in Hong Kong, 70% of *A. pittii* isolates carried *adeE*. Moreover, *adeE* was detected in the same *A. nosocomialis* and *Acinetobacter* genomic species 17 isolate that harboured *adeY* [253].

In 2011, Roca *et al.* found a tripartite efflux pump including an upstream encoded two-component system in *A. nosocomialis* with high similarity to AdeRSABC (99%, 94%, 96%, 99%, 95% amino acid identity, respectively) [279]. This finding contradicts previous studies, which suggest that AdeABC is an *A. baumannii* specific pump. The substrate profile of the pump was investigated by insertional inactivation of "AdeB" and included aminoglycosides, β-lactams, chloramphenicol, quinolones, tetracycline, tigecycline and trimethoprim. Except for ceftazidime, this substrate profile matched with that of the *A. baumannii* AdeABC efflux system (Table 1.2). Additionally, gene amplicons highly similar to *adeJ* and *adeY* were detected in their strain. However, as AdeJ and AdeY share an amino acid identity of 99%, Roca *et al.* propose that AdeXYZ does not represent an independent pump but rather the same as AdeIJK.

Homologs of the new PACE-family transporter protein AceI were found in *A. radioresistens* and *A. baylyi [277]*.

1.3.5 Acquired efflux pumps in Acinetobacter spp.

In *A. baumannii*, acquired efflux determinants are mainly associated with the AbaR1 resistance island (see 1.1.4). These include the MFS pumps CmlA and FloR conferring resistance to fenicols, and the *qacE* gene, encoding an SMR transporter that was shown to extrude quaternary ammonium compounds in *E. coli* [37].

Regarding tetracycline resistance, several acquired transporters of the MFS-type superfamily have been characterized in *A. baumannii*, with TetA and TetB being the most prevalent [280]. TetA, which is only exporting tetracycline, is encoded on a Tn1721-like transposon together with its regulatory protein TetR [106]. This part of the Tn1721-like transposon was also identified within the AbaR1 resistance island [37]. In contrast, TetB is pumping out minocycline in addition to tetracycline, and the gene is located on plasmids in MDR *A. baumannii* [281]. Moreover, the *tetH* gene was found on a plasmid in an *A. radioresistens* strain isolated from a fish farm [282] and in the oil degrader *A. oleivorans* [283].

1.4 Aim of the study

1) Different study designs have been used to investigate the prevalence of RND-type efflux transporters among *A. baumannii* isolates. The origin of isolates investigated was limited to a specific hospital, a city or single countries and species identification was not always performed using reference methods. In order to determine the prevalence of genes encoding the RND transporters AdeB, AdeJ and AdeG in isolates of worldwide origin, 144 geographically diverse and epidemiologically characterized *A. baumannii* isolates, representing IC1–8 and genotypically unique isolates, were investigated using a PCR-based detection method. Applying an *in silico* approach, five putative RND-type transporter genes were identified and also included in the prevalence study.

2) The RND efflux pump with the locus tag A1S_2660 in *A. baumannii* ATCC 17978, which displayed the highest amino acid similarity to AdeB amongst the five putative exporters identified *in silico*, was chosen for further characterization. Substances inducing the expression of A1S_2660 (referred to as *rnd1*) were determined using a β-galactosidase reporter assay. Furthermore, substrates of the putative pump should be identified.

3) The amino acid substitution Asp20→Asn in the response regulator AdeR (see 1.3.1) was previously reported in our research group. This replacement, residing in the acidic triad making up the active site for phosphorylation, was associated with *adeB* overexpression and reduced susceptibility to the antimicrobials levofloxacin, tigecycline, and co-trimoxazole. As most amino acid changes in the regulatory genes have only been allied to increased expression of *adeB,* in the present study, it was aimed to further characterize the effect of the substitution on antimicrobial susceptibility, the expression of the efflux genes *adeB*, *adeJ*, and *adeG*, bacterial growth, and substrate accumulation by the use of recombinant *adeR(Asp20)S*, *adeR(Asn20)S*, or *adeR(Asp20)SABC*, and *adeR(Asn20)SABC* constructs, respectively.

2. Materials & Methods

2.1 Materials

Materials used within the course of the study are listed in Table 2.1-2.5.

2.1.1 Antimicrobials

Antimicrobial discs (Table 2.1) were purchased from Oxoid (Wesel, Germany). Antimicrobials used for determination of the minimal inhibitory concentration, for selection of transformants and for induction of efflux pump expression are indicated in Table 2.2.

Table 2.1 Antimicrobial discs

Antimicrobial disc	Abbreviation
Amikacin	AK
Amoxacillin/Clavulanic acid	AMC
Ampicillin	AMP
Ampicillin/Sulbactam	SAM
Aztreonam	ATM
Azithromycin	AZM
Cefepime	FEP
Cefsulodine	CFS
Ceftriaxone	CRO
Chloramphenicol	C
Ciprofloxacin	CIP
Clindamycin	DA
Doxycycline	DO
Ertapenem	ETP
Erythromycin	E
Gentamicin	CN
Imipenem	IPM
Meropenem	MEM
Ofloxacin	OFX
Oxacillin	OX
Penicillin	P
Piperacillin/Tazobactam	TZP
Rifampicin	RD
Tetracycline	TE
Ticarcillin	TIC
Ticarcillin/Clavulanic acid	TIM
Trimethoprim/Sulfamethoxazole	SXT
Vancomycin	VA

Table 2.2 Antimicrobial powder

Antimicrobial	Abbreviation	Manufacturer
Amikacin sulfate	AMK	Molekula, Munich
Ampicillin sodium salt	AMP	Sigma-Aldrich; Steinheim
Azithromycin	AZI	Pfizer, Berlin
Chloramphenicol	CHL	Serva, Heidelberg
Ciprofloxacin	CIP	Bayer, Leverkusen
Erythromycin	ERY	AppliChem, Darmstadt
Gentamicin sulfate	GEN	Sigma-Aldrich
Kanamycin sulfate	KAN	AppliChem
Levofloxacin	LEV	Sanofi Aventis, Frankfurt
Meropenem	MEM	Molekula, Munich
Minocycline hydrochloride	MIN	Molekula
Moxifloxacin	MOX	Bayer
Nalidixic acid	NAL	Sigma-Aldrich
Novobiocin	NOV	Sigma-Aldrich
Rifampicin	RIF	Sigma-Aldrich
Tetracycline hydrochloride	TET	Sigma-Aldrich
Ticarcillin	TIC	Roth, Karlsruhe
Tigecycline	TGC	Sigma-Aldrich

2.1.2 Equipment

In Table 2.3 the equipment used and the manufacturers are listed.

Table 2.3 Equipment

Equipment	Manufacturer
96-well plate	BIOplastics BV, Landgraaf, The Netherlands
Disc Dispenser	Oxoid, Wesel, Germany
Gene Pulser II System	BioRad, Munich, Germany
Gel Doc XR$^+$ System	BioRad
LightCycler® 480	Roche, Mannheim, Germany
Multipoint inoculator	Mast Laboratories, Liverpool, United Kingdom
NanoDrop 2000 Spectrophotometer	Thermo Fisher Scientific, Schwerte, Germany
Plate Reader Infinite M1000	Tecan, Crailsheim, Germany
Thermal Cycler C1000 Touch®	BioRad
VITEK Densicheck	Biomerieux, Nürtingen, Germany

2.1.3 Chemicals and other materials

All chemicals and other materials and their abbreviations used for the purpose of the study are presented in Table 2.4.

Table 2.4 Chemicals and other materials

Chemical	Abbreviation	Manufacturer
100 bp and 1 kb ladder		New England Biolabs, Frankfurt
1-(1-naphtylmethyl)-piperazine	NMP	Sigma-Aldrich
5-bromo-4-chloro-3-indolyl-β-D-galactopyranoside	X-Gal	AppliChem, Darmstadt
Acriflavine		Sigma-Aldrich
Agarose		Sigma-Aldrich
BBL™ Mueller Hinton II Agar		BD Clonetech, Heidelberg
BBL™ Mueller Hinton II Broth		BD Clonetech
β-mercaptoethanol		Merck, Darmstadt
Benzalkonium chloride		Sigma-Aldrich
Carbonyl cyanide m-chlorophenyl hydrazone	CCCP	Sigma-Aldrich
Comassie blue		Serva, Heidelberg
Difco Agar Noble	Agar	BD Clonetech
Dimethyl sulfoxide	DMSO	Merck
Di-potassium hydrogen phosphate	K_2HPO_4	Roth, Karlsruhe
DNA Gel loading dye		New England Biolabs
Ethidium bromide powder		Merck
Ethidium bromide solution		Roth
Ethanol 96% absolute		Th. Geyer, Hamburg
Glucose monohydrate		Merck
Isopropyl β-D-1-thiogalactopyranoside	IPTG	Sigma-Aldrich
Isopropanol		Roth
Magnesium sulfate	$MgSO_4$	Sigma-Aldrich
Manganese chloride tetrahydrate	Mn(II)Cl	Sigma-Aldrich
Potassium dihydrogen phosphate	KH_2PO_4	AppliChem
Potassium tellurite hydrate	Tellurite	Sigma-Aldrich
RNA Protect Bacteria Reagent		Qiagen, Hilden
Rhodamine 6G		Sigma-Aldrich
Rothiphorese® 50x TAE Buffer		Roth, Karlsruhe
Safranin O		Sigma-Aldrich
Sodium chloride	NaCl	Sigma-Aldrich
Sodium dodecyl sulfate	SDS	AppliChem
Sodium deoxycholate		Sigma-Aldrich
Sucrose		Sigma-Aldrich
Sulbactam		Pfizer, Berlin
Triclosan		Molekula, München
Tris-acetate EDTA buffer	TAE buffer	Qiagen, Hilden
Tryptone		Oxoid, Wesel
Ultrapure H_2O		Sigma-Aldrich
Yeast extract		Oxoid

2.1.4 Culture media

All culture media were resuspended in demineralised water and autoclaved for 20 min at 120°C and 100 kPa. In addition to the listed self-made media (recipe for 1 L), commercially available blood agar and Mueller-Hinton agar plates (Oxoid, Wesel) were used.

Luria-Bertani Agar
10g Tryptone
10g NaCl
5g Yeast extract
16g Agar

Luria-Bertani Broth
10g Tryptone
10g NaCl
5g Yeast extract

Mueller-Hinton Agar
38g BBL™ Mueller Hinton II Agar

Mueller-Hinton Broth
22g BBL™ Mueller Hinton II Broth

2.1.5 Master Mix and enzymes

The enzymes listed in Table 2.5 were used for PCR, qRT-PCR or cloning.

Table 2.5 Enzymes and Master Mix

Enzymes or Master Mix	Manufacturer
Antarctic phosphatase + buffer	New England BioLabs, Frankfurt, Germany
Blunting enzyme mix + Deoxynucleotide Solution Mix	New England BioLabs
DNase	Qiagen, Hilden, Germany
Endonucleases (PstI-HF, SmaI, EagI-HF, HindIII-HF, EcroRV-HF, EcoRI-HF, NcoI-HF, PvuII-HF, ScaI-HF) + buffer	New England BioLabs
In-Fusion® HD Enzyme Premix	ClonTech, Saint-Germain-en-Laye, France
Lysozyme	Sigma-Aldrich, Steinheim, Germany
Q5 High-Fidelity Hot Start Master Mix	New England BioLabs
Quantiscript Reverse Transcriptase	Qiagen
Quick Ligase + buffer	New England BioLabs
SYBR Green Master Mix	Qiagen
T4 polynucleotide kinase + buffer	New England BioLabs
Taq PCR Master Mix	Qiagen

2.1.6 Bacterial strains and growth conditions

Plasmids and routinely used bacterial strains are listed in Table 2.6. *A. baumannii* strains were routinely grown on blood agar at 37°C or in LB broth at 37°C and 220 rpm shaking. NEB 5-alpha *E. coli* cells were used for transformation of plasmid constructs. For plasmid selection and maintenance, *E. coli* and *A. baumannii* transformants were grown on media

supplemented with tetracycline, ampicillin or ticarcillin, depending on the introduced plasmid.

Table 2.6 Bacterial strains and plasmids

Strain		Relevant characteristics	Reference
E. coli	NEB 5-alpha	Chemically competent	New England BioLabs, Frankfurt
A. baumannii	ATCC 17978	Reference strain	[17, 284]
	ATCC 19606	Reference strain, relatively high *adeB* expression (10^5-10^6 µg RNA)	[17]
	BMBF 320	Clinical isolate; moderate *adeB* expression (10^4-10^5 µg RNA)	[65]
	Isolate F	Clinical isolate, *adeR*(Asp20) variant	[89]
	Isolate G	Clinical isolate, *adeR*(Asn20) variant	[89]
	NIPH 60*	Clinical isolate; *adeRSABC*-deficient	[244]
	Scope 23	Clinical isolate; low *adeB* expression (10^1-10^2 µg RNA)	[285]
Plasmids	pMC1871	LacZ, TetR	Fungal Biodiversity Centre, Utrecht, The Netherlands
	pWH1266	*E. coli-A. baumannii* shuttle vector, *A. baumannii* replication origin, TetR	ATCC Catalog No. 77092 [286]
	pQE80L	IPTG-inducible lac-promoter expression vector; AmpR	Qiagen, Hilden
	pBHR1	KanR	MoBiTec, Göttingen
	pIG14/09	pWH1266 backbone with *lacZ* insertion obtained from pMC1871	This study
	pIG14/09::*rnd1*	pIG14/09 backbone, *rnd1-lacZ* fusion obtained by insertion	This study
	pIG14/09::*adeA*	pIG14/09 backbone, *adeA-lacZ* fusion obtained by insertion	This study
	pBA03/05	pQE80L backbone with *A. baumannii* ori obtained from pWH1266	This study
	pBA03/05::*rnd1_oe*	pBA03/05 backbone with complete A1S_2660 ORF fused in-frame to IPTG-inducable lac-promoter	This study
	pBA03/05::*rnd1_oof*	pBA03/05 backbone with complete A1S_2660 ORF fused out-of-frame to IPTG-inducable lac-promoter	This study
	pJN17/04	pBHR1 backbone with *A. baumannii* ori obtained from pWH1266	This study

*kindly provided by Alexandr Nemec

2.1.7 Primers

Primers were designed using Primer3 software (http://bioinfo.ut.ee/primer3/) or with the help of the Clontech primer design tool (http://www.clontech.com/US/Products/Cloning_and_Competent_Cells/Cloning_Resources/Online_In-Fusion_Tools).

Table 2.7 Primers

Primer name	Primer sequence (5´-3´)	Feature/Purpose	Annealing temperature	Extension time
lacZ_F lacZ_R	TTGCCGGGAAGCTAGAGTAA GATAACACTGCGGCCAACTT	Amplify *lacZ* gene from pMC1871	55°C	1.5 min
rnd1_F rnd1_R	ATCCGGGGAATTCCCGTTGGCGTCGTTTCAGTTTT AACGACGGGATCCCCCCGTTCTACAGGCAAATTCAT	Amplify promoter region of A1S_2660 + first 21 nucleotides; tails (underlined) complementary to SmaI restricted pIG14/09	57°C	30 sec
adeA_F adeA_R	ATCCGGGGAATTCCCAAGAATGATCAAACATAGAAAATCTG AACGACGGGATCCCCAAGTAAAAGATGCTTTTGCAT	Amplify promoter region of *adeA* + first 21 nucleotides; tails (underlined) complementary to SmaI restricted pIG14/09	57°C	30 sec
ori_F_EcoRI ori_R_NcoI	cggaattccAAGAACGCAACCCTATAGCAG gcccatggtgCATTTTGCGTTGTTCCAAAA	Amplify *A. baumannii* ori from pWH1266; tails (lower case) designed with respective restriction site	55 + 60°C	1.5 min
rnd1_oe_F rnd1_oe_R	*TCACCATCACGGATCC*ATGCTATCTAAATTTTTTATTCAAC **TTGGAATTCCGTGGC**CTTGATTTGATGCCCGTTTT	Amplify complete ORF of A1S_2660; tails complementary to BamHI (underlined, italics) + PstI (underlined, bold) restricted pBA03/04	57°C	3 min

2.2 Methods

2.2.1 General methods

2.2.1.1 PCR amplifications

Standard PCR amplifications were performed using either purified plasmids or crude lysates as DNA template. Crude lysates were prepared by heat-lysis: one colony was resuspended in 100 µl pure water and incubated at 99°C for 10 min and snap-cooled on ice; cells were pelleted at 13000 rpm for 1 min and the supernatant was used as template. For amplification, either the 2x Taq PCR Master Mix or the Q5® Hot Start High-Fidelity 2x Master Mix was used. With the 2x Taq PCR Master Mix the reaction was prepared as follows:

12.5 µl Taq PCR Master Mix (2x)
0.5 µl primer 1 (10 pmol/µl)
0.5 µl primer 2 (10 pmol/µl)
1 µl DNA template
10.5 µl RNase-free H_2O
25 µl final volume

The reaction mixture was subjected to the following conditions:

Step	Temperature	Time	
1 Initial denaturation	95°C	3 min	
2 Denaturation	95°C	30 sec	35 cycles
3 Annealing	55-57°C*	20 sec	
4 Extension	72°C	1- 4 min**	
5 Final elongation	72°C	5 min	
6 Storage	4°C	∞	

*dependent on primer sequence
**dependent on amplicon size

Using the Q5® Hot Start High-Fidelity 2x Master Mix, the reaction was set up in the following way:

25 µl Q5® Hot Start High-Fidelity Master Mix (2x)
2.5 µl primer 1 (10 pmol/µl)
2.5 µl primer 2 (10 pmol/µl)
2 µl DNA template
18 µl RNase-free H_2O
50 µl final volume

The reaction mixture was subjected to the following conditions:

Step	Temperature	Time	
1 Initial denaturation	98°C	3 min	
2 Denaturation	98°C	30 sec	35 cycles
3 Annealing	55-57°C*	20 sec	
4 Extension	72°C	1- 4 min**	
5 Final elongation	72°C	5 min	
6 Storage	4°C	∞	

*dependent on primer sequence
**dependent on amplicon size

After thermal cycling, amplicons were mixed with 6x DNA Loading Dye and electrophoresis of PCR amplicons was performed in 1% agarose in 1% TAE buffer at 100 V for 30 min. DNA was stained with 0.5 ng ethidium bromide and visualised using the Gel Doc XR^+ System. If necessary, PCR products were purified using the QIAquick PCR Purification Kit (Qiagen, Hilden, Germany) unless otherwise stated.

2.2.1.2 Restriction digest

DNA restriction was performed according to the manufacturer's recommendation. Restriction enzymes with their respective restriction buffer, incubation time and temperature are listed in Table 2.8.

Table 2.8 Restriction enzymes

Restriction enzyme	Buffer	Incubation time	Incubation temperature
EagI-HF	NEB4	5 min	37°C
EcoRI-HF	NEB4	5 min	37°C
EcroRV-HF	NEB4	5 min	37°C
HindIII-HF	NEB4	5 min	37°C
NcoI-HF	NEB4	5 min	37°C
PstI-HF	NEB4	5 min	37°C
PvuII-HF	NEB4	5 min	37°C
ScaI-HF	NEB4	5 min	37°C
SmaI	NEB4	1 h	25°C

Amplicon restrictions for subsequent cloning, or plasmid restrictions after cloning (to confirm the correct size) were prepared as follows:

650 ng purified plasmid DNA
1 µl enzyme (5 U)
2 µl restriction buffer
x µl RNase-free H_2O
20 µl final volume

If plasmids were linearized for subsequent cloning, the reaction was set up in the following way:

1 µg purified plasmid DNA
3 µl enzyme (15 U)
7 µl restriction buffer
x µl RNase-free H_2O
70 µl final volume

The restricted plasmids were mixed with 6x DNA Loading Dye, subjected to a 1% agarose gel and electrophoresis was run for 45 min to check whether the plasmid was properly restricted.

2.2.1.3 Cloning

Cloning was performed using either the Quick ligation kit or the In-fusion® HD cloning kit.

In the case of Quick ligation, purified PCR amplicons were phosphorylated using T4 polynucleotide kinase, restricted plasmids were dephosphorylated using the Antarctic phosphatase. Insert and donor were ligated according to the manufacturer's recommendation.

The In-fusion® HD cloning kit uses a recombinase which recognizes complementary overlaps and fuses them together. Therefore, no phosphatase treatment or ligation is necessary. Plasmids were linearized by restriction and DNA inserts were amplified using primers that generate a 15 bp overhang complementary to the linearized vector (unless otherwise stated). In this case, primers were designed with the help of the Clontech primer design tool. Restricted vectors and amplified DNA fragments were purified using the NucleoSpin Extract II PCR clean-up kit (Macherey-Nagel, Düren) and mixed with 5x In-Fusion HD Enzyme Premix according to the manufacturer's recommendation.

Transformation of plasmids into competent *E. coli* NEB5-alpha was conducted by heat shock and transformants were selected on LB plates supplemented with the appropriate antimicrobial. Plasmids were isolated using the QIAprep Spin Miniprep Kit (Qiagen, Hilden, Germany) and analysed by restriction and/or by sequencing to confirm the correct insertion. 100 ng of purified plasmids were used to transform electro-competent *A. baumannii* cells as previously described for *P. aeruginosa* (28) using the Gene Pulser II system (settings: 25 µF; 200Ω; 2.5 kV). All kits were used according to the manufacturer's instructions.

2.2.1.4 DNA sequencing

DNA sequencing was performed by LGC (Berlin) and the sequencing reaction was prepared according to their instructions. Primers used for sequencing are listed in Table 2.9. Primers were named after their position in the freezer box.

Table 2.9 Sequencing primers

Target	Primer name	Primer sequence (5´-3´)
rnd1-lacZ in pIG14/09	A15	TACGCGTACTGTGAGCCAGA
adeA-lacZ in pIG14/09	E18	TTGCCGGGAAGCTAGAGTAA
rnd1 in pBA03/05	E33	AAGTTGGCCGCAGTGTTATC
	JE76	ATGCTATCTAAATTTTTTATTCAAC
	JE3	ATGAAGTTCAACGCCAAGGT
	C13	ATTGCCGTTTTTACGCTGTT
	JE63	CTTGATTTGATGCCCGTTTT
	JE38	CCTGCGATGTGTGTAGCACT
	B42	CTGTGCCCGAATAATTTCGT
adeR in pJN17/04	JE23	TTTGAGAAGCACACGGTCAC
	D5	GCTCAGCTTGAGCGACTTCT
	D2	AATCCAGCCTTTTTCAATCG
	D4	ATCGCTTGCTTTCCATTCAT

Table 2.9 contd. Sequencing primers

Target	Primer name	Primer sequence (5´-3´)
adeS in pJN17/04	C81	GAGGGAGTGCTCGAATTTGT
	D3	TGCATGAATGATAGCGATGC
	D13	TTAGTCACGGCGACCTCTCT
	JE24	TCATCCTGCCCTTATGTTCC
adeRS in pJN17/04	C81	GAGGGAGTGCTCGAATTTGT
	D3	TGCATGAATGATAGCGATGC
	D31	GGAGTAAGTGTGGAGAAATACGG
adeRS of ATCC 17978, ATCC 19606, BMBF 320 and Scope 23	C79	CCGAGCACAGTCCATTTACA
	D1	GGCACAGGTTTAGGTCTTGC
	D2	AATCCAGCCTTTTTCAATCG
	D3	TGCATGAATGATAGCGATGC
	D4	ATCGCTTGCTTTCCATTCAT
	D5	GCTCAGCTTGAGCGACTTCT
	F79	AGGAAAATGCCACAAAATGG
mutated *adeS* in pJN17/04	D3	TGCATGAATGATAGCGATGC
	D13	TTAGTCACGGCGACCTCTCT
	JE24	TCATCCTGCCCTTATGTTCC
adeR(Asn20)S(17978) in pJN17/04	JE23	TTTGAGAAGCACACGGTCAC
	H18	AATCCAGCCTTTTTCAATTG
	D3	TGCATGAATGATAGCGATGC
	JE24	TCATCCTGCCCTTATGTTCC
adeABC in pJN17/04	JE23	TTTGAGAAGCACACGGTCAC
	D6	TGGGTTAAAAGGCTTCACCA
	D5	GCTCAGCTTGAGCGACTTCT
	JE1	AAGAATGATCAAACATAGAAAATCTG
	C5	CGGAAATTCGTCCTATCGAA
	C1	GATGTGGAAATGGCTCAGGT
	A2	CATGTTCGGTATGGTGCTTG
	A3	AATACTGCCGCCAATACCAG
	A48	GTATGAATTGATGCTGC
	C26	TTTCGCAATCAGTTGTTCCA
	D64	CTGGTCAGTTTCCGCAATTT
	JE24	TCATCCTGCCCTTATGTTCC
adeRSABC in pJN17/04	F79	AGGAAAATGCCACAAAATGG
	JE67	ACGCCATCAATAATTCCCTG
	D3	TGCATGAATGATAGCGATGC
	JE1	AAGAATGATCAAACATAGAAAATCTG
	C5	CGGAAATTCGTCCTATCGAA
	C1	GATGTGGAAATGGCTCAGGT
	A2	CATGTTCGGTATGGTGCTTG
	A3	AATACTGCCGCCAATACCAG
	A48	GTATGAATTGATGCTGC
	C26	TTTCGCAATCAGTTGTTCCA
	D64	CTGGTCAGTTTCCGCAATTT
	JE24	TCATCCTGCCCTTATGTTCC

2.2.1.5 Semi-quantitative reverse transcription PCR (qRT-PCR)

Gene expression was measured using the real-time, two-step RT-PCR approach. Total RNA was prepared using RNA Mini Prep Kit (Qiagen, Hilden) and extracted from *A. baumannii* cells that were grown until mid-log phase (optical density (OD) OD 0.7 - 0.8). 500 µl of the cell culture was mixed with 1 ml of RNAprotect Bacteria Reagent and incubated for 5 min. Following centrifugation at 8000 rpm for 12 min, the supernatant was carefully removed and RNA was extracted according to the manufacturer's recommendations. The RNA concentration was measured with the NanoDrop 2000 spectrophotometer. For the synthesis of cDNA, 1 µg of RNA was reverse-transcribed using the QuantiTect Reverse Transcription Kit (Qiagen, Hilden). Standard curves for each measured gene were prepared using PCR fragments. These were generated by PCR using the Q5® Hot Start High-Fidelity 2x Master Mix (elongation time: 30 sec) and the respective primers listed in Table 2.10. After amplicon purification and quantification, 5 dilutions were prepared in RNase free water so that the amount of unknown target was within the range (Table 2.11). *rpoB*, encoding the β-subunit of bacterial RNA polymerase, was used as a reference gene and quantified concurrent with efflux pump expression. qRT-PCR reactions, including the samples of interest and the standard curves, were prepared in 96-well plates using the QuantiFast SYBR Green RT-PCR Kit as follows:

12.5 µl SYBR Green master mix
1 µl freshly synthesised cDNA
1 µl primer 1 (10 pmol/µl)
1 µl primer 2 (10 pmol/µl)
9.5 µl RNase free H_2O
25 µl final volume

Gene specific primers are listed in Table 2.10. qRT-PCR was run in triplicates using the LightCycler® 480. Experiments were independently repeated at least three times. The reaction mixtures were subjected to the conditions recommended by the supplier and run for 30 cycles.

Table 2.10 Primer and standard curve range used for expression analysis

Target gene	Primer name	Primer sequence (5'-3')	Amplicon size (bp)
A1S_2660	ACICU_02904 2_F	ATTGCCGTTTTTACGCTGTT	147
	ACICU_02904 2_R	ATATTGGCGGACTTGCTCAC	
adeB	adeB 2_F	GAATAAGGCACCGCAACAAT	124
	adeB 2_R	TTTCGCAATCAGTTGTTCCA	
adeJ	adeJ_qRT_F	GCGAATGGACGTATGGTTCT	113
	adeJ_qRT_R	CATTGCTTTCATGGCATCAC	
adeG	adeG 2_F	GCGTTGCTGTGACAGATGTT	104
	adeG 2_R	TTGTGCACGGACCTGATAAA	
rpoB	rpoB_qRT_F	GAGTCTAATGGCGGTGGTTC	110
	rpoB_qRT_R	ATTGCTTCATCTGCTGGTTG	

Table 2.11 Standard curve range for expression analysis of efflux pump genes

Target Gene	Strain	Range for standard curve	Target Gene	Strain	Range for standard curve
adeB	ATCC 17978	10^1-10^5	*adeG*	ATCC 17978	10^2-10^6
	ATCC 19606	10^3-10^7		ATCC 19606	10^1-10^5
	BMBF 320	10^3-10^7		BMBF 320	10^1-10^5
	Scope 23	10^1-10^5		Scope 23	10^1-10^5
	NIPH 60	10^3-10^7		NIPH 60	10^1-10^5
adeJ	ATCC 17978	10^3-10^7	*rpoB*	ATCC 17978	10^3-10^7
	ATCC 19606	10^2-10^6		ATCC 19606	10^3-10^7
	BMBF 320	10^3-10^7		BMBF 320	10^3-10^7
	Scope 23	10^2-10^6		Scope 23	10^3-10^7
	NIPH 60	10^2-10^6		NIPH 60	10^4-10^8
A1S_2660	ATCC 17978	10^4-10^8			
	NIPH 60	10^4-10^8			

2.2.1.6 Growth kinetics

Growth kinetics of transformants were determined by recording their colony forming units per microliter (cfu/ml) for 4 h. Fresh overnight cultures of each transformant were diluted to a McFarland 0.5 suspension and 100 µl were used to inoculate a fresh 10 ml MH broth, and incubated at 37°C with 220 rpm shaking. At hourly intervals, a 200 µl aliquot was taken, which was serially diluted 1:10 in saline solution (0.45% NaCl). 0.1 ml aliquots of the 10-fold serial dilutions were plated on MH agar. Colonies were counted after overnight incubation, and cfu/ml was calculated using the following equation:

$$\mathrm{cfu/ml} = \frac{\mathrm{cfu} * \mathrm{x}}{\mathrm{dilution}}$$

x=10; as 0.1 ml of diluted aliquots were plated on agar

2.2.1.7 Antimicrobial susceptibility testing

Antimicrobial susceptibility was determined by agar dilution or disc diffusion.

For agar dilution, two-fold serial dilutions (of antimicrobials) were performed according to the current guidelines of the Clinical Laboratory Standards Institute [287]. For sample preparation, overnight cultures were diluted 1:10 in 0.85% saline solution, and MH agar plates, supplemented with serial dilutions of antimicrobial agents, were inoculated using a multipoint inoculator. The minimal inhibitory concentration (MIC; concentration of antimicrobial agent that completely inhibited visible growth of bacteria) was determined after overnight incubation at 37°C.

Regarding disc diffusion, a McFarland 0.5 suspension of the respective transformant was spread onto the surface of MH agar plates. Antimicrobial discs were applied on the agar plate using the Disc Dispenser. The diameter of inhibition was measured after overnight incubation at 37°C.

2.2.1.8 Accumulation studies

Accumulation kinetics of ethidium bromide was monitored by a fluorimetric assay as described previously with minor changes (30). Cells were grown aerobically in LB broth until mid-log phase, harvested at 4000 x g for 5 min at 4°C, washed twice in potassium phosphate buffer (50 mM potassium phosphate buffer, 1 mM $MgSO_4$, pH 7.4) and resuspended to an OD of 20 at 600 nm. The suspension was transferred into a 96-well plate with 0.2% (w/v) glucose, and ethidium bromide was added to a final concentration of 10 µM. The fluorescence of the supernatant was recorded at λexcite 530nm and λemit 600nm using the Infinite M1000 PRO plate reader every 10 sec for 30 min after ethidium bromide addition. The change in fluorescence intensity was directly proportional to the accumulation of ethidium.

2.2.2 Prevalence of eight resistance-nodulation-cell division-type efflux pump genes in epidemiologically characterized A. baumannii of worldwide origin

2.2.2.1 Bacterial isolates and growth conditions

One hundred and forty-four MDR *A. baumannii* isolates (*Suppl. Table II*) were selected from a global cohort (n = 492) which was part of the larger Tigecycline Evaluation and Surveillance Trial programme [288]. To accomplish a wide geographical origin, isolates recovered from 68 centres in 26 countries in Africa, Asia, Europe, North and South America were included. Molecular typing of the isolates was performed during a previous study using DiversiLab [65], a semi-automated strain typing system using repetitive sequence-based PCR to discriminate bacteria at the subspecies level. Using these data, isolates belonging to IC1–8 and genotypically unique (GtU) isolates were chosen to cover a wide epidemiological background (Fig. 2.1). Multiple isolates from single centres were only included where multiple clonal lineages were present. All isolates, with the exception of three, were carbapenem resistant and therefore exhibited a high clinical relevance.

Figure 2.1 Distribution of ICs among selected *A. baumannii* isolates.

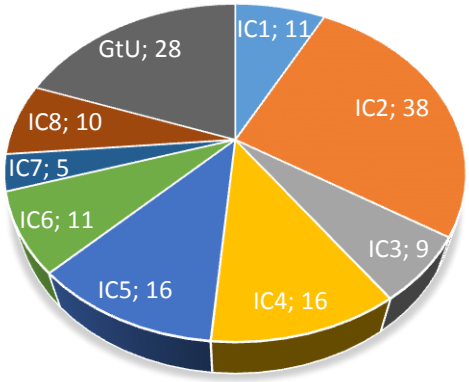

IC; international clone, GtU; Genotypically unique

2.2.2.2 Identification of putative RND efflux pump genes

An *in-silico* approach was taken to identify putative RND-type pumps and to determine their prevalence among published *A. baumannii* genomes. For their identification, open reading frames (ORFs) from *A. baumannii* genomes ACICU (CP000863.1), AB0057 (CP001182.1) and ATCC 17978 (CP000521.1), published at the National Center for Biotechnology Information

(NCBI) database, were analysed using the *A. baumannii* pump AdeB (GI:16118478) as a search query for BLAST search. To determine the prevalence, the amino acid and nucleotide sequence of the putative RND pumps were used for a BLAST search against all published complete *A. baumannii* genomes listed in the NCBI database.

2.2.2.3 Detection of RND efflux pump genes

A PCR-based detection was used to investigate the presence of the genes encoding the efflux pumps AdeB, AdeG, AdeJ and the five putative RND-type efflux pumps identified *in silico* amongst the 144 selected *A. baumannii* isolates. For amplification, crude lysates of the isolates were used as DNA template and the PCR was set-up using the Taq PCR Master Mix (55°C annealing temperature and 1 min extension time). Primers are listed in Table 2.12. To avoid false-negative results due to small genetic variations of DNA regions targeted by the first primer pair, a second primer pair was designed for each gene and used where necessary.

Table 2.12 List of primers used for the detection of efflux pump genes.
. Adapted from Nowak *et al.* [289].

Efflux pump gene	Primer name	Primer sequence (5'-3')	Expected size (bp)
adeB	O3†	GTATGAATTGATGCTGC	981
	O4†	CACTCGTAGCCAATACC	
	adeB 2_F	GAATAAGGCACCGCAACAAT	124
	adeB 2_R	TTTCGCAATCAGTTGTTCCA	
adeG	adeG 1_F	TGAACGATGCTGCTCAAAAC	681
	adeG 1_R	CTCCAGCTGTCAACCAGACA	
	adeG 2_F	GCGTTGCTGTGACAGATGTT	104
	adeG 2_R	TTGTGCACGGACCTGATAAA	
adeJ	adeJ 1_F	CTTGGTGTAACTGCCGGATT	605
	adeJ 1_R	TGAGCACCAGACTCACGTTC	
ACICU_02904*	ACICU_02904 1_F	ATGACGCGATTGTGGTTGTA	623
	ACICU_02904 1_R	CTGTGCCCGAATAATTTCGT	
	ACICU_02904 2_F	ATTGCCGTTTTTACGCTGTT	147
	ACICU_02904 2_R	ATATTGGCGGACTTGCTCAC	
ACICU_00143*	ACICU_00143 1_F	TTCCGCTCAATATTCCGAAC	646
	ACICU_00143 1_R	AGTGTCGTGGTTCCTTGGAC	
	ACICU_00143 2_F	GGTATTGGTGCGGATTATGC	134
	ACICU_00143 2_R	GTCGCGACAAAAAGAGAAGC	

† previously described by Magnet *et al*. [126]
*locus tag in *A. baumannii* ACICU

Table 2.12 contd. List of primers used for the detection of the efflux pump genes.
Adapted from Nowak *et al*. [289].

Efflux pump gene	Primer name	Primer sequence (5'-3')	Expected size (bp)
ACICU_03412*	ACICU_03412 1_F	TATGGGCTTTCCCAAGTCAC	734
	ACICU_03412 1_R	CGGTCATAAACCGTCTCGAT	
	ACICU_03412 2_F	ACCAATGGGTGGTAAAAGCA	135
	ACICU_03412 2_R	TAATTTCGGCCACACCTTTC	
ACICU_03066*	ACICU_03066 1_F	TCCGCGATGAAATTGATACA	660
	ACICU_03066 1_R	CAATAATGGTGCGAACAACG	
	ACICU_03066 2_F	AAAAAGTTCCGATGCCAATG	118
	ACICU_03066 2_R	TTTAGAGCTGTCAGCGACGA	
ACICU_03646*	ACICU_03646 1_F	AGAATATGCCGATCGTTTGC	793
	ACICU_03646 1_R	AATTCGGCTATACCCCTGCT	

† previously described by Magnet *et al*. [126]
*locus tag in *A. baumannii* ACICU

2.2.3 Characterization of the putative RND-type efflux pump A1S_2660

2.2.3.1 Construction of the reporter plasmid pIG14/09

A 3340 bp DNA fragment containing the promoterless β-galactosidase encoding *lacZ* gene flanked by PstI restriction sites was amplified from pMC1871 by PCR using the primer pair lacZ_F and lacZ_R (Table 2.7). The reaction mixture contained 60 ng of purified plasmid as DNA template and for amplification with the Q5® Hot Start High-Fidelity 2x Master Mix was used (55°C annealing temperature and 1.5 min elongation time).

The purified amplicon was digested with 5 U of PstI-HF and ligated into the similarly digested and dephosphorylated shuttle vector pWH1266. Transformed *E. coli* cells were selected on LB agar supplemented with 10 mg/L tetracycline. Restriction of the resulting plasmid pIG14/09, to confirm the correct insertion, was performed using the endonucleases SmaI and EagI-HF. The reaction was first incubated with 5U SmaI at 25°C for 1h, followed by the addition of 5U of EagI-HF and incubation at 37°C for 10 min.

2.2.3.2 Construction of pIG14/09::rnd1-lacZ

To determine the natural expression of the putative RND-type efflux pump A1S_2660, a reporter system was constructed. A 451 bp DNA fragment containing the predicted promoter region and the first 21 nucleotides of A1S_2660 was amplified from heat-lysed ATCC 17978 using the primer rnd1_F and rnd1_R (Table 2.7) and the Q5® Hot Start High-Fidelity 2x Master Mix. Using the In-Fusion® HD Enzyme Premix, the amplicon was cloned in-frame to the promoterless β-galactosidase gene *lacZ* of the SmaI restricted pIG14/09 (Fig. 2.2), yielding pIG14/09::*rnd1-lacZ* (*Suppl. Fig. I*). In ATCC 17978, it was previously found that *adeA* was constitutively expressed. Therefore, as a positive control for *lacZ* expression, a construct containing the promoter region of *adeA* and its first 21 nucleotides was generated using the primers adeA_F and adeA_R (Table 2.7) as described above leading to pIG14/09::*adeA-lacZ*.

Figure 2.2 pIG14/09::*rnd1-lacZ* in-fusion cloning

PCR primers rnd1_F and rnd1_R amplifying the promoter region and the first 21 nucleotides of A1S_2660 were extended by 15 nucleotides which are homologous to the ends of the SmaI linearized plasmid pIG14/09. In this way, the PCR fragment is elongated by the sequence homology ensuring a successful insertion into the plasmid by In-Fusion cloning (Section 2.2.3.2).

E. coli transformants were selected on LB plates supplemented with 10 mg/L tetracycline. To confirm the insertion, restriction of pIG14/09::*rnd1-lacZ* and *pIG14/09::adeA-lacZ* was performed using the endonuclease PstI-HF. In addition, successful cloning was confirmed by sequencing using primer E18 and A15 (Table 2.9). Both pIG14/09 constructs and empty vector control were introduced into competent *A. baumannii* 17978, and transformants were selected on LB plates supplemented with 30 mg/L tetracycline.

2.2.3.3 Reporter assay

To determine the effect of different antimicrobials and potential efflux substrates on the expression of A1S_2660, *A. baumannii* ATCC 17978 transformants harbouring *rnd1-lacZ* or *adeA-lacZ*, respectively, were grown on gradient plates or were tested by disc diffusion.

In the case of the gradient plates, two different MH agar layers were poured successively into the petri dish (Fig. 2.3). The bottom layer (1; 20 ml), supplemented with a test substance (antimicrobial, bile salt, detergent, dye or salt; see Table 2.13) and 40 mg/L X-gal, was solidified on a slant so that the agar covered the whole plate, but not with an even thickness; the top layer (2, 20 ml), supplemented with 40 mg/L X-gal only, was poured and the plate was placed horizontally. This resulted in an antimicrobial gradient from low to high concentration (Fig. 2.3). In order to check whether selective pressure has an effect on A1S_2660 induction, the antimicrobial concentration supplemented to layer 1 was adjusted in a way that the transformants grew until half the plate (if applicable; Table 2.13).

Figure 2.3 Schematic depiction of a gradient plate.

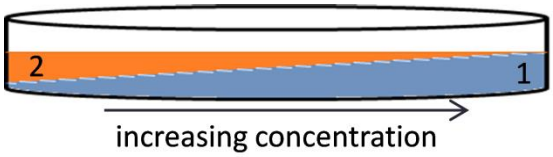

Table 2.13 List of substances used for the reporter assay applying gradient plates.

Substance category	Substance class	Substance	Concentration
Antimicrobials	Aminoglycosides	Amikacin	2 mg/L
		Gentamicin	0.5 mg/L
		Kanamycin	2 mg/L
	ß-lactams	Ampicillin	64 mg/L
		Ticarcillin	32 mg/L
	Carbapenems	Meropenem	2 mg/L
	Fenicols	Chloramphenicol	64 mg/L
	Fluoroquinolones	Ciprofloxacin	0.25 mg/L
		Levofloxacin	0.125 mg/L
		Moxifloxacin	0.125 mg/L
	Glycylcyclines	Tigecycline	0.5 mg/L
	Macrolides	Azithromycin	2 mg/L
		Erythromycin	16 mg/L
	Tetracyclines	Minocycline	1 mg/L
ß-lactamase inhibitors		Sulbactam	2 mg/L
Bile salts		Sodium deoxycholate	20 mM
Disinfectants		Benzalkonium chloride	256 mg/L
		Ethanol	10 %
Detergents		SDS	1%
Dyes		Acriflavine	16 mg/L
		Comassie blue	8 mg/L
		Rhodamine 6G	256 mg/L
		Safranin O	1 mg/L
Metal salts		Tellurite	2 mg/L
Salts		Mn(II) Cl	20 mM
		NaCl	170 mM, 200 mM

For inoculation, a McFarland 0.5 suspension of cells was streaked along the gradient, starting from the lowest to the highest concentration. Gradient plates were incubated for 16 – 48 h at 37°C. During incubation, the substance in layer 1 diffused into the upper layer and was diluted proportional to the thickness of the second layer. As a consequence, a uniform concentration gradient was established (described previously by Szybalski *et al.* [290]). The empty vector control was used as a negative control, whereas the pIG14/09::*adeA-lacZ* transformant was used as a positive control.

X-gal is an analogue of lactose and can therefore be hydrolysed to galactose by β-galactosidase. As a by-product, 5-bromo-4-chloro-3-hydroxyindole forms dimers and is oxidised to 5,5'-dibromo-4,4'-dichloro-indigo, which is blue in colour. As the promoterless β-galactosidase gene *lacZ* was cloned in-frame to A1S_2660 or *adeA*, respectively, its expression could be detected by blue colouring of the media.

In the case of disc diffusion, square MH agar plates, supplemented with 40 mg/L X-gal, had a McFarland 0.5 suspension of cells spread evenly on the plate. Antimicrobial discs were applied using a Disc Dispenser. *A. baumannii* transformants were tested with the following compounds; aminoglycosides (amikacin, gentamicin), β-lactams (ampicillin, cefepime, ertapenem, imipenem, meropenem, ticarcillin), β-lactam/β-lactamase inhibitor (ampicillin/sulbactam, piperacillin/tazobactam), chloramphenicol, clindamycin, fluoroquinolones (ciprofloxacin, ofloxacin), macrolides (azithromycin, erythromycin), rifampicin, tetracyclines (doxycycline, tetracycline), and vancomycin.

2.2.3.4 Construction of the E. coli – A. baumannii expression plasmid pBA03/05

A 1300 bp DNA fragment containing the *A. baumannii* origin of replication was amplified by PCR from pWH1266 using the primer pair ori_F_EcoRI and ori_R_NcoI (Table 2.7). The reaction mixture containing Q5® Hot Start High-Fidelity 2x Master Mix and 110 ng purified plasmid pWH1266 as DNA template was amplified using the following conditions:

	Step	Temperature	Time	
1	Initial denaturation	98°C	3 min	
2	Denaturation	98°C	30 sec	5 cycles
3	Annealing	55°C	20 sec	
4	Extension	72°C	1.5 min	
5	Denaturation	98°C	30 sec	25 cycles
6	Annealing	60°C	20 sec	
7	Extension	72°C	1.5min	
8	Final elongation	72°C	5 min	
9	Storage	4°C	∞	

The plasmid pQE80L was linearized using HindIII_HF. The resulting 3' overhangs were blunted and phosphorylated using 1.7 µl of the blunting enzyme mix with 7 µl of deoxynucleotide solution mix. The reaction mixture was incubated for 15 min at room temperature followed by heat inactivation at 70°C for 10 min. The purified amplicon was cloned into the linearized plasmid using the Quick ligation kit. Transformed *E. coli* cells were selected in LB agar supplemented with 50 mg/L ampicillin. Restriction of pBA03/05 to confirm the correct insertion was performed using the endonuclease EcoRV-HF.

2.2.3.5 Construction of pBA03/05::rnd1_oe and pBA03/05::rnd1_oof

To overexpress A1S_2660 (*rnd1*), the gene-encoding A1S_2660 was cloned in-frame to the IPTG-inducible lac-promoter encoded on the expression vector pBA03/05. The complete ORF including the start codon was amplified from crude lysates of ATCC 17978 using the Q5® Hot Start High-Fidelity 2x Master Mix and the primers rnd1_oe_F and rnd1_oe_R (Table 2.7). The purified amplicon and the shuttle vector pBA03/05 were restricted using BamHI-HF and PstI-HF (15 Units each). After purification of the linearized pBA03/05, the amplicon was fused to the plasmid using the In-fusion® HD cloning kit leading to pBA03/05::*rnd1_oe*. *(Suppl. Fig. II)*. *E. coli* transformants were selected on LB plates supplemented with 50 mg/L ampicillin. In addition to the pBA03/05::*rnd1_oe* construct, a control out-of-frame construct (*rnd1_oof*) was generated by deleting one nucleotide (in red) of primer rnd1_oe_F, resulting in the primer oof_F: TCACCATCACGGATC~~C~~ATGCTATCTAAATTTTTTATTCAAC. The pBA03/05::*rnd1_oe* construct and its oof control pBA03/05::*rnd1_oof* were introduced into competent *A. baumannii* ATCC 17978 and NIPH 60 and selected on LB plates supplemented with 150 mg/L ticarcillin. Restriction of the plasmids to confirm the correct amplicon insertion was performed using the endonuclease PstI-HF. In addition, successful cloning was confirmed by sequencing using the primers E33, JE76, JE3, C13, JE63, JE38, B42 (Table 2.9).

Expression of *rnd1* could be induced by the addition of IPTG. Usually, the lac repressor encoded on pBA03/05 binds to the lac operator when transcribed, thereby preventing the transcription of downstream encoded genes (Fig. 2.4). In *E. coli*, repressor-operator binding is naturally prevented by lactose, which allosterically binds to the repressor, changing its conformation. IPTG, a molecular analogue of lactose, can therefore be used for a controlled gene expression of *rnd1*.

Figure 2.4 Schematic depiction of the mechanism of action of IPTG

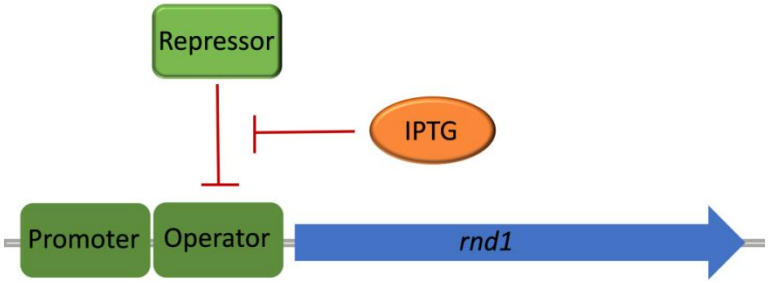

2.2.3.6 Semi-quantitative reverse transcription PCR (qRT-PCR)

Expression of the efflux pump gene A1S_2660 in pBA03/05::*rnd1_oe* transformants was measured using the real-time, two-step RT-PCR approach described in 2.2.1.5 with minor modifications. ATCC 17978 and NIPH 60 transformants were grown until mid-log phase and 2 ml of the cultures were split into 5 tubes supplemented with 0, 0.005, 0.01, 0.1, and 1 mM IPTG. After 20 min incubation, 500 µl of the cell suspension was mixed with 1 ml of RNAprotect Bacteria Reagent as described in 2.2.1.5. Gene specific primers for qRT-PCR as well as the range for the standard curves are listed in Tables 2.10 and 2.11, respectively.

2.2.3.7 Growth kinetics

Growth kinetics of ATCC 17978 and NIPH 60 pBA03/05::*rnd1_oe* and *rnd1_oof* transformants were performed as described in 2.2.1.6 with minor modifications; each transformant was diluted to a McFarland 0.5 suspension and 100 µl were used to inoculate 5 fresh 10 ml MH broth. After 2 hours of incubation, 0, 0.005, 0.01, 0.1, or 1 mM IPTG, respectively, was added and serial dilutions were plated as described previously.

2.2.3.8 Antimicrobial susceptibility testing

To identify substrates of A1S_2660, antimicrobial susceptibility of *A. baumannii* ATCC 17978 and NIPH 60 transformed with pBA03/05::*rnd1_oe* and *rnd1_oof* was determined by agar dilution or disc diffusion as described in 2.2.1.7. MH agar plates were supplemented with 0.05, 0.1 or 1 mM IPTG, respectively.

The MIC to the following antimicrobial agents was determined by agar dilution: acriflavine, benzalkonium chloride, deoxycholic acid, meropenem, nalidixic acid, novobiocin, tigecycline and triclosan. Antimicrobial concentrations tested ranged from 0.125 to 512 mg/l.

Furthermore, antimicrobial susceptibility to aminoglycosides (amikacin, gentamicin), aztreonam, β-lactams (imipenem, meropenem, penicillin), β-lactam/β-lactamase inhibitor (ampicillin/sulbactam), cephalosporins (ceftriaxone), chloramphenicol, fluoroquinolones (ciprofloxacin, ofloxacin), macrolides (erythromycin), tetracyclines (doxycycline, tetracycline), co-trimoxazole and vancomycin was performed by disc diffusion.

2.2.3.9 Accumulation studies

Accumulation kinetics of ethidium bromide in all NIPH 60 transformants was monitored by a fluorimetric assay as described in 2.2.1.8 with a minor modification; after ethidium bromide addition, 1 mM IPTG was added, followed by fluorescence readings.

2.2.4 Characterization of the Asp20→Asn substitution in the response regulator AdeR

2.2.4.1 Construction of the E. coli – A. baumannii shuttle vector pJN17/04

A DNA fragment containing the *A. baumannii* origin of replication from pWH1266 was amplified by PCR as described in 2.2.3.4. The purified amplicon was double digested with NcoI-HF and EcoRI-HF (5 U each), ligated into the similarly digested and dephosphorylated pBHR1, which does not replicate in *A. baumannii*. Transformed *E. coli* cells were selected on LB agar supplemented with 10 mg/L kanamycin. Restriction of the constructed plasmid pJN17/04 to confirm the correct insertion was performed using the endonuclease PvuII-HF. Electro-transformation of the resulting shuttle vector in competent *A. baumannii* ATCC 17978, using 50 mg/L kanamycin for selection, confirmed the replication of the shuttle vector.

2.2.4.2 Construction of pJN17/04::adeR, pJN17/04::adeS, pJN17/04::adeRS, pJN17/04::adeRSABC and pJN17/04::adeABC

To elucidate the individual impact of the *adeABC* regulators AdeRS, eight different plasmids were generated (Table 2.14). The two variants of *adeR* [referred to as *adeR*(Asp20) and *adeR*(Asn20)], including 233 bp upstream of the *adeR* start codon, were amplified alone or in combination with *adeS* [*adeR*(Asp20)*S* or *adeR*(Asn20)*S*] from *A. baumannii* isolate F and isolate G (Table. 2.6), respectively. Furthermore, *adeR*(Asp20)*SABC* and *adeR*(Asn20)*SABC* fragments (7977bp) were obtained using the primer pair adeRSABC_F and adeABC_R (Fig. 2.5;). *adeS* including 190 bp upstream of the *ade*S start codon and *adeABC* including the promoter region of *adeA* were amplified from isolate F using the primer pairs adeS_F/R or adeABC_F/R, respectively. The PCR reaction was set up using the Q5® Hot Start High-Fidelity 2x Master Mix and 2 µl of crude lysates as DNA template. Annealing was set to 57°C and extension times of each PCR were adjusted to the expected size of the PCR product (Table 2.14).

Figure 2.5 Schematic illustration of primer binding sites for cloning of the *adeRSABC* genes

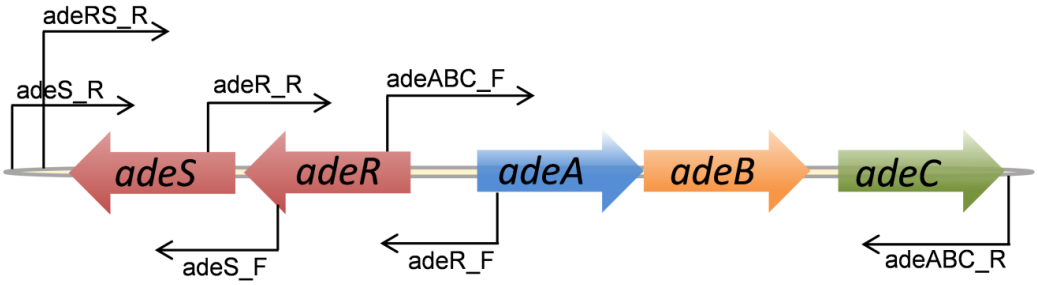

The purified amplicons were individually ligated into the ScaI (8 Units) linearized and dephosphorylated pJN17/04 using Quick ligase. Transformed *E. coli* cells were selected on LB agar supplemented with 10 mg/L kanamycin. Restriction of constructed plasmids to confirm the correct amplicon insertion was performed using the endonucleases PvuII-HF (pJN17/04::*adeS*), EcoRI-HF (pJN17/04::*adeR* variants, pJN17/04::*adeRS* variants and pJN17/04::*adeABC*) or EagI-HF for pJN17/04::*adeRSABC* constructs. *S*uccessful cloning of the generated plasmids was confirmed by sequencing (see Table 2.9 for primers). All eight constructs and the empty vector were introduced into competent *A. baumannii* as indicated in Table 2.14 by electroporation and transformants were selected on LB plates supplemented with kanamycin.

2.2.4.3 Site-directed mutagenesis in adeS of A. baumannii ATCC 17978

Single point mutations in *adeS* of *A. baumannii* ATCC 17978 leading to L173P, Y303F and double point mutations leading to L173P/Y303F were introduced using PCR in combination with the In-fusion® HD cloning kit. To introduce the single mutations, 2 amplicons were spliced together (Fig. 2.6), for the introduction of double mutations, 3 amplicons were ligated. Primers for each site-directed mutagenesis are listed in Table 2.15 (57°C annealing temperature and 80 sec elongation). For higher yields of the *adeS* gene carrying the particular mutation, the ligated product was re-amplified using 2 µl of the ligation mixture, Q5® Hot Start High-Fidelity 2x Master Mix and the primers adeRS2_R and adeS_F. Following, the purified amplicons were individually ligated into the ScaI-linearized vector pJN17/04 generating pJN17/04::*adeS*(L173P), pJN17/04::*adeS*(Y303F) and pJN17/04::*adeS*(L173P/Y303F).

Table 2.14 Cloning information on various pJN17/04 constructs

Target	Primer name	Primer sequence (5'-3')	Target size (bp)	PCR extension time	Generated plasmid	Transformed into	Kanamycin conc. for transformation
adeR(Asp20)/ adeR(Asn20)	adeR_F adeR_R	GCTCAGCTTGAGCGACTTCT AATCCAGCCTTTTTCAATCG	1137	45 sec	pJN17/04::*adeR*(Asp20) pJN17/04::*adeR*(Asn20)	ATCC 17978	50 mg/L
adeS	adeS_F adeS_R	TGCATGAATGATAGCGATGC CCGAGCACAGTCCATTTACA	1885	1 min	pJN17/04::*adeS*	ATCC 17978	50 mg/L
adeR(Asp20)S/ adeR(Asn20)S	adeR_F adeRS_R	GCTCAGCTTGAGCGACTTCT GAGGGAGTGCTCGAATTTGT	2293	1:30 min	pJN17/04::*adeR(Asp20)S* pJN17/04::*adeR(Asn20)S* *[Suppl. Fig. III]*	ATCC 17978 ATCC 19606 BMBF 320 Scope 23 NIPH 60	50 mg/L 10 mg/L 30 mg/L 50 mg/L 8 mg/L
adeABC	adeABC_F adeABC_R	TGGGTTAAAAGGCTTCACCA TTAGACTTTTGATATTCCTCCTCCTAAAAC	6265	3:30 min	pJN17/04::*adeABC*	NIPH 60	8 mg/L
adeR(Asp20)SABC/ adeR(Asn20)SABC	adeR_R adeABC_R	GAGGGAGTGCTCGAATTTGT TTAGACTTTTGATATTCCTCCTCCTAAAAC	7977	4 min	pJN17/04::*adeR(Asp20)SABC* pJN17/04::*adeR(Asn20)SABC*	NIPH 60	8 mg/L

Figure 2.6 Generation of *adeS*(L173P)

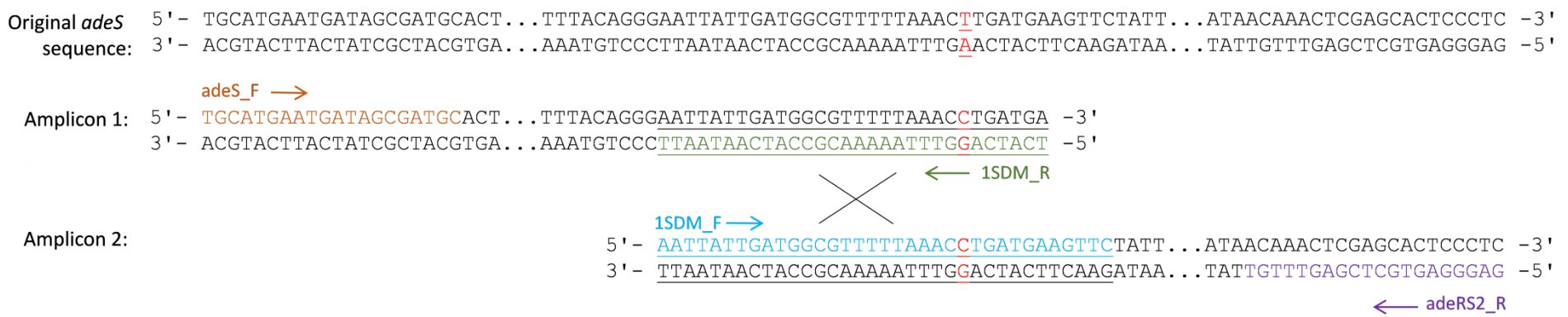

Specific primers were designed to generate *adeS*(L173P) (Section 2.2.4.3). *adeS* was amplified in two parts using primer adeS_F/1SDM_R (Amplicon 1) and 1SDM_F/adeRS2_R (Amplicon 2). The wildtype nucleotide was replaced by incorporation of the desired nucleotide (marked in red) within the primer sequence of primer 1SDM_R and 1SDM_F, resulting in the amino acid substitution L173→P. Furthermore these primers were designed homologous to each other (underlined). As a result, both amplicons were fused together using the In-fusion enzyme mix yielding *adeS*(L173P).

To confirm successful cloning, restriction digests using the endonuclease PvuII-HF and sequencing (see Table 2.9 for primers) were performed. Purified plasmids were electro-transformed into ATCC 17978.

Table 2.15 Primers used for site-directed mutagenesis in *adeS* of ATCC 17978

Amino acid substitution	Primer name	Primer sequence (5´-3´)
L173P	adeS_F	TGCATGAATGATAGCGATGC
	1SDM_R	TCATCAGGTTTAAAAACGCCATCAATAATTCCCTG
	1SDM_F	AATTATTGATGGCGTTTTTAAACCTGATGAAGTTCT
	adeRS2_R	GAGGGAGTGCTCGAGTTTGT
Y303F	adeS_F	TGCATGAATGATAGCGATGC
	2SDM_R	AGGCTTAAATAAATCGTCTTGGAACTCGGTTGCAA
	2SDM_F	AACCGAGTTCCAAGACGATTTATTTAAGCCTTTCT
	adeRS2_R	GAGGGAGTGCTCGAGTTTGT
L173P/Y303F	adeS_F	TGCATGAATGATAGCGATGC
	1SDM_R	TCATCAGGTTTAAAAACGCCATCAATAATTCCCTG
	1SDM_F	AATTATTGATGGCGTTTTTAAACCTGATGAAGTTCT
	2SDM_R	AGGCTTAAATAAATCGTCTTGGAACTCGGTTGCAA
	2SDM_F	AACCGAGTTCCAAGACGATTTATTTAAGCCTTTCT
	adeRS2_R	GAGGGAGTGCTCGAGTTTGT

In red: introduced mutation

2.2.4.4 Construction of pJN17/04::adeR(Asn20)S(17978)

To determine, whether increased expression of *adeB* is induced by a specific interaction between AdeR(Asn20) and its cognate sensor kinase AdeS, the sequence of a 'foreign' *adeS* (from *A. baumannii* ATCC 17978) was fused to *adeR*(Asn20). For the construction of the pJN17/04::*adeR*(Asn20)*S*(17978) plasmid a two-step approach using PCR and the In-fusion® HD cloning procedure was taken. First, *adeR*(Asn20), including 233 bp upstream of the *adeR* start codon, and *adeS*(17978) (1086 bp) were amplified from isolate G or ATCC 17978, respectively. For *adeR*(Asn20) the primer pair JE70/JE72, and for *adeS*(17978) the primer pair JE71/JE73 was used (Table 2.16). The PCR reaction was set up using the Q5® Hot Start High-Fidelity 2x Master Mix and 2 µl of crude lysates as DNA template (57°C annealing, 90 sec extension time).

In the second step, the two purified amplicons were fused in frame into the ScaI (15 Units) linearized and dephosphorylated vector pJN17/04 using the In-Fusion® HD cloning kit. The reaction was set up as follows:

150 ng *adeS*(17978) amplicon
130 ng *adeR*(Asn20) amplicon
75 ng restricted pJN17/04
x µl RNase free H_2O
10 µl final volume

Table 2.16 Primers used to amplify *adeR*(Asn20) and *adeS*(17978)

Primer name	Primer sequence (5´-3´)	Purpose
JE70	ATTTTTTAATATTATTTAGGCATCATCTTTTACAG	Amplify *adeR*(Asn20); underlined tail complementary to JE71 tail; italicized tail complementary to ScaI cut pJN17/04
JE72	*GCCACTCATCGCAGT*GCTCAGCTTGAGCGACTTCT	
JE71	ATAATATTAAAAAATAGCTAGGGAATATTTTATGA	Amplify AdeS(17978); underlined tail complementary to JE70 tail; italicized tail complementary to ScaI cut pJN17/04
JE73	*ATGAATTACAACAGT*GAGGGAGTGCTCGAGTTTGT	

Thereby, JE70 and JE71 were extended by 15 nucleotides, which are homologous to each other reflecting the intergenic region of *adeS*(17978) and *adeR*(Asn20), so that they fused together (Table 2.16). As the nucleotide sequence of intergenic region between *adeR* and *adeS* was identical in isolate G and 17978, no additional changes had to be added. Primers JE72 and JE73 each had tails homologous to the ScaI linearized plasmid pJN17/04. In this way, the fusion product of *adeR*(Asn20) and *adeS*(17978) could ligate to the vector.

Transformed *E. coli* cells were selected on LB agar supplemented with 10 mg/L kanamycin. Restriction of constructed plasmids to confirm the correct amplicon insertion was performed using the endonuclease EcoRI-HF. *S*uccessful cloning of the generated plasmid was confirmed by sequencing (see Table 2.9 for primers). The construct was introduced into competent *A. baumannii* ATCC 17978 by electroporation and transformants were selected on LB plates supplemented with 50 mg/L kanamycin.

2.2.4.5 Antimicrobial susceptibility testing

Antimicrobial susceptibility of *A. baumannii* parent strains and transformants was determined by agar dilution as described in 2.2.1.7. The MICs to the following 12 antimicrobial agents was determined: amikacin, azithromycin, chloramphenicol, ciprofloxacin, erythromycin, gentamicin, levofloxacin, meropenem, minocycline, rifampicin,

tetracycline, and tigecycline. Antimicrobial concentrations tested ranged from 0.03 to 256 mg/l. Where stated, 100 mg/L of the efflux pump inhibitor NMP was added to the medium.

2.2.4.6 Semi-quantitative reverse transcription PCR (qRT-PCR)

Expression of the efflux pump genes *adeB*, *adeJ* and *adeG* was measured using the real-time, two-step RT-PCR approach as described in 2.2.1.5. Gene specific primers for qRT-PCR are listed in Table 2.10 and the dilution range of PCR fragments for standard curves are listed in Table 2.11.

2.2.4.7 Growth kinetics

Growth kinetics were performed for all *adeRS* and *adeRSABC* transformants and empty vector control as described in 2.2.1.6.

2.2.3.8 Accumulation studies

Accumulation kinetics of ethidium bromide in all NIPH 60 transformants were performed as described in 2.2.1.8. With the addition of azithromycin (32 mg/L), gentamicin (4 mg/L), tetracycline (2 mg/L) or tigecycline (2.5 mg/L) at sub-inhibitory concentrations immediately after ethidium bromide addition, competition assays were accomplished.

To check whether changes in the accumulation of ethidium were caused by a proton-motive force, the proton uncoupler carbonyl cyanide m-chlorophenylhydrazone (CCCP) was added to the mixture (final concentration: 500 µM) 15 minutes after the measurement of ethidium accumulation was started. For this experiment, cells were prepared to an OD of 2 at 600nm.

In addition to ethidium bromide, accumulation studies were also performed using acriflavine at a final concentration of 5 µM or rhodamine 6G (50 µM final concentration) as substrates. Thereby, the fluorescence of the supernatant was recorded at λexcite 416 nm and λemit 514 nm for acriflavine or λexcite 480 nm and λemit 558 nm for rhodamine 6G. The fluorescence intensity was inversely proportional to the accumulation of acriflavine and rhodamine 6G.

3. Results

3.1 Prevalence of eight resistance-nodulation-cell division-type efflux pump genes in epidemiologically characterized A. baumannii of worldwide origin

3.1.1 Identification of putative RND efflux pumps

BLAST analysis identified five putative RND pumps in the three *A. baumannii* genomes ACICU, AB0057 and ATCC 17978 with the *A. baumannii* ACICU accession numbers ACICU_02904, ACICU_00143, ACICU_03412, ACICU_03066 and ACICU_03646 (Table 3.1, Fig. 3.1). ACICU_02904, annotated as a cation/multidrug efflux pump, was 1031 amino acid residues in size and was 40% identical to the AdeB amino acid sequence. No further genes characteristic for the RND-type complex (MFP or outer membrane pore) were encoded immediately upstream or downstream of the pump. The same was true for the RND superfamily exporter ACICU_00143, 1216 amino acid residues in size and 23% identical to the AdeB amino acid sequence. For both RND family cation/multidrug efflux pumps ACICU_03066 and ACICU_03646, a MFP was encoded upstream of the pump. Additionally, in the case of ACICU_03646, a *TetR*-type transcriptional regulator was found adjacent to the MFP. The latter pump was 1041 amino acids in size and 24% identical to the AdeB amino acid sequence, whereas ACICU_03066 was 1011 amino acids in size and displayed 29% similarity to AdeB. Regarding the efflux transporter ACICU_03412, both the MFP and outer membrane pore were encoded upstream of the pump displaying a putative tripartite RND efflux system, as the outer membrane pore does not necessarily have to be encoded next to the transporter. Similar to *adeAB*, the start and the stop codon of the genes encoding the MFP and the pump ACICU_03412 overlapped, which is indicative of an operon organization.

Table 3.1 Features of the five uncharacterized RND efflux pump genes. Adapted from Nowak *et al.* [289].

Locus tag	Annotated as	Size (amino acids)	Features	Similarity to AdeB
ACICU_02904	Cation/multidrug efflux pump	1031	Upstream: Zn-dependent hydrolase, glycerophosphoryl diester phosphodiesterase Downstream: hypothetical protein, htpX	40 %
ACICU_03066	Cation/multidrug efflux pump	1011	Upstream: hypothetical protein (nodulation protein), membrane-fusion protein Downstream: prolyl-tRNA synthetase, hypothetical protein	29%
ACICU_03412	Putative silver efflux pump	1052	Upstream: membrane fusion protein, outer membrane protein Downstream: Hypothetical protein, Co/Zn/Cd efflux system component	27%
ACICU_03646	Cation/multidrug efflux pump	1041	Upstream: TetR transcriptional regulator; membrane-fusion protein Downstream: hypothetical protein, chaperon protein DnaJ	24%
ACICU_00143	RND superfamily exporter	1216	Upstream: polyketide synthetase module, non-ribosomal peptide synthetase protein Downstream: hypothetical protein, NAD-dependent epimerase	23%

Figure 3.1 Schematic illustration of the five uncharacterized RND efflux pump genes and their surrounding

3.1.2 Prevalence of RND-type efflux pumps in A. baumannii isolates

The prevalence of the eight RND efflux pumps amongst sequenced *A. baumannii* genomes was determined *in silico* using the NCBI database. Twenty-five complete *A. baumannii* genomes were available to compare against *A. baumannii* ACICU. Unassembled whole-genome-shotgun sequences were not considered as complete genomes, as they might have gaps and thus sequence validity was not given. Due to the incomplete sequence, draft genomes were also excluded. Efflux pumps showing >95% sequence similarity were rated as present in the query isolate. Under these conditions, *adeG*, *adeJ*, ACICU_3066 and ACICU_3646 were present in all of the twenty-five fully sequenced *A. baumannii* genomes. Twenty-four isolates (96%) harboured ACICU_2904 and ACICU_00143, whereas 23 (92%) harboured *adeB*. In contrast, ACICU_03412 was present in less than half of the isolates (44%). The results were the same regardless of whether the amino acid sequence or the nucleotide sequence was compared.

The PCR-based detection of the eight RND efflux pump encoding genes amongst our 144 *A. baumannii* isolates revealed that five of the pump genes (*adeG*, *adeJ*, ACICU_02904, ACICU_03066 and ACICU_03646) were present in all of the *A. baumannii* isolates (Table 3.2). The gene encoding AdeB, the pump most often associated with MDR, was present in 97% of all isolates; one isolate each in IC5 and IC8, and three of the genotypically unique isolates were missing the gene. Similarly, the uncharacterized ACICU_00143 was present in all *A. baumannii* isolates of IC2, IC3, IC6 and IC7, whereas one to three isolates were negative for this pump in IC1, IC4, IC5 isolates and in the genotypically unique isolates. In IC8, less than 50% of the isolates were positive for this gene. The highest diversity in the prevalence of the eight investigated RND efflux pumps was observed with ACICU_03412; ≥ 90% of the IC1, IC3, IC6 and IC8 isolates carried the gene, while 60% of the genotypically unique isolates and IC5 gave a positive PCR product. Furthermore, only 40% of isolates in IC7, 29% in IC2 and 6% in IC4 isolates amplified ACICU_03412. Overall, there was no association between the presence of one or multiple pumps to a specific clonal lineage. However, all isolates of IC3 and IC6 were positive for all the genes investigated. With an overall prevalence of 56%, ACICU_03412 was detected least of all (for IC2, IC4 and IC7 the prevalence was <50%).

In cases when no amplicon was achieved with the first primer pair, a separate second primer pair per gene was used. For *adeJ* and ACICU_03646 no second primer pair was necessary; a

positive amplicon was detected with all isolates using the first primer pair. With regards to *adeB* and *adeG*, 5 isolates had to be re-tested with the second primer pair which revealed that all isolates were positive for *adeG*, whereas the *adeB* gene was still missing in 4 isolates. However, the use of both primer sets was frequently required for the remaining efflux pump genes. Re-testing 80 strains for ACICU_02904 and 58 strains for ACICU_03066, all strains were found positive for the respective putative RND pump. On the other hand, only 3 of 66 and 1 of 16 retested strains were positive for ACICU_03412 and ACICU_00143. BLAST analysis of whole genomes revealed that polymorphisms within the second primer-binding sites were rare.

The total prevalence of the efflux pumps amongst our strain collection showed a high similarity to the prevalence in the publicly available completely sequenced *A. baumannii* genomes in the NCBI database. Therefore, the PCR-based method to determine the prevalence of RND-type efflux pumps was reliable.

Table 3.2 Prevalence of efflux pump genes (%) for each of the eight international clones as determined by PCR. Adapted from Nowak *et al*. [289].

International clone (No. of isolates)	*adeB*	*adeG*	*adeJ*	ACICU_02904*	ACICU_00143*	ACICU_03412*	ACICU_03066*	ACICU_03646*
IC 1 (11)	100	100	100	100	82	91	100	100
IC 2 (38)	100	100	100	100	100	29	100	100
IC 3 (9)	100	100	100	100	100	100	100	100
IC 4 (16)	100	100	100	100	94	6	100	100
IC 5 (16)	94	100	100	100	88	63	100	100
IC 6 (11)	100	100	100	100	100	100	100	100
IC 7 (5)	100	100	100	100	100	40	100	100
IC 8 (10)	90	100	100	100	30	100	100	100
GtU (28)	89	100	100	100	89	61	100	100
Total (144)	97	100	100	100	87	65	100	100

*locus tag in *A. baumannii* ACICU; GtU, Genotypically Unique

3.2 Characterization of the putative RND-type efflux pump A1S_2660

3.2.1 Induced expression of A1S_2660 (rnd1)

The putative RND-type efflux pump ACICU_02904 was one of five uncharacterized pumps identified in *A. baumannii* ACICU during BLAST analysis, which was present in all 144 isolates we tested (Table 3.2). Showing the highest similarity to the AdeB amino acid sequence amongst all other putative pumps, we wanted to further characterize this pump (annotated as a cation/multidrug efflux pump), with regards to its expression and substrate specificity. For this investigation we used the *A. baumannii* reference strain ATCC 17978, in which A1S_2660 is the equivalent to ACICU_02904. Henceforth, A1S_2660 will be referred to as *rnd1*.

In contrast to the RND-type efflux pumps already described in *A. baumannii*, no further genes characteristic for the RND complex (MFP or outer membrane pore) were encoded immediately upstream or downstream of *rnd1*. To determine whether *rnd1* is constitutively expressed in ATCC 17978, reverse transcription was performed with freshly prepared cDNA using nested primers specific to the *rnd1* sequence. As a positive control genomic DNA was taken.

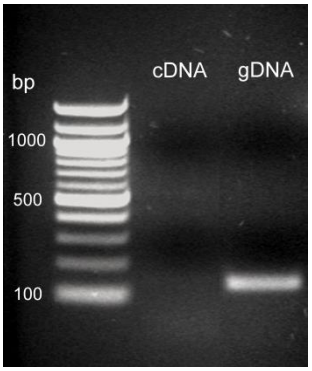

Figure 3.2 Expression of *rnd1* in *A. baumannii* ATCC 17978. Primers ACICU_02904 2_F and ACICU_02904 2_R were used to amplify *rnd1* from freshly synthetized cDNA as well as gDNA obtained from crude lysates. A positive amplicon of the gDNA sample confirmed the presence of *rnd1*, but the lack of an amplicon with the cDNA sample showed that it is not constitutively expressed.

In contrast to the genomic DNA sample of ATCC 17978, no amplified product could be detected using cDNA (Fig. 3.2). This indicated that *rnd1* is not constitutively expressed and we suggest that it is a cryptic pump.

In order to identify conditions or substances, which induce the expression of the putative pump, the β-galactosidase reporter assay was used fusing the promoter region of *rnd1* and its first 21 nucleotides to the β-galactosidase encoding gene *lacZ*. As *adeA* is constitutively expressed in ATCC 17978, an *adeA-lacZ* construct was generated as a positive control. The empty vector served as a negative control. All three constructs were transformed into the *A. baumannii* reference strain ATCC 17978 and streaked on gradient agar plates which were supplemented with different antimicrobial agents, disinfectants, detergents, chemicals or salts (Table 2.13). In addition, the LacZ substrate X-gal was added to the agar.

No colouring of the agar was observed under any of the tested conditions, neither with the wildtype strain nor the empty vector transformant (Fig. 3.3). In contrast, the agar around the *adeA-lacZ* transformants was constantly blue, confirming a constitutive expression of *adeA* in ATCC 17978. With the *rnd1-lacZ* transformants, expression could not be observed under most of the tested conditions and substances (exemplified by ampicillin in Fig.3.3 E), suggesting that the pump was not constitutively expressed. However, blue colouring of the agar was observed when meropenem (Fig. 3.3 A), chloramphenicol (B), ethanol (C) or sodium chloride (D), respectively, were supplemented, indicating that these substances were inducers of *rnd1* expression. *rnd1* was already expressed at low concentrations of meropenem, chloramphenicol and ethanol. However, its expression was induced at a NaCl concentration of ~80-100 mM and was further increased up to a final concentration of 200 mM, visible through a light blue to dark blue colour shift of the agar. Nevertheless, expression was considered low as the colour change was visible only after ≥ 24 hours of incubation. In contrast, with the *adeA-lacZ* transformant a strong colour change could be observed already after 16 h of incubation.

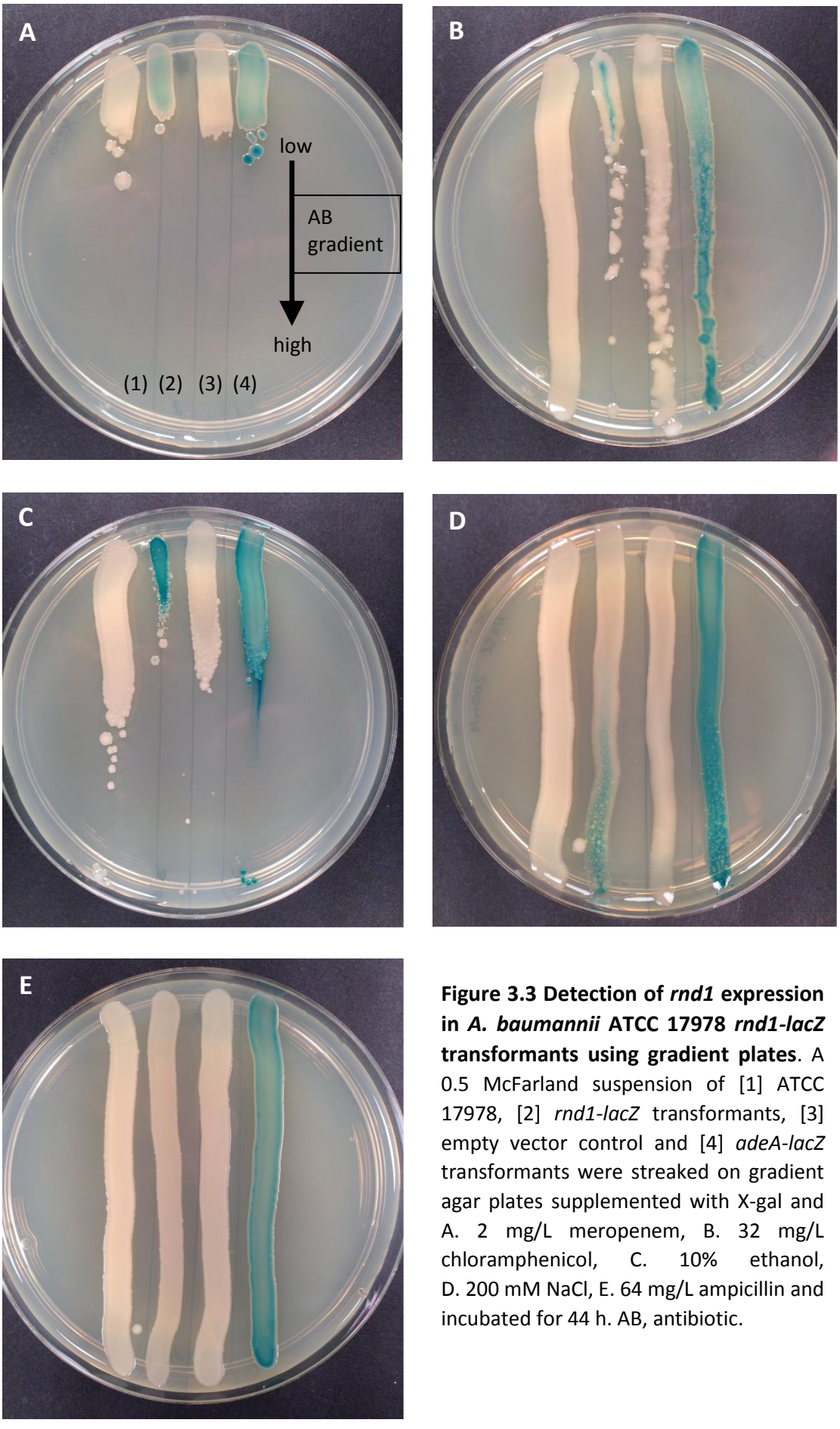

Figure 3.3 Detection of *rnd1* expression in *A. baumannii* ATCC 17978 *rnd1-lacZ* transformants using gradient plates. A 0.5 McFarland suspension of [1] ATCC 17978, [2] *rnd1-lacZ* transformants, [3] empty vector control and [4] *adeA-lacZ* transformants were streaked on gradient agar plates supplemented with X-gal and A. 2 mg/L meropenem, B. 32 mg/L chloramphenicol, C. 10% ethanol, D. 200 mM NaCl, E. 64 mg/L ampicillin and incubated for 44 h. AB, antibiotic.

To further confirm the induction of *rnd1* expression by meropenem and chloramphenicol, disc diffusion was performed with the *rnd1-lacZ* transformants. The agar was again supplemented with X-gal.

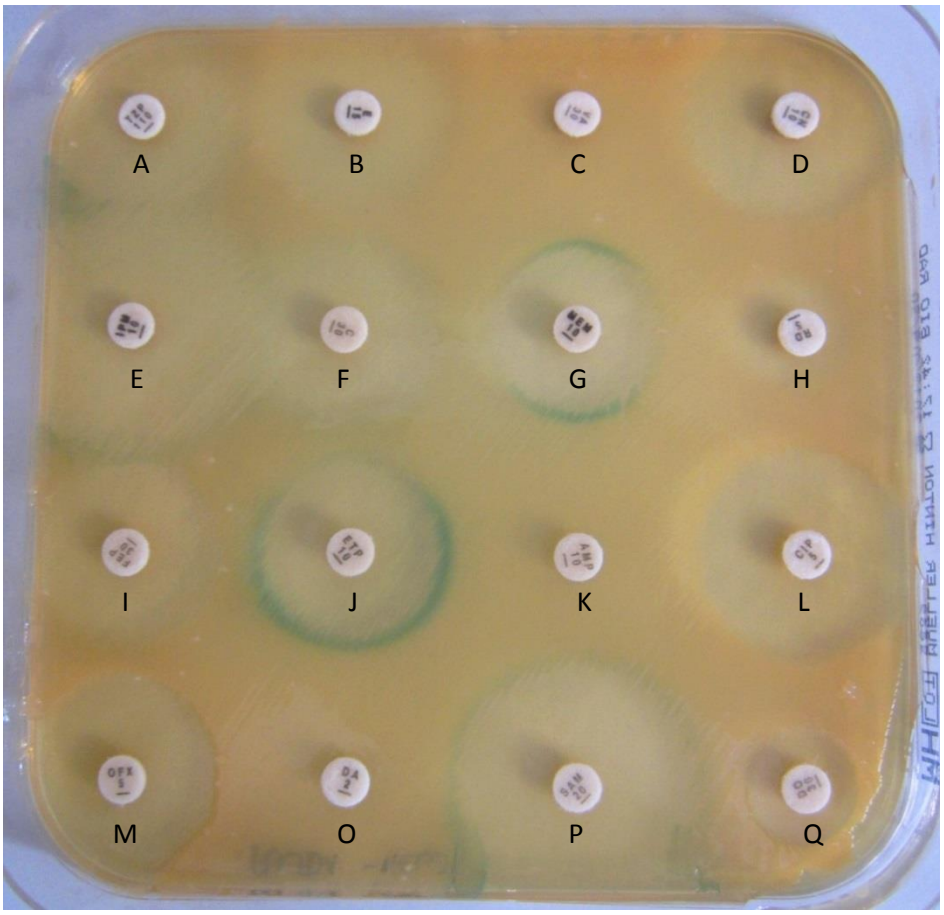

Figure 3.4 Detection of *rnd1* expression in *A. baumannii* ATCC 17978 *rnd1-lacZ* transformants using disc diffusion. A 0.5 McFarland suspension of *rnd1-lacZ* transformants was plated on a MH plate supplemented with X-gal. After antimicrobial discs were applied, the plate was incubated for 42 h. Blue colouring of the agar indicates induced expression of *rnd1*. The MH plate shown is a representative of three independent experiments.

Similar to the results of the gradient agar plates, a blue coloured inhibition zone was observed around the meropenem discs after 36 h incubation (Fig. 3.4 G). Additionally, imipenem (E) and ertapenem (J) also induced the expression of the reporter gene which led to blue colouring. Likewise, expression of *rnd1* was induced by ampicillin/sulbactam (P), but as ampicillin (K) itself did not cause any colour change, the effect could be induced by sulbactam. Using the disc diffusion method, induction could only very weakly be observed by chloramphenicol (F). With other antimicrobials tested, no colour change occurred.

3.2.2 Induced overexpression of rnd1 for substrate identification

rnd1 expression was considered low as the colour change was visible only after prolonged incubation. In order to identify substrates of Rnd1, the complete ORF of *rnd1* was cloned into an IPTG inducible expression vector for overexpression, generating *rnd1_oe*. As a control, an out-of-frame *rnd1_oof* construct was generated. Both constructs were transformed into *A. baumannii* ATCC 17978. IPTG-induced expression of *rnd1* was determined by qRT-PCR.

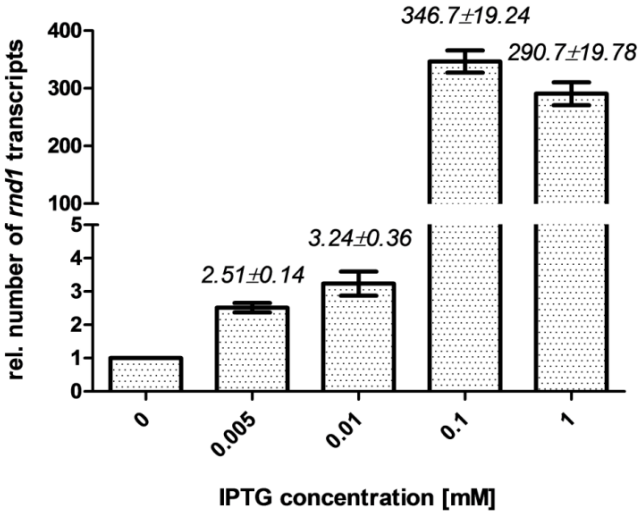

Figure 3.5 Relative *rnd1* expression in *A. baumannii* ATCC 17978 *rnd1_oe* transformants after IPTG addition. Transformants were grown until mid-log phase and IPTG was added for 20 min. Total RNA was isolated and cDNA was synthesized. *rnd1* expression was determined by qRT-PCR. The number of *rnd1* transcripts was related to the zero control after being normalized to the expression of the reference gene *rpoB*. Data displayed are representative of three independent experiments and results are shown as mean ± standard error of the mean.

After the addition of 0.005 or 0.01 mM IPTG for 20 minutes, minor changes in the *rnd1* expression by 2.5- and 3.2-fold, respectively, were determined compared to the zero control (Fig. 3.5). However, adding 0.1 or 1 mM IPTG a maximum expression was reached, which was ~300-fold higher than the *rnd1* expression of the control sample. Further experiments, which required overexpression of *rnd1* were performed adding 0.1 mM IPTG.

Substrate identification of *rnd1* was performed by disc diffusion. If increased expression of the pump leads to increased efflux of antimicrobials, disc diameter should be reduced compared to the control. However, after overnight incubation of the test plates, we observed less growth of the *rnd1_oe* transformants compared to the oof control. Supplementing the agar with 0.1 mM IPTG, growth of *rnd1_oe* transformants was reduced to

single colonies, whereas the *rnd1_oof* transformants showed confluent growth on the plate. These results suggested that overexpression of *rnd1* might be toxic for *A. baumannii* ATCC 17978. Thus, growth curves were conducted to determine bacterial fitness at different levels of *rnd1* expression.

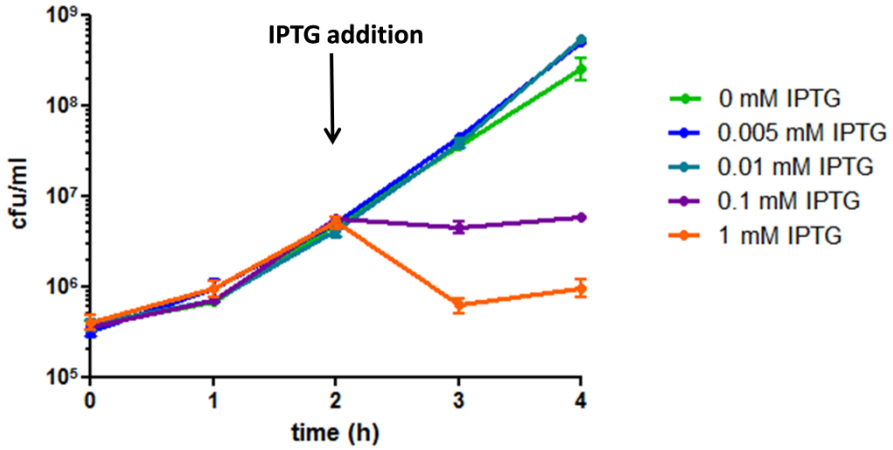

Figure 3.6 Growth of *A. baumannii* ATCC 17978 *rnd1_oe* transformants before and after IPTG addition. Growth was recording at hourly intervals for 4 hours; after 2 hours IPTG was added. Data displayed are representative of two independent experiments and results are shown as mean ± standard error of the mean.

Inducing *rnd1* expression with the addition of 0.005 or 0.01 mM IPTG, no difference in the growth of the transformants was observed compared to the control (Fig. 3.6). These results indicated that low-level expression of *rnd1* had little or no impact on survival of the transformants. However, high-level expression induced by 0.1 mM IPTG had a bacteriostatic effect, inhibiting further growth after IPTG addition. Although no further increase in *rnd1* expression was detected by qRT-PCR when raising the IPTG concentration by another 10-fold (Fig. 3.5), a bactericidal effect could be observed after 1 mM IPTG was added (Fig. 3.6). These results suggest that high-level expression of *rnd1* had a negative impact on the transformants' fitness, explaining why single colonies were visible on solid media after overnight incubation.

AdeB was originally considered to be a cryptic RND-type efflux pump, however in ATCC 17978 the *adeB* gene is constitutively expressed. Therefore, we hypothesised that the overexpression of another efflux pump might influence bacterial fitness in this strain. In order to investigate a possible correlation between *adeB* and *rnd1* expression, the *rnd1_oe* and the *rnd1_oof* construct were introduced into the clinical *A. baumannii* isolate NIPH 60.

Whole-genome sequencing previously revealed that NIPH 60 is deficient in the AdeRSABC encoding genes but is carrying *adeIJK* and *adeFGH* on the chromosome [244].

Reverse transcription of NIPH 60 gDNA and cDNA revealed that *rnd1* is also not constitutively expressed in this strain (Fig. 3.7).

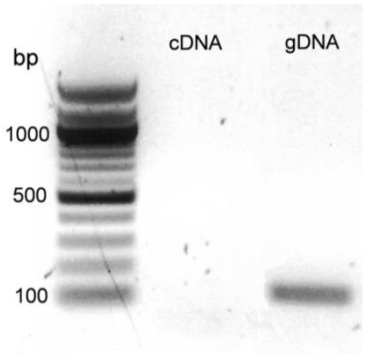

Figure 3.7 Expression of *rnd1* in *A. baumannii* NIPH 60. Primers ACICU_02904 2_F and ACICU_02904 2_R were used to amplify *rnd1* from freshly synthetized cDNA as well as gDNA obtained from crude lysates. A positive amplicon of the gDNA sample confirmed the presence of *rnd1*, but the lack of an amplicon with the cDNA sample showed that it is not constitutively expressed.

IPTG-induced expression of *rnd1* in NIPH 60 *rnd1_oe* transformants was determined by qRT-PCR. Similar to the *rnd1_o*e transformants in ATCC 17978 (Fig. 3.5), only a 6-fold change in expression of *rnd1* was induced with the addition of 0.01 mM IPTG compared to the control (Fig. 3.8). With the addition of 0.1 or 1 mM IPTG a maximum expression of ~300-fold higher compared to the control was observed.

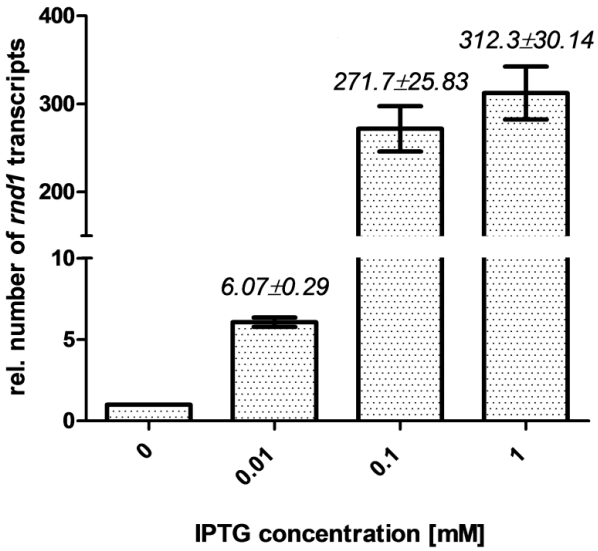

Figure 3.8 Relative *rdn1* expression in *A. baumannii* NIPH 60 *rnd1_oe* transformants after IPTG addition. Transformants were grown until mid-log phase and IPTG was added for 20 min. Total RNA was isolated and cDNA was synthesized. *rnd1* expression was determined by qRT-PCR. The number of *rnd1* transcripts was related to the zero control after being normalized to the expression of the reference gene *rpoB*. Data displayed are representative of three independent experiments and results are shown as mean ± standard error of the mean.

Growth kinetics were performed to determine if the overexpression of *rnd1* had a negative effect on bacterial growth of *adeRSABC*-deficient NIPH 60 transformants as seen with ATCC 17978 (Fig. 3.6).

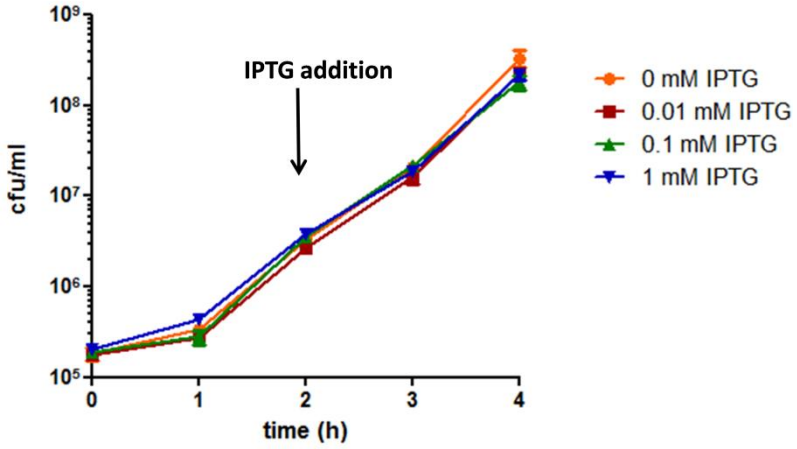

Figure 3.9 Growth of *A. baumannii* NIPH 60 *rnd1_oe* transformants before and after IPTG addition. Growth kinetics were performed recording growth at hourly intervals, for 4 hours; after 2 hours IPTG was added. Data displayed are representative of two independent experiments and results are shown as mean ± standard error of the mean.

In contrast to the ATCC 17978 *rnd1_oe* transformants (Fig. 3.6), no impact on the survival of NIPH 60 transformants was determined irrespective of which IPTG concentration was added (Fig. 3.9). Further experiments which required overexpression of *rnd1* were performed adding 1 mM IPTG, as the highest expression of *rnd1* was achieved at this concentration.

As bacterial growth of NIPH 60 *rnd1_oe* transformants was not affected by *rnd1* overexpression, substrate identification of the putative pump was performed by disc diffusion adding 1 mM IPTG to the medium. Using disc diffusion, no difference in the susceptibility to any of the tested antimicrobials was observed with the NIPH 60 *rnd1_oe* transformants compared to the *rnd1_oof* control (Table 3.3).

Table 3.3 Antibiotic disc diameter (mm) of NIPH 60 transformants

		NIPH60 pBA03/05::rnd1_*oof*		NIPH60 pBA03/05::*rnd1_oe*	
Antimicrobial class	**Antimicrobial**	**0 mM IPTG**	**1 mM IPTG**	**0 mM IPTG**	**1 mM IPTG**
Aminoglycosides	Amikacin	20	19	19	19
	Gentamicin	20	20	20	20
ß-lactams	Penicillin	9	9	9	9
Carbapenems	Imipenem	29	30	29	29
	Meropenem	26	25	26	26
Cephalosporins	Ceftriaxone	18	18	18	18
Fenicols	Chloramphenicol	11	11	10	10
Fluoroquinolones	Ciprofloxacin	29	29	29	29
	Ofloxacin	30	31	30	30
Quinolones	Nalidixic acid	23	23	22	23
Macrolides	Erythromycin	16	17	16	17
Rifamycines	Rifampicin	17	17	16	16
Tetracyclines	Doxycycline	26	26	26	26
	Tetracycline	23	24	23	23
ß-lactam/β-lactamase inhibitor	Ampicillin/Sulbactam	14	14	13	14
Folate pathway inhibitors	Co-trimoxazole	23	23	23	23

Further antimicrobials were tested by agar dilution.

Table 3.4 MIC values (mg/L) of NIPH 60 transformants

Strain	Triclosan	Acriflavine	MEM	TGC	Deoxycholic acid	Nalidixic acid	Novobiocin	Benzalkonium chloride
NIPH 60	2	64	0.25	0.25	>512	4	32	16
NIPH 60 – *rnd1_oof*	2	64	0.25	0.25	>512	4	32	16
NIPH 60 – *rnd1_oe*	2	64	0.25	0.25	>512	4	32	16

MEM, meropenem; TGC, tigecycline

Likewise, no change in the susceptibility to any of the tested substances was detected between *rnd1_oe* and *rnd1_oof* transformants using agar dilution (Table 3.4).

As there was no difference in susceptibility, we conclude that the substances tested are not substrates of this pump. Following, the accumulation assay performed in liquid culture was used as another approach, with which ethidium was tested as a potential substrate. The levels of ethidium accumulation of NIPH 60 *rnd1_oof* transformants and *rnd1_oe* transformants are summarized in Figure 3.10. No difference in ethidium accumulation was observed between *rnd1_oof* and *rnd1_oe* transformants (Fig. 3.10).

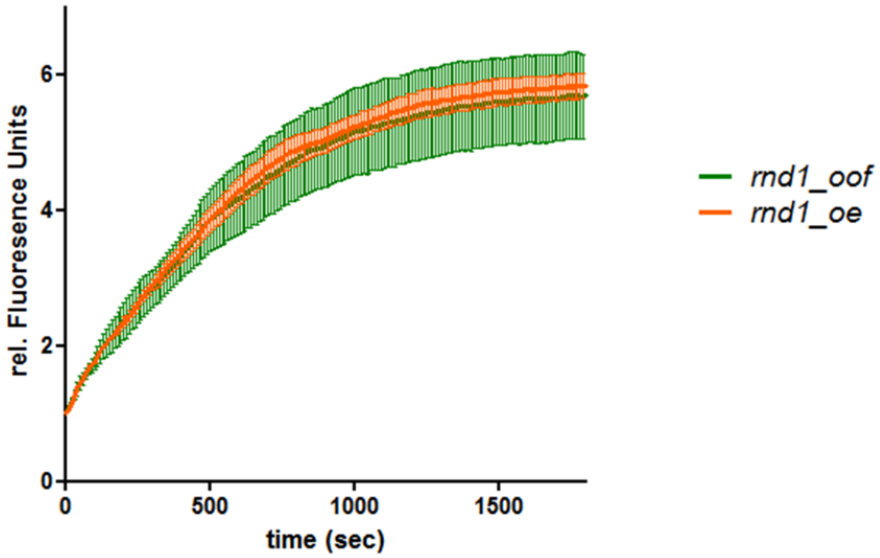

Figure 3.10 Ethidium accumulation of NIPH 60 *rnd1_oe* and *rdn1_oof* transformants. The fluorescence intensity was recorded after ethidium bromide (10 µM) and IPTG (1 mM) addition at excitation and emission wavelengths of 530 and 600 nm, respectively, every 10 seconds over a 30 min incubation period. Data displayed are representative of two independent experiments and results are shown as mean ± standard error of the mean.

As a consequence it can be said that although overexpression of the cryptic A1S_2660 (Rnd1) RND-type efflux pump was induced in the AdeRSABC-deficient isolate NIPH 60, and no negative effect on the growth rate was detected, we did not observe any difference in the susceptibility to any of the tested compounds, nor did its overexpression affect ethidium accumulation. These results implied that either I) a compound other than the applied ones might be a substrate of this pump, II) Rnd1 has another function within the cell or III) the pump, as we tested it, is not functional.

3.3 Characterization of the Asp20→Asn substitution in the response regulator AdeR

3.3.1 Synergistic interaction of AdeR(Asn20) and AdeS leads to increased expression of adeB

To determine the contribution of the Asp20→Asn substitution in AdeR on *adeB* expression and decreased antimicrobial susceptibility, two recombinant variants of *adeR* [*adeR*(Asp20) and *adeR*(Asn20)] were introduced into the *A. baumannii* reference strain ATCC 17978. As ATCC 17978 has the Asp20 variant encoded on the chromosome, any detectable differences in *adeB* expression measured by qRT-PCR or in antimicrobial susceptibility could be correlated to the substitution in AdeR. Testing the transformants against eight structurally diverse antimicrobial classes, the introduction of the empty vector control pJN17/04 into ATCC 17978 had no effect on antimicrobial susceptibility with the exception of amikacin and chloramphenicol where the MIC was reproducibly reduced from 4 mg/L to 2 mg/L, and 128 mg/L to 64 mg/L, respectively, compared to the reference strain (Table 3.5). Therefore, MIC values of all ATCC 17978 transformants were henceforth compared to the empty vector control. With the *adeR*(Asp20) variant only a minor reproducible increase in the MIC by 2-fold was seen with amikacin, gentamicin, tigecycline and azithromycin (Table 3.5). For amikacin and azithromycin these changes were further increased by another 2-fold with the *adeR*(Asn20) construct leading to an MIC of 8 mg/L for amikacin and 16 mg/L for azithromycin. Furthermore, levofloxacin and tetracycline MICs of the *adeR*(Asn20) transformants were 2-fold higher compared to the empty vector transformants.

Measuring the *adeB* expression, the number of transcripts increased by 5.5-fold with the *adeR*(Asp20) variant or by 7.5-fold with the *adeR*(Asn20) transformant relative to the vector only control (Fig 3.11). However, comparing the two *adeR* transformants with each other to catch the effect which is only due to the missense mutation in *adeR*, no significant difference in the number of *adeB* transcripts could be detected.

Table 3.5 MIC values (mg/L) of *A. baumannii* ATCC 17978 transformants

Antimicrobial class	Antimicrobial	17978	pJN17/04	*adeR(Asp20)*	*adeR(Asn20)*
Aminoglycosides	Amikacin	4	2	4	8
	Gentamicin	1	1	2	2
Carbapenems	Meropenem	1	1	1	1
Fenicols	Chloramphenicol	128	64	64	64
Fluoroquinolones	Ciprofloxacin	0.5	0.5	0.5	0.5
	Levofloxacin	0.125	0.125	0.125	0.25
Glycylcyclines	Tigecycline	0.25	0.25	0.5	0.5
Macrolides	Azithromycin	4	4	8	16
	Erythromycin	16	16	16	16
Rifamycins	Rifampicin	4	4	4	4
Tetracyclines	Tetracycline	1	1	1	2
	Minocycline	0.125	0.125	0.125	0.125

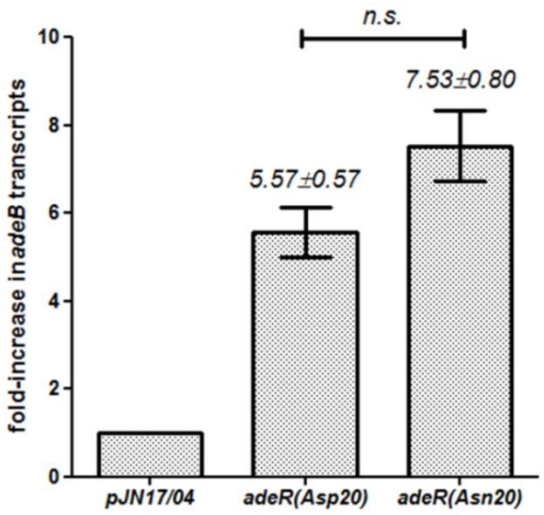

Figure 3.11 Relative *adeB* expression in the *A. baumannii* ATCC 17978 *adeR* transformants. The number of *adeB* transcripts was related to the empty vector control after being normalized to the expression of the reference gene *rpoB*. Data displayed are representative of six independent experiments and results are shown as mean ± standard error of the mean. Statistical analysis was carried out with the recorded absolute values by performing an unpaired t-test. n.s. not significant.

In contrast to the previous study with isolate F and G [89], no significant change in the expression of *adeB* (Fig. 3.11) and only minor MIC changes were detected (Table 3.5) when introducing the *adeR*(Asn20) construct compared to *adeR*(Asp20). These results suggested that the response regulator AdeR alone does not affect *adeB* expression and subsequently the susceptibility phenotype observed previously. Therefore, we took a

closer look at the amino acid sequence of the sensor kinase AdeS of the clinical isolate F and the reference strain ATCC 17978.

Comparing the AdeS amino acid sequence of isolate F with ATCC 17978, eleven differences were detected, e.g. V94A, L214F, R299Q (Fig. 3.12).

Figure 3.12 Comparison of the AdeS amino acid sequence of *A. baumannii* ATCC 17978 and isolate F and G.

To elucidate the effect of these amino acid changes, *adeS* from the clinical isolate F was introduced into ATCC 17978 and *adeB* expression was determined. This introduction led to a 22-fold increase in *adeB* expression compared to the vector only transformants (Fig. 3.13). Regarding susceptibility, amikacin, levofloxacin, tigecycline and tetracycline MICs increased slightly by 2-fold. In addition, an increase in the MICs to gentamicin by 4-fold and by 8-fold with azithromycin was found.

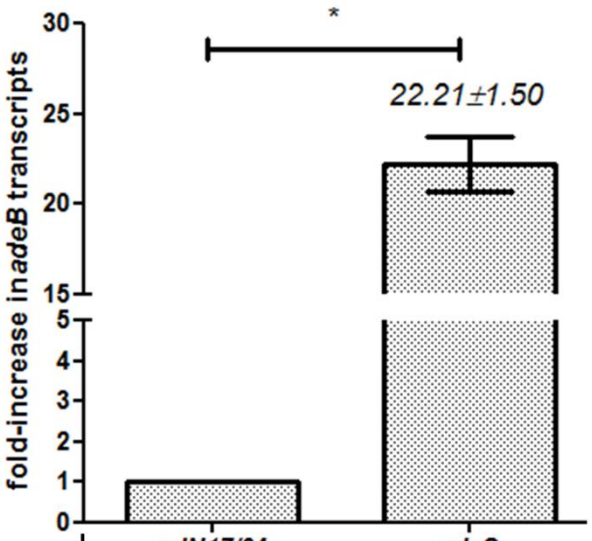

Antimicrobial class	Antimicrobial	pJN17/04	adeS
Aminoglycosides	Amikacin	2	4
	Gentamicin	1	4
Carbapenems	Meropenem	1	1
Fenicols	Chloramphenicol	64	64
Fluoroquinolones	Ciprofloxacin	0.5	0.5
	Levofloxacin	0.125	0.25
Glycylcyclines	Tigecycline	0.25	0.5
Macrolides	Azithromycin	4	32
	Erythromycin	16	16
Rifamycins	Rifampicin	4	4
Tetracyclines	Tetracycline	1	2
	Minocycline	0.125	0.125

Figure 3.13 Relative *adeB* expression and MICs (mg/L) of ATCC 17978 *adeS* transformants. The number of *adeB* transcripts was related to the empty vector control after being normalized to the expression of the reference gene *rpoB*. Data displayed are representative of three independent experiments and results are shown as mean ± standard error of the mean. Statistical analysis was carried out with the recorded absolute values by performing an unpaired t-test. *, $P < 0.05$. Antimicrobial susceptibility was determined by agar dilution.

In comparison to the *adeR* transformants (Table 3.5), susceptibilities to a larger number of antimicrobials were affected when introducing *adeS* of isolate F into ATCC 17978. Having a closer look at the amino acid differences between both strains, in particular the substitutions

at position 173 and 303 might have an impact on *adeB* expression as they lie within functional domains (other substitutions were not considered as relevant compared to the sequence of *A. baumannii* ATCC 19606, BMBF 320, Scope 23; see Fig. 3.25). The amino acid difference at position 173 lies within the histidine kinase domain close to the autophosphorylation site, which might affect the phosphorylation of AdeR and thus its activation (Fig. 3.12). The substitution at position 303 on the other hand, lies within the ATP binding site which is equally important for the phosphoryl-transfer to the response regulator. To elucidate whether one of these amino acid changes or both combined affect *adeB* expression, the *adeS* sequence of ATCC 17978 was altered by applying a site-directed mutagenesis approach. The following recombinant *adeS* constructs were generated: *adeS*(L173P), *adeS*(Y303F) and *adeS*(L173P/Y303F). These *adeS* variants were transformed into the reference strain ATCC 17978, and *adeB* expression was recorded by qRT-PCR. The chosen amino acid differences alone or in combination did not affect the number of *adeB* transcripts compared to the empty vector control (Fig. 3.14).

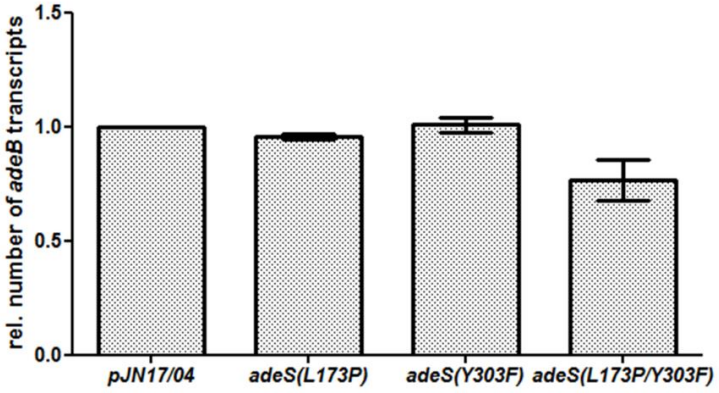

Figure 3.14 Relative *adeB* expression in ATCC 17978 *adeS* site-directed mutagenesis transformants. The number of *adeB* transcripts was related to the empty vector control after being normalized to the expression of the reference gene *rpoB*. Data displayed are representative of three independent experiments and results are shown as mean ± standard error of the mean.

Nevertheless, the fact that the susceptibilities to a larger number of antimicrobials were decreased when introducing *adeS* of the clinical isolate F, as well as the accompanying 22-fold increase in *adeB* expression (Fig. 3.13), led us to the question of whether AdeR is dependent on its cognate sensor kinase and if their interaction is synergistic or additive. Thus, *adeR*(Asp20)*S* or *adeR*(Asn20)*S* genes from isolates F or G, respectively, were transformed into ATCC 17978 and *adeB* expression as well as their antimicrobial susceptibility were determined. The introduction of the *adeR*(Asp20)*S* construct led to a

78-fold increase in *adeB* expression, compared to the empty vector control (Fig. 3.15). However, no further changes in the MICs to the tested antimicrobials were detected in addition to the elevated MICs seen previously with the *adeS* transformant (Fig. 3.13). With the *adeR*(Asn20)*S* construct, *adeB* expression was increased by over 400-fold and MICs to ciprofloxacin, levofloxacin, and tetracycline increased by 4-fold, while amikacin and tigecycline MICs increased by 8-fold compared to the control (Fig. 3.15). Furthermore, gentamicin and azithromycin MICs increased by 16-fold from 1 mg/L to 16 mg/L and 4 mg/L to 64 mg/L, respectively. Comparing both *adeRS* constructs with each other to catch the effect which is only due to the mutation in *adeR*, a 5-fold increase in *adeB* expression and a 4-fold increase of the MIC to antimicrobials belonging to the three different antimicrobial classes aminoglycosides, fluoroquinolones and glycylcyclines was detected.

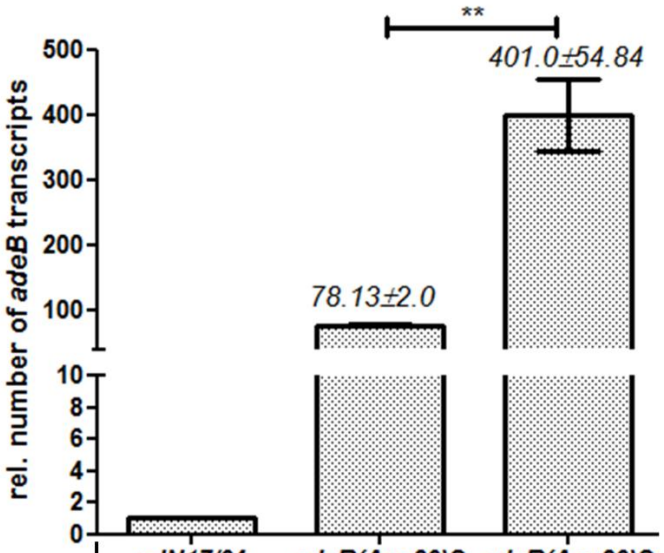

Antimicrobial class	Antimicrobial	pJN17/04	adeR(Asp20)S	adeR(Asn20)S
Aminoglycosides	Amikacin	2	4	16
	Gentamicin	1	4	16
Carbapenems	Meropenem	1	1	2
Fenicols	Chloramphenicol	64	64	64
Fluoroquinolones	Ciprofloxacin	0.5	0.5	2
	Levofloxacin	0.125	0.25	0.5
Glycylcyclines	Tigecycline	0.25	0.5	2
Macrolides	Azithromycin	4	32	64
	Erythromycin	16	16	32
Rifamycins	Rifampicin	4	4	4
Tetracyclines	Tetracycline	1	2	4
	Minocycline	0.125	0.125	0.125

Figure 3.15 Relative *adeB* expression and MICs (mg/L) of the ATCC 17978 *adeRS* transformants. The number of *adeB* transcripts was related to the empty vector control after being normalized to the expression of the reference gene *rpoB*. Data displayed are representative of three independent experiments and results are shown as mean ± standard error of the mean. Statistical analysis was carried out with the recorded absolute values by performing an unpaired t-test. **, $P < 0.01$. Antimicrobial susceptibility was determined by agar dilution.

In conclusion, the introduction of both *adeR* and *adeS* combined show a synergistic effect on the number of *adeB* transcripts as well as on reduced antimicrobial susceptibility, especially with the *adeRS* transformant harboring the Asn20 variant. However, introducing *adeS* and *adeR*(Asp20) of isolate F together, no further changes in the MICs compared to the *adeS* only transformants were detected. These results indicated that the Asn20 substitution in AdeR has a specific effect on the interaction with its cognate sensor kinase leading to the significant increase in *adeB* expression and decrease in the susceptibility profile. To investigate the dependence of AdeR(Asn20) on its cognate sensor kinase, a plasmid was constructed harboring *adeS* of ATCC 17978 in frame with *adeR*(Asn20) of isolate G, rendering *adeR*(Asn20)*S*(17978). The intergenic region between *adeRS* of ATCC 17978 was the same compared to isolate F and G, therefore the only difference to *adeR*(Asn20)S was the 'new' *adeS* sequence downstream of *adeR*(Asn20). The *adeR*(Asn20)*S*(17978) was introduced into ATCC 17978 and *adeB* expression was determined by qRT-PCR.

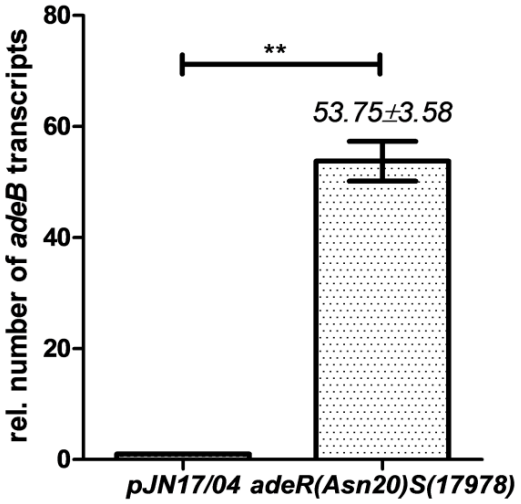

Figure 3.16 Relative *adeB* expression in ATCC 17978 *adeR*(Asn20)*S*(17978) transformants. The number of *adeB* transcripts was related to the empty vector control after being normalized to the expression of the reference gene *rpoB*. Data displayed are representative of two independent experiments and results are shown as mean ± standard error of the mean. Statistical analysis was carried out with the recorded absolute values by performing an unpaired t-test. **, $P < 0.01$.

With the introduction of the *adeR*(Asn20)*S*(17978) construct *adeB* expression was increased by almost 54-fold compared to the empty vector control (Fig. 3.16). This increase is comparable to the effect of the *adeR*(Asp20)*S* transformant (Fig. 3.15). These results suggest that the 400-fold increase in the number of *adeB* transcripts observed for the *adeR*(Asn20)*S*

transformant (Fig. 3.15) is due to the Asp20→Asn substitution in AdeR which might specifically affect the interaction with its cognate AdeS.

Concluding these results, with the introduction of the different *adeR*, *adeS* and *adeRS* constructs of isolate F and G a stepwise increase in the expression of *adeB* and a stepwise decrease in the susceptibility to multiple antibiotics was achieved in the *A. baumannii* reference strain ATCC 17978 (Fig. 3.17). The *adeR* transformants showed a 5.5-7.5 fold increase in the number of *adeB* transcripts but minor changes in the MICs by 2-fold were observed compared to the empty vector control. With the *adeS* and the *adeR*(Asp20)*S* construct, which led to elevated *adeB* transcription levels by 22- to 78-fold, respectively, an identical susceptibility profile could be observed; a 4-fold increase in the MIC to gentamicin and an 8-fold increase in azithromycin MIC (Fig. 3.17). Although *adeR*(Asp20)*S* had a synergistic effect on *adeB* expression compared to the *adeS* and *adeR*(Asp20) single transformants, it was the synergistic effect of *adeR*(Asn20) in combination with its cognate sensor kinase that increased the *adeB* expression by over 400-fold compared to the control and thereby caused a significant decrease in the susceptibility to antimicrobials belonging to three different classes in *A. baumannii* strain ATCC 17978.

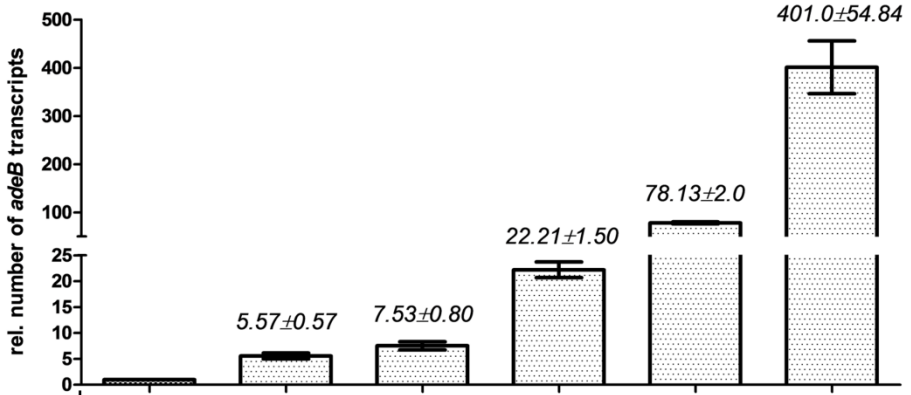

Antimicrobial class	Antimicrobial	pJN17/04	adeR(Asp20)	adeR(Asn20)	adeS	adeR(Asp20)S	adeR(Asn20)S
Aminoglycosides	Amikacin	2	2	4	2	2	8
	Gentamicin	1	2	2	4	4	16
Carbapenems	Meropenem	1	-	-	-	-	2
Fenicols	Chloramphenicol	64	-	-	-	-	-
Fluoroquinolones	Ciprofloxacin	0.5	-	-	-	-	4
	Levofloxacin	0.125	-	2	2	2	4
Glycylcyclines	Tigecycline	0.25	2	2	2	2	8
Macrolides	Azithromycin	4	2	4	8	8	16
	Erythromycin	16	-	-	-	-	2
Rifamycins	Rifampicin	4	-	-	-	-	-
Tetracyclines	Tetracycline	1	-	2	2	2	4
	Minocycline	0.125	-	-	-	-	-

Figure 3.17 Relative *adeB* expression and MICs of the ATCC 17978 transformants. The number of *adeB* transcripts was related to the empty vector control after being normalized to the expression of the reference gene *rpoB*. Results are shown as mean ± standard error of the mean. Antimicrobial susceptibility was determined by agar dilution and is shown in mg/L for the empty vector transformant and as fold-increase for the other transformants compared to the control.

As the overexpression of the other two efflux pump genes *adeG* and *adeJ* have also been associated with decreased susceptibility in *A. baumannii* isolates, their expression was also investigated.

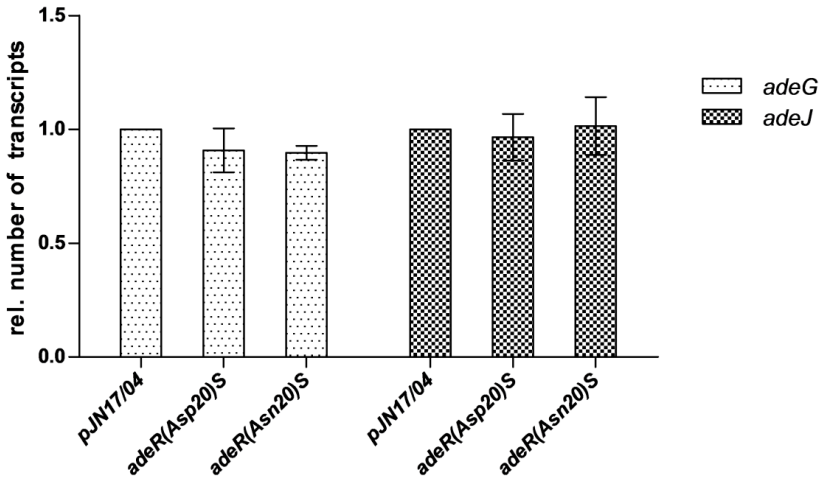

Figure 3.18 Relative *adeG* and *adeJ* expression in the ATCC 17978 *adeRS* transformants. The number of *adeG* or *adeJ* transcripts was related to the empty vector control after being normalized to the expression of the reference gene *rpoB.* Data displayed are representative of three independent experiments and results are shown as mean ± standard error of the mean.

No significant difference in the expression of *adeG* or *adeJ* was detected between the *adeRS* transformants and the empty vector control (Fig. 3.18).

To determine if the increased expression of *adeB* was accompanied by a fitness cost for the transformants, growth curves were conducted. No difference in growth rates between either of the *adeRS* transformants and the empty vector control were observed (Fig. 3.19).

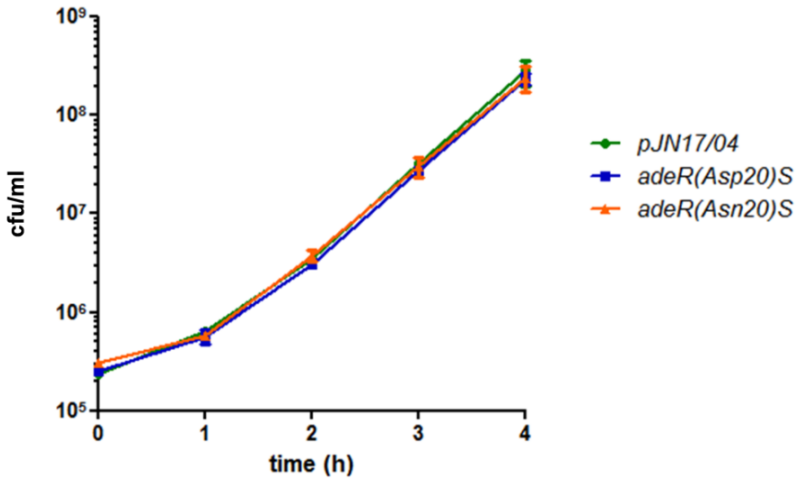

Figure 3.19 Growth of the *A. baumannii* ATCC 17978 *adeRS* transformants. Growth kinetics were performed recording growth at hourly intervals, for 4 hours. Data displayed are representative of two separate experiments and results are shown as mean ± standard error of the mean.

3.3.2 The effect of adeR(Asn20)S differs among A. baumannii strains

To investigate whether the downstream effects of the introduced *adeRS* constructs are uniform among other *A. baumannii* strains, both *adeRS* variants [*adeR(Asp20)S*, *adeR(Asn20)S*] were transformed into three further isolates; the *A. baumannii* reference strain ATCC 19606, which naturally has a relatively high number of *adeB* transcripts (10^5-10^6µg RNA); the *A. baumannii* isolate BMBF 320 with a moderate number of *adeB* transcripts (10^4-10^5µg RNA) and the clinical isolate Scope 23, which has the lowest number of *adeB* transcripts (10^1-10^2 µg RNA). *adeB* expression was determined by qRT-PCR and antimicrobial susceptibility by agar dilution.

3.3.2.1 ATCC 19606

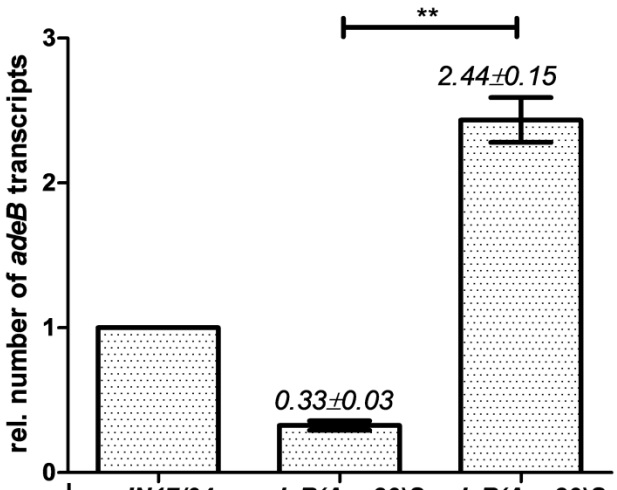

Antimicrobial class	Antimicrobial	pJN17/04	adeR(Asp20)S	adeR(Asn20)S
Aminoglycosides	Amikacin	8	8	8
	Gentamicin	8	4	16
Carbapenems	Meropenem	1	0.5	1
Fenicols	Chloramphenicol	128	128	128
Fluoroquinolones	Ciprofloxacin	1	1	2
	Levofloxacin	0.25	0.25	0.5
Glycylcyclines	Tigecycline	1	0.5	1
Macrolides	Erythromycin	32	32	32
	Azithromycin	32	16	32
Rifamycins	Rifampicin	2	2	2
Tetracyclines	Tetracycline	2	2	4
	Minocycline	0.25	0.125	0.25

Figure 3.20 Relative *adeB* expression and MICs (mg/L) of the ATCC 19606 *adeRS* transformants. The number of *adeB* transcripts was related to the empty vector control after being normalized to the expression of the reference gene *rpoB*. qRT-PCR data displayed are representative of four independent experiments and results are shown as mean ± standard error of the mean. Statistical analysis was carried out with the recorded absolute values by performing an unpaired t-test. **, $P < 0.01$. Antimicrobial susceptibility was determined by agar dilution.

Introducing the *adeR*(Asp20)*S* construct into ATCC 19606, the number of *adeB* transcripts was reduced by almost 70% compared to the empty vector control (Fig. 3.20). Correlating, the MICs to gentamicin, meropenem, tigecycline, azithromycin and minocycline were reproducably reduced by 2-fold. The susceptibility to the other tested antimicrobials was not affected. In contrast, *adeB* expression was increased by 2.5-fold with the *adeR(Asn20)S* construct (Fig. 3.20). Compared to the control, MICs of gentamicin, ciprofloxacin, levofloxacin and tetracycline were reproducably increased by 2-fold from 8 mg/L to 16 mg/L, 1 mg/L to 2 mg/L, 0.25 mg/L to 0.5 mg/L, and 2 mg/L to 4 mg/L, respectively. Comparing both *adeRS* transformants with each other, *adeB* expression was significantly elevated by 7.4-fold with the *adeR*(Asn20)*S* variant. Regarding the susceptibility data, a minor increase in the MIC by 2-fold was induced for 5 of the 8 tested antimicrobial classes (carbapenems, fluoroquinoloes, glycylcyclines, macrolides and tetracylines). A reduced susceptibility by 4-fold was observed for gentamicin.

3.3.2.2 BMBF 320

With the *adeR*(Asp20)*S* construct, no changes in the number of *adeB* transcripts was determined in the *A. baumannii* isolate BMBF 320 compared to the empty vector control (Fig. 3.21). Similarly, the susceptibility to all tested antimicrobials was unaffected with the exception of ciprofloxacin, where the already high MIC value of 64 mg/L was reproducibly increased by 2-fold to 128 mg/L. However, *adeB* expression was elevated by 18-fold in the *adeR*(Asn20)*S* transformant compared to the control and 12-fold compared to the *adeR*(Asp20)*S* construct. Regarding susceptibility, comparing both *adeRS* constructs minor changes in the MIC to amikacin, the tested fluoroquinolones, macrolides and tetracyclines by 2-fold were observed (Fig. 3.21). Furthermore, the MIC to tigecycline increased by 4-fold from 2 mg/L to 8mg/L.

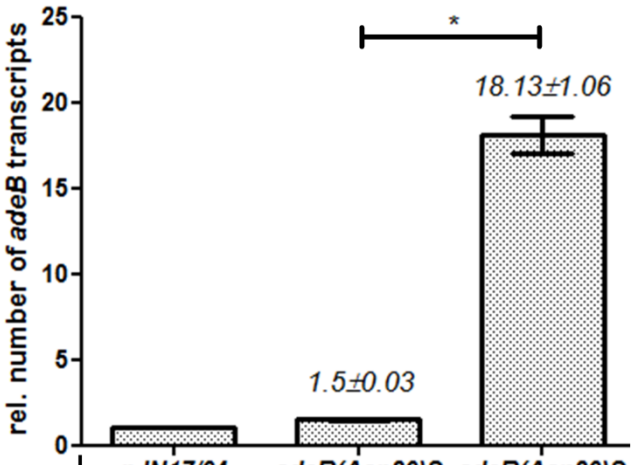

Antimicrobial class	Antimicrobial	pJN17/04	adeR(Asp20)S	adeR(Asn20)S
Aminoglycosides	Amikacin	4	4	8
	Gentamicin	>512	>512	>512
Carbapenems	Meropenem	32	32	32
Fenicols	Chloramphenicol	128	128	128
Fluoroquinolones	Ciprofloxacin	64	128	256
	Levofloxacin	8	8	16
Glycylcyclines	Tigecycline	2	2	8
Macrolides	Erythromycin	32	32	64
	Azithromycin	32	32	64
Rifamycins	Rifampicin	4	4	4
Tetracyclines	Tetracycline	8	8	16
	Minocycline	0.25	0.25	0.5

Figure 3.21 Relative *adeB* expression and MICs (mg/L) of the BMBF 320 *adeRS* transformants. The number of *adeB* transcripts was related to the empty vector control after being normalized to the expression of the reference gene *rpoB*. qRT-PCR data displayed are representative of three independent experiments and results are shown as mean ± standard error of the mean. Statistical analysis was carried out with the recorded absolute values by performing an unpaired t-test. *, $P < 0.05$. Antimicrobial susceptibility was determined by agar dilution.

3.3.2.3 Scope 23

In the *A. baumannii* isolate Scope 23, introducing both *adeRS* variants led to a stepwise increase in *adeB* expression and a stepwise decrease in antimicrobial susceptibility, compared to the empty vector control (Fig. 3.22). The 40-fold increase in the number of *adeB* transcripts induced with the *adeR*(Asp20)*S* construct was accompanied by minor changes in the MICs of amikacin, the fluoroquinolones and minocycline by 2-fold. In addition, susceptibilities to gentamicin and azithromycin were decreased by 4- and 8-fold, respectively. With the introduction of *adeR*(Asn20)*S* the increase in *adeB* expression by almost 350-fold was reflected by a 4-fold increase in the MIC to amikacin, the fluoroquinolones and tigecycline compared to the empty vector control. Gentamicin and

azithromycin MICs were increased by 16- or 32-fold, respectively from 1 mg/ml, and 4 mg/L, to 16 mg/L and 128 mg/L, respectively. Comparing both *adeRS* transformants to catch the effect of the Asp20→Asn substitution, *adeB* expression significantly differed by 8.6-fold. Furthermore, the susceptibility to 8 of 10 tested antimicrobials was affected, with reproducible minor changes by 2-fold for amikacin, the fluoroquinolones, erythromycin and tetracycline. The MICs to gentamicin, azithromycin and tigecycline were increased by 4-fold.

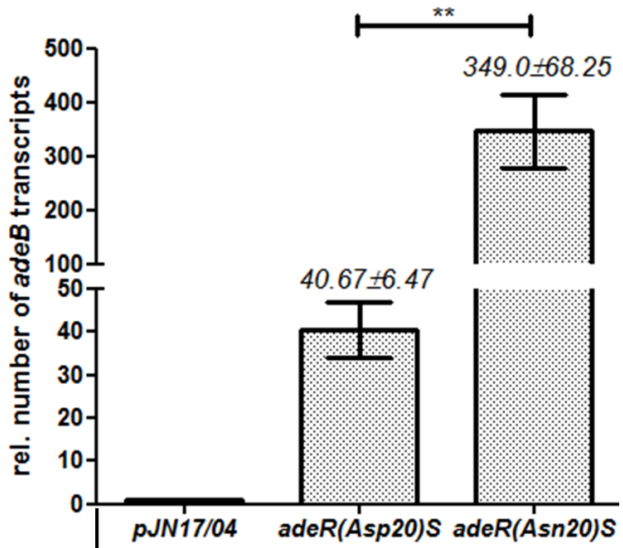

Antimicrobial class	Antimicrobial	pJN17/04	adeR(Asp20)S	adeR(Asn20)S
Aminoglycosides	Amikacin	4	8	16
	Gentamicin	1	4	16
Carbapenems	Meropenem	4	4	4
Fenicols	Chloramphenicol	256	256	256
Fluoroquinolones	Ciprofloxacin	0.5	1	2
	Levofloxacin	0.25	0.5	1
Glycylcyclines	Tigecycline	1	1	4
Macrolides	Erythromycin	32	32	64
	Azithromycin	4	32	128
Rifamycins	Rifampicin	n.t.	n.t.	n.t
Tetracyclines	Tetracycline	4	4	8
	Minocycline	0.125	0.25	0.25

Figure 3.22 Relative *adeB* expression and MICs (mg/L) of the Scope 23 *adeRS* transformants. The number of *adeB* transcripts was related to the empty vector control after being normalized to the expression of the reference gene *rpoB*. qRT-PCR data displayed are representative of three independent experiments and results are shown as mean ± standard error of the mean. Statistical analysis was carried out with the recorded absolute values by performing an unpaired t-test. **, $P < 0.01$. Antimicrobial susceptibility was determined by agar dilution.

In addition to *adeB* expression and the susceptibility testing, *adeG* and *adeJ* expression were determined and growth curves were conducted for all *adeRS* and empty vector transformants. Results are shown in Figure 3.23 and 3.24.

A. ATCC 19606

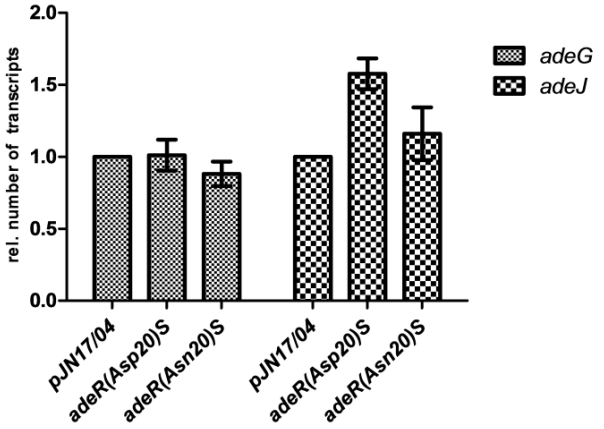

B. BMBF 320

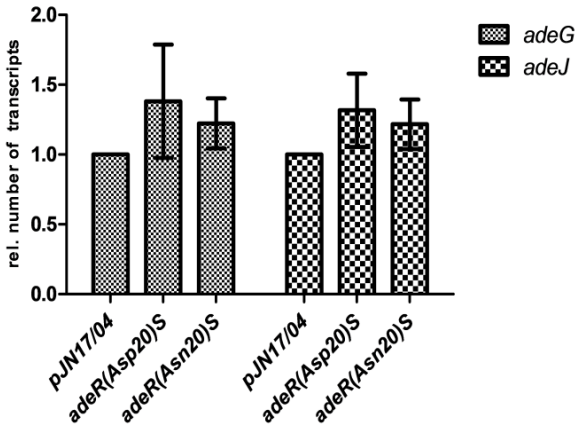

C. Scope 23

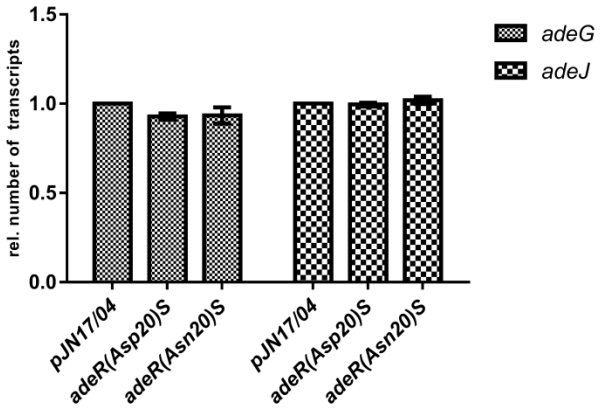

Figure 3.23 Relative *adeG* and *adeJ* expression in (A) ATCC 19606, (B) BMBF 320, and (C) Scope 23 *adeRS* transformants. The number of *adeG* or *adeJ* transcripts was related to the empty vector control after being normalized to the expression of the reference gene *rpoB*. Data displayed are representative of three independent experiments and results are shown as mean ± standard error of the mean.

As observed previously for the *A. baumannii* ATCC 17978 transformants (Fig. 3.18), no significant change in either *adeG* or *adeJ* expression was observed in the other *A. baumannii* transformants (Fig. 3.23). Similarly, no fitness cost could be detected for the ATCC 19606, BMBF 320 or Scope 23 *adeRS* transformants compared to their empty vector controls (Fig. 3.24).

A. ATCC 19606

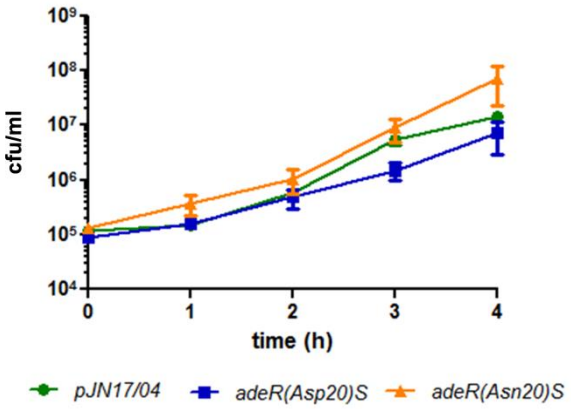

B. BMBF 320

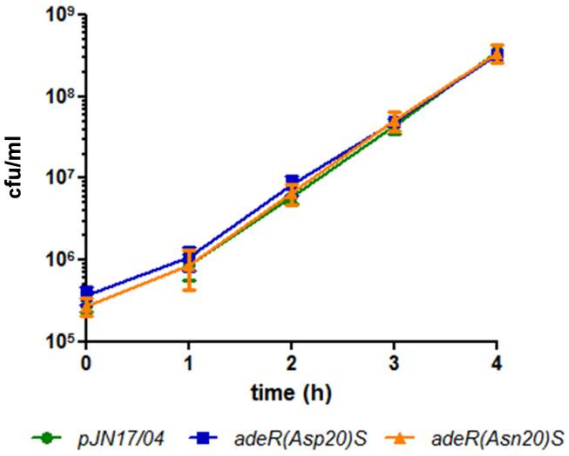

C. Scope 23

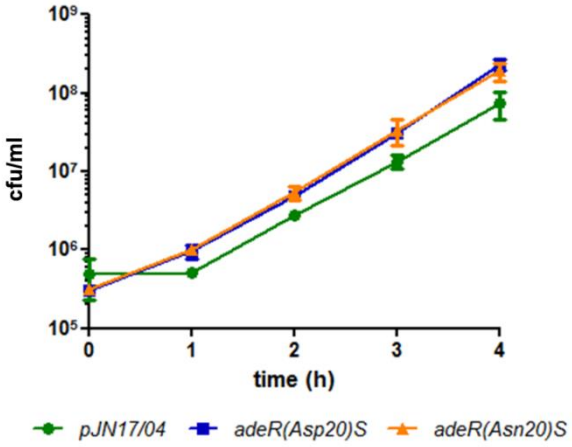

Figure 3.24 Growth of the *A. baumannii* (A) ATCC 19606, (B) BMBF 320, and (C) Scope 23 *adeRS* transformants. Growth kinetics were performed recording growth at hourly intervals, for 4 hours. Data displayed are representative of at least two independent experiments and results are shown as mean ± standard error of the mean.

Having determined both *adeB* expression and antimicrobial susceptibility, in three further *A. baumannii* strains transformed with both *adeRS* constructs, we observed that the downstream effects were not equal in each isolate. Whereas the introduction of *adeR(Asp20)S* lowered the number of *adeB* transcripts by 70% compared to the empty vector control in the *A. baumannii* reference strain ATCC 19606 (Fig. 3.20), no change was observed in BMBF 320 (Fig. 3.21), and in Scope 23 *adeB* expression was elevated (Fig. 3.22; comparable to ATCC 17978, Fig. 3.15). With the *adeR*(Asn20)*S* construct, *adeB* expression was increased in all *A. baumannii* strains, with the lowest fold-difference in ATCC 19606, and the highest in Scope 23, relative to the empty vector control. Overall it can be said that the lower the initial *adeB* expression of the recipient strain, the higher the *adeB* expression after introducing *adeR*(Asn20)*S*. Furthermore, we could show that by increasing the number of *adeB* transcripts, the susceptibilities to multiple classes of antimicrobials was affected.

Neither *adeG* or *adeJ* expression, nor the fitness were changed in any of the four *A. baumannii* strains.

However, as we introduced the *adeRS* copies of the clinical isolates F and G on top of the chromosomally encoded genes of each recipient strain, we cannot rule out possible interactions between the plasmid and chromosomally encoded proteins and the impact it might have. Furthermore, looking at the AdeS amino acid sequence of all tested *A. baumannii* strains, we could determine 20 amino acid differences (Fig. 3.25). Whereas certain polymorphisms were common in all strains compared to isolate F and G (e.g. V94A, R299Q, K339Q), others might be strain specific (e.g. P172L for ATCC 17978, T153A for ATCC 19606, S179I for BMBF 320 and N273H for Scope 23). Regarding AdeR, the amino acid sequence was found to be more conserved, as only three polymorphisms were found (L241P for ATCC 19606, L142I and V243I in BMBF 320) (Fig. 3.26).

Figure 3.25 Comparison of the AdeS amino acid sequences among the tested *A. baumannii* strains.

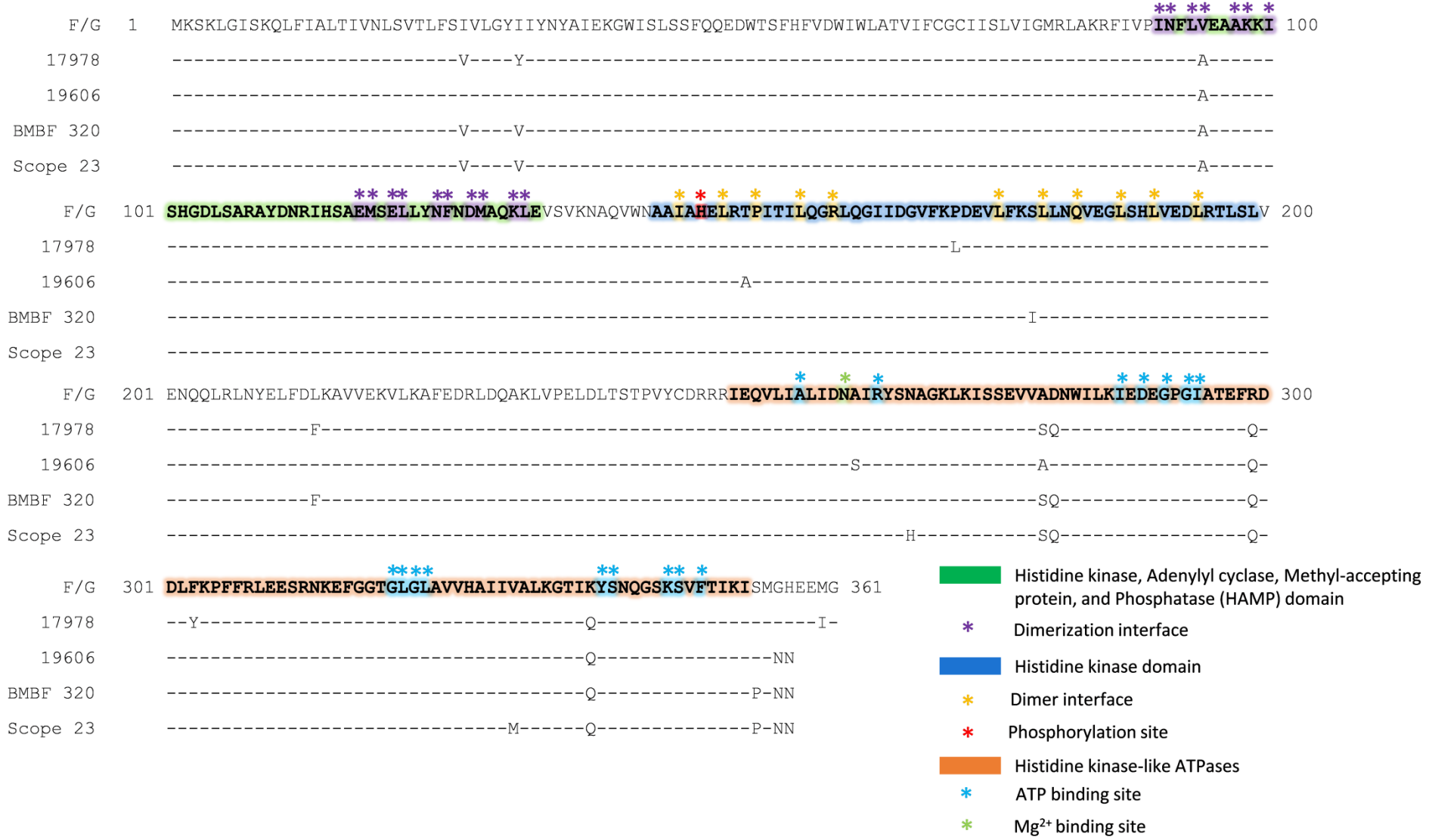

Figure 3.26 Comparison of the AdeR amino acid sequences among the tested *A. baumannii* strains.

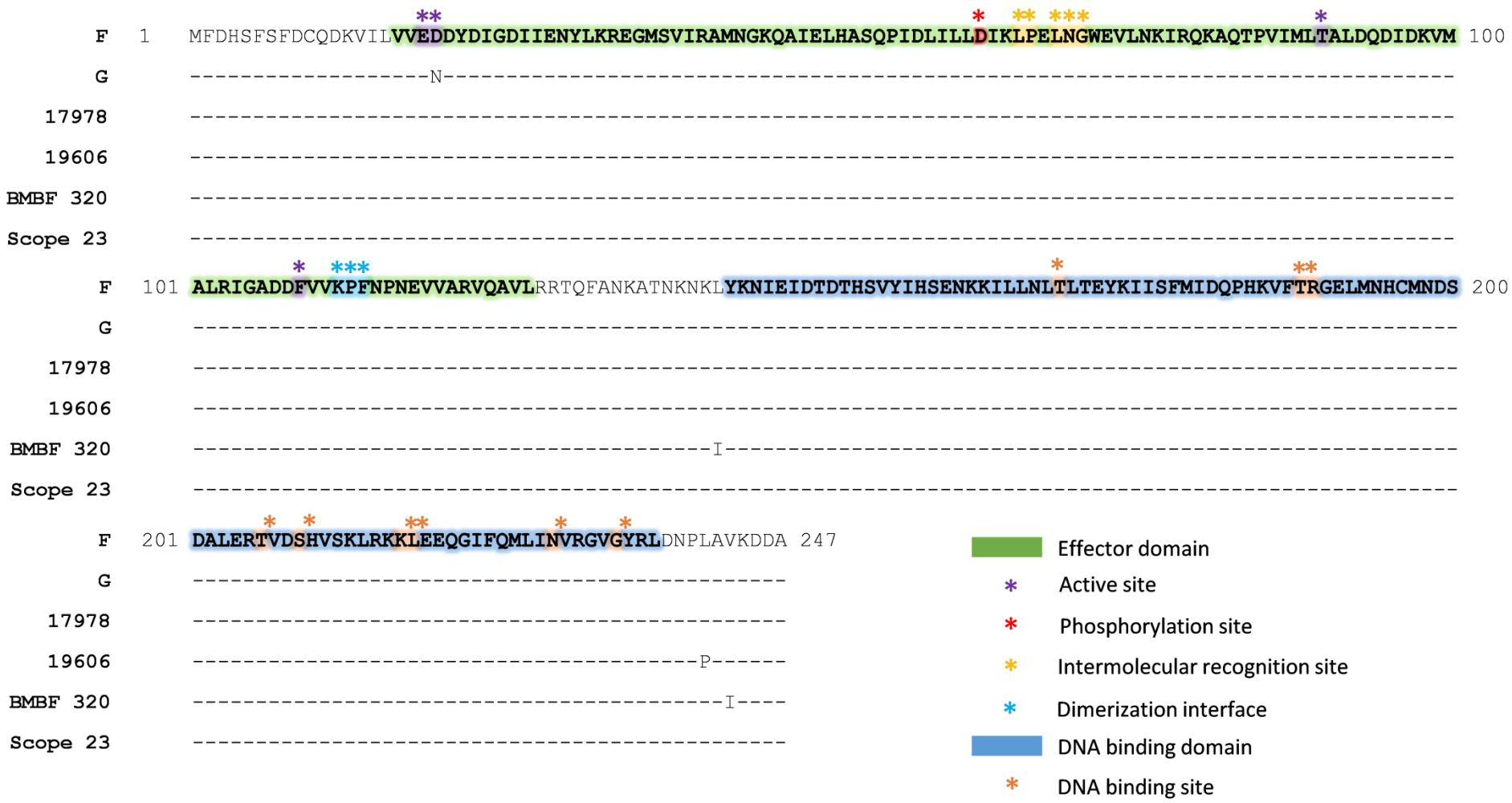

3.3.3 Investigation of the Asp20→Asn substitution in the adeRSABC deficient isolate NIPH 60

In order to test the impact of the Asp20→Asn substitution in AdeR without the influence of AdeRS encoded on the chromosome, in the next step we chose the clinical isolate NIPH 60. Whole-genome sequencing revealed that NIPH 60 is deficient in the AdeRSABC cassette [244]. In this way, any detectable differences could directly be correlated to the mutation in the introduced *adeR* gene. The two forms of *adeRS* alone or in combination with the whole *adeABC* operon were introduced and their impact on antimicrobial susceptibility was investigated for the previously used eight structurally diverse antimicrobial classes. In addition, a control *adeABC* construct (without the regulators *adeRS*) was generated and transformed into NIPH 60. Results are summarized in Table 3.6.

With the introduction of *adeRS,* no change in antimicrobial susceptibility was observed in either the *adeR*(Asp20)*S* or the *adeR*(Asn20)*S* transformant compared to the empty vector control. The same was true for the *adeABC* construct. With the *adeR*(Asp20)*SABC* construct an increase in the MICs to six antimicrobials was recorded compared to the empty vector control; minor changes in the MICs of amikacin, ciprofloxacin, levofloxacin, tigecycline and erythromycin by 2-fold, as well as an 8-fold and 32-fold increase in gentamicin and azithromycin MIC, respectively, were observed. However, the introduction of the *adeR*(Asn20)*SABC* construct had a greater impact on the susceptibility to six of eight tested antimicrobial classes. Besides a 2-fold increase in the meropenem MIC, a 4-fold increase in the MIC was observed for amikacin, levofloxacin, erythromycin and tetracycline. Ciprofloxacin, tigecycline and gentamicin MICs increased by 6-, 8- and 16-fold, respectively, and azithromycin increased by 64-fold. Comparing the two *adeRSABC* transformants with each other to catch the effect which is only due to the missense mutation in *adeR*, the Asn20 transformants recorded higher MICs compared to the Asp20 transformants especially with ciprofloxacin, tetracycline and tigecycline, where a 4-fold increase in the MIC was observed.

Table 3.6 MIC values (mg/L) of *A. baumannii* NIPH 60 transformants. Adapted from Nowak *et al*. [292].

Antimicrobial class	Antimicrobial	pJN17/04	*adeR(Asp20)S*	*adeR(Asn20)S*	*adeABC*	*adeR(Asp20) SABC*	*adeR(Asn20) SABC*
Aminoglycosides	Amikacin	4	4	4	4	8	16
	Gentamicin	1	1	1	1	8	16
Carbapenems	Meropenem	0.5	0.5	0.5	0.5	0.5	1
Fenicols	Chloramphenicol	128	128	128	128	128	128
Fluoroquinolones	Ciprofloxacin	0.25	0.25	0.25	0.25	0.5	2
	Levofloxacin	0.125	0.125	0.125	0.125	0.25	0.5
Glycylcyclines	Tigecycline	0.5	0.5	0.5	0.5	1	4
Macrolides	Azithromycin	1	1	1	1	32	64
	Erythromycin	8	8	8	8	16	32
Rifamycins	Rifampicin	4	4	4	4	4	4
Tetracyclines	Tetracycline	2	2	2	2	2	8
	Minocycline	0.125	0.125	0.125	0.125	0.125	0.125

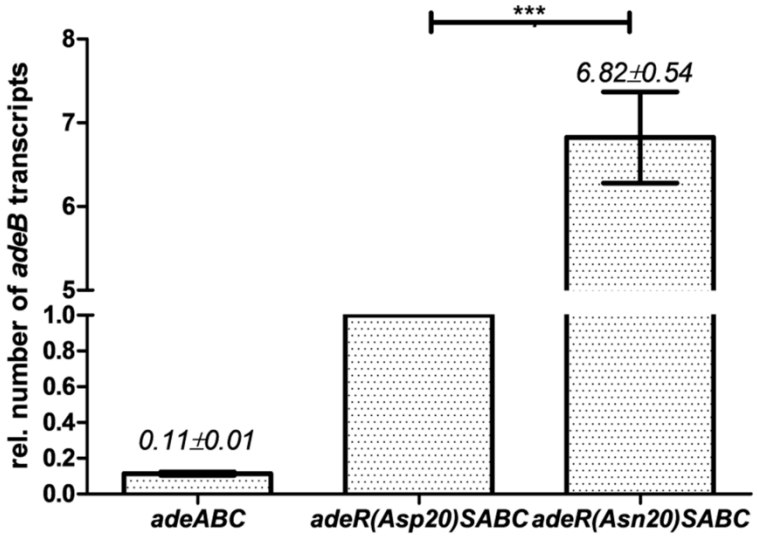

Figure 3.27 Relative *adeB* expression in NIPH 60 *adeRSABC* transformants. The number of transcripts of the *adeR(Asn20)SABC* and *adeABC* transformants have been related to the *adeR(Asp20)SABC* transformants after being normalized to the expression of the reference gene *rpoB*. Data displayed are representative of four independent experiments and results are shown as mean ± standard error of the mean. Statistical analysis was carried out with the recorded absolute values by performing an unpaired t test. ***, $P < 0.001$.

To confirm whether the difference in the susceptibility profile between the two *adeRSABC* transformants is due to a different expression of *adeB*, qRT-PCR was performed. As a control, the *adeABC* construct was included in the expression measurement. A 6.8-fold increase in *adeB* expression of the *adeR*(Asn20)*SABC* transformants was recorded compared to the *adeR*(Asp20)*SABC* transformants (Fig. 3.27). Very low *adeB* expression was recorded with the transformants harbouring only the *adeABC* operon.

The efflux pump inhibitor NMP has been shown to effectively inhibit antimicrobial extrusion in *adeB*-overexpressing *A. baumannii* strains [291]. To further investigate whether the MIC changes induced by our *adeRSABC* constructs are reversible, 100 mg/L NMP was added to the agar during agar dilution. Results are shown in Table 3.7.

Table 3.7 MIC values (mg/L) of NIPH 60 transformants with and without the addition of the efflux pump inhibitor NMP

Antimicrobial class	Antimicrobial	pJN17/04		*adeR*(Asp20)*SABC*		*adeR*(Asn20)*SABC*	
		- NMP	+NMP	-NMP	+NMP	-NMP	+NMP
Aminoglycosides	Amikacin	4	8	8	8	16	16
	Gentamicin	1	1	8	4	16	8
Carbapenems	Meropenem	0.5	1	0.5	1	1	1
Fenicols	Chloramphenicol	128	16	128	16	128	16
Fluoroquinolones	Ciprofloxacin	0.25	0.25	0.5	0.5	2	1
	Levofloxacin	0.125	0.125	0.25	0.25	0.5	0.5
Glycylcyclines	Tigecycline	0.5	0.25	1	0.25	4	0.25
Macrolides	Azithromycin	1	0.25	32	8	64	16
	Erythromycin	8	4	16	8	32	16
Rifamycins	Rifampicin	4	4	4	4	4	4
Tetracyclines	Tetracycline	2	1	2	1	8	1
	Minocycline	0.125	0.03	0.125	0.03	0.125	0.03

With the addition of efflux pump inhibitor NMP, no reduction in the MICs to amikacin, meropenem, levofloxacin and rifampicin was observed compared to the control values in the absence of NMP (Table 3.7). In the case of chloramphenicol and minocycline, the MICs were consistently reduced from 128 mg/L and 0.125 mg/L to 16 mg/L and 0.03 mg/L, respectively, for all NIPH 60 transformants, including the vector control. Based on the fact that chloramphenicol and minocycline MICs did not increase with the introduction of the *adeRSABC* constructs, compared to the empty vector control, these result suggest that efflux pumps other than AdeABC (targeting chloramphenicol and minocycline) are also inhibited by NMP. Minor reductions in the MICs to gentamicin, ciprofloxacin, and erythromycin by 2-fold and a 4-fold reduction in the azithromycin MICs were observed compared to the control

values of the *adeRSABC* transformants. However, the susceptibility to tigecycline and tetracycline (that was initially decreased by the *adeRSABC* constructs) was increased in the presence of NMP. Tigecycline and tetracycline MICs were reduced 4- to 8-fold in comparison to the control values in the absence of NMP, from 1 or 4 mg/L to 0.25 mg/L in the case of tigecycline and from 8 mg/L to 1 mg/L in the case of tetracycline.

In order to get a complete picture of RND-pump expression, expression of *adeG* and *adeJ* was also investigated with NIPH 60 transformants. No significant difference in the expression of *adeG* or *adeJ* was detected between the *adeRS, adeABC* and *adeRSABC* transformants compared to the empty vector control (Fig. 3.28).

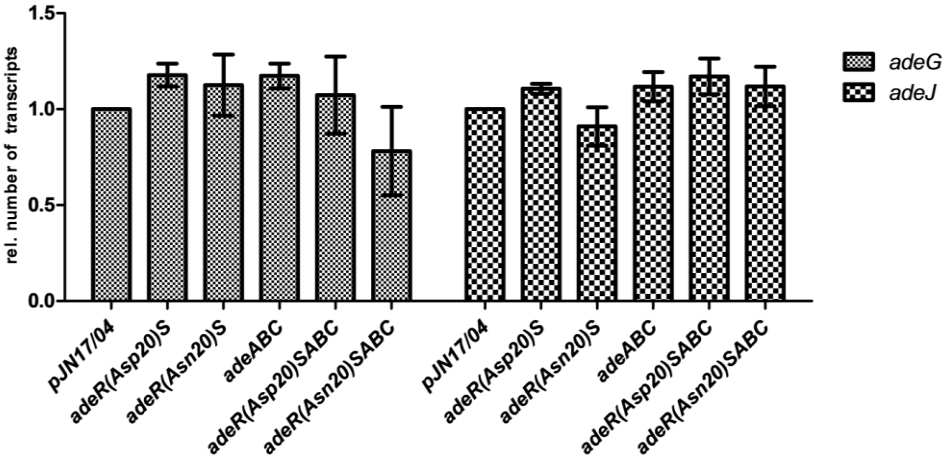

Figure 3.28 Relative *adeG* and *adeJ* expression in NIPH 60 transformants. The number of *adeG* or *adeJ* transcripts was related to the empty vector control after being normalized to the expression of the reference gene *rpoB*. Data displayed are representative of three independent experiments results are shown as mean ± standard error of the mean.

To determine if increased expression of *adeB* was accompanied by fitness costs for the transformants, growth curves were performed. In this case, only the *adeRSABC* transformants were considered, as they were the only transformants expressing *adeB*. Although growth of the *adeRSABC* transformants was slightly decreased after 1h, no difference in growth rates between either of the *adeRSABC* transformants and the empty vector control was observed over the recording course of 4h (Fig. 3.29), suggesting that the introduced pump had no effect on the overall fitness of NIPH 60.

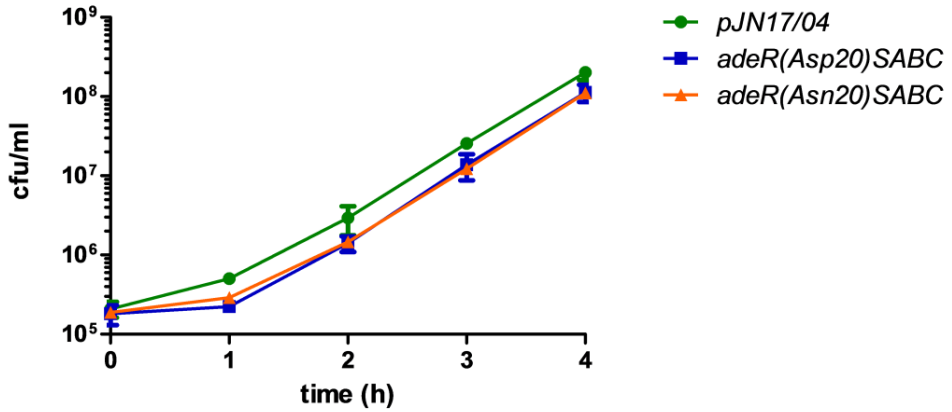

Figure 3.29 Growth of the *A. baumannii* NIPH 60 *adeRSABC* transformants. Growth kinetics were performed recording growth at hourly intervals, for 4 hours. Data displayed are representative of three independent experiments and results are shown as mean ± standard error of the mean.

To determine whether the substitution in AdeR has an impact on substrate extrusion, an ethidium accumulation assay was performed using all NIPH 60 transformants. The levels of ethidium accumulation of the empty vector control and the different transformants are summarized in Figure 3.30 and 3.31. There was no significant difference between the *adeRS* and the *adeABC* transformants as all three showed a similar ethidium accumulation compared to the empty vector control (Fig. 3.30).

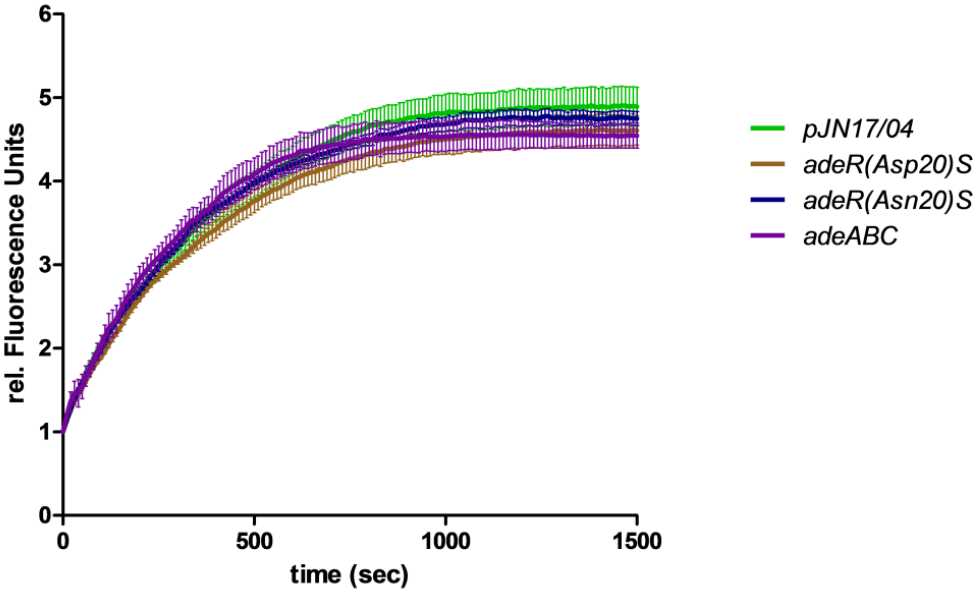

Figure 3.30 Ethidium accumulation of NIPH 60 *adeRS* and *adeABC* transformants. The fluorescence intensity was recorded at excitation and emission wavelengths of 530 and 600 nm, respectively, every 10 seconds over a 25 min incubation period. Data displayed are representative examples of four independent experiments and results are shown as mean ± standard error of the mean.

However, ethidium accumulation was significantly reduced in the *adeRSABC* transformants (Fig. 3.31). At steady state, which was reached approximately 15 min after ethidium bromide addition, the *adeR(Asp20)SABC* transformant accumulated about 12% less ethidium compared to the empty vector control whereas with the *adeR(Asn20)SABC* construct, ethidium accumulation was approximately 72% of that observed for the control.

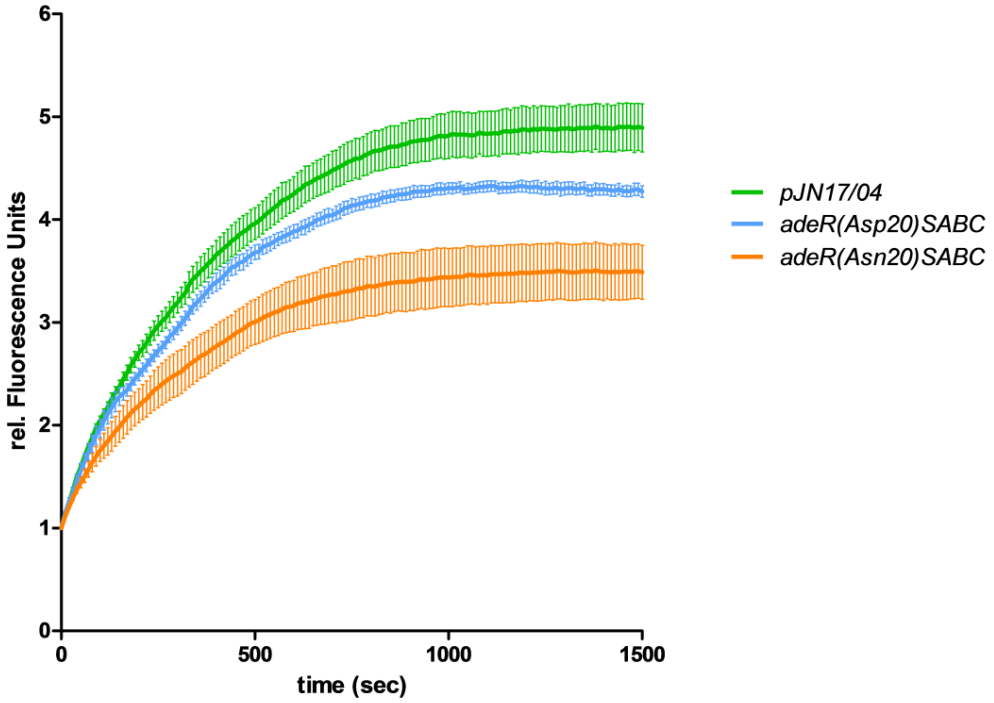

Figure 3.31 Ethidium accumulation of NIPH 60 *adeRSABC* transformants. The fluorescence intensity was recorded at excitation and emission wavelengths of 530 and 600 nm, respectively, every 10 seconds over a 25 min incubation period. Data displayed are representative examples of four independent experiments and results are shown as mean ± standard error of the mean. Taken from Nowak *et al*. [292].

Addition of the proton motive force uncoupler CCCP induced a rapid increase in accumulated ethidium in all three transformants, so that their accumulation of ethidium was nearly identical (Fig. 3.32). This indicated that the reduced ethidium accumulation observed before (Fig. 3.31) was due to the activity of the proton motif force-driven transporter AdeABC.

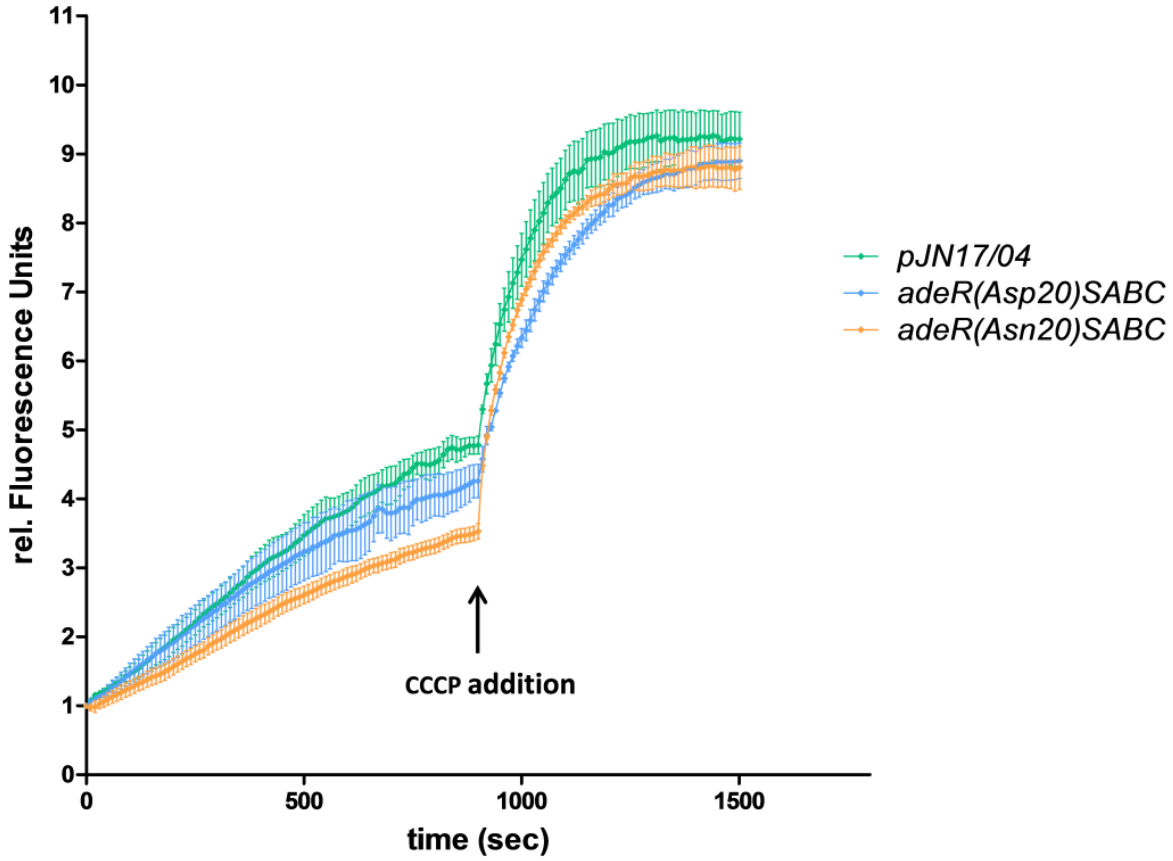

Figure 3.32 Ethidium accumulation of NIPH 60 *adeRSABC* transformants after CCCP addition. Cells were resuspended to an OD of 2 at 600 nm. CCCP (500 µM) was added at the time indicated by the arrow. Data displayed are representative examples of three independent experiments and results are shown as mean ± standard error of the mean. Taken from Nowak *et al.* [292].

In addition to ethidium, the accumulation of the efflux substrates acriflavine and rhodamine 6G was also assayed. However, no significant difference in their accumulation was detected comparing the *adeR(Asn20)SABC* transformant with the empty vector control during two independent runs (Fig. 3.33), suggesting that acriflavine and rhodamine 6G are not substrates of AdeABC.

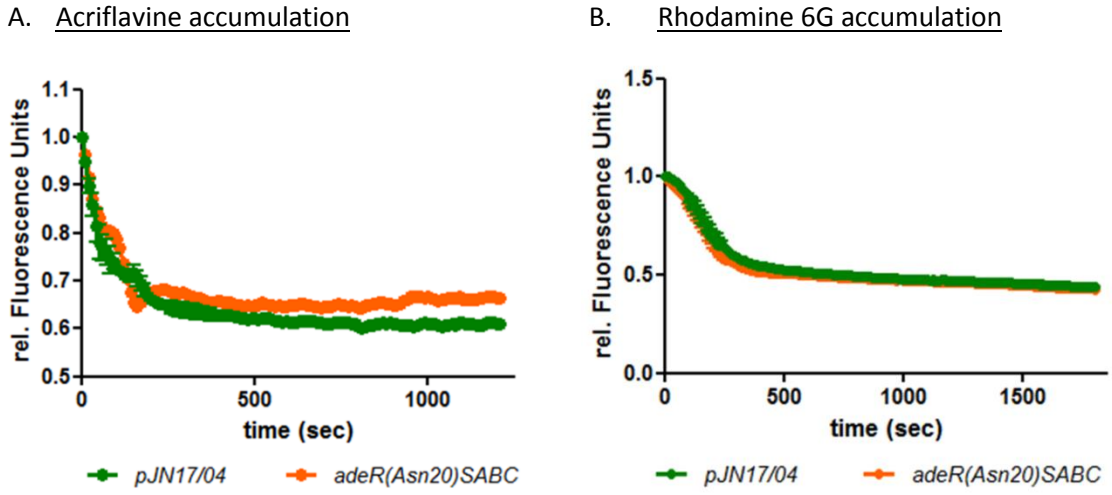

Figure 3.33 Acriflavine (A) and rhodamine 6G (B) accumulation of NIPH 60 *adeR*(Asn20)*SABC* transformants. The fluorescence intensity was recorded at excitation and emission wavelengths of 416 and 514 nm in the case of acriflavine or 480 nm and 558 nm for rhodamine 6G, respectively, every 10 seconds over a 20 to 30 min incubation period. Data displayed are representative examples of two independent experiments and results are shown as mean ± standard error of the mean.

Furthermore, competition assays were performed adding sub-inhibitory concentrations of antimicrobials to the cell suspension in addition to ethidium. In this way, it could be determined whether one of the antimicrobials is preferably exported over ethidium. As tetracycline and tigecycline showed the greatest difference in MIC values between both *adeRSABC* transformants (Table 3.6), they were chosen as promising potential competitors. No change in the accumulation of ethidium could be detected with either antimicrobial (Fig. 3.34 C and D). Additionally, competition experiments were performed using azithromycin and gentamicin at sub-inhibitory concentrations. Similar to tetracycline and tigecycline, with the addition of 32 mg/L azithromycin or 4 mg/L gentamicin, respectively, no change in ethidium accumulation was observed (Fig. 3.34 A and B), suggesting that ethidium is preferably extruded or both substrates (ethidium and the respective antimicrobial) do not compete for the same binding site within AdeB.

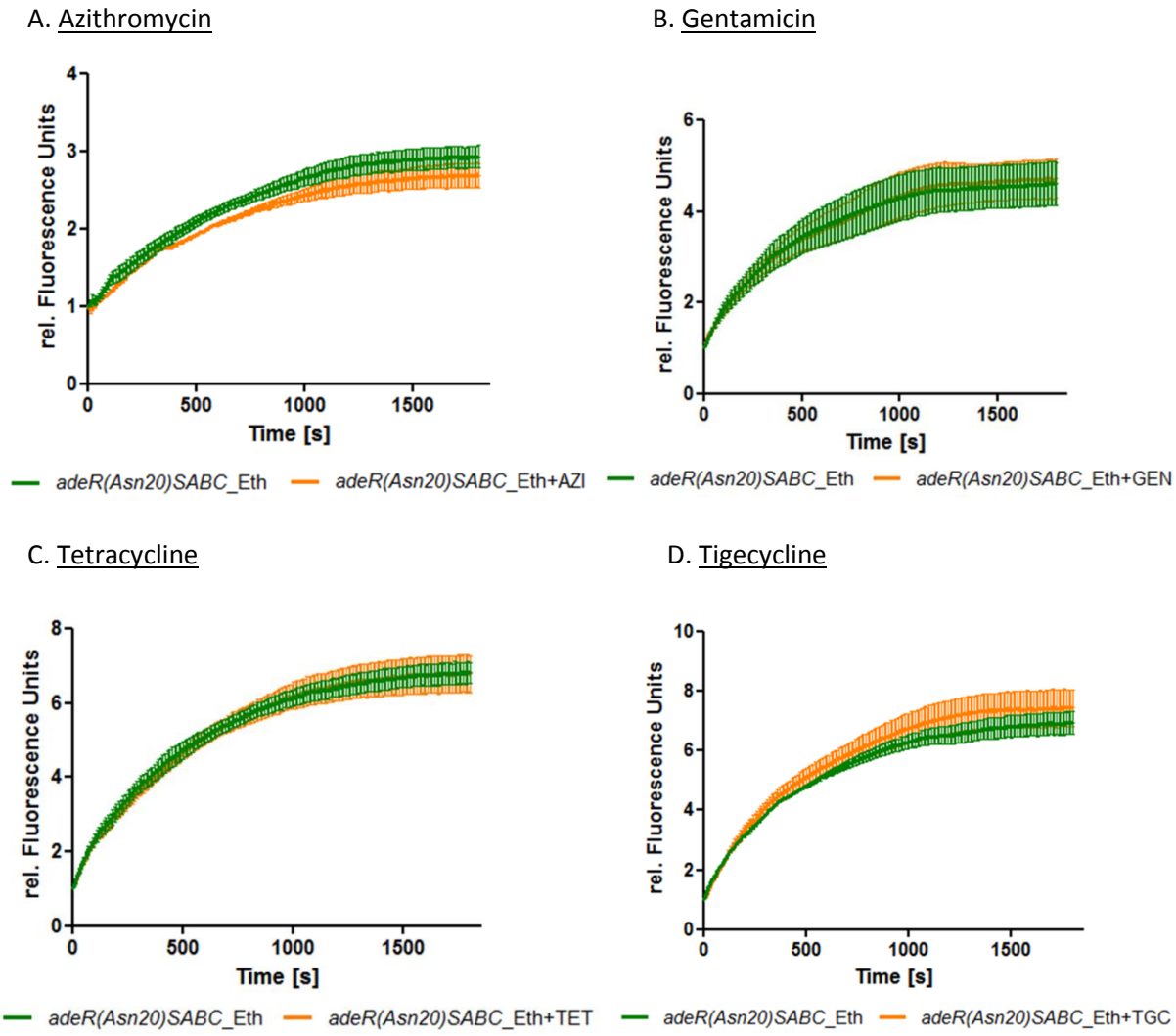

Figure 3.34 Ethidium bromide competition assay. (A) 32 mg/L azithromycin, (B) 4 mg/L gentamicin, (C) 2 mg/L tetracycline and (D) 2.5 mg/L tigecycline were added to the cell suspension shortly after ethidium bromide addition. The fluorescence intensity was recorded at excitation and emission wavelengths of 530 and 600 nm, respectively, every 10 seconds over a 30 min incubation period. Data displayed are representative examples of three independent experiments and results are shown as mean ± standard error of the mean.

Concluding this chapter, the Asn20 substitution in AdeR leads to an increased expression of *adeB* (Fig. 3.27). Accumulation assays revealed that the accompanied decrease in multiple, structurally unrelated antimicrobials (Table. 3.6) seems to be due to the enhanced efflux activity of the proton-motive force-dependent AdeABC efflux system (Fig. 3.31-32).

4. Discussion

4.1 Prevalence of eight resistance-nodulation-cell division-type efflux pump genes in epidemiologically characterized A. baumannii of worldwide origin

Investigating the prevalence of RND-type efflux pump encoding genes, we report that these efflux systems are widely distributed in *A. baumannii*; 5 of 8 RND-efflux pump encoding genes were present in all 144 tested isolates and the other 3 genes had a prevalence varying between 56% and 97%. To our knowledge, this is the first report describing the distribution of both characterized and uncharacterised RND efflux pumps in a genotypically diverse pool of clinically relevant *A. baumannii* isolates of worldwide origin.

In 2006, Chu *et al*. reported the presence of three efflux systems in different *Acinetobacter* genomic DNA groups. In their collection of 56 *A. baumannii* isolates 70% were positive for *adeB* by PCR [253]. However these isolates came from only one hospital in Hong Kong and might include duplicate strains. Similarly, working with isolates from one hospital in Sichuan, China, Lin *et al*. reported that 84% and 90% of their 112 non-repetitive isolates carried *adeB* or *adeJ*, respectively [254]. Yet, the isolates they investigated belonged to the Acb-complex and thus did not only include *A. baumannii.* Focusing on a predominantly European collection, Nemec *et al*. investigated 116 *A. baumannii* isolates belonging to IC1-3 as well as genotypically unique strains [244]. Eighty-two percent of the isolates carried a*deB*. In another European study that included related and unrelated isolates belonging to IC1, IC2 and genotypically unique strains, 49 out of 51 isolates harboured *adeB* [105].

In these previous studies, only one primer pair was used. However, if there are nucleotide polymorphisms within the primer annealing site that lead to no amplicon, a false negative result can occur. The finding of 11 *adeB* sequence types among 50 *A. baumannii* isolates belonging to European clones 1-3 (IC1-3) demonstrate the sequence variability in this gene [252]. For this reason we used two separate primer pairs per gene, when necessary. Whereas no second primer pair was necessary for the detection of *adeJ* and ACICU_03646; the use of both primer sets was frequently required for the remaining efflux pump genes. In 66% of cases, in which a negative result was obtained with the first pair of primers, using the second pair gave a positive result. While it still is possible that nucleotide polymorphisms

within the second primer annealing sites could result in a false negative result, when we analysed available genome sequences, these polymorphisms were rarely found.

We found no association between the epidemiological background of an isolate and its efflux gene profile. It is noteworthy that 5 of the 8 investigated RND-family genes were present in all isolates tested. The other three pumps, including *adeB*, showed a high prevalence in our diverse pool of isolates. As bacterial genomes are highly plastic and genes of no need or function are rapidly removed or replaced [293], this finding supports a defined function of each individual pump that has still to be determined. In *P. aeruginosa* it has been shown that MexAB, MexCD, MexEF and MexXY each have fixed functions, e.g. MexCD functions as part of the envelope stress response (expression is induced in response to membrane damage) [294], while MexEF is linked to the organism's nitrosative stress response (if reactive nitrogen and oxygen species cause cell damage) [295], and oxidative stress activates MexXY expression [296]. Except for the overlapping substrate profile of AdeB, AdeJ and AdeG, and a growth phase-dependent expression of these genes [259] little is known about regulation of the RND-type efflux systems in *A. baumannii*. A synergy of efflux combined with other resistance mechanisms has been observed to achieve high-level antimicrobial resistance [89, 245, 297]. Investigating 40 isolates endemic to New York, Bratu *et al.* for example detected increased levels of β-lactamases and *adeABC* expression, the presence of aminoglycoside-modifying enzymes as well as mutations in DNA gyrase, which in combination were responsible for cephalosporin, meropenem, aminoglycoside and fluoroquinolone resistance, and reduced susceptibilities to cefepime and tigecycline [245]. Further insight into the functionality of each pump including a characterization of the reported putative RND-type efflux pumps might reveal their individual importance in this organism.

In conclusion, the presence of the eight RND-efflux pumps in our geographically and genotypically diverse collection of worldwide *A. baumannii* isolates varied between 56 and 100%. No association between IC clusters and the presence or absence of the pumps was observed. However, the fact, that at least another five uncharacterised RND-pumps are encoded on the chromosome illustrates the need for further investigations to gain a better understanding of their contribution to the ever-increasing emergence of multidrug resistant *A. baumannii*.

4.2 Characterization of the putative RND-type efflux pump A1S_2660

To date three RND-type efflux systems have been characterized in *A. baumannii* [112, 126, 133]. Whereas AdeABC seems to be the predominant transporter system most often associated to an acquired MDR phenotype in clinical isolates worldwide, AdeIJK is involved in intrinsic resistance having a minor effect on high-level resistance as its overexpression is toxic to the cell [127]. The role and clinical significance of AdeFGH has not yet been elucidated. It is not expressed constitutively and strains overexpressing this pump have rarely been reported. However, depending on the strain and genome annotation, 7-19 RND pumps are encoded on the chromosome of *A. baumannii* [90, 284]. Using the sequenced genomes of *A. baumannii* ACICU, AB0057 and ATCC 17978 and the amino acid sequence of AdeB as a reference, we identified 5 putative RND transporters in addition to the previously characterized ones. Showing the highest amino acid identity to AdeB among all of the putative exporters (40% similarity), it was the aim to further characterize the pump ACICU_02904/A1S_2660 (locus tag in *A. baumannii* ACICU and *A. baumannii* ATCC 17978, respectively) by determining its inducers and substrates. According to our prevalence study, this pump was present in all of the 144 tested genotypically and geographically diverse clinically relevant *A. baumannii* isolates as well as in 25 fully sequenced and annotated genomes available in the NCBI database, suggesting a function relevant to *A. baumannii*.

RT-PCR revealed that this putative transporter is not constitutively expressed in *A. baumannii* ATCC 17978. Using the β-galactosidase reporter assay, we were able to confirm the cryptic nature of this pump and identify substances inducing its transcription. Expression of A1S_2660 was induced by antimicrobial agents (carbapenems and chloramphenicol) as well as ethanol, NaCl and sulbactam.

To date, practically no data have been published linking specific substances or environmental changes to the induced expression of characterized RND-type efflux pumps in *A. baumannii*. Merely, *adeA* has been reported to be overexpressed upon NaCl exposure [260]. However, in other bacterial genera a wide variety of stimuli and effector molecules could be linked to the induced transcription of RND transporters in order to export these toxic substances, including different stress signals (oxidative stress, envelope stress; see Chapter 4.1.), antimicrobials, detergents, disinfectants and bile salts, [199, 298]. Especially of concern is the induction of A1S_2660 by carbapenems, which may constitute a significant

threat to the hospital environment as these are the antibiotics of choice to treat infections with MDR Gram-negative bacteria, including *A. baumannii*. Additionally, NaCl at physiological concentrations (170-200 mM) is not only present in health care environments (as a constituent of drug formulations, wound dressings, intravenous fluids) but also in the human host (e.g. in body fluids and on the skin surface) [260]. Thus, expression of this putative pump could easily be induced in hospital settings as well as in the community. However, the induced expression of A1S_2660 was still relatively low, as with the β-galactosidase assay the expression was only visible after ≥24 hours. With this induced low-level expression, possible changes in the resistance phenotype of the cell would not have been detectable with conventional susceptibility testing methods.

Overexpression of A1S_2660 in the *A. baumannii* reference strain ATCC 17978 using an expression plasmid reduced cell growth, suggesting that the energy consumed for the synthesis and/or functioning of the transporter resulted in a fitness cost to the cell. This was supported by experimental findings, which correlated the overexpression of some exporters to decreased cell growth [225, 299]. For AdeIJK a similar phenomenon has been described; overexpression of *adeJ* up to a certain threshold led to low-level resistance, whereas overexpression above this undefined threshold was toxic to the cell and led to impaired growth [127]. Additionally, nutrients essential to the cell could be substrates of the pump, so that extruding them could lead to cell stasis [222, 223]. In *A. baumannii* ATCC 17978 *adeABC*, *adeIJK* and *adeFGH* are constitutively expressed. Although overexpression of more than one efflux pump at the same time has been shown without any negative effect on cell survival [300-302], it is possible that ATCC 17978 could not compensate the (over-) production of another efflux pump.

Several RND-type efflux systems of *P. aeruginosa* (MexPQ-OpmE, Mex MN-OprM, Mex VW-Oprm, and TriABC-OpmH) have been shown to confer antimicrobial resistance if the host was deficient in the major RND pumps like MexAB, MexCD-OprJ, MexEF-OprN and MexXY [303-305]. Due to overlapping substrate profiles, it is possible that the impact of these 'minor' transporters on antimicrobial resistance is dwarfed by the major pumps making their contribution difficult to detect. Furthermore, the expression of minor exporters might especially be enhanced when major pumps are not present. Supporting the latter assumption, Eaves *et al*. reported increased expression of *acrD* in *Salmonella* when *acrB* or *acrF* were inactivated [306]. To mimic such a scenario, A1S_2660 was overexpressed in the

A. baumannii clinical isolate NIPH 60, which is deficient in the *adeRSABC* genes. As AdeIJK and AdeFGH show only minor effects on resistance, their presence could be neglected. Under these conditions, overexpression of A1S_2660 did not lead to impaired growth of NIPH 60 cells. It remains speculative whether NIPH 60 has a low overall energy cost, so that the overexpression of A1S_2660 was not harmful to the cell, or whether it can adapt better to this new condition and compensate the additional energy consumed. In MexEF-OprN-overproducing *P. aeruginosa* for example, the accompanied fitness cost (due to cytoplasmic acidification caused by MexEF-mediated proton influx) was metabolically compensated by increasing the oxygen uptake and enhancing the expression of the nitrate respiratory chain [307]. In this way, cytoplasmic acidification was prevented.

When overexpressing A1S_2660 in NIPH 60, we could not detect any changes in the resistance phenotype to the tested compounds which included antibiotics (aminoglycosides, aztreonam, β-lactams, cephalosporins, chloramphenicol, fluoroquinolones, macrolides, nalidixic acid, novobiocin, and tetracyclines), disinfectants (benzalkonium chloride, triclosan), bile salts (deoxycholic acid) and organic dyes (acriflavine, ethidium). All of these substances used have been reported to be extruded by various efflux pumps in other bacteria [199, 308, 309]. It has been reported that substrates of an efflux pump might as well induce its expression [310]. However, identified as inducers of A1S_2660, carbapenems and chloramphenicol could not be identified as substrates. It is possible, that compounds other than the applied ones are substrates of this pump, including bacitracin, chlorhexidine, doxorubicin, fatty acids, metal salts, protamine, puromycin, quaternary ammonium compounds, and toluene. Furthermore, this putative exporter could be involved in cellular responses that were not tested in this study, e.g. responses to nitrosative or oxidative stress as reported for efflux pumps in *P. aeruginosa* [295, 296]. Given that the expression is induced by carbapenems and ethanol, compounds which disrupt the cell wall, this could indicate a function during envelope stress responses.

Based on current knowledge about RND-type efflux pumps, it is possible that A1S_2660 is not functional under the tested conditions. Usually, RND-efflux systems are composed of a periplasmic adaptor protein, the transporter and an outer membrane pore in order to facilitate the extrusion of compounds to the extracellular environment [138]. It is common that the three components are encoded as an operon with a cognate MFP upstream and a cognate outer membrane pore downstream of the transporter. We could neither detect an

MFP nor an outer membrane pore encoded close to this putative pump in the three *A. baumannii* genomes ACICU, AB0057 and ATCC 17978. As these strains belong to diverse epidemiological groups, it is likely that no *A. baumannii* strain has an MFP adjacent to A1S_2660. In *P. aeruginosa* and *Vibrio cholera* it has been demonstrated that a cognate outer membrane pore is not essential for the composition of a functional RND system as the pores can be sequestered from elsewhere. A substrate-dependent utilization of either OprM or OpmH by the MexJK complex was reported, whereby neither outer membrane pore was encoded adjacent to *mexIJ* [255]. In the case of *V. cholerae* the *tolC* encoded outer membrane pore seems to interact with six different RND systems [311, 312]. Even in the case of the major RND efflux system AcrAB-TolC in *E. coli*, TolC is encoded elsewhere on the chromosome [197]. However, the MFP is required for the functionality of the tripartite complex. On the one hand, the MFP is thought to recruit the outer membrane pore to the transporter and assembling them together [173]. On the other hand, conformational changes in the MFP seem to induce a shift within the inner channel of the pore from a closed to an open state in order to let substrates be extruded from the inner cleft of the pump through the pore to the extracellular environment [173]. To date, no RND-type efflux pump has been reported without an associated MFP. In fact, even RND transporters requiring two adaptor proteins have been identified, e.g. the TriABC-OmpH exporter with the two MFPs TriA and TriB [305]. Nevertheless, it is possible that MFPs can be sequestered by A1S_2660, like it has been shown for outer membrane pores. Compounds inducing A1S_2660 expression (carbapenems, chloramphenicol, ethanol and NaCl) might also induce the expression of a specific MFP that is required for A1S_2660 functioning. A transcriptomic approach used under the conditions tested initially (e.g. non-induced vs. NaCl-induced) might help identify an MFP. Subsequently, the MFP could be overexpressed together with A1S_2660, and susceptibility testing of the transformants might reveal substrates of the pump. Thus, further investigations are needed to elucidate the function of this putative efflux pump, which is highly prevalent in *A. baumannii*.

4.3 Characterization of the Asp20→Asn substitution in the response regulator AdeR

To date, numerous substitutions within every functional domain of the AdeRS two-component regulatory system have been associated with the overexpression of the genes encoding AdeABC (Fig. 1.13). Changes in the periplasmic input domain [261] or near to the autophosphorylation site [257] of AdeS for example, could lead to a permanent signal transduction including a constitutive activation of the sensor kinase. Consequently, AdeR would constitutively be activated leading to elevated *adeABC* expression. Similarly, substitutions in the HAMP domain (e.g. G103D) or the ATPase domain could affect signal transduction, ATP binding and/or the autophosphorylation of AdeS, promoting an enhanced transcription of *adeABC* [257, 262]. Amino acid substitutions within the signal receiver domain of AdeR [246, 257] or at its effector domain [262] could further lead to its constitutive activation or enhanced binding to the *adeABC* promoter, respectively. However, these substitutions were merely associated with increased *adeB* expression (and decreased antimicrobial susceptibility) and the detailed mechanisms were not further investigated.
Complementing *adeRS* in an *adeRS* knockout strain, Sun *et al.* were the first to describe the mechanism behind elevated *adeB* expression levels and the concomitant antimicrobial resistance phenotype, which were caused by insertion of the IS element IS*Aba1* in *adeS* [99]. In addition, Yoon *et al.* revealed that the mutation leading to the Ala94→Val substitution in the HAMP linker domain of AdeS is a polymorphism of isolates belonging to IC1 and thus was erroneously reported to be responsible for increased *adeABC* expression [262]. Based on these findings, deeper investigations are necessary in order to unravel the direct impact of the individual mutations on efflux pump expression and the concomitant susceptibility phenotype, instead of speculating on the effect they might have.

The previously reported Asp20→Asn substitution in the response regulator AdeR, which was investigated in thirteen isogenic isolates from one patient, was associated with increased expression of *adeB* and with decreased susceptibility to co-trimoxazole, levofloxacin and tigecycline [89]. The Asp20 residue corresponds to Asp10 in the response regulator PhoB in *E. coli* which has been described to be part of an acidic triad making up the active site for phosphorylation [313, 314]. A mutation at this functionally important phosphorylation site may alter the interaction between AdeS and AdeR mediating the overexpression of *adeABC*.

In order to further characterize this amino acid change, we determined its effect on antimicrobial susceptibility, the expression of the efflux genes *adeB*, *adeJ*, and *adeG*, bacterial growth, and substrate accumulation.

Usually, when investigating the effect of mutations, a knock-out of the specific gene by insertional inactivation, often followed by complementation, is performed in the isolate the mutation was initially detected [111, 126]. In our previous study, the clinical isolate G, in which the Asp20→Asn substitution was recorded, was multidrug resistant [89], rendering it difficult to find a selective marker to generate a knock-out. Therefore, other approaches were taken.

As a first approach *adeR(Asp20)*, *adeR(Asn20)* and *adeS* constructs were introduced into the *A. baumannii* reference strain ATCC 17978 on top of the chromosomally encoded genes. Surprisingly, no significant change in *adeB* expression and antimicrobial susceptibility was detected with the mutant *adeR(Asn20)* construct compared to *adeR(Asp20)*. However, by introducing only the *adeS* construct, the number of *adeB* transcripts increased significantly. Insertional inactivation of *adeS*, performed by Marchand *et al*., provided evidence for an essential role in regulating *adeABC* expression [257]. As the sensor kinase AdeS is the key component in sensing environmental stimuli and transmitting the signal to the response regulator which in turn drives different gene expression, elevated transcripts of *adeB* as a result of additional copies of *adeS* are reasonable. On the other hand, inactivation of *adeR* would impair the signal transduction induced by *adeS*, thus the role of the response regulator alone could not be determined [257].

As the combination of the chromosomally encoded *adeS* and the plasmid encoded *adeR(Asn20)* did not significantly impact *adeB* expression in comparison to *adeR(Asp20)*, we suggested that the synergistic interplay specifically driven by *adeR*(Asn20) and its cognate sensor kinase is responsible for increased *adeB* expression. Introducing the *adeR(Asn20)S* construct this assumption could be verified. Thereby, the fold-difference in the relative number of *adeB* transcripts induced by the *adeR(Asp20)S* and *adeR(Asn20)S* variants was similar to that previously observed for the clinical isolates F and G [89]. Transformants with an *adeR*(Asn20)*AdeS(*17978) construct, which showed a comparable *adeB* expression and antimicrobial susceptibility as the *adeR(Asp20)S* transformants, further supported the assumption that the Asp20→Asn substitution specifically enhances the interaction of AdeR(Asn20) with its cognate AdeS. Evidence supporting this hypothesis comes from

investigations on the response regulator Spo0F, responsible for initiating sporulation in *Bacillus subtilis*. McLaughlin *et al*. propose that the recognition of sensor kinases and their respective response regulators is driven by residues in the core of the response regulator [315]. They suggest that specific buried residues are responsible for presenting the correct surface to the specific sensor kinase, facilitating a defined discrimination of binding partners among multiple kinases in the cell. Thus, it is possible that the Asp20→Asn substitution within the acidic triad of AdeR has an impact on AdeS binding, showing greater specificity for AdeS of the clinical isolates F and G than for the *A. baumannii* reference strains ATCC 17978 (which differs by 11 amino acids).

Introducing the two *adeRS* constructs into three additional *A. baumannii* isolates that differ in their *adeB* expression level [low- (Scope 23), medium- (BMBF 320) to high-level expression (ATCC 19606)], a limited rise in *adeB* expression was detected - the higher the initial expression level, the least increased expression was observed in the *adeRS* transformants. As the synthesis and the function of efflux transporters is an energy-consuming process, it is possible that the cells reach a maximum of *adeABC* expression and concomitant AdeABC synthesis that they can maintain without resulting in a fitness cost. Furthermore, in correlation with the limited increase in *adeB* expression, there was no further decrease in antimicrobial susceptibility. The impact of RND transporters on the susceptibility phenotype is limited to the amount of antimicrobials that enter the periplasm via membrane diffusion and antimicrobials that are extruded from the cytoplasm to the periplasm by primary efflux pumps. As no additional changes in the membrane permeability or the expression of primary efflux transporters were introduced, the contribution of elevated levels of the RND-type exporter AdeABC on the susceptibility phenotype of the cell was restricted.

However, there are limitations to our first approach. Introducing additional *adeRS* copies (from the isolates F and G) on top of the chromosomally encoded ones, we cannot rule out possible interactions between the plasmid and the chromosomally encoded proteins. Furthermore, differences in the genetic background of the strains leading to minor or major distinctions in cellular processes (e.g. stability of mRNA, influx, protein half-life, *adeB* sequences, second regulators not yet identified) may also impact the expression and/or the susceptibility outcome. It had been previously determined in our laboratory that BMBF 320 belongs to IC4, whereas the other three *A. baumannii* strains are genotypically unique. Thus, they cannot directly be compared to one another. In order to test the impact of the

Asp20→Asn substitution in AdeR without the influence of AdeRS encoded on the chromosome, in our next approach the *adeRSABC*-deficient clinical isolate NIPH 60 was used. In this way, the two forms of AdeRS alone or in combination with the whole *adeABC* operon were introduced and specifically investigated with regards to their impact on antimicrobial susceptibility, efflux pump expression, and substrate accumulation. Any detectable differences could directly be correlated to the substitution in AdeR.

Based on the susceptibility data, AdeRS did not appear to regulate any other resistance mechanisms than AdeABC. In the absence of the efflux pump encoding genes *adeABC*, the two-component regulatory system had no effect on antimicrobial susceptibility in NIPH 60. Differences in the MIC values to structurally unrelated antimicrobials, in the number of *adeB* transcripts and ethidium accumulation were only observed when the genes encoding the regulators AdeRS were combined with the *adeABC* operon. Nevertheless, this system might still regulate other genes or cellular processes, which were not addressed in this study. In *E.coli*, the two-component system BaeSR for example does not only regulate gene expression of the RND efflux genes *mdtABC* [316], but more than 60 other genes involved in signal transduction, sugar transport, flagellum biosynthesis, homeostasis or chemotactic response are part of its regulon [317]. To investigate this further, transcriptomics using whole-genome sequencing will be necessary.

By introducing the recombinant *adeRSABC* constructs into *A. baumannii* NIPH 60, we demonstrated that the amino acid change Asp20→Asn in the response regulator AdeR led to increased expression of *adeB*. The fold-difference in the relative number of *adeB* transcripts between the NIPH 60 *adeRSABC* variants was similar to that previously observed for the clinical isolates F and G [89]. The accompanying decrease in susceptibility to a multitude of structurally diverse antimicrobials was due to enhanced efflux activity, as determined by the ethidium accumulation assay. Reversing this increased efflux activity upon CCCP addition, the results provide evidence that the proton-motive force-dependent active efflux mediated by AdeABC is responsible for decreased susceptibility in the *adeRSABC* transformants. The impact of the NIPH 60 *adeRSABC* transformant harbouring the *adeR*(*Asn20)* variant on the decrease in antimicrobial susceptibility was markedly higher compared to the unmutated *adeR(Asp20)SABC* transformant. Thereby, bacterial fitness was not reduced in the *adeRSABC* transformants although efflux pump synthesis and their functioning have been reported to cause decreased growth [183, 199, 234]. Furthermore, no impact on the transcription of

adeG or *adeJ* was detected. As *adeG* and *adeJ* expression have been reported to be regulated by the LysR-type transcriptional regulator AdeL [112] or the TetR-type regulator AdeN [133], respectively, cross-regulation can be ruled out.

Ethidium accumulation in the *adeR(Asn20)SABC* transformant was not altered by the addition of antimicrobials at sub-inhibitory concentrations. In the *E. coli* AdeB-homolog AcrB, two binding portions within the distal binding pocket have been described in the inner periplasmic cleft [177]. Minocycline, levofloxacin, erythromycin, rifampicin and tetracycline are predicted to bind to the upper 'groove' portion, whereas chloramphenicol seems to bind to the lower 'cave portion. Adapting this to our investigations, ethidium is either preferably extruded over the other compounds or both ethidium and the antimicrobials are not in competition for the same binding site in AdeB. It is also possible, that the concentration of the antimicrobials was too low, as we used sub-inhibitory concentrations. In *Salmonella enteritidis*, for example, changes in the ethidium accumulation were only visible when tetracycline concentrations of >100 mg/L were added [318]. With regards to the present study, sub-inhibitory concentrations were used to avoid any interfering stress responses due to antimicrobial challenge and we wanted to remain within pharmacokinetic boundaries.

Using the efflux pump inhibitor NMP, antimicrobial susceptibilities were not restored to the control values completely; six out of nine antimicrobials, to which the MIC was increased with the introduction of the *adeRSABC* constructs, showed reduced MICs in the presence of NMP. In particular, the susceptibility to tigecycline and tetracycline were increased by this inhibitor. Investigations in *E. coli* have shown that NMP acts as a substrate of the RND pump AcrB binding to the groove portion of the distal binding pocket, thereby inhibiting substrate binding [190]. Our results suggest that tetracycline, which is predicted to bind to the same portion of the pocket [177], is a good substrate of the AcrB-homolog AdeB and its extrusion is inhibited by the addition of NMP. As a consequence, less tetracycline is extruded out of the cell and the intracellular accumulation increases so that toxicity to the cell is achieved by lower concentrations. The same might apply for tigecycline, however its binding pattern has not yet been investigated. The two efflux pump inhibitors showing the highest efficiency against *A. baumannii* RND efflux pumps *in vitro* are NMP and PAβN [319]. In *P. aeruginosa* PAβN successfully inhibits the four clinically most relevant efflux pumps (MexAB-OprM, MexCD-OprJ, MexEF-OprN and MexXY-OprM) [188]. In *A. baumannii* its activity has been shown against AdeFGH potentiating the activity of clindamycin and, to a lesser extent, to

trimethoprim and chloramphenicol [320]. Reduced MICs to tigecycline, gentamicin, chloramphenicol and nalidixic acid but not ciprofloxacin were demonstrated in other studies [264, 321]. NMP restored ciprofloxacin susceptibility in a number of intermediate resistant clinical *A. baumannii* isolates [322]. Comparing both compounds in fluoroquinolone resistant and susceptible *A. baumannii* isolates revealed that PAβN is more active than NMP at low concentration (25 mg/L), especially reducing the MIC of clarithromycin and rifampicin. In contrast, NMP showed greater efficacy at high concentration (100 mg/L), particularly lowering the MICs of tetracycline, chloramphenicol and linezolid [291]. Overall, in *A. baumannii* NMP was more efficient in reducing MICs than PaβN. However, reducing the MIC values of antimicrobial agents not targeted by the introduced AdeABC (chloramphenicol and minocycline) our results indicate that other efflux pumps are also inhibited by NMP. These might include RND-type efflux pumps other than AdeABC (AdeIJK and AdeFGH) which have also been reported to extrude chloramphenicol and minocycline [112, 127]. Furthermore, chloramphenicol has been shown to be the only substrate of the MFS-type transporter CraA and minocycline is extruded by plasmid encoded MFS-type efflux pumps [270, 281]. Further investigations could elucidate which other efflux pumps in *A. baumannii* are targeted by NMP. Nevertheless, causing renal toxicity or likely acting as a serotonin agonist, respectively, PAβN and NMP were not further developed to be used as clinically useful drugs [323, 324]. Although the development of derivatives with reduced toxicity and the search for alternative compounds continues, no efflux pump inhibitor has yet been licensed for the treatment of bacterial infections.

As *adeB* has often been reported to be overexpressed in clinically relevant MDR *A. baumannii* isolates, it is important to understand the source of overexpression as well as the individual impact and contribution on increased resistance rates. In this part of the study we demonstrated that *adeB* overexpression can be caused by the Asp20→Asn substitution in AdeR and that the accompanying decrease in antimicrobial susceptibility is due to enhanced efflux activity.

5. Summary & Conclusion

Over the past three decades *A. baumannii* has evolved into a clinically important nosocomial pathogen causing epidemic outbreaks worldwide. Due to its intrinsic antimicrobial resistance and its ability to easily acquire new resistance determinants, *A. baumannii* can display resistance to all of today's commonly prescribed antimicrobials, leaving limited treatment options. Among all reported resistance mechanisms, chromosomally encoded efflux pumps contribute most to multidrug resistance owing to their broad substrate specificity. In *A. baumannii* particularly, the overexpression of RND-type efflux pumps, extruding antimicrobials from the periplasm to the extracellular environment, plays a significant role in the appearance of MDR clones worldwide.

With this PhD project it was aimed to further investigate and characterize RND-type efflux transporters in *A. baumannii*. Using BLAST analysis five putative RND pumps in addition to the three characterized systems AdeABC, AdeIJK and AdeFGH were identified. Testing the prevalence of these eight exporter genes within a genotypically and geographically diverse pool of clinical *A. baumannii* isolates using a PCR-based approach, five of eight RND-type efflux genes were present in all isolates. Two of them were present in ≥87% of isolates, highlighting the great distribution and relevance of these efflux pumps for this nosocomial pathogen.

Further investigating one of the identified putative exporters (A1S_2660 locus tag in *A. baumannii* ATCC 17978), low-level expression of this pump was induced by antimicrobials (carbapenems, chloramphenicol), disinfectants (ethanol) and NaCl, substances which are frequently used in the healthcare environment. Carbapenems are used as a last resort antibiotic against *A. baumannii* infections. Overexpression of this exporter was toxic in the *A. baumannii* reference strain ATCC 17978, but did not have a fitness cost in the AdeABC-deficient isolate NIPH 60. Testing a large collection of antimicrobials, bile salts, disinfectants and organic dyes, substrates of A1S_2660 could not be identified.

Substitutions in the two-component regulatory system AdeRS, which regulates the expression of the clinically most significant RND-type efflux pump AdeABC, are rarely further investigated and remain merely associated to increased *adeB* expression and decreased antimicrobial susceptibility. Within this thesis, we report that the Asp→Asn20 substitution in

the response regulator AdeR induced increased *adeB* expression levels, which was accompanied by decreased susceptibility to a multitude of structurally diverse antimicrobials. With the application of the ethidium accumulation assay enhanced efflux was determined to be the cause of the changed susceptibility phenotype. Furthermore, the Asn20 substitution seemed to specifically enhance the interaction between AdeR and its cognate sensor kinase AdeS. Further investigations are needed to verify this hypothesis.

Being aware of the significant contribution of RND-type efflux pumps to antimicrobial resistance and understanding their structure, regulation and transport mechanism will help to find new treatment options against infections caused by MDR pathogens.

On the one hand new antibiotic molecules can be designed which are not extruded by polyspecific efflux transporters, like tigecycline for example, which was initially developed not to be a substrate of the MFS-type efflux pumps Tet(A-E), that are responsible for acquired resistance to tetracyclines like tetracycline, minocycline and doxycycline. However, it was later investigated that tigecycline is a substrate of polyspecific RND-type efflux pumps in various species. It is another strategy to find compounds which inhibit efflux function. Thereby, an ideal efflux pump inhibitor would enhance the activity of multiple antibiotics but must be relatively stable and nontoxic to eukaryotic cells. Especially, efflux pumps of the RND family are a good target for inhibition as no homologues exist in mammals. Inhibitors would be most efficient when used in combination therapy, administered together with an antibiotic. As antimicrobial adjuvants, efflux pump inhibitors are hoped to restore the effectiveness of the agent active against the pathogen. This kind of therapy is already applied successfully when administering β-lactam antibiotics together with β-lactamase inhibitors in order to prevent β-lactam degrading enzymes of lowering the effectiveness of the antimicrobial agent. Deeper insights into the functionality of polyspecific efflux pumps may facilitate the development of new, effective compounds that will combat MDR bacteria.

6. References

1. World Health Organization (WHO). *Antimicrobial resistance: no action today, no cure tomorrow.* [Web Page]: WHO Press; 7 April 2011 [cited 15 April 2016]; Available from: http://www.who.int/world-health-day/2011/en/index.html.
2. Tanwar, J., Das, S., Fatima, Z., and Hameed, S. 2014. *Multidrug resistance: an emerging crisis.* Interdiscip Perspect Infect Dis, **2014**: 541340.
3. Rice, L.B. 2008. *Federal funding for the study of antimicrobial resistance in nosocomial pathogens: no ESKAPE.* J Infect Dis, **197**: 1079-81.
4. Valencia, R., Arroyo, L.A., Conde, M., Aldana, J.M., Torres, M.J., Fernandez-Cuenca, F., Garnacho-Montero, J., Cisneros, J.M., Ortiz, C., Pachon, J., and Aznar, J. 2009. *Nosocomial outbreak of infection with pan-drug-resistant Acinetobacter baumannii in a tertiary care university hospital.* Infect Control Hosp Epidemiol, **30**: 257-63.
5. Gottig, S., Gruber, T.M., Higgins, P.G., Wachsmuth, M., Seifert, H., and Kempf, V.A. 2014. *Detection of pan drug-resistant Acinetobacter baumannii in Germany.* J Antimicrob Chemother, **69**: 2578-9.
6. Peleg, A.Y., Seifert, H., and Paterson, D.L. 2008. *Acinetobacter baumannii: emergence of a successful pathogen.* Clin Microbiol Rev, **21**: 538-82.
7. Rossau, R., Vanlandschoot, A., Gillis, M., and Deley, J. 1991. *Taxonomy of Moraxellaceae Fam-Nov, a New Bacterial Family to Accommodate the Genera Moraxella, Acinetobacter, and Psychrobacter and Related Organisms.* International Journal of Systematic Bacteriology, **41**: 310-319.
8. Jakubů, V. *Očekávané výsledky EHK-626 - bakteriologická diagnostika*. [Web Page]: Státní zdravotní ústav; 9 October 2009 [cited 15 April 2016]; Avaiable from: http://www.szu.cz/ocekavane-vysledky-ehk-626-bakteriologicka-diagnostika.
9. Visca, P., Seifert, H., and Towner, K.J. 2011. *Acinetobacter infection--an emerging threat to human health.* IUBMB life, **63**: 1048-54.
10. Brisou, J., and Prevot, A.R. 1954. *[Studies on bacterial taxonomy. X. The revision of species under Acromobacter group].* Annales de l'Institut Pasteur, **86**: 722-8.
11. Baumann, P., Doudoroff, M., and Stanier, R.Y. 1968. *A study of the Moraxella group. II. Oxidative-negative species (genus Acinetobacter).* J Bacteriol, **95**: 1520-41.
12. Lessel EF. 1971. International Committee on Nomenclature of Bacteria Subcommittee on the Taxonomy of Moraxella and Allied Bacteria: Minutes of the Meeting, 11. August 1970 Room Constitution C Maria-Isabel Hotel, MexicoCity, Mexico. Int J Syst Bacteriol; **21**:213-4: https://dx.doi.org/10.1099/00207713-21-2-213.
13. Skiebe, E., de Berardinis, V., Morczinek, P., Kerrinnes, T., Faber, F., Lepka, D., Hammer, B., Zimmermann, O., Ziesing, S., Wichelhaus, T.A., Hunfeld, K.P., Borgmann, S., Grobner, S., Higgins, P.G., Seifert, H., Busse, H.J., Witte, W., Pfeifer, Y., and Wilharm, G. 2012. *Surface-associated motility, a common trait of clinical isolates of Acinetobacter baumannii, depends on 1,3-diaminopropane.* International journal of medical microbiology : IJMM, **302**: 117-28.
14. Mussi, M.A., Gaddy, J.A., Cabruja, M., Arivett, B.A., Viale, A.M., Rasia, R., and Actis, L.A. 2010. *The opportunistic human pathogen Acinetobacter baumannii senses and responds to light.* J Bacteriol, **192**: 6336-45.
15. Clemmer, K.M., Bonomo, R.A., and Rather, P.N. 2011. *Genetic analysis of surface motility in Acinetobacter baumannii.* Microbiology, **157**: 2534-44.
16. Wilharm, G. *RKI - P 2 Acinetobacter baumannii – Biologie eines Krankenhauserregers*. [Web Page]: Robert Koch Institut; 24 November 2015 [cited 15 April 2016]; Available from: http://www.rki.de/DE/Content/Forsch/Projektgruppen/Projektgruppe_2/P2_node.html.

17. Bouvet, P.J.M., and Grimont, P.A.D. 1986. *Taxonomy of the Genus Acinetobacter with the Recognition of Acinetobacter-Baumannii Sp-Nov, Acinetobacter-Haemolyticus Sp-Nov, Acinetobacter-Johnsonii Sp-Nov, and Acinetobacter-Junii Sp-Nov and Emended Descriptions of Acinetobacter-Calcoaceticus and Acinetobacter-Lwoffii.* International journal of systematic bacteriology, **36**: 228-240.
18. Gerner-Smidt, P., Tjernberg, I., and Ursing, J. 1991. *Reliability of phenotypic tests for identification of Acinetobacter species.* J Clin Microbiol, **29**: 277-82.
19. Nemec, A., Krizova, L., Maixnerova, M., Sedo, O., Brisse, S., and Higgins, P.G. 2015. *Acinetobacter seifertii sp. nov., a member of the Acinetobacter calcoaceticus-Acinetobacter baumannii complex isolated from human clinical specimens.* Int J Syst Evol Microbiol, **65**: 934-42.
20. Bergogne-Berezin, E., and Towner, K.J. 1996. *Acinetobacter spp. as nosocomial pathogens: microbiological, clinical, and epidemiological features.* Clin Microbiol Rev, **9**: 148-65.
21. Houang, E.T., Chu, Y.W., Chu, K.Y., Ng, K.C., Leung, C.M., and Cheng, A.F. 2003. *Significance of genomic DNA group delineation in comparative studies of antimicrobial susceptibility of Acinetobacter spp.* Antimicrob Agents Chemother, **47**: 1472-5.
22. Lee, J.H., Choi, C.H., Kang, H.Y., Lee, J.Y., Kim, J., Lee, Y.C., Seol, S.Y., Cho, D.T., Kim, K.W., Song do, Y., and Lee, J.C. 2007. *Differences in phenotypic and genotypic traits against antimicrobial agents between Acinetobacter baumannii and Acinetobacter genomic species 13TU.* J Antimicrob Chemother, **59**: 633-9.
23. Dijkshoorn, L., Van Harsselaar, B., Tjernberg, I., Bouvet, P.J., and Vaneechoutte, M. 1998. *Evaluation of amplified ribosomal DNA restriction analysis for identification of Acinetobacter genomic species.* Systematic and applied microbiology, **21**: 33-9.
24. Janssen, P., Maquelin, K., Coopman, R., Tjernberg, I., Bouvet, P., Kersters, K., and Dijkshoorn, L. 1997. *Discrimination of Acinetobacter genomic species by AFLP fingerprinting.* International journal of systematic bacteriology, **47**: 1179-87.
25. Espinal, P., Seifert, H., Dijkshoorn, L., Vila, J., and Roca, I. 2012. *Rapid and accurate identification of genomic species from the Acinetobacter baumannii (Ab) group by MALDI-TOF MS.* Clin Microbiol Infect, **18**: 1097-103.
26. David H. *Microbial identification using the bioMérieux Vitek® 2 system*, Pincus bioMérieux, Inc. Hazelwood, MO, USA, https://store.pda.org/TableOfContents/ERMM_V2_Ch01.pdf.
27. Turton, J.F., Woodford, N., Glover, J., Yarde, S., Kaufmann, M.E., and Pitt, T.L. 2006. *Identification of Acinetobacter baumannii by detection of the blaOXA-51-like carbapenemase gene intrinsic to this species.* J Clin Microbiol, **44**: 2974-6.
28. Higgins, P.G., Lehmann, M., Wisplinghoff, H., and Seifert, H. 2010. *gyrB multiplex PCR to differentiate between Acinetobacter calcoaceticus and Acinetobacter genomic species 3.* J Clin Microbiol, **48**: 4592-4.
29. Baumann, P. 1968. *Isolation of Acinetobacter from soil and water.* J Bacteriol, **96**: 39-42.
30. Peix, A., Lang, E., Verbarg, S., Sproer, C., Rivas, R., Santa-Regina, I., Mateos, P.F., Martinez-Molina, E., Rodriguez-Barrueco, C., and Velazquez, E. 2009. *Acinetobacter strains IH9 and OCI1, two rhizospheric phosphate solubilizing isolates able to promote plant growth, constitute a new genomovar of Acinetobacter calcoaceticus.* Systematic and applied microbiology, **32**: 334-41.
31. Pontiroli, A., Rizzi, A., Simonet, P., Daffonchio, D., Vogel, T.M., and Monier, J.M. 2009. *Visual evidence of horizontal gene transfer between plants and bacteria in the phytosphere of transplastomic tobacco.* Appl Environ Microbiol, **75**: 3314-22.
32. Carr, E.L., Kampfer, P., Patel, B.K., Gurtler, V., and Seviour, R.J. 2003. *Seven novel species of Acinetobacter isolated from activated sludge.* International journal of systematic and evolutionary microbiology, **53**: 953-63.
33. Ordonez, O.F., Flores, M.R., Dib, J.R., Paz, A., and Farias, M.E. 2009. *Extremophile culture collection from Andean lakes: extreme pristine environments that host a wide diversity of microorganisms with tolerance to UV radiation.* Microbial ecology, **58**: 461-73.

34. Seifert, H., Dijkshoorn, L., Gerner-Smidt, P., Pelzer, N., Tjernberg, I., and Vaneechoutte, M. 1997. *Distribution of Acinetobacter species on human skin: comparison of phenotypic and genotypic identification methods.* J Clin Microbiol, **35**: 2819-25.
35. Berlau, J., Aucken, H., Malnick, H., and Pitt, T. 1999. *Distribution of Acinetobacter species on skin of healthy humans.* European journal of clinical microbiology & infectious diseases : official publication of the European Society of Clinical Microbiology, **18**: 179-83.
36. Dijkshoorn, L., van Aken, E., Shunburne, L., van der Reijden, T.J., Bernards, A.T., Nemec, A., and Towner, K.J. 2005. *Prevalence of Acinetobacter baumannii and other Acinetobacter spp. in faecal samples from non-hospitalised individuals.* Clin Microbiol Infect, **11**: 329-32.
37. Fournier, P.E., Vallenet, D., Barbe, V., Audic, S., Ogata, H., Poirel, L., Richet, H., Robert, C., Mangenot, S., Abergel, C., Nordmann, P., Weissenbach, J., Raoult, D., and Claverie, J.M. 2006. *Comparative genomics of multidrug resistance in Acinetobacter baumannii.* PLoS Genet, **2**: e7.
38. Berlau, J., Aucken, H.M., Houang, E., and Pitt, T.L. 1999. *Isolation of Acinetobacter spp. including A. baumannii from vegetables: implications for hospital-acquired infections.* J Hosp Infect, **42**: 201-4.
39. Houang, E.T., Chu, Y.W., Leung, C.M., Chu, K.Y., Berlau, J., Ng, K.C., and Cheng, A.F. 2001. *Epidemiology and infection control implications of Acinetobacter spp. in Hong Kong.* J Clin Microbiol, **39**: 228-34.
40. Huys, G., Bartie, K., Cnockaert, M., Hoang Oanh, D.T., Phuong, N.T., Somsiri, T., Chinabut, S., Yusoff, F.M., Shariff, M., Giacomini, M., Teale, A., and Swings, J. 2007. *Biodiversity of chloramphenicol-resistant mesophilic heterotrophs from Southeast Asian aquaculture environments.* Res Microbiol, **158**: 228-35.
41. La Scola, B., and Raoult, D. 2004. *Acinetobacter baumannii in human body louse.* Emerg Infect Dis, **10**: 1671-3.
42. Choi, J.Y., Kim, Y., Ko, E.A., Park, Y.K., Jheong, W.H., Ko, G., and Ko, K.S. 2012. *Acinetobacter species isolates from a range of environments: species survey and observations of antimicrobial resistance.* Diagn Microbiol Infect Dis, **74**: 177-80.
43. Belmonte, O., Pailhories, H., Kempf, M., Gaultier, M.P., Lemarie, C., Ramont, C., Joly-Guillou, M.L., and Eveillard, M. 2014. *High prevalence of closely-related Acinetobacter baumannii in pets according to a multicentre study in veterinary clinics, Reunion Island.* Vet Microbiol, **170**: 446-50.
44. Endimiani, A., Hujer, K.M., Hujer, A.M., Bertschy, I., Rossano, A., Koch, C., Gerber, V., Francey, T., Bonomo, R.A., and Perreten, V. 2011. *Acinetobacter baumannii isolates from pets and horses in Switzerland: molecular characterization and clinical data.* J Antimicrob Chemother, **66**: 2248-54.
45. Goodhart, G.L., Abrutyn, E., Watson, R., Root, R.K., and Egert, J. 1977. *Community-acquired Acinetobacter calcoaceticus var anitratus pneumonia.* JAMA, **238**: 1516-8.
46. Falagas, M.E., Karveli, E.A., Kelesidis, I., and Kelesidis, T. 2007. *Community-acquired Acinetobacter infections.* Eur J Clin Microbiol Infect Dis, **26**: 857-68.
47. Chang, W.N., Lu, C.H., Huang, C.R., and Chuang, Y.C. 2000. *Community-acquired Acinetobacter meningitis in adults.* Infection, **28**: 395-7.
48. Falagas, M.E., Karveli, E.A., Kelesidis, I., and Kelesidis, T. 2007. *Community-acquired Acinetobacter infections.* European journal of clinical microbiology & infectious diseases : official publication of the European Society of Clinical Microbiology, **26**: 857-68.
49. Rodriguez-Bano, J., Cisneros, J.M., Fernandez-Cuenca, F., Ribera, A., Vila, J., Pascual, A., Martinez-Martinez, L., Bou, G., and Pachon, J. 2004. *Clinical features and epidemiology of Acinetobacter baumannii colonization and infection in Spanish hospitals.* Infection control and hospital epidemiology, **25**: 819-24.
50. Scott, PT. 2004. *Acinetobacter baumannii infections among patients at military medical facilities treating injured U.S. service members, 2002-2004.* MMWR. Morbidity and mortality weekly report, **53**: 1063-6.

51. Falagas, M.E., and Rafailidis, P.I. 2007. *Attributable mortality of Acinetobacter baumannii: no longer a controversial issue.* Critical care, **11**: 134.
52. Oncul, O., Keskin, O., Acar, H.V., Kucukardali, Y., Evrenkaya, R., Atasoyu, E.M., Top, C., Nalbant, S., Ozkan, S., Emekdas, G., Cavuslu, S., Us, M.H., Pahsa, A., and Gokben, M. 2002. *Hospital-acquired infections following the 1999 Marmara earthquake.* J Hosp Infect, **51**: 47-51.
53. Wang, Y., Hao, P., Lu, B., Yu, H., Huang, W., Hou, H., and Dai, K. 2010. *Causes of infection after earthquake, China, 2008.* Emerg Infect Dis, **16**: 974-5.
54. Uckay, I., Sax, H., Harbarth, S., Bernard, L., and Pittet, D. 2008. *Multi-resistant infections in repatriated patients after natural disasters: lessons learned from the 2004 tsunami for hospital infection control.* J Hosp Infect, **68**: 1-8.
55. Leung, W.S., Chu, C.M., Tsang, K.Y., Lo, F.H., Lo, K.F., and Ho, P.L. 2006. *Fulminant community-acquired Acinetobacter baumannii pneumonia as a distinct clinical syndrome.* Chest, **129**: 102-9.
56. Choi, S.H., Choo, E.J., Kwak, Y.G., Kim, M.Y., Jun, J.B., Kim, M.N., Kim, N.J., Jeong, J.Y., Kim, Y.S., and Woo, J.H. 2006. *Clinical characteristics and outcomes of bacteremia caused by Acinetobacter species other than A. baumannii: comparison with A. baumannii bacteremia.* J Infect Chemother, **12**: 380-6.
57. Seifert, H., Strate, A., Schulze, A., and Pulverer, G. 1994. *Bacteremia due to Acinetobacter species other than Acinetobacter baumannii.* Infection, **22**: 379-85.
58. Cisneros, J.M., Reyes, M.J., Pachon, J., Becerril, B., Caballero, F.J., Garcia-Garmendia, J.L., Ortiz, C., and Cobacho, A.R. 1996. *Bacteremia due to Acinetobacter baumannii: epidemiology, clinical findings, and prognostic features.* Clin Infect Dis, **22**: 1026-32.
59. Koch, F.H., Cusumano, A., Seifert, P., Mougharbel, M., and Augustin, A.J. 1995. *Ultrastructure of the anterior lens capsule after vitrectomy with silicone oil injection. Correlation of clinical and morphological features.* Doc Ophthalmol, **91**: 233-42.
60. Chuang, Y.C., Sheng, W.H., Li, S.Y., Lin, Y.C., Wang, J.T., Chen, Y.C., and Chang, S.C. 2011. *Influence of genospecies of Acinetobacter baumannii complex on clinical outcomes of patients with acinetobacter bacteremia.* Clin Infect Dis, **52**: 352-60.
61. Munoz-Price, L.S., and Weinstein, R.A. 2008. *Acinetobacter infection.* N Engl J Med, **358**: 1271-81.
62. Joly-Guillou, M.L. 2005. *Clinical impact and pathogenicity of Acinetobacter.* Clin Microbiol Infect, **11**: 868-73.
63. Dijkshoorn, L., Aucken, H., Gerner-Smidt, P., Janssen, P., Kaufmann, M.E., Garaizar, J., Ursing, J., and Pitt, T.L. 1996. *Comparison of outbreak and nonoutbreak Acinetobacter baumannii strains by genotypic and phenotypic methods.* J Clin Microbiol, **34**: 1519-25.
64. Diancourt, L., Passet, V., Nemec, A., Dijkshoorn, L., and Brisse, S. 2010. *The population structure of Acinetobacter baumannii: expanding multiresistant clones from an ancestral susceptible genetic pool.* PLoS One, **5**: e10034.
65. Higgins, P.G., Dammhayn, C., Hackel, M., and Seifert, H. 2010. *Global spread of carbapenem-resistant Acinetobacter baumannii.* J Antimicrob Chemother, **65**: 233-8.
66. Schulte, B., Goerke, C., Weyrich, P., Grobner, S., Bahrs, C., Wolz, C., Autenrieth, I.B., and Borgmann, S. 2005. *Clonal spread of meropenem-resistant Acinetobacter baumannii strains in hospitals in the Mediterranean region and transmission to South-west Germany.* J Hosp Infect, **61**: 356-7.
67. van den Broek, P.J., Arends, J., Bernards, A.T., De Brauwer, E., Mascini, E.M., van der Reijden, T.J., Spanjaard, L., Thewessen, E.A., van der Zee, A., van Zeijl, J.H., and Dijkshoorn, L. 2006. *Epidemiology of multiple Acinetobacter outbreaks in The Netherlands during the period 1999-2001.* Clin Microbiol Infect, **12**: 837-43.
68. Dijkshoorn, L., Nemec, A., and Seifert, H. 2007. *An increasing threat in hospitals: multidrug-resistant Acinetobacter baumannii.* Nat Rev Microbiol, **5**: 939-51.

69. Peleg, A.Y., Bell, J.M., Hofmeyr, A., and Wiese, P. 2006. *Inter-country transfer of Gram-negative organisms carrying the VIM-4 and OXA-58 carbapenem-hydrolysing enzymes.* J Antimicrob Chemother, **57**: 794-5.
70. Naas, T., Kernbaum, S., Allali, S., and Nordmann, P. 2007. *Multidrug-resistant Acinetobacter baumannii, Russia.* Emerg Infect Dis, **13**: 669-71.
71. Maragakis, L.L., Cosgrove, S.E., Song, X., Kim, D., Rosenbaum, P., Ciesla, N., Srinivasan, A., Ross, T., Carroll, K., and Perl, T.M. 2004. *An outbreak of multidrug-resistant Acinetobacter baumannii associated with pulsatile lavage wound treatment.* JAMA, **292**: 3006-11.
72. Consales, G., Gramigni, E., Zamidei, L., Bettocchi, D., and De Gaudio, A.R. 2011. *A multidrug-resistant Acinetobacter baumannii outbreak in intensive care unit: antimicrobial and organizational strategies.* J Crit Care, **26**: 453-9.
73. El Shafie, S.S., Alishaq, M., and Leni Garcia, M. 2004. *Investigation of an outbreak of multidrug-resistant Acinetobacter baumannii in trauma intensive care unit.* J Hosp Infect, **56**: 101-5.
74. Kuo, S.C., Chang, S.C., Wang, H.Y., Lai, J.F., Chen, P.C., Shiau, Y.R., Huang, I.W., Lauderdale, T.L., and Hospitals, T. 2012. *Emergence of extensively drug-resistant Acinetobacter baumannii complex over 10 years: nationwide data from the Taiwan Surveillance of Antimicrobial Resistance (TSAR) program.* BMC Infect Dis, **12**: 200.
75. Teo, J., Lim, T.P., Hsu, L.Y., Tan, T.Y., Sasikala, S., Hon, P.Y., Kwa, A.L., and Apisarnthanarak, A. 2015. *Extensively drug-resistant Acinetobacter baumannii in a Thai hospital: a molecular epidemiologic analysis and identification of bactericidal Polymyxin B-based combinations.* Antimicrob Resist Infect Control, **4**: 2.
76. Jones, C.L., Clancy, M., Honnold, C., Singh, S., Snesrud, E., Onmus-Leone, F., McGann, P., Ong, A.C., Kwak, Y., Waterman, P., Zurawski, D.V., Clifford, R.J., and Lesho, E. 2015. *Fatal outbreak of an emerging clone of extensively drug-resistant Acinetobacter baumannii with enhanced virulence.* Clin Infect Dis, **61**: 145-54.
77. Magiorakos, A.P., Srinivasan, A., Carey, R.B., Carmeli, Y., Falagas, M.E., Giske, C.G., Harbarth, S., Hindler, J.F., Kahlmeter, G., Olsson-Liljequist, B., Paterson, D.L., Rice, L.B., Stelling, J., Struelens, M.J., Vatopoulos, A., Weber, J.T., and Monnet, D.L. 2012. *Multidrug-resistant, extensively drug-resistant and pandrug-resistant bacteria: an international expert proposal for interim standard definitions for acquired resistance.* Clin Microbiol Infect, **18**: 268-81.
78. Jawad, A., Seifert, H., Snelling, A.M., Heritage, J., and Hawkey, P.M. 1998. *Survival of Acinetobacter baumannii on dry surfaces: comparison of outbreak and sporadic isolates.* J Clin Microbiol, **36**: 1938-41.
79. Jawad, A., Heritage, J., Snelling, A.M., Gascoyne-Binzi, D.M., and Hawkey, P.M. 1996. *Influence of relative humidity and suspending menstrua on survival of Acinetobacter spp. on dry surfaces.* J Clin Microbiol, **34**: 2881-7.
80. Musa, E.K., Desai, N., and Casewell, M.W. 1990. *The survival of Acinetobacter calcoaceticus inoculated on fingertips and on formica.* J Hosp Infect, **15**: 219-27.
81. Wendt, C., Dietze, B., Dietz, E., and Ruden, H. 1997. *Survival of Acinetobacter baumannii on dry surfaces.* J Clin Microbiol, **35**: 1394-7.
82. Bernards, A.T., Frenay, H.M., Lim, B.T., Hendriks, W.D., Dijkshoorn, L., and van Boven, C.P. 1998. *Methicillin-resistant Staphylococcus aureus and Acinetobacter baumannii: an unexpected difference in epidemiologic behavior.* Am J Infect Control, **26**: 544-51.
83. Weernink, A., Severin, W.P., Tjernberg, I., and Dijkshoorn, L. 1995. *Pillows, an unexpected source of Acinetobacter.* J Hosp Infect, **29**: 189-99.
84. Gaddy, J.A., and Actis, L.A. 2009. *Regulation of Acinetobacter baumannii biofilm formation.* Future Microbiol, **4**: 273-8.
85. Gayoso, C.M., Mateos, J., Mendez, J.A., Fernandez-Puente, P., Rumbo, C., Tomas, M., Martinez de Ilarduya, O., and Bou, G. 2014. *Molecular mechanisms involved in the response to desiccation stress and persistence in Acinetobacter baumannii.* J Proteome Res, **13**: 460-76.

86. Marti, S., Rodriguez-Bano, J., Catel-Ferreira, M., Jouenne, T., Vila, J., Seifert, H., and De, E. 2011. *Biofilm formation at the solid-liquid and air-liquid interfaces by Acinetobacter species.* BMC Res Notes, **4**: 5.
87. Pour, N.K., Dusane, D.H., Dhakephalkar, P.K., Zamin, F.R., Zinjarde, S.S., and Chopade, B.A. 2011. *Biofilm formation by Acinetobacter baumannii strains isolated from urinary tract infection and urinary catheters.* FEMS Immunol Med Microbiol, **62**: 328-38.
88. Montefour, K., Frieden, J., Hurst, S., Helmich, C., Headley, D., Martin, M., and Boyle, D.A. 2008. *Acinetobacter baumannii: an emerging multidrug-resistant pathogen in critical care.* Critical care nurse, **28**: 15-25; quiz 26.
89. Higgins, P.G., Schneiders, T., Hamprecht, A., and Seifert, H. 2010. *In vivo selection of a missense mutation in adeR and conversion of the novel blaOXA-164 gene into blaOXA-58 in carbapenem-resistant Acinetobacter baumannii isolates from a hospitalized patient.* Antimicrob Agents Chemother, **54**: 5021-7.
90. Iacono, M., Villa, L., Fortini, D., Bordoni, R., Imperi, F., Bonnal, R.J., Sicheritz-Ponten, T., De Bellis, G., Visca, P., Cassone, A., and Carattoli, A. 2008. *Whole-genome pyrosequencing of an epidemic multidrug-resistant Acinetobacter baumannii strain belonging to the European clone II group.* Antimicrob Agents Chemother, **52**: 2616-25.
91. Adams, M.D., Goglin, K., Molyneaux, N., Hujer, K.M., Lavender, H., Jamison, J.J., MacDonald, I.J., Martin, K.M., Russo, T., Campagnari, A.A., Hujer, A.M., Bonomo, R.A., and Gill, S.R. 2008. *Comparative genome sequence analysis of multidrug-resistant Acinetobacter baumannii.* J Bacteriol, **190**: 8053-64.
92. Adams, M.D., Chan, E.R., Molyneaux, N.D., and Bonomo, R.A. 2010. *Genomewide analysis of divergence of antibiotic resistance determinants in closely related isolates of Acinetobacter baumannii.* Antimicrob Agents Chemother, **54**: 3569-77.
93. Post, V., and Hall, R.M. 2009. *AbaR5, a large multiple-antibiotic resistance region found in Acinetobacter baumannii.* Antimicrob Agents Chemother, **53**: 2667-71.
94. Post, V., White, P.A., and Hall, R.M. 2010. *Evolution of AbaR-type genomic resistance islands in multiply antibiotic-resistant Acinetobacter baumannii.* J Antimicrob Chemother, **65**: 1162-70.
95. Krizova, L., Dijkshoorn, L., and Nemec, A. 2011. *Diversity and evolution of AbaR genomic resistance islands in Acinetobacter baumannii strains of European clone I.* Antimicrob Agents Chemother, **55**: 3201-6.
96. Zhu, L., Yan, Z., Zhang, Z., Zhou, Q., Zhou, J., Wakeland, E.K., Fang, X., Xuan, Z., Shen, D., and Li, Q.Z. 2013. *Complete genome analysis of three Acinetobacter baumannii clinical isolates in China for insight into the diversification of drug resistance elements.* PLoS One, **8**: e66584.
97. Figueiredo, S., Poirel, L., Croize, J., Recule, C., and Nordmann, P. 2009. *In vivo selection of reduced susceptibility to carbapenems in Acinetobacter baumannii related to ISAba1-mediated overexpression of the natural bla(OXA-66) oxacillinase gene.* Antimicrob Agents Chemother, **53**: 2657-9.
98. Segal, H., Thomas, R., and Gay Elisha, B. 2003. *Characterization of class 1 integron resistance gene cassettes and the identification of a novel IS-like element in Acinetobacter baumannii.* Plasmid, **49**: 169-78.
99. Sun, J.R., Perng, C.L., Chan, M.C., Morita, Y., Lin, J.C., Su, C.M., Wang, W.Y., Chang, T.Y., and Chiueh, T.S. 2012. *A truncated AdeS kinase protein generated by ISAba1 insertion correlates with tigecycline resistance in Acinetobacter baumannii.* PLoS One, **7**: e49534.
100. Hujer, K.M., Hujer, A.M., Hulten, E.A., Bajaksouzian, S., Adams, J.M., Donskey, C.J., Ecker, D.J., Massire, C., Eshoo, M.W., Sampath, R., Thomson, J.M., Rather, P.N., Craft, D.W., Fishbain, J.T., Ewell, A.J., Jacobs, M.R., Paterson, D.L., and Bonomo, R.A. 2006. *Analysis of antibiotic resistance genes in multidrug-resistant Acinetobacter sp. isolates from military and civilian patients treated at the Walter Reed Army Medical Center.* Antimicrob Agents Chemother, **50**: 4114-23.

101. Nemec, A., Dolzani, L., Brisse, S., van den Broek, P., and Dijkshoorn, L. 2004. *Diversity of aminoglycoside-resistance genes and their association with class 1 integrons among strains of pan-European Acinetobacter baumannii clones.* J Med Microbiol, **53**: 1233-40.
102. Seward, R.J., Lambert, T., and Towner, K.J. 1998. *Molecular epidemiology of aminoglycoside resistance in Acinetobacter spp.* J Med Microbiol, **47**: 455-62.
103. Doi, Y., Adams, J.M., Yamane, K., and Paterson, D.L. 2007. *Identification of 16S rRNA methylase-producing Acinetobacter baumannii clinical strains in North America.* Antimicrob Agents Chemother, **51**: 4209-10.
104. Lee, H., Yong, D., Yum, J.H., Roh, K.H., Lee, K., Yamane, K., Arakawa, Y., and Chong, Y. 2006. *Dissemination of 16S rRNA methylase-mediated highly amikacin-resistant isolates of Klebsiella pneumoniae and Acinetobacter baumannii in Korea.* Diagn Microbiol Infect Dis, **56**: 305-12.
105. Huys, G., Cnockaert, M., Vaneechoutte, M., Woodford, N., Nemec, A., Dijkshoorn, L., and Swings, J. 2005. *Distribution of tetracycline resistance genes in genotypically related and unrelated multiresistant Acinetobacter baumannii strains from different European hospitals.* Res Microbiol, **156**: 348-55.
106. Ribera, A., Roca, I., Ruiz, J., Gibert, I., and Vila, J. 2003. *Partial characterization of a transposon containing the tet(A) determinant in a clinical isolate of Acinetobacter baumannii.* J Antimicrob Chemother, **52**: 477-80.
107. Ribera, A., Ruiz, J., and Vila, J. 2003. *Presence of the Tet M determinant in a clinical isolate of Acinetobacter baumannii.* Antimicrob Agents Chemother, **47**: 2310-2.
108. Petersen, P.J., Jacobus, N.V., Weiss, W.J., Sum, P.E., and Testa, R.T. 1999. *In vitro and in vivo antibacterial activities of a novel glycylcycline, the 9-t-butylglycylamido derivative of minocycline (GAR-936).* Antimicrob Agents Chemother, **43**: 738-44.
109. Hoban, D.J., Bouchillon, S.K., Johnson, B.M., Johnson, J.L., Dowzicky, M.J., Tigecycline, E., and Surveillance Trial, G. 2005. *In vitro activity of tigecycline against 6792 Gram-negative and Gram-positive clinical isolates from the global Tigecycline Evaluation and Surveillance Trial (TEST Program, 2004).* Diagn Microbiol Infect Dis, **52**: 215-27.
110. Sader, H.S., Jones, R.N., Stilwell, M.G., Dowzicky, M.J., and Fritsche, T.R. 2005. *Tigecycline activity tested against 26,474 bloodstream infection isolates: a collection from 6 continents.* Diagn Microbiol Infect Dis, **52**: 181-6.
111. Ruzin, A., Keeney, D., and Bradford, P.A. 2007. *AdeABC multidrug efflux pump is associated with decreased susceptibility to tigecycline in Acinetobacter calcoaceticus-Acinetobacter baumannii complex.* J Antimicrob Chemother, **59**: 1001-4.
112. Coyne, S., Rosenfeld, N., Lambert, T., Courvalin, P., and Perichon, B. 2010. *Overexpression of resistance-nodulation-cell division pump AdeFGH confers multidrug resistance in Acinetobacter baumannii.* Antimicrob Agents Chemother, **54**: 4389-93.
113. Chen, Q., Li, X., Zhou, H., Jiang, Y., Chen, Y., Hua, X., and Yu, Y. 2014. *Decreased susceptibility to tigecycline in Acinetobacter baumannii mediated by a mutation in trm encoding SAM-dependent methyltransferase.* J Antimicrob Chemother, **69**: 72-6.
114. Li, X., Liu, L., Ji, J., Chen, Q., Hua, X., Jiang, Y., Feng, Y., and Yu, Y. 2015. *Tigecycline resistance in Acinetobacter baumannii mediated by frameshift mutation in plsC, encoding 1-acyl-sn-glycerol-3-phosphate acyltransferase.* Eur J Clin Microbiol Infect Dis, **34**: 625-31.
115. Poirel, L., Mansour, W., Bouallegue, O., and Nordmann, P. 2008. *Carbapenem-resistant Acinetobacter baumannii isolates from Tunisia producing the OXA-58-like carbapenem-hydrolyzing oxacillinase OXA-97.* Antimicrob Agents Chemother, **52**: 1613-7.
116. Zarrilli, R., Vitale, D., Di Popolo, A., Bagattini, M., Daoud, Z., Khan, A.U., Afif, C., and Triassi, M. 2008. *A plasmid-borne blaOXA-58 gene confers imipenem resistance to Acinetobacter baumannii isolates from a Lebanese hospital.* Antimicrob Agents Chemother, **52**: 4115-20.
117. Galimand, M., Sabtcheva, S., Courvalin, P., and Lambert, T. 2005. *Worldwide disseminated armA aminoglycoside resistance methylase gene is borne by composite transposon Tn1548.* Antimicrob Agents Chemother, **49**: 2949-53.

118. Hamouda, A., and Amyes, S.G. 2004. *Novel gyrA and parC point mutations in two strains of Acinetobacter baumannii resistant to ciprofloxacin.* J Antimicrob Chemother, **54**: 695-6.
119. Vila, J., Ruiz, J., Goni, P., Marcos, A., and Jimenez de Anta, T. 1995. *Mutation in the gyrA gene of quinolone-resistant clinical isolates of Acinetobacter baumannii.* Antimicrob Agents Chemother, **39**: 1201-3.
120. Higgins, P.G., Wisplinghoff, H., Stefanik, D., and Seifert, H. 2004. *Selection of topoisomerase mutations and overexpression of adeB mRNA transcripts during an outbreak of Acinetobacter baumannii.* J Antimicrob Chemother, **54**: 821-3.
121. Mulvey, M.R., and Simor, A.E. 2009. *Antimicrobial resistance in hospitals: how concerned should we be?* CMAJ, **180**: 408-15.
122. Houang, E.T., Chu, Y.W., Lo, W.S., Chu, K.Y., and Cheng, A.F. 2003. *Epidemiology of rifampin ADP-ribosyltransferase (arr-2) and metallo-beta-lactamase (blaIMP-4) gene cassettes in class 1 integrons in Acinetobacter strains isolated from blood cultures in 1997 to 2000.* Antimicrob Agents Chemother, **47**: 1382-90.
123. Evans, B.A., Hamouda, A., and Amyes, S.G. 2013. *The rise of carbapenem-resistant Acinetobacter baumannii.* Curr Pharm Des, **19**: 223-38.
124. Poirel, L., Bonnin, R.A., and Nordmann, P. 2011. *Genetic basis of antibiotic resistance in pathogenic Acinetobacter species.* IUBMB Life, **63**: 1061-7.
125. Beceiro, A., Llobet, E., Aranda, J., Bengoechea, J.A., Doumith, M., Hornsey, M., Dhanji, H., Chart, H., Bou, G., Livermore, D.M., and Woodford, N. 2011. *Phosphoethanolamine modification of lipid A in colistin-resistant variants of Acinetobacter baumannii mediated by the pmrAB two-component regulatory system.* Antimicrob Agents Chemother, **55**: 3370-9.
126. Magnet, S., Courvalin, P., and Lambert, T. 2001. *Resistance-nodulation-cell division-type efflux pump involved in aminoglycoside resistance in Acinetobacter baumannii strain BM4454.* Antimicrob Agents Chemother, **45**: 3375-80.
127. Damier-Piolle, L., Magnet, S., Bremont, S., Lambert, T., and Courvalin, P. 2008. *AdeIJK, a resistance-nodulation-cell division pump effluxing multiple antibiotics in Acinetobacter baumannii.* Antimicrob Agents Chemother, **52**: 557-62.
128. Obara, M., and Nakae, T. 1991. *Mechanisms of resistance to beta-lactam antibiotics in Acinetobacter calcoaceticus.* J Antimicrob Chemother, **28**: 791-800.
129. Sato, K., and Nakae, T. 1991. *Outer membrane permeability of Acinetobacter calcoaceticus and its implication in antibiotic resistance.* J Antimicrob Chemother, **28**: 35-45.
130. Dupont, M., Pages, J.M., Lafitte, D., Siroy, A., and Bollet, C. 2005. *Identification of an OprD homologue in Acinetobacter baumannii.* J Proteome Res, **4**: 2386-90.
131. Limansky, A.S., Mussi, M.A., and Viale, A.M. 2002. *Loss of a 29-kilodalton outer membrane protein in Acinetobacter baumannii is associated with imipenem resistance.* J Clin Microbiol, **40**: 4776-8.
132. Siroy, A., Molle, V., Lemaitre-Guillier, C., Vallenet, D., Pestel-Caron, M., Cozzone, A.J., Jouenne, T., and De, E. 2005. *Channel formation by CarO, the carbapenem resistance-associated outer membrane protein of Acinetobacter baumannii.* Antimicrob Agents Chemother, **49**: 4876-83.
133. Rosenfeld, N., Bouchier, C., Courvalin, P., and Perichon, B. 2012. *Expression of the resistance-nodulation-cell division pump AdeIJK in Acinetobacter baumannii is regulated by AdeN, a TetR-type regulator.* Antimicrob Agents Chemother, **56**: 2504-10.
134. Nikaido, H. 1996. *Multidrug efflux pumps of gram-negative bacteria.* J Bacteriol, **178**: 5853-9.
135. Li, X.Z., Plesiat, P., and Nikaido, H. 2015. *The challenge of efflux-mediated antibiotic resistance in Gram-negative bacteria.* Clin Microbiol Rev, **28**: 337-418.
136. Du, D., van Veen, H.W., Murakami, S., Pos, K.M., and Luisi, B.F. 2015. *Structure, mechanism and cooperation of bacterial multidrug transporters.* Curr Opin Struct Biol, **33**: 76-91.
137. Zgurskaya, H.I., and Nikaido, H. 2000. *Multidrug resistance mechanisms: drug efflux across two membranes.* Mol Microbiol, **37**: 219-25.
138. Piddock, L.J. 2006. *Clinically relevant chromosomally encoded multidrug resistance efflux pumps in bacteria.* Clin Microbiol Rev, **19**: 382-402.

139. Ma, D., Cook, D.N., Alberti, M., Pon, N.G., Nikaido, H., and Hearst, J.E. 1993. *Molecular cloning and characterization of acrA and acrE genes of Escherichia coli.* J Bacteriol, **175**: 6299-313.
140. Poole, K., Krebes, K., McNally, C., and Neshat, S. 1993. *Multiple antibiotic resistance in Pseudomonas aeruginosa: evidence for involvement of an efflux operon.* J Bacteriol, **175**: 7363-72.
141. Higgins, C.F. 1992. *ABC transporters: from microorganisms to man.* Annu Rev Cell Biol, **8**: 67-113.
142. Holland, I.B., and Blight, M.A. 1999. *ABC-ATPases, adaptable energy generators fuelling transmembrane movement of a variety of molecules in organisms from bacteria to humans.* J Mol Biol, **293**: 381-99.
143. ter Beek, J., Guskov, A., and Slotboom, D.J. 2014. *Structural diversity of ABC transporters.* J Gen Physiol, **143**: 419-35.
144. Hopfner, K.P., Karcher, A., Shin, D.S., Craig, L., Arthur, L.M., Carney, J.P., and Tainer, J.A. 2000. *Structural biology of Rad50 ATPase: ATP-driven conformational control in DNA double-strand break repair and the ABC-ATPase superfamily.* Cell, **101**: 789-800.
145. Smith, P.C., Karpowich, N., Millen, L., Moody, J.E., Rosen, J., Thomas, P.J., and Hunt, J.F. 2002. *ATP binding to the motor domain from an ABC transporter drives formation of a nucleotide sandwich dimer.* Mol Cell, **10**: 139-49.
146. Chen, J., Lu, G., Lin, J., Davidson, A.L., and Quiocho, F.A. 2003. *A tweezers-like motion of the ATP-binding cassette dimer in an ABC transport cycle.* Mol Cell, **12**: 651-61.
147. Wilkens, S. 2015. *Structure and mechanism of ABC transporters.* F1000Prime Rep, **7**: 14.
148. Kobayashi, N., Nishino, K., and Yamaguchi, A. 2001. *Novel macrolide-specific ABC-type efflux transporter in Escherichia coli.* J Bacteriol, **183**: 5639-44.
149. Lin, H.T., Bavro, V.N., Barrera, N.P., Frankish, H.M., Velamakanni, S., van Veen, H.W., Robinson, C.V., Borges-Walmsley, M.I., and Walmsley, A.R. 2009. *MacB ABC transporter is a dimer whose ATPase activity and macrolide-binding capacity are regulated by the membrane fusion protein MacA.* J Biol Chem, **284**: 1145-54.
150. Lu, S., and Zgurskaya, H.I. 2012. *Role of ATP binding and hydrolysis in assembly of MacAB-TolC macrolide transporter.* Mol Microbiol, **86**: 1132-43.
151. Huang, Y., Lemieux, M.J., Song, J., Auer, M., and Wang, D.N. 2003. *Structure and mechanism of the glycerol-3-phosphate transporter from Escherichia coli.* Science, **301**: 616-20.
152. Abramson, J., Smirnova, I., Kasho, V., Verner, G., Kaback, H.R., and Iwata, S. 2003. *Structure and mechanism of the lactose permease of Escherichia coli.* Science, **301**: 610-5.
153. McMurry, L., Petrucci, R.E., Jr., and Levy, S.B. 1980. *Active efflux of tetracycline encoded by four genetically different tetracycline resistance determinants in Escherichia coli.* Proc Natl Acad Sci U S A, **77**: 3974-7.
154. Yin, Y., He, X., Szewczyk, P., Nguyen, T., and Chang, G. 2006. *Structure of the multidrug transporter EmrD from Escherichia coli.* Science, **312**: 741-4.
155. Nishino, K., and Yamaguchi, A. 2001. *Analysis of a complete library of putative drug transporter genes in Escherichia coli.* J Bacteriol, **183**: 5803-12.
156. Heng, J., Zhao, Y., Liu, M., Liu, Y., Fan, J., Wang, X., Zhao, Y., and Zhang, X.C. 2015. *Substrate-bound structure of the E. coli multidrug resistance transporter MdfA.* Cell Res, **25**: 1060-73.
157. Tanabe, M., Szakonyi, G., Brown, K.A., Henderson, P.J., Nield, J., and Byrne, B. 2009. *The multidrug resistance efflux complex, EmrAB from Escherichia coli forms a dimer in vitro.* Biochem Biophys Res Commun, **380**: 338-42.
158. Morita, Y., Kodama, K., Shiota, S., Mine, T., Kataoka, A., Mizushima, T., and Tsuchiya, T. 1998. *NorM, a putative multidrug efflux protein, of Vibrio parahaemolyticus and its homolog in Escherichia coli.* Antimicrob Agents Chemother, **42**: 1778-82.
159. He, G.X., Kuroda, T., Mima, T., Morita, Y., Mizushima, T., and Tsuchiya, T. 2004. *An H(+)-coupled multidrug efflux pump, PmpM, a member of the MATE family of transporters, from Pseudomonas aeruginosa.* J Bacteriol, **186**: 262-5.

160. He, X., Szewczyk, P., Karyakin, A., Evin, M., Hong, W.X., Zhang, Q., and Chang, G. 2010. *Structure of a cation-bound multidrug and toxic compound extrusion transporter.* Nature, **467**: 991-4.
161. Tanaka, Y., Hipolito, C.J., Maturana, A.D., Ito, K., Kuroda, T., Higuchi, T., Katoh, T., Kato, H.E., Hattori, M., Kumazaki, K., Tsukazaki, T., Ishitani, R., Suga, H., and Nureki, O. 2013. *Structural basis for the drug extrusion mechanism by a MATE multidrug transporter.* Nature, **496**: 247-51.
162. Lu, M., Radchenko, M., Symersky, J., Nie, R., and Guo, Y. 2013. *Structural insights into H+-coupled multidrug extrusion by a MATE transporter.* Nat Struct Mol Biol, **20**: 1310-7.
163. Lu, M., Symersky, J., Radchenko, M., Koide, A., Guo, Y., Nie, R., and Koide, S. 2013. *Structures of a Na+-coupled, substrate-bound MATE multidrug transporter.* Proc Natl Acad Sci U S A, **110**: 2099-104.
164. Chen, Y.J., Pornillos, O., Lieu, S., Ma, C., Chen, A.P., and Chang, G. 2007. *X-ray structure of EmrE supports dual topology model.* Proc Natl Acad Sci U S A, **104**: 18999-9004.
165. Schuldiner, S. 2012. *Undecided membrane proteins insert in random topologies. Up, down and sideways: it does not really matter.* Trends Biochem Sci, **37**: 215-9.
166. Dutta, S., Morrison, E.A., and Henzler-Wildman, K.A. 2014. *Blocking dynamics of the SMR transporter EmrE impairs efflux activity.* Biophys J, **107**: 613-20.
167. Morrison, E.A., DeKoster, G.T., Dutta, S., Vafabakhsh, R., Clarkson, M.W., Bahl, A., Kern, D., Ha, T., and Henzler-Wildman, K.A. 2012. *Antiparallel EmrE exports drugs by exchanging between asymmetric structures.* Nature, **481**: 45-50.
168. Yerushalmi, H., and Schuldiner, S. 2000. *An essential glutamyl residue in EmrE, a multidrug antiporter from Escherichia coli.* J Biol Chem, **275**: 5264-9.
169. Li, X.Z., Poole, K., and Nikaido, H. 2003. *Contributions of MexAB-OprM and an EmrE homolog to intrinsic resistance of Pseudomonas aeruginosa to aminoglycosides and dyes.* Antimicrob Agents Chemother, **47**: 27-33.
170. Srinivasan, V.B., and Rajamohan, G. 2013. *KpnEF, a new member of the Klebsiella pneumoniae cell envelope stress response regulon, is an SMR-type efflux pump involved in broad-spectrum antimicrobial resistance.* Antimicrob Agents Chemother, **57**: 4449-62.
171. Lomovskaya, O., Zgurskaya, H.I., Totrov, M., and Watkins, W.J. 2007. *Waltzing transporters and 'the dance macabre' between humans and bacteria.* Nat Rev Drug Discov, **6**: 56-65.
172. Du, D., Wang, Z., James, N.R., Voss, J.E., Klimont, E., Ohene-Agyei, T., Venter, H., Chiu, W., and Luisi, B.F. 2014. *Structure of the AcrAB-TolC multidrug efflux pump.* Nature, **509**: 512-5.
173. Symmons, M.F., Bokma, E., Koronakis, E., Hughes, C., and Koronakis, V. 2009. *The assembled structure of a complete tripartite bacterial multidrug efflux pump.* Proc Natl Acad Sci U S A, **106**: 7173-8.
174. Seeger, M.A., Schiefner, A., Eicher, T., Verrey, F., Diederichs, K., and Pos, K.M. 2006. *Structural asymmetry of AcrB trimer suggests a peristaltic pump mechanism.* Science, **313**: 1295-8.
175. Murakami, S., Nakashima, R., Yamashita, E., Matsumoto, T., and Yamaguchi, A. 2006. *Crystal structures of a multidrug transporter reveal a functionally rotating mechanism.* Nature, **443**: 173-9.
176. Blair, J.M., and Piddock, L.J. 2009. *Structure, function and inhibition of RND efflux pumps in Gram-negative bacteria: an update.* Curr Opin Microbiol, **12**: 512-9.
177. Nakashima, R., Sakurai, K., Yamasaki, S., Nishino, K., and Yamaguchi, A. 2011. *Structures of the multidrug exporter AcrB reveal a proximal multisite drug-binding pocket.* Nature, **480**: 565-9.
178. Eicher, T., Cha, H.J., Seeger, M.A., Brandstatter, L., El-Delik, J., Bohnert, J.A., Kern, W.V., Verrey, F., Grutter, M.G., Diederichs, K., and Pos, K.M. 2012. *Transport of drugs by the multidrug transporter AcrB involves an access and a deep binding pocket that are separated by a switch-loop.* Proc Natl Acad Sci U S A, **109**: 5687-92.

179. Aires, J.R., and Nikaido, H. 2005. *Aminoglycosides are captured from both periplasm and cytoplasm by the AcrD multidrug efflux transporter of Escherichia coli.* J Bacteriol, **187**: 1923-9.
180. Vargiu, A.V., and Nikaido, H. 2012. *Multidrug binding properties of the AcrB efflux pump characterized by molecular dynamics simulations.* Proc Natl Acad Sci U S A, **109**: 20637-42.
181. Feng, Z., Hou, T., and Li, Y. 2012. *Unidirectional peristaltic movement in multisite drug binding pockets of AcrB from molecular dynamics simulations.* Mol Biosyst, **8**: 2699-709.
182. Cha, H.J., Muller, R.T., and Pos, K.M. 2014. *Switch-loop flexibility affects transport of large drugs by the promiscuous AcrB multidrug efflux transporter.* Antimicrob Agents Chemother, **58**: 4767-72.
183. Takatsuka, Y., Chen, C., and Nikaido, H. 2010. *Mechanism of recognition of compounds of diverse structures by the multidrug efflux pump AcrB of Escherichia coli.* Proc Natl Acad Sci U S A, **107**: 6559-65.
184. Yu, E.W., Aires, J.R., McDermott, G., and Nikaido, H. 2005. *A periplasmic drug-binding site of the AcrB multidrug efflux pump: a crystallographic and site-directed mutagenesis study.* J Bacteriol, **187**: 6804-15.
185. Yu, E.W., Aires, J.R., and Nikaido, H. 2003. *AcrB multidrug efflux pump of Escherichia coli: composite substrate-binding cavity of exceptional flexibility generates its extremely wide substrate specificity.* J Bacteriol, **185**: 5657-64.
186. Tornroth-Horsefield, S., Gourdon, P., Horsefield, R., Brive, L., Yamamoto, N., Mori, H., Snijder, A., and Neutze, R. 2007. *Crystal structure of AcrB in complex with a single transmembrane subunit reveals another twist.* Structure, **15**: 1663-73.
187. Nikaido, H., and Pages, J.M. 2012. *Broad-specificity efflux pumps and their role in multidrug resistance of Gram-negative bacteria.* FEMS Microbiol Rev, **36**: 340-63.
188. Lomovskaya, O., Warren, M.S., Lee, A., Galazzo, J., Fronko, R., Lee, M., Blais, J., Cho, D., Chamberland, S., Renau, T., Leger, R., Hecker, S., Watkins, W., Hoshino, K., Ishida, H., and Lee, V.J. 2001. *Identification and characterization of inhibitors of multidrug resistance efflux pumps in Pseudomonas aeruginosa: novel agents for combination therapy.* Antimicrob Agents Chemother, **45**: 105-16.
189. Bohnert, J.A., and Kern, W.V. 2005. *Selected arylpiperazines are capable of reversing multidrug resistance in Escherichia coli overexpressing RND efflux pumps.* Antimicrob Agents Chemother, **49**: 849-52.
190. Vargiu, A.V., Ruggerone, P., Opperman, T.J., Nguyen, S.T., and Nikaido, H. 2014. *Molecular mechanism of MBX2319 inhibition of Escherichia coli AcrB multidrug efflux pump and comparison with other inhibitors.* Antimicrob Agents Chemother, **58**: 6224-34.
191. Seeger, M.A., von Ballmoos, C., Eicher, T., Brandstatter, L., Verrey, F., Diederichs, K., and Pos, K.M. 2008. *Engineered disulfide bonds support the functional rotation mechanism of multidrug efflux pump AcrB.* Nat Struct Mol Biol, **15**: 199-205.
192. Yamane, T., Murakami, S., and Ikeguchi, M. 2013. *Functional rotation induced by alternating protonation states in the multidrug transporter AcrB: all-atom molecular dynamics simulations.* Biochemistry, **52**: 7648-58.
193. Seeger, M.A., von Ballmoos, C., Verrey, F., and Pos, K.M. 2009. *Crucial role of Asp408 in the proton translocation pathway of multidrug transporter AcrB: evidence from site-directed mutagenesis and carbodiimide labeling.* Biochemistry, **48**: 5801-12.
194. Mikolosko, J., Bobyk, K., Zgurskaya, H.I., and Ghosh, P. 2006. *Conformational flexibility in the multidrug efflux system protein AcrA.* Structure, **14**: 577-87.
195. Koronakis, V., Sharff, A., Koronakis, E., Luisi, B., and Hughes, C. 2000. *Crystal structure of the bacterial membrane protein TolC central to multidrug efflux and protein export.* Nature, **405**: 914-9.
196. Tamura, N., Murakami, S., Oyama, Y., Ishiguro, M., and Yamaguchi, A. 2005. *Direct interaction of multidrug efflux transporter AcrB and outer membrane channel TolC detected via site-directed disulfide cross-linking.* Biochemistry, **44**: 11115-21.

197. Nikaido, H. 1998. *Antibiotic resistance caused by gram-negative multidrug efflux pumps.* Clin Infect Dis, **27 Suppl 1**: S32-41.
198. Levy, S.B. 2002. *Active efflux, a common mechanism for biocide and antibiotic resistance.* Symp Ser Soc Appl Microbiol: 65S-71S.
199. Li, X.Z., and Nikaido, H. 2009. *Efflux-mediated drug resistance in bacteria: an update.* Drugs, **69**: 1555-623.
200. Piddock, L.J. 2006. *Multidrug-resistance efflux pumps - not just for resistance.* Nat Rev Microbiol, **4**: 629-36.
201. Zgurskaya, H.I., and Nikaido, H. 1999. *Bypassing the periplasm: reconstitution of the AcrAB multidrug efflux pump of Escherichia coli.* Proc Natl Acad Sci U S A, **96**: 7190-5.
202. Martins, A., Iversen, C., Rodrigues, L., Spengler, G., Ramos, J., Kern, W.V., Couto, I., Viveiros, M., Fanning, S., Pages, J.M., and Amaral, L. 2009. *An AcrAB-mediated multidrug-resistant phenotype is maintained following restoration of wild-type activities by efflux pump genes and their regulators.* Int J Antimicrob Agents, **34**: 602-4.
203. Martins A, *et al.* 2012*. Sequential Responses of Bacteria to Noxious Agents (Antibiotics) Leading To Accumulation of Mutations and Permanent Resistance*. Biochem Pharmacol **1**:104.
204. Nikaido, H. 2001. *Preventing drug access to targets: cell surface permeability barriers and active efflux in bacteria.* Semin Cell Dev Biol, **12**: 215-23.
205. Davin-Regli, A., Bolla, J.M., James, C.E., Lavigne, J.P., Chevalier, J., Garnotel, E., Molitor, A., and Pages, J.M. 2008. *Membrane permeability and regulation of drug "influx and efflux" in enterobacterial pathogens.* Curr Drug Targets, **9**: 750-9.
206. Liu, X., and Ferenci, T. 2001. *An analysis of multifactorial influences on the transcriptional control of ompF and ompC porin expression under nutrient limitation.* Microbiology, **147**: 2981-9.
207. Viveiros, M., Dupont, M., Rodrigues, L., Couto, I., Davin-Regli, A., Martins, M., Pages, J.M., and Amaral, L. 2007. *Antibiotic stress, genetic response and altered permeability of E. coli.* PLoS One, **2**: e365.
208. Tal, N., and Schuldiner, S. 2009. *A coordinated network of transporters with overlapping specificities provides a robust survival strategy.* Proc Natl Acad Sci U S A, **106**: 9051-6.
209. Lee, A., Mao, W., Warren, M.S., Mistry, A., Hoshino, K., Okumura, R., Ishida, H., and Lomovskaya, O. 2000. *Interplay between efflux pumps may provide either additive or multiplicative effects on drug resistance.* J Bacteriol, **182**: 3142-50.
210. Poole, K. 2007. *Efflux pumps as antimicrobial resistance mechanisms.* Ann Med, **39**: 162-76.
211. Ma, D., Cook, D.N., Alberti, M., Pon, N.G., Nikaido, H., and Hearst, J.E. 1995. *Genes acrA and acrB encode a stress-induced efflux system of Escherichia coli.* Mol Microbiol, **16**: 45-55.
212. Bogomolnaya, L.M., Andrews, K.D., Talamantes, M., Maple, A., Ragoza, Y., Vazquez-Torres, A., and Andrews-Polymenis, H. 2013. *The ABC-type efflux pump MacAB protects Salmonella enterica serovar typhimurium from oxidative stress.* MBio, **4**: e00630-13.
213. Huang, Y.W., Liou, R.S., Lin, Y.T., Huang, H.H., and Yang, T.C. 2014. *A linkage between SmeIJK efflux pump, cell envelope integrity, and sigmaE-mediated envelope stress response in Stenotrophomonas maltophilia.* PLoS One, **9**: e111784.
214. Srinivasan, V.B., Mondal, A., Venkataramaiah, M., Chauhan, N.K., and Rajamohan, G. 2013. *Role of oxyRKP, a novel LysR-family transcriptional regulator, in antimicrobial resistance and virulence in Klebsiella pneumoniae.* Microbiology, **159**: 1301-14.
215. Baugh, S., Ekanayaka, A.S., Piddock, L.J., and Webber, M.A. 2012. *Loss of or inhibition of all multidrug resistance efflux pumps of Salmonella enterica serovar Typhimurium results in impaired ability to form a biofilm.* J Antimicrob Chemother, **67**: 2409-17.
216. De Kievit, T.R., Parkins, M.D., Gillis, R.J., Srikumar, R., Ceri, H., Poole, K., Iglewski, B.H., and Storey, D.G. 2001. *Multidrug efflux pumps: expression patterns and contribution to antibiotic resistance in Pseudomonas aeruginosa biofilms.* Antimicrob Agents Chemother, **45**: 1761-70.
217. Kvist, M., Hancock, V., and Klemm, P. 2008. *Inactivation of efflux pumps abolishes bacterial biofilm formation.* Appl Environ Microbiol, **74**: 7376-82.

218. Buckley, A.M., Webber, M.A., Cooles, S., Randall, L.P., La Ragione, R.M., Woodward, M.J., and Piddock, L.J. 2006. *The AcrAB-TolC efflux system of Salmonella enterica serovar Typhimurium plays a role in pathogenesis.* Cell Microbiol, **8**: 847-56.
219. Padilla, E., Llobet, E., Domenech-Sanchez, A., Martinez-Martinez, L., Bengoechea, J.A., and Alberti, S. 2010. *Klebsiella pneumoniae AcrAB efflux pump contributes to antimicrobial resistance and virulence.* Antimicrob Agents Chemother, **54**: 177-83.
220. Hirakata, Y., Srikumar, R., Poole, K., Gotoh, N., Suematsu, T., Kohno, S., Kamihira, S., Hancock, R.E., and Speert, D.P. 2002. *Multidrug efflux systems play an important role in the invasiveness of Pseudomonas aeruginosa.* J Exp Med, **196**: 109-18.
221. Salunkhe, P., Smart, C.H., Morgan, J.A., Panagea, S., Walshaw, M.J., Hart, C.A., Geffers, R., Tummler, B., and Winstanley, C. 2005. *A cystic fibrosis epidemic strain of Pseudomonas aeruginosa displays enhanced virulence and antimicrobial resistance.* J Bacteriol, **187**: 4908-20.
222. Webber, M.A., and Piddock, L.J. 2003. *The importance of efflux pumps in bacterial antibiotic resistance.* J Antimicrob Chemother, **51**: 9-11.
223. Kurland, C.G., and Dong, H. 1996. *Bacterial growth inhibition by overproduction of protein.* Mol Microbiol, **21**: 1-4.
224. Lee, S.W., and Edlin, G. 1985. *Expression of tetracycline resistance in pBR322 derivatives reduces the reproductive fitness of plasmid-containing Escherichia coli.* Gene, **39**: 173-80.
225. Wood, K.B., and Cluzel, P. 2012. *Trade-offs between drug toxicity and benefit in the multi-antibiotic resistance system underlie optimal growth of E. coli.* BMC Syst Biol, **6**: 48.
226. Ramos, J.L., Martinez-Bueno, M., Molina-Henares, A.J., Teran, W., Watanabe, K., Zhang, X., Gallegos, M.T., Brennan, R., and Tobes, R. 2005. *The TetR family of transcriptional repressors.* Microbiol Mol Biol Rev, **69**: 326-56.
227. Perera, I.C., and Grove, A. 2010. *Molecular mechanisms of ligand-mediated attenuation of DNA binding by MarR family transcriptional regulators.* J Mol Cell Biol, **2**: 243-54.
228. Brown, N.L., Stoyanov, J.V., Kidd, S.P., and Hobman, J.L. 2003. *The MerR family of transcriptional regulators.* FEMS Microbiol Rev, **27**: 145-63.
229. Westbrock-Wadman, S., Sherman, D.R., Hickey, M.J., Coulter, S.N., Zhu, Y.Q., Warrener, P., Nguyen, L.Y., Shawar, R.M., Folger, K.R., and Stover, C.K. 1999. *Characterization of a Pseudomonas aeruginosa efflux pump contributing to aminoglycoside impermeability.* Antimicrob Agents Chemother, **43**: 2975-83.
230. Lucas, C.E., Balthazar, J.T., Hagman, K.E., and Shafer, W.M. 1997. *The MtrR repressor binds the DNA sequence between the mtrR and mtrC genes of Neisseria gonorrhoeae.* J Bacteriol, **179**: 4123-8.
231. Xiong, A., Gottman, A., Park, C., Baetens, M., Pandza, S., and Matin, A. 2000. *The EmrR protein represses the Escherichia coli emrRAB multidrug resistance operon by directly binding to its promoter region.* Antimicrob Agents Chemother, **44**: 2905-7.
232. Ahmed, M., Borsch, C.M., Taylor, S.S., Vazquez-Laslop, N., and Neyfakh, A.A. 1994. *A protein that activates expression of a multidrug efflux transporter upon binding the transporter substrates.* J Biol Chem, **269**: 28506-13.
233. Martin, R.G., Gillette, W.K., Rhee, S., and Rosner, J.L. 1999. *Structural requirements for marbox function in transcriptional activation of mar/sox/rob regulon promoters in Escherichia coli: sequence, orientation and spatial relationship to the core promoter.* Mol Microbiol, **34**: 431-41.
234. Sulavik, M.C., Gambino, L.F., and Miller, P.F. 1995. *The MarR repressor of the multiple antibiotic resistance (mar) operon in Escherichia coli: prototypic member of a family of bacterial regulatory proteins involved in sensing phenolic compounds.* Mol Med, **1**: 436-46.
235. Vinue, L., McMurry, L.M., and Levy, S.B. 2013. *The 216-bp marB gene of the marRAB operon in Escherichia coli encodes a periplasmic protein which reduces the transcription rate of marA.* FEMS Microbiol Lett, **345**: 49-55.
236. Blair, J.M., Richmond, G.E., and Piddock, L.J. 2014. *Multidrug efflux pumps in Gram-negative bacteria and their role in antibiotic resistance.* Future Microbiol, **9**: 1165-77.

237. Rosenberg, E.Y., Bertenthal, D., Nilles, M.L., Bertrand, K.P., and Nikaido, H. 2003. *Bile salts and fatty acids induce the expression of Escherichia coli AcrAB multidrug efflux pump through their interaction with Rob regulatory protein.* Mol Microbiol, **48**: 1609-19.
238. Demple, B. 1996. *Redox signaling and gene control in the Escherichia coli soxRS oxidative stress regulon--a review.* Gene, **179**: 53-7.
239. Nikaido, E., Shirosaka, I., Yamaguchi, A., and Nishino, K. 2011. *Regulation of the AcrAB multidrug efflux pump in Salmonella enterica serovar Typhimurium in response to indole and paraquat.* Microbiology, **157**: 648-55.
240. Capra, E.J., and Laub, M.T. 2012. *Evolution of two-component signal transduction systems.* Annu Rev Microbiol, **66**: 325-47.
241. Cann, AJ. *Two-component signal transduction in bacteria*. [Web Page]: MicrobiologyBytes; 15 February 2010 [cited 15 April 2016]; Available from: http://microbiologybytes.wordpress.com/2010/02/15/two-component-signal-transduction-in-bacteria.
242. Bearson, B.L., Wilson, L., and Foster, J.W. 1998. *A low pH-inducible, PhoPQ-dependent acid tolerance response protects Salmonella typhimurium against inorganic acid stress.* J Bacteriol, **180**: 2409-17.
243. Nishino, K., Nikaido, E., and Yamaguchi, A. 2007. *Regulation of multidrug efflux systems involved in multidrug and metal resistance of Salmonella enterica serovar Typhimurium.* J Bacteriol, **189**: 9066-75.
244. Nemec, A., Maixnerova, M., van der Reijden, T.J., van den Broek, P.J., and Dijkshoorn, L. 2007. *Relationship between the AdeABC efflux system gene content, netilmicin susceptibility and multidrug resistance in a genotypically diverse collection of Acinetobacter baumannii strains.* J Antimicrob Chemother, **60**: 483-9.
245. Bratu, S., Landman, D., Martin, D.A., Georgescu, C., and Quale, J. 2008. *Correlation of antimicrobial resistance with beta-lactamases, the OmpA-like porin, and efflux pumps in clinical isolates of Acinetobacter baumannii endemic to New York City.* Antimicrob Agents Chemother, **52**: 2999-3005.
246. Hornsey, M., Ellington, M.J., Doumith, M., Thomas, C.P., Gordon, N.C., Wareham, D.W., Quinn, J., Lolans, K., Livermore, D.M., and Woodford, N. 2010. *AdeABC-mediated efflux and tigecycline MICs for epidemic clones of Acinetobacter baumannii.* J Antimicrob Chemother, **65**: 1589-93.
247. Hu, W.S., Yao, S.M., Fung, C.P., Hsieh, Y.P., Liu, C.P., and Lin, J.F. 2007. *An OXA-66/OXA-51-like carbapenemase and possibly an efflux pump are associated with resistance to imipenem in Acinetobacter baumannii.* Antimicrob Agents Chemother, **51**: 3844-52.
248. Pournaras, S., Markogiannakis, A., Ikonomidis, A., Kondyli, L., Bethimouti, K., Maniatis, A.N., Legakis, N.J., and Tsakris, A. 2006. *Outbreak of multiple clones of imipenem-resistant Acinetobacter baumannii isolates expressing OXA-58 carbapenemase in an intensive care unit.* J Antimicrob Chemother, **57**: 557-61.
249. Jeong, H.W., Cheong, H.J., Kim, W.J., Kim, M.J., Song, K.J., Song, J.W., Kim, H.S., and Roh, K.H. 2009. *Loss of the 29-kilodalton outer membrane protein in the presence of OXA-51-like enzymes in Acinetobacter baumannii is associated with decreased imipenem susceptibility.* Microb Drug Resist, **15**: 151-8.
250. Lee, Y., Yum, J.H., Kim, C.K., Yong, D., Jeon, E.H., Jeong, S.H., Ahn, J.Y., and Lee, K. 2010. *Role of OXA-23 and AdeABC efflux pump for acquiring carbapenem resistance in an Acinetobacter baumannii strain carrying the blaOXA-66 gene.* Ann Clin Lab Sci, **40**: 43-8.
251. Sugawara, E., and Nikaido, H. 2014. *Properties of AdeABC and AdeIJK efflux systems of Acinetobacter baumannii compared with those of the AcrAB-TolC system of Escherichia coli.* Antimicrob Agents Chemother, **58**: 7250-7.
252. Huys, G., Cnockaert, M., Nemec, A., and Swings, J. 2005. *Sequence-based typing of ade B as a potential tool to identify intraspecific groups among clinical strains of multidrug-resistant Acinetobacter baumannii.* J Clin Microbiol, **43**: 5327-31.

253. Chu, Y.W., Chau, S.L., and Houang, E.T. 2006. *Presence of active efflux systems AdeABC, AdeDE and AdeXYZ in different Acinetobacter genomic DNA groups.* J Med Microbiol, **55**: 477-8.
254. Lin, L., Ling, B.D., and Li, X.Z. 2009. *Distribution of the multidrug efflux pump genes, adeABC, adeDE and adeIJK, and class 1 integron genes in multiple-antimicrobial-resistant clinical isolates of Acinetobacter baumannii-Acinetobacter calcoaceticus complex.* Int J Antimicrob Agents, **33**: 27-32.
255. Chuanchuen, R., Murata, T., Gotoh, N., and Schweizer, H.P. 2005. *Substrate-dependent utilization of OprM or OpmH by the Pseudomonas aeruginosa MexJK efflux pump.* Antimicrob Agents Chemother, **49**: 2133-6.
256. Thanabalu, T., Koronakis, E., Hughes, C., and Koronakis, V. 1998. *Substrate-induced assembly of a contiguous channel for protein export from E.coli: reversible bridging of an inner-membrane translocase to an outer membrane exit pore.* EMBO J, **17**: 6487-96.
257. Marchand, I., Damier-Piolle, L., Courvalin, P., and Lambert, T. 2004. *Expression of the RND-type efflux pump AdeABC in Acinetobacter baumannii is regulated by the AdeRS two-component system.* Antimicrob Agents Chemother, **48**: 3298-304.
258. Bazyleu, A., and Kumar, A. 2014. *Incubation temperature, osmolarity, and salicylate affect the expression of resistance-nodulation-division efflux pumps and outer membrane porins in Acinetobacter baumannii ATCC19606T.* FEMS Microbiol Lett, **357**: 136-43.
259. Fernando, D., and Kumar, A. 2012. *Growth phase-dependent expression of RND efflux pump- and outer membrane porin-encoding genes in Acinetobacter baumannii ATCC 19606.* J Antimicrob Chemother, **67**: 569-72.
260. Hood, M.I., Jacobs, A.C., Sayood, K., Dunman, P.M., and Skaar, E.P. 2010. *Acinetobacter baumannii increases tolerance to antibiotics in response to monovalent cations.* Antimicrob Agents Chemother, **54**: 1029-41.
261. Coyne, S., Guigon, G., Courvalin, P., and Perichon, B. 2010. *Screening and quantification of the expression of antibiotic resistance genes in Acinetobacter baumannii with a microarray.* Antimicrob Agents Chemother, **54**: 333-40.
262. Yoon, E.J., Courvalin, P., and Grillot-Courvalin, C. 2013. *RND-type efflux pumps in multidrug-resistant clinical isolates of Acinetobacter baumannii: major role for AdeABC overexpression and AdeRS mutations.* Antimicrob Agents Chemother, **57**: 2989-95.
263. Lopes, B.S., and Amyes, S.G. 2013. *Insertion sequence disruption of adeR and ciprofloxacin resistance caused by efflux pumps and gyrA and parC mutations in Acinetobacter baumannii.* Int J Antimicrob Agents, **41**: 117-21.
264. Peleg, A.Y., Adams, J., and Paterson, D.L. 2007. *Tigecycline Efflux as a Mechanism for Nonsusceptibility in Acinetobacter baumannii.* Antimicrob Agents Chemother, **51**: 2065-9.
265. Lin, M.F., Lin, Y.Y., Yeh, H.W., and Lan, C.Y. 2014. *Role of the BaeSR two-component system in the regulation of Acinetobacter baumannii adeAB genes and its correlation with tigecycline susceptibility.* BMC Microbiol, **14**: 119.
266. Lin, M.F., Lin, Y.Y., and Lan, C.Y. 2015. *The Role of the Two-Component System BaeSR in Disposing Chemicals through Regulating Transporter Systems in Acinetobacter baumannii.* PLoS One, **10**: e0132843.
267. Coyne, S., Courvalin, P., and Perichon, B. 2011. *Efflux-mediated antibiotic resistance in Acinetobacter spp.* Antimicrob Agents Chemother, **55**: 947-53.
268. Rajamohan, G., Srinivasan, V.B., and Gebreyes, W.A. 2010. *Novel role of Acinetobacter baumannii RND efflux transporters in mediating decreased susceptibility to biocides.* J Antimicrob Chemother, **65**: 228-32.
269. Fernando, D.M., Xu, W., Loewen, P.C., Zhanel, G.G., and Kumar, A. 2014. *Triclosan can select for an AdeIJK-overexpressing mutant of Acinetobacter baumannii ATCC 17978 that displays reduced susceptibility to multiple antibiotics.* Antimicrob Agents Chemother, **58**: 6424-31.
270. Roca, I., Marti, S., Espinal, P., Martinez, P., Gibert, I., and Vila, J. 2009. *CraA, a major facilitator superfamily efflux pump associated with chloramphenicol resistance in Acinetobacter baumannii.* Antimicrob Agents Chemother, **53**: 4013-4.

271. Rajamohan, G., Srinivasan, V.B., and Gebreyes, W.A. 2010. *Molecular and functional characterization of a novel efflux pump, AmvA, mediating antimicrobial and disinfectant resistance in Acinetobacter baumannii.* J Antimicrob Chemother, **65**: 1919-25.
272. Su, X.Z., Chen, J., Mizushima, T., Kuroda, T., and Tsuchiya, T. 2005. *AbeM, an H+-coupled Acinetobacter baumannii multidrug efflux pump belonging to the MATE family of transporters.* Antimicrob Agents Chemother, **49**: 4362-4.
273. Srinivasan, V.B., Rajamohan, G., and Gebreyes, W.A. 2009. *Role of AbeS, a novel efflux pump of the SMR family of transporters, in resistance to antimicrobial agents in Acinetobacter baumannii.* Antimicrob Agents Chemother, **53**: 5312-6.
274. Hassan, K.A., Jackson, S.M., Penesyan, A., Patching, S.G., Tetu, S.G., Eijkelkamp, B.A., Brown, M.H., Henderson, P.J., and Paulsen, I.T. 2013. *Transcriptomic and biochemical analyses identify a family of chlorhexidine efflux proteins.* Proc Natl Acad Sci U S A, **110**: 20254-9.
275. Chen, Y., Pi, B., Zhou, H., Yu, Y., and Li, L. 2009. *Triclosan resistance in clinical isolates of Acinetobacter baumannii.* J Med Microbiol, **58**: 1086-91.
276. Lytvynenko, I., Brill, S., Oswald, C., and Pos, K.M. 2015. *Residues involved in substrate recognition of the small multidrug resistance efflux pump AbeS from Acinetobacter baumannii.* J Mol Biol.
277. Hassan, K.A., Liu, Q., Henderson, P.J., and Paulsen, I.T. 2015. *Homologs of the Acinetobacter baumannii AceI transporter represent a new family of bacterial multidrug efflux systems.* MBio, **6**.
278. Chau, S.L., Chu, Y.W., and Houang, E.T. 2004. *Novel resistance-nodulation-cell division efflux system AdeDE in Acinetobacter genomic DNA group 3.* Antimicrob Agents Chemother, **48**: 4054-5.
279. Roca, I., Espinal, P., Marti, S., and Vila, J. 2011. *First identification and characterization of an AdeABC-like efflux pump in Acinetobacter genomospecies 13TU.* Antimicrob Agents Chemother, **55**: 1285-6.
280. Vila, J., Marti, S., and Sanchez-Cespedes, J. 2007. *Porins, efflux pumps and multidrug resistance in Acinetobacter baumannii.* J Antimicrob Chemother, **59**: 1210-5.
281. Srinivasan, V.B., Rajamohan, G., Pancholi, P., Stevenson, K., Tadesse, D., Patchanee, P., Marcon, M., and Gebreyes, W.A. 2009. *Genetic relatedness and molecular characterization of multidrug resistant Acinetobacter baumannii isolated in central Ohio, USA.* Ann Clin Microbiol Antimicrob, **8**: 21.
282. Miranda, C.D., Kehrenberg, C., Ulep, C., Schwarz, S., and Roberts, M.C. 2003. *Diversity of tetracycline resistance genes in bacteria from Chilean salmon farms.* Antimicrob Agents Chemother, **47**: 883-8.
283. Hong, H., Jung, J., and Park, W. 2014. *Plasmid-encoded tetracycline efflux pump protein alters bacterial stress responses and ecological fitness of Acinetobacter oleivorans.* PLoS One, **9**: e107716.
284. Smith, M.G., Gianoulis, T.A., Pukatzki, S., Mekalanos, J.J., Ornston, L.N., Gerstein, M., and Snyder, M. 2007. *New insights into Acinetobacter baumannii pathogenesis revealed by high-density pyrosequencing and transposon mutagenesis.* Genes Dev, **21**: 601-14.
285. Wisplinghoff, H., Hippler, C., Bartual, S.G., Haefs, C., Stefanik, D., Higgins, P.G., and Seifert, H. 2008. *Molecular epidemiology of clinical Acinetobacter baumannii and Acinetobacter genomic species 13TU isolates using a multilocus sequencing typing scheme.* Clin Microbiol Infect, **14**: 708-15.
286. Hunger, M., Schmucker, R., Kishan, V., and Hillen, W. 1990. *Analysis and nucleotide sequence of an origin of DNA replication in Acinetobacter calcoaceticus and its use for Escherichia coli shuttle plasmids.* Gene, **87**: 45-51.
287. Clinical and Laboratory Standards Institute (CLSI). 2015. *Performance standards for antimicrobial susceptibility testing*. Twenty-fifth informational supplement. CLSI document M100–S25. CLSI, Wayne, PA.

288. Halstead, D.C., Abid, J., and Dowzicky, M.J. 2007. *Antimicrobial susceptibility among Acinetobacter calcoaceticus-baumannii complex and Enterobacteriaceae collected as part of the Tigecycline Evaluation and Surveillance Trial.* J Infect, **55**: 49-57.
289. Nowak, J., Seifert, H., and Higgins, P.G. 2015. *Prevalence of eight resistance-nodulation-division efflux pump genes in epidemiologically characterized Acinetobacter baumannii of worldwide origin.* J Med Microbiol, **64**: 630-5.
290. Szybalski, W., and Bryson, V. 1952. *Genetic studies on microbial cross resistance to toxic agents. I. Cross resistance of Escherichia coli to fifteen antibiotics.* J Bacteriol, **64**: 489-99.
291. Pannek, S., Higgins, P.G., Steinke, P., Jonas, D., Akova, M., Bohnert, J.A., Seifert, H., and Kern, W.V. 2006. *Multidrug efflux inhibition in Acinetobacter baumannii: comparison between 1-(1-naphthylmethyl)-piperazine and phenyl-arginine-beta-naphthylamide.* J Antimicrob Chemother, **57**: 970-4.
292. Nowak, J., Schneiders, T., Seifert, H., and Higgins, P.G. 2015. *The Asp20-to-Asn Substitution in the Response Regulator AdeR Leads to Enhanced Efflux Activity of AdeB in Acinetobacter baumannii.* Antimicrob Agents Chemother, **60**: 1085-90.
293. Lan, R., and Reeves, P.R. 2000. *Intraspecies variation in bacterial genomes: the need for a species genome concept.* Trends Microbiol, **8**: 396-401.
294. Fraud, S., Campigotto, A.J., Chen, Z., and Poole, K. 2008. *MexCD-OprJ multidrug efflux system of Pseudomonas aeruginosa: involvement in chlorhexidine resistance and induction by membrane-damaging agents dependent upon the AlgU stress response sigma factor.* Antimicrob Agents Chemother, **52**: 4478-82.
295. Fetar, H., Gilmour, C., Klinoski, R., Daigle, D.M., Dean, C.R., and Poole, K. 2011. *mexEF-oprN multidrug efflux operon of Pseudomonas aeruginosa: regulation by the MexT activator in response to nitrosative stress and chloramphenicol.* Antimicrob Agents Chemother, **55**: 508-14.
296. Fraud, S., and Poole, K. 2011. *Oxidative stress induction of the MexXY multidrug efflux genes and promotion of aminoglycoside resistance development in Pseudomonas aeruginosa.* Antimicrob Agents Chemother, **55**: 1068-74.
297. Luo, L., Jiang, X., Wu, Q., Wei, L., Li, J., and Ying, C. 2011. *Efflux pump overexpression in conjunction with alternation of outer membrane protein may induce Acinetobacter baumannii resistant to imipenem.* Chemotherapy, **57**: 77-84.
298. Poole, K. 2014. *Stress responses as determinants of antimicrobial resistance in Pseudomonas aeruginosa: multidrug efflux and more.* Can J Microbiol, **60**: 783-91.
299. Andersson, D.I. 2006. *The biological cost of mutational antibiotic resistance: any practical conclusions?* Curr Opin Microbiol, **9**: 461-5.
300. Llanes, C., Hocquet, D., Vogne, C., Benali-Baitich, D., Neuwirth, C., and Plesiat, P. 2004. *Clinical strains of Pseudomonas aeruginosa overproducing MexAB-OprM and MexXY efflux pumps simultaneously.* Antimicrob Agents Chemother, **48**: 1797-802.
301. Pumbwe, L., and Piddock, L.J. 2000. *Two efflux systems expressed simultaneously in multidrug-resistant Pseudomonas aeruginosa.* Antimicrob Agents Chemother, **44**: 2861-4.
302. Akiba, M., Lin, J., Barton, Y.W., and Zhang, Q. 2006. *Interaction of CmeABC and CmeDEF in conferring antimicrobial resistance and maintaining cell viability in Campylobacter jejuni.* J Antimicrob Chemother, **57**: 52-60.
303. Mima, T., Sekiya, H., Mizushima, T., Kuroda, T., and Tsuchiya, T. 2005. *Gene cloning and properties of the RND-type multidrug efflux pumps MexPQ-OpmE and MexMN-OprM from Pseudomonas aeruginosa.* Microbiol Immunol, **49**: 999-1002.
304. Li, Y., Mima, T., Komori, Y., Morita, Y., Kuroda, T., Mizushima, T., and Tsuchiya, T. 2003. *A new member of the tripartite multidrug efflux pumps, MexVW-OprM, in Pseudomonas aeruginosa.* J Antimicrob Chemother, **52**: 572-5.
305. Mima, T., Joshi, S., Gomez-Escalada, M., and Schweizer, H.P. 2007. *Identification and characterization of TriABC-OpmH, a triclosan efflux pump of Pseudomonas aeruginosa requiring two membrane fusion proteins.* J Bacteriol, **189**: 7600-9.

306. Eaves, D.J., Ricci, V., and Piddock, L.J. 2004. *Expression of acrB, acrF, acrD, marA, and soxS in Salmonella enterica serovar Typhimurium: role in multiple antibiotic resistance.* Antimicrob Agents Chemother, **48**: 1145-50.
307. Olivares, J., Alvarez-Ortega, C., and Martinez, J.L. 2014. *Metabolic compensation of fitness costs associated with overexpression of the multidrug efflux pump MexEF-OprN in Pseudomonas aeruginosa.* Antimicrob Agents Chemother, **58**: 3904-13.
308. Poole, K. 2004. *Efflux-mediated multiresistance in Gram-negative bacteria.* Clin Microbiol Infect, **10**: 12-26.
309. Lin, J., Michel, L.O., and Zhang, Q. 2002. *CmeABC functions as a multidrug efflux system in Campylobacter jejuni.* Antimicrob Agents Chemother, **46**: 2124-31.
310. Taylor, D.L., Ante, V.M., Bina, X.R., Howard, M.F., and Bina, J.E. 2015. *Substrate-dependent activation of the Vibrio cholerae vexAB RND efflux system requires vexR.* PLoS One, **10**: e0117890.
311. Bina, X.R., Provenzano, D., Nguyen, N., and Bina, J.E. 2008. *Vibrio cholerae RND family efflux systems are required for antimicrobial resistance, optimal virulence factor production, and colonization of the infant mouse small intestine.* Infect Immun, **76**: 3595-605.
312. Cerda-Maira, F.A., Ringelberg, C.S., and Taylor, R.K. 2008. *The bile response repressor BreR regulates expression of the Vibrio cholerae breAB efflux system operon.* J Bacteriol, **190**: 7441-52.
313. Allen, M.P., Zumbrennen, K.B., and McCleary, W.R. 2001. *Genetic evidence that the alpha5 helix of the receiver domain of PhoB is involved in interdomain interactions.* J Bacteriol, **183**: 2204-11.
314. Sola, M., Gomis-Ruth, F.X., Serrano, L., Gonzalez, A., and Coll, M. 1999. *Three-dimensional crystal structure of the transcription factor PhoB receiver domain.* J Mol Biol, **285**: 675-87.
315. McLaughlin, P.D., Bobay, B.G., Regel, E.J., Thompson, R.J., Hoch, J.A., and Cavanagh, J. 2007. *Predominantly buried residues in the response regulator Spo0F influence specific sensor kinase recognition.* FEBS Lett, **581**: 1425-9.
316. Baranova, N., and Nikaido, H. 2002. *The baeSR two-component regulatory system activates transcription of the yegMNOB (mdtABCD) transporter gene cluster in Escherichia coli and increases its resistance to novobiocin and deoxycholate.* J Bacteriol, **184**: 4168-76.
317. Nishino, K., Honda, T., and Yamaguchi, A. 2005. *Genome-wide analyses of Escherichia coli gene expression responsive to the BaeSR two-component regulatory system.* J Bacteriol, **187**: 1763-72.
318. Cerca, P., Martins, A., Couto, I., Viveiros, M., and Amaral, L. 2011. *Competition between substrates of the efflux pump system of Salmonella enteritidis.* In Vivo, **25**: 597-602.
319. Yang, Y., and Chua, K.L. 2013. *Assessment of the effect of efflux pump inhibitors on in vitro antimicrobial susceptibility of multidrug-resistant Acinetobacter baumannii.* Int J Antimicrob Agents, **42**: 283-4.
320. Cortez-Cordova, J., and Kumar, A. 2011. *Activity of the efflux pump inhibitor phenylalanine-arginine beta-naphthylamide against the AdeFGH pump of Acinetobacter baumannii.* Int J Antimicrob Agents, **37**: 420-4.
321. Ribera, A., Ruiz, J., Jiminez de Anta, M.T., and Vila, J. 2002. *Effect of an efflux pump inhibitor on the MIC of nalidixic acid for Acinetobacter baumannii and Stenotrophomonas maltophilia clinical isolates.* J Antimicrob Chemother, **49**: 697-8.
322. Coban, A.Y., Guney, A.K., Tanriverdi Cayci, Y., and Durupinar, B. 2011. *Effect of 1-(1-Naphtylmethyl)-piperazine, an efflux pump inhibitor, on antimicrobial drug susceptibilities of clinical Acinetobacter baumannii isolates.* Curr Microbiol, **62**: 508-11.
323. Lomovskaya, O., and Bostian, K.A. 2006. *Practical applications and feasibility of efflux pump inhibitors in the clinic--a vision for applied use.* Biochem Pharmacol, **71**: 910-8.
324. Pages, J.M., and Amaral, L. 2009. *Mechanisms of drug efflux and strategies to combat them: challenging the efflux pump of Gram-negative bacteria.* Biochim Biophys Acta, **1794**: 826-33.

7. Supplementary Material

Suppl. Table I *List of approved antimicrobials active against Acinetobacter spp.*
Adapted from Magiorakos *et al*. [77] with permission from Elsevier.

Antimicrobial category	**Antimicrobial agent**
Aminoglycosides	Gentamicin Tobramycin Amikacin Netilmicin
Antipseudomonal carbapenems	Imipenem Meropenem Doripenem
Antipseudomonal fluoroquinolones	Ciprofloxacin Levofloxacin
Antipseudomonal penicillins + β-lactanase inhibitors	Piperacillin-tazobactam Ticarcillin-clavulanic acid
Extended-spectrum cephalosporins	Cefotaxime Ceftriaxone Ceftazidime Cefepime
Folate pathway inhibitors	Trimethoprim-sulfamethoxazole
Penicillins + β-lactamase inhibitors	Ampicillin-sulbactam
Polymyxins	Colistin Polymyxin B
Tetracyclines	Tetracycline Doxycycline Minocycline

Suppl. Table II *Characterisation of isolates used to study the prevalence of RND-type efflux pump genes*

Cluster	Investigator	Country	*adeB*		*adeJ*	*adeG*		ACICU_00143		ACICU_02904		ACICU_03066		ACICU_3412		ACICU_03646
			O3/O4	2_F/R	1_F/R	1_F/R	2_F/R	1_F/R	2_F/R	1_F/R	2_F/R	1_F/R	2_F/R	1_F/R	2_F/R	1_F/R
IC1	34252	Italy	1	n.t.	1	n.t.	n.t.	1	n.t.	1	n.t.	0	1	1	n.t.	1
IC1	34261	Italy	1	n.t.	1	1	n.t.	1	n.t.	1	n.t.	0	1	1	n.t.	1
IC1	34609	Greece	1	n.t.	1	1	n.t.	0	0	1	1	0	1	1	1	1
IC1	34625	Pakistan	1	n.t.	1	1	n.t.	1	n.t.	1	n.t.	0	1	1	n.t.	1
IC1	34632	Spain	1	n.t.	1	1	n.t.	1	n.t.	1	n.t.	0	1	1	n.t.	1
IC1	34632	Spain	1	n.t.	1	1	n.t.	1	n.t.	1	n.t.	0	1	1	n.t.	1
IC1	35428	United States	1	n.t.	1	1	n.t.	1	1	0	1	0	1	0	0	1
IC1	35679	Greece	1	n.t.	1	1	n.t.	0	0	1	1	0	1	1	1	1
IC1	35695	India	1	n.t.	1	1	n.t.	1	n.t.	1	n.t.	0	1	1	n.t.	1
IC1	35695	India	1	n.t.	1	1	n.t.	1	n.t.	1	n.t.	0	1	1	n.t.	1
IC1	37762	Puerto Rico	1	n.t.	1	1	n.t.	1	n.t.	1	n.t.	0	1	1	n.t.	1
IC2	34261	Italy	1	n.t.	1	1	n.t.	1	n.t.	0	1	1	n.t.	1	1	1
IC2	34534	United States	1	n.t.	1	1	n.t.	1	n.t.	0	1	1	n.t.	1	1	1
IC2	34565	United States	1	n.t.	1	1	n.t.	1	n.t.	0	1	1	n.t.	0	0	1
IC2	34576	United States	1	n.t.	1	1	n.t.	1	n.t.	0	1	1	1	0	0	1
IC2	34576	United States	1	n.t.	1	1	n.t.	1	n.t.	0	1	1	n.t.	0	0	1
IC2	34590	Austria	1	n.t.	1	1	n.t.	1	n.t.	0	1	1	n.t.	1	1	1
IC2	34601	China	1	n.t.	1	1	n.t.	1	n.t.	0	1	1	1	0	0	1
IC2	34609	Greece	1	n.t.	1	1	n.t.	1	n.t.	0	1	1	n.t.	1	0	1
IC2	34625	Pakistan	1	n.t.	1	1	n.t.	1	n.t.	0	1	1	n.t.	0	0	1
IC2	34625	Pakistan	1	n.t.	1	1	n.t.	1	n.t.	0	1	1	n.t.	0	0	1
IC2	34628	Portugal	1	n.t.	1	1	n.t.	1	n.t.	0	1	1	n.t.	1	1	1
IC2	34628	Portugal	1	n.t.	1	1	n.t.	1	n.t.	0	1	1	n.t.	1	1	1
IC2	34995	United States	1	n.t.	1	1	n.t.	1	n.t.	0	1	1	n.t.	0	0	1
IC2	35029	United States	1	n.t.	1	1	n.t.	1	n.t.	0	1	1	n.t.	1	1	1
IC2	35035	United States	1	n.t.	1	1	n.t.	1	n.t.	0	1	0	1	0	0	1

Suppl. Table II contd. *Characterisation of isolates used to study the prevalence of RND-type efflux pump genes*

Cluster	Investigator	Country	*adeB*		*adeJ*	*adeG*		ACICU_00143		ACICU_02904		ACICU_03066		ACICU_3412		ACICU_03646
			O3/O4	2_F/R	1_F/R	1_F/R	2_F/R	1_F/R	2_F/R	1_F/R	2_F/R	1_F/R	2_F/R	1_F/R	2_F/R	1_F/R
IC2	35099	United States	1	n.t.	1	1	n.t.	1	n.t.	0	1	1	n.t.	1	1	1
IC2	35262	United States	1	n.t.	1	1	n.t.	1	n.t.	0	1	1	n.t.	0	0	1
IC2	35314	United States	1	n.t.	1	1	n.t.	1	n.t.	0	1	1	n.t.	1	1	1
IC2	35411	Singapore	1	n.t.	1	1	n.t.	1	n.t.	0	1	1	n.t.	0	0	1
IC2	35411	Singapore	1	n.t.	1	1	n.t.	1	n.t.	0	1	1	n.t.	0	0	1
IC2	35491	United States	1	n.t.	1	1	n.t.	1	n.t.	0	1	1	n.t.	0	0	1
IC2	35491	United States	1	n.t.	1	1	n.t.	1	n.t.	0	1	1	n.t.	0	0	1
IC2	35656	Australia	1	n.t.	1	1	n.t.	1	n.t.	0	1	1	n.t.	0	0	1
IC2	35656	Australia	1	n.t.	1	1	n.t.	1	n.t.	0	1	1	n.t.	0	0	1
IC2	35679	Greece	1	n.t.	1	1	n.t.	1	n.t.	0	1	1	1	1	1	1
IC2	35683	Italy	1	n.t.	1	1	n.t.	1	n.t.	0	1	1	n.t.	1	1	1
IC2	35718	Ireland	1	n.t.	1	1	n.t.	1	n.t.	0	1	1	n.t.	0	0	1
IC2	35718	Ireland	1	n.t.	1	1	n.t.	1	n.t.	0	1	1	n.t.	0	0	1
IC2	35733	South Africa	1	n.t.	1	1	n.t.	1	n.t.	0	1	1	n.t.	0	0	1
IC2	35878	United States	1	n.t.	1	1	n.t.	1	n.t.	0	1	1	n.t.	0	0	1
IC2	36094	United States	1	n.t.	1	1	n.t.	1	n.t.	0	1	1	n.t.	0	0	1
IC2	36098	United States	1	n.t.	1	1	n.t.	1	n.t.	0	1	1	n.t.	0	0	1
IC2	36873	United States	1	n.t.	1	1	n.t.	1	n.t.	0	1	1	n.t.	0	0	1
IC2	36873	United States	1	n.t.	1	1	n.t.	1	n.t.	0	1	1	n.t.	0	0	1
IC2	37562	United States	1	n.t.	1	1	n.t.	1	n.t.	0	1	1	n.t.	0	0	1
IC2	38215	Israel	1	n.t.	1	1	n.t.	1	n.t.	0	1	1	n.t.	0	0	1
IC2	38249	South Africa	1	n.t.	1	1	n.t.	1	n.t.	0	1	1	n.t.	0	0	1
IC2	38249	South Africa	1	n.t.	1	1	n.t.	1	n.t.	0	1	1	n.t.	0	0	1
IC3	34542	United States	1	n.t.	1	1	n.t.	1	n.t.	1	n.t.	1	n.t.	1	n.t.	1
IC3	34542	United States	1	n.t.	1	1	n.t.	1	n.t.	1	n.t.	1	0	1	n.t.	1
IC3	34564	United States	1	n.t.	1	1	n.t.	1	n.t.	1	n.t.	1	1	1	n.t.	1
IC3	34630	Spain	1	n.t.	1	1	n.t.	1	n.t.	1	n.t.	1	n.t.	1	n.t.	1

Suppl. Table II contd. *Characterisation of isolates used to study the prevalence of RND-type efflux pump genes*

Cluster	Investigator	Country	*adeB*		*adeJ*	*adeG*		ACICU_00143		ACICU_02904		ACICU_03066		ACICU_3412		ACICU_03646
			O3/O4	2_F/R	1_F/R	1_F/R	2_F/R	1_F/R	2_F/R	1_F/R	2_F/R	1_F/R	2_F/R	1_F/R	2_F/R	1_F/R
IC3	35080	United States	1	n.t.	1	1	n.t.	1	n.t.	1	n.t.	1	n.t.	1	n.t.	1
IC3	35489	United States	1	n.t.	1	1	n.t.	1	n.t.	1	n.t.	0	1	1	n.t.	1
IC3	36185	United States	1	n.t.	1	1	n.t.	1	n.t.	1	n.t.	1	n.t.	1	n.t.	1
IC3	36852	United States	1	n.t.	1	1	n.t.	1	n.t.	1	n.t.	1	n.t.	1	n.t.	1
IC3	39418	United States	1	n.t.	1	1	n.t.	1	n.t.	1	n.t.	1	n.t.	1	n.t.	1
IC4	34595	Argentina	1	n.t.	1	1	n.t.	1	n.t.	0	1	0	1	0	0	1
IC4	34595	Argentina	1	n.t.	1	1	n.t.	1	n.t.	0	1	0	1	0	0	1
IC4	34596	Argentina	1	n.t.	1	1	n.t.	1	n.t.	0	1	0	1	0	0	1
IC4	34596	Argentina	1	n.t.	1	1	n.t.	1	n.t.	0	1	0	1	0	0	1
IC4	34596	Argentina	1	n.t.	1	1	0	1	0	0	1	0	1	0	0	1
IC4	34596	Argentina	1	n.t.	1	1	n.t.	1	n.t.	0	1	0	1	0	0	1
IC4	34611	Hungary	1	n.t.	1	1	n.t.	1	1	0	1	0	1	0	0	1
IC4	34637	Turkey	1	n.t.	1	1	n.t.	1	n.t.	0	1	0	1	0	0	1
IC4	34637	Turkey	1	n.t.	1	1	n.t.	1	n.t.	0	1	0	1	0	0	1
IC4	34637	Turkey	1	n.t.	1	1	n.t.	1	n.t.	0	1	0	1	0	0	1
IC4	34637	Turkey	1	n.t.	1	1	n.t.	0	0	0	1	1	1	1	1	1
IC4	34637	Turkey	1	n.t.	1	1	n.t.	1	n.t.	0	1	0	1	0	0	1
IC4	35651	Argentina	1	n.t.	1	1	n.t.	1	n.t.	0	1	0	1	0	0	1
IC4	35651	Argentina	1	n.t.	1	1	n.t.	1	n.t.	0	1	0	1	0	0	1
IC4	35652	Argentina	1	n.t.	1	1	n.t.	1	n.t.	0	1	0	1	0	0	1
IC4	35695	India	1	n.t.	1	1	n.t.	1	n.t.	0	1	0	1	0	0	1
IC5	34255	United States	1	n.t.	1	1	n.t.	1	n.t.	1	n.t.	1	n.t.	0	0	1
IC5	34572	United States	1	n.t.	1	1	n.t.	1	n.t.	1	n.t.	1	n.t.	0	0	1
IC5	34632	Spain	1	1	1	1	n.t.	1	n.t.	1	1	1	n.t.	0	0	1
IC5	34632	Spain	1	n.t.	1	1	n.t.	1	n.t.	1	1	1	n.t.	0	0	1
IC5	35649	Argentina	1	n.t.	1	1	n.t.	1	n.t.	1	n.t.	1	n.t.	1	n.t.	1
IC5	35649	Argentina	1	n.t.	1	1	n.t.	1	n.t.	1	n.t.	1	n.t.	1	1	1

Suppl. Table II contd. *Characterisation of isolates used to study the prevalence of RND-type efflux pump genes*

Cluster	Investigator	Country	*adeB*		*adeJ*	*adeG*		ACICU_00143		ACICU_02904		ACICU_03066		ACICU_3412		ACICU_03646
			O3/O4	2_F/R	1_F/R	1_F/R	2_F/R	1_F/R	2_F/R	1_F/R	2_F/R	1_F/R	2_F/R	1_F/R	2_F/R	1_F/R
IC5	35649	Argentina	1	n.t.	1	1	n.t.	1	n.t.	1	1	1	n.t.	1	1	1
IC5	35651	Argentina	1	1	1	1	n.t.	1	n.t.	1	n.t.	1	n.t.	1	1	1
IC5	35652	Argentina	1	n.t.	1	1	n.t.	1	n.t.	1	n.t.	1	n.t.	1	n.t.	1
IC5	35652	Argentina	1	n.t.	1	1	n.t.	1	1	0	1	1	n.t.	0	1	1
IC5	35652	Argentina	0	0	1	1	n.t.	1	n.t.	1	n.t.	1	n.t.	1	1	1
IC5	35652	Argentina	1	n.t.	1	1	n.t.	1	n.t.	1	n.t.	1	n.t.	1	1	1
IC5	35828	United States	1	n.t.	1	1	n.t.	1	n.t.	1	n.t.	1	n.t.	0	0	1
IC5	38268	Venezuela	1	n.t.	1	1	n.t.	1	1	1	n.t.	1	n.t.	0	0	1
IC5	39581	Mexico	1	n.t.	1	1	n.t.	0	0	1	n.t.	1	n.t.	1	1	1
IC5	39581	Mexico	1	n.t.	1	1	n.t.	0	0	1	n.t.	1	n.t.	1	1	1
IC6	38188	Honduras	1	n.t.	1	1	n.t.	1	n.t.	n.t.	1	0	1	1	n.t.	1
IC6	38188	Honduras	1	n.t.	1	1	n.t.	1	n.t.	n.t.	1	0	1	1	n.t.	1
IC6	38188	Honduras	1	n.t.	1	n.t.	1	1	n.t.	n.t.	1	0	1	1	n.t.	1
IC6	38188	Honduras	1	n.t.	1	1	n.t.	1	n.t.	n.t.	1	0	1	1	n.t.	1
IC6	38188	Honduras	1	n.t.	1	1	n.t.	1	n.t.	0	1	0	1	1	n.t.	1
IC6	38188	Honduras	1	n.t.	1	1	n.t.	1	n.t.	n.t.	1	0	1	1	n.t.	1
IC6	38188	Honduras	1	n.t.	1	1	n.t.	1	n.t.	n.t.	1	0	1	1	n.t.	1
IC6	38225	Italy	1	n.t.	1	1	n.t.	1	n.t.	n.t.	1	0	1	1	n.t.	1
IC6	38225	Italy	1	n.t.	1	1	n.t.	1	n.t.	0	1	0	1	1	n.t.	1
IC6	38225	Italy	1	n.t.	1	1	n.t.	1	n.t.	n.t.	1	0	1	1	n.t.	1
IC6	38225	Italy	1	n.t.	1	1	n.t.	1	n.t.	n.t.	1	0	1	1	n.t.	1
IC7	35411	Singapore	1	n.t.	1	1	n.t.	1	n.t.	0	1	1	n.t.	0	0	1
IC7	35652	Argentina	1	n.t.	1	1	n.t.	1	n.t.	0	1	1	n.t.	0	0	1
IC7	35666	Columbia	1	n.t.	1	1	n.t.	1	n.t.	0	1	1	n.t.	0	0	1
IC7	38268	Venezuela	1	n.t.	1	1	n.t.	1	n.t.	0	1	1	n.t.	1	1	1
IC7	39581	Mexico	1	n.t.	1	1	n.t.	1	n.t.	0	1	1	n.t.	1	1	1
IC8	34601	China	1	1	1	1	n.t.	0	0	0	1	0	1	0	1	1

Suppl. Table II contd. *Characterisation of isolates used to study the prevalence of RND-type efflux pump genes*

Cluster	Investigator	Country	*adeB*		*adeJ*	*adeG*		ACICU_00143		ACICU_02904		ACICU_03066		ACICU_3412		ACICU_03646
			O3/O4	2_F/R	1_F/R	1_F/R	2_F/R	1_F/R	2_F/R	1_F/R	2_F/R	1_F/R	2_F/R	1_F/R	2_F/R	1_F/R
IC8	34630	Spain	1	n.t.	1	1	n.t.	0	0	n.t.	1	1	n.t.	1	n.t.	1
IC8	34630	Spain	1	n.t.	1	1	n.t.	0	0	1	n.t.	1	n.t.	1	n.t.	1
IC8	34630	Spain	1	n.t.	1	1	n.t.	0	0	1	n.t.	1	n.t.	1	n.t.	1
IC8	34637	Turkey	1	n.t.	1	1	n.t.	0	0	n.t.	1	1	n.t.	1	n.t.	1
IC8	34637	Turkey	1	n.t.	1	1	n.t.	1	1	0	1	0	1	1	n.t.	1
IC8	34637	Turkey	1	n.t.	1	1	n.t.	1	1	n.t.	1	1	n.t.	1	n.t.	1
IC8	34637	Turkey	1	n.t.	1	1	n.t.	1	n.t.	0	1	0	1	1	1	1
IC8	35670	France	1	n.t.	1	1	n.t.	0	0	n.t.	1	1	n.t.	1	n.t.	1
IC8	38229	Korea	0	0	1	1	n.t.	0	0	1	n.t.	1	n.t.	1	n.t.	1
GtU	34596	Argentina	1	n.t.	1	0	1	1	n.t.	0	1	0	1	0	1	1
GtU	34596	Argentina	1	n.t.	1	1	n.t.	1	n.t.	1	n.t.	0	1	1	n.t.	1
GtU	34597	Argentina	1	n.t.	1	1	n.t.	1	n.t.	1	n.t.	0	1	1	1	1
GtU	34597	Argentina	1	n.t.	1	1	n.t.	1	n.t.	1	n.t.	1	n.t.	1	n.t.	1
GtU	34599	Brazil	0	0	1	1	n.t.	1	1	0	1	0	1	1	1	1
GtU	34599	Brazil	1	n.t.	1	1	n.t.	1	n.t.	0	1	1	n.t.	0	0	1
GtU	34627	Poland	1	n.t.	1	1	n.t.	1	n.t.	1	n.t.	0	1	1	n.t.	1
GtU	34632	Spain	1	n.t.	1	1	n.t.	1	n.t.	1	n.t.	0	1	1	1	1
GtU	34639	United States	1	n.t.	1	1	n.t.	1	n.t.	1	n.t.	0	1	0	0	1
GtU	34804	United States	1	n.t.	1	1	n.t.	1	1	1	n.t.	0	1	0	0	1
GtU	35028	United States	0	0	1	0	1	0	1	0	1	1	n.t.	1	n.t.	1
GtU	35029	United States	1	n.t.	1	1	n.t.	1	n.t.	1	n.t.	1	n.t.	0	0	1
GtU	35029	United States	1	n.t.	1	0	1	1	n.t.	1	n.t.	0	1	0	0	1
GtU	35411	Singapore	1	n.t.	1	1	n.t.	1	n.t.	1	n.t.	1	n.t.	1	n.t.	1
GtU	35411	Singapore	1	n.t.	1	1	n.t.	1	n.t.	0	1	1	n.t.	0	0	1
GtU	35432	United States	1	1	1	1	n.t.	0	0	0	1	1	n.t.	0	0	1
GtU	35474	United States	1	n.t.	1	0	1	0	n.t.	0	1	0	1	1	1	1
GtU	35491	United States	1	n.t.	1	0	1	1	n.t.	0	1	0	1	1	1	1

Suppl. Table II contd. *Characterisation of isolates used to study the prevalence of RND-type efflux pump genes*

Cluster	Investigator	Country	*adeB*		*adeJ*	*adeG*		ACICU_00143		ACICU_02904		ACICU_03066		ACICU_3412		ACICU_03646
			O3/O4	2_F/R	1_F/R	1_F/R	2_F/R	1_F/R	2_F/R	1_F/R	2_F/R	1_F/R	2_F/R	1_F/R	2_F/R	1_F/R
GtU	35649	Argentina	1	n.t.	1	1	n.t.	1	n.t.	1	n.t.	0	1	1	1	1
GtU	35656	Australia	1	n.t.	1	1	n.t.	1	n.t.	0	1	0	1	0	0	1
GtU	35666	Columbia	1	n.t.	1	1	n.t.	1	n.t.	0	1	1	n.t.	0	0	1
GtU	35683	Italy	1	n.t.	1	1	n.t.	1	n.t.	1	n.t.	0	1	1	n.t.	1
GtU	35683	Italy	0	0	1	1	1	1	n.t.	1	n.t.	1	n.t.	1	1	1
GtU	35695	India	1	n.t.	1	1	n.t.	0	0	1	n.t.	1	n.t.	1	1	1
GtU	35828	United States	1	n.t.	1	1	n.t.	1	n.t.	0	1	1	n.t.	0	0	1
GtU	36094	United States	1	n.t.	1	1	n.t.	1	n.t.	0	1	0	1	1	n.t.	1
GtU	38268	Venezuela	1	n.t.	1	1	n.t.	1	n.t.	0	1	1	n.t.	0	0	1
GtU	39581	Mexico	1	n.t.	1	1	n.t.	1	n.t.	1	n.t.	1	n.t.	1	1	1

IC: international clone; GtU: genotypically unique; n.t.: not tested, 0: no product, 1: positive PCR product

Suppl. Figure I *Plasmid card pIG14/09::rnd1-lacZ*

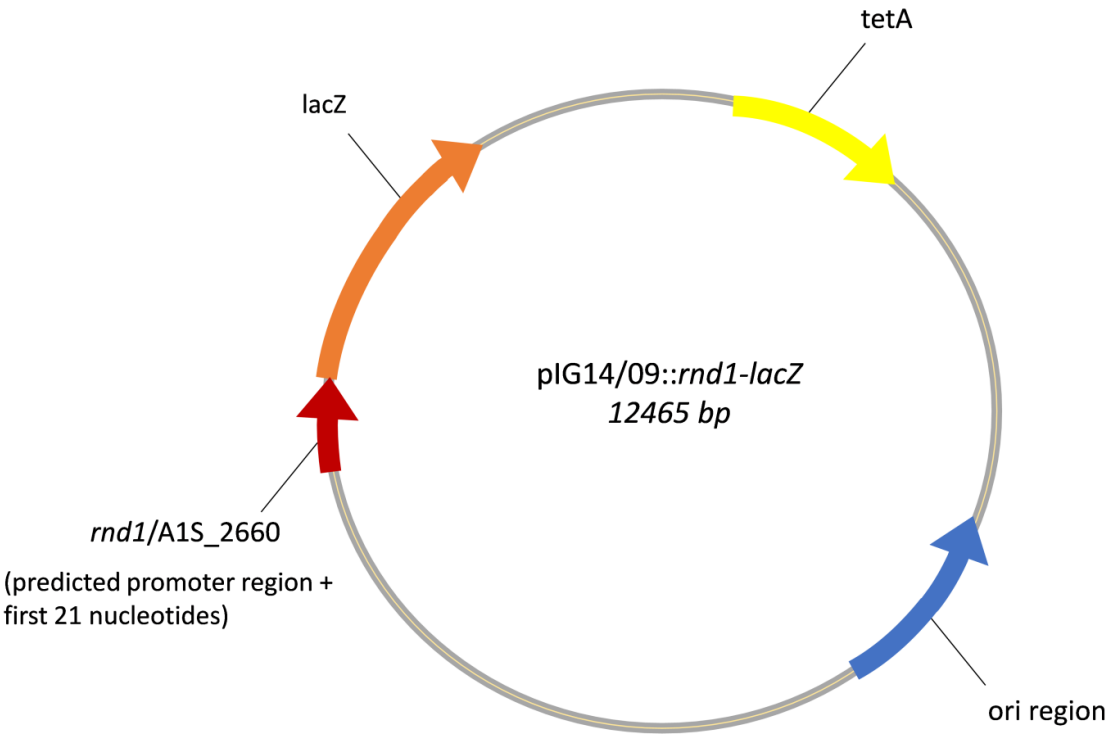

For the generation of pIG14/09, the β-galactosidase encoding gene *lacZ*, amplified from pMC1871, was cloned into the PstI restriction site of pWH1266 (Section 2.2.3.1). The predicted promoter region of A1S_2660 and its first 21 nucleotides were cloned in frame to the *lacZ* gene using the In-fusion enzyme mix (Section 2.2.3.2). β-galactosidase breaks down the lactose analogue X-gal (5-bromo-4-chloro-3-indolyl-β-D-galactopyranoside) to galactose and 5-bromo-4-chloro-3-hydroxyindole. The latter forms dimers and is oxidised to 5,5'-dibromo-4,4'-dichloro-indigo, which appears blue and can therefore be used for a reporter assay.

Suppl. Figure II *Plasmid card pBA03/05::rnd1_oe*

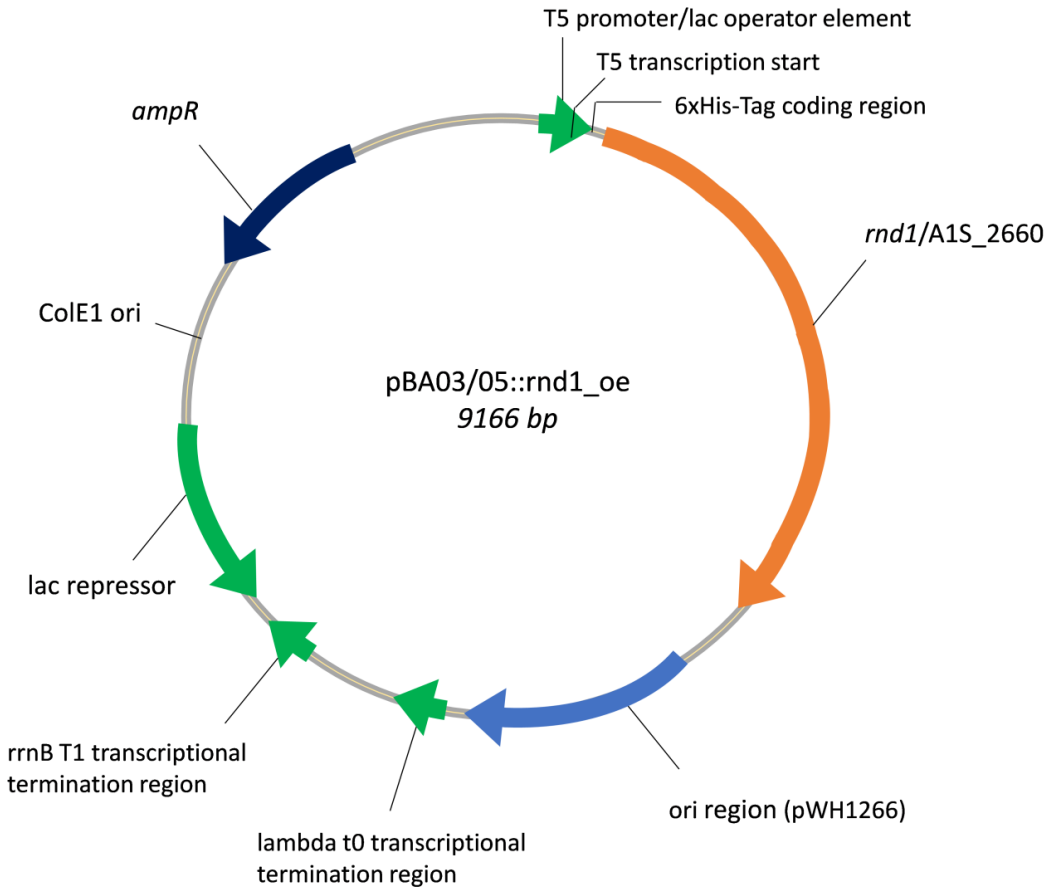

For the generation of pBA03/05, the origin of replication amplified from pWH1266 was cloned into the HindIII restricted and blunted pQE80L (Section 2.2.3.4). The *rnd1* (A1S_2660) gene was cloned into the polylinker in frame with the T5 promoter using the In-fusion enzyme mix (Section 2.2.3.5).

Suppl. Figure III *Plasmid card pJN17/04::adeRS*

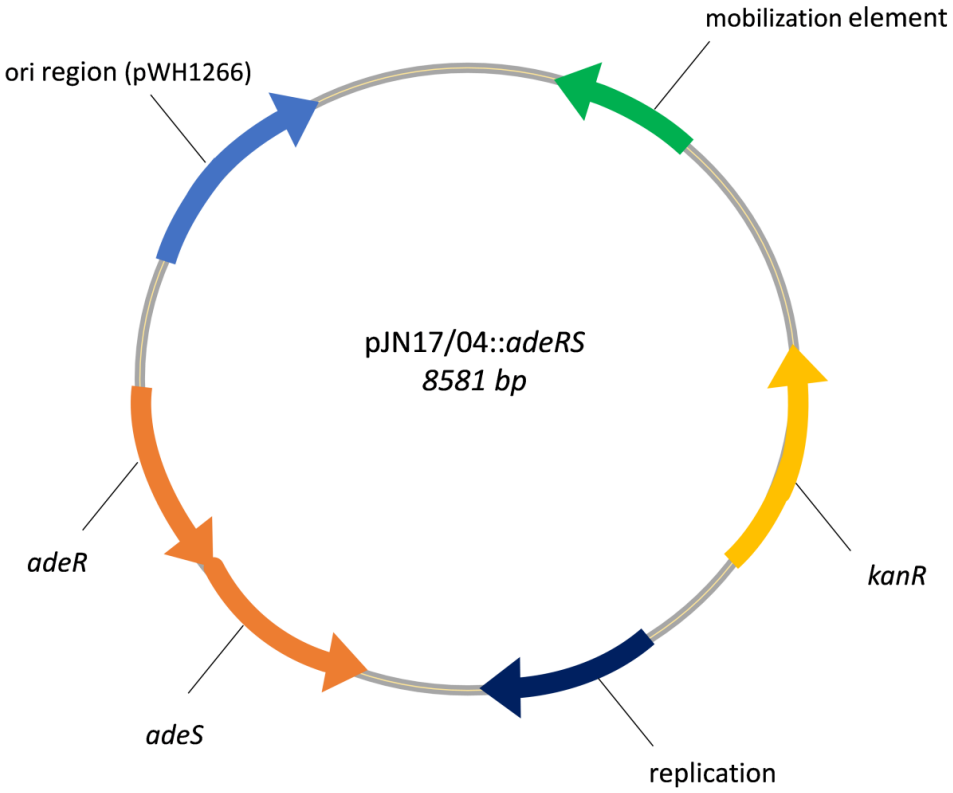

For the generation of pJN17/04, the origin of replication amplified from pWH1266 was cloned into the multiple cloning site of pBHR1 (Section 2.2.4.1). *adeRS* genes were blunt ligated with pJN17/04 which was linearized by the endonuclease ScaI (Section 2.2.4.2).